Parameter Sensitivity, Estimation and Convergence

-- An Information Approach

by

Victor E. DeBrunner

Dissertation submitted to the Faculty of the

Virginia Polytechnic Institute and State University

in partial fulfillment of the requirements for the degree of

Doctor of Philosophy

in

Electrical Engineering

APPROVED:

A. A. (Louis) Beex, Chairman

C. A. Beattie

S. Bingulac

D. K. Lindner

S. M. Riad

April 18, 1990

Blacksburg, Virginia

Parameter Sensitivity, Estimation and Convergence

-- An Information Approach

by

Victor E. DeBrunner

A. A. (Louis) Beex, Chairman

Electrical Engineering

(ABSTRACT)

Convergence rates are analyzed for Recursive Prediction (Output) Error Methods (RPEM) in the identification of linear state-space systems from (noisy) impulse response data. RPEM algorithms are derived which are suitable for the identification of the parameters in arbitrary state-space structures. Deterministic and stochastic versions of these identification algorithms are presented. These two classes indicate the number of realizations used in the identification, not the presence or absence of noise. The convergence analysis uses the eigen-information of the correlation matrix (really its inverse, the Fisher information matrix) for a chosen parameterization. This analysis explains why various state-space structures have different convergence properties, i.e., why for the same system the estimation processes corresponding to different identification structures converge at different rates. The eigen-information of the parameter information matrix relates the system sensitivity and numerical conditioning in a manner which provides insight into the identification process. The relevant eigen-information is combined in the proposed scalar convergence time constant τ. One important result is that identification of the usually identified direct form II parameters (the standard ARMA parameters) does not necessarily yield the fastest parameter set convergence for the system being identified. Identification from arbitrary input is also briefly considered, as is identification when the model order is different from the "true" system order.

Acknowledgements

I would like to thank Dr. A. A. (Louis) Beex for his encouragement and help; without it this would have been a much more difficult project, and not nearly as much fun. He let me flounder just enough so that I discovered much by myself, and "calmed the waters" when that seemed appropriate. He also provided the initial comment on sensitivity and identification which initiated this dissertation. I would also like to thank Dr. Chris Beattie, with whom I had several lively discussions -- these helped me clarify ideas immensely, even if it didn't appear so at the time. I want to thank Dr. Baja Bingulac for interesting me in system identification, as the 2 courses that I took under him in this area were 2 of my more enjoyable classes. I would like to thank Dr. D. K. Lindner for his discussions of the dual generalized Hessenberg representation structure. I would like to thank Dr. S. Riad for his interest in this work. Finally, I would like to thank my wife Linda for her support during this stressful experience.

Table of Contents

List of Illustrations

List of Tables

1.0 Introduction

In the 1986 M.S. Thesis [24], *Sensitivity Analysis of Digital Filters,* the identification of structures with low coefficient sensitivities for the purpose of reducing digital-filter parameter-quantization noise power was considered. As a natural extension to this previous work, we now investigate the opposite question of the usefulness of structures with high parameter sensitivities for the purpose of increasing the convergence rate of parameter and state identification algorithms. In particular, we are examining the effects of parameter sensitivity on the identification of SISO linear systems from measurements of the impulse response (the partial realization problem) with an eye toward its possible application for the identification from estimated correlation data (the stochastic partial realization problem).

The notion of parametric modeling (identifying system model parameters) from observed data was initiated by Gauss in the early 19th century [40]. The stochastic version of identification, time series analysis, was developed at least as early as 1914 [39], with many disciplines involved in this work. With the advent of digital computers in the 1960's, these algorithms became computationally practical for a wide variety of situations and many uses. A proliferation of algorithms resulted from this development. These new identification algorithms were motivated by the desire to quickly identify the model parameters (for real time use) and the desire to increase the accuracy of the resulting estimates. As usual, these two desirable features are incompatible, and therefore some

optimal middle-ground must be found between speed and accuracy. This issue is tackled directly, with the hope of increasing both speed and accuracy by examining the structure of SISO systems. By examining the information content of the parameters which describe the system, some interesting convergence speed-up results can be predicted. This effort is strongly supported by observation and simulation.

In practice, only one particular class of this problem is examined in any detail, the partial realization problem. The name partial realization is derived from the fact that only a partial subsequence of an entire (infinite) sequence is used in the identification. In the (approximate) partial realization (A)PR problem, this infinite sequence is a (noisy) impulse response, and in the approximate stochastic partial realization problem (A)SPR, this sequence is the (estimated) covariance sequence. In particular, we focus on the convergence aspects of gradient (conjugate direction) algorithms in the identification procedure.

Since any observed linear system has an infinite number of parameterizations, and these different parameterizations have different characteristics, why not choose parameterizations which specifically have properties useful in identification? The parameter characteristics of interest depend in full on the information content of the chosen system parameterization. In particular, the following is shown with regard to partial realization:

1. An identifier structure with high parameter sensitivity leads to fast convergence of the associated parameter estimates;
2. An identifier structure exhibiting a wide variation of parameter sensitivities leads to poor convergence of all associated parameter estimates.

We combine these two different mechanisms affecting convergence into one measure τ, a self-styled "time constant" of system parameter convergence. From this measure, we have formulated a conjecture (see Conjecture (C.1) in Chapter 5). We have not been able to find counter-examples to the conjecture, but we also have not been able to prove it. Upper bound arguments may be given which, under local conditions, indicate that the conjecture is reasonable.

Care should be exercised with making statements about absolute convergence rates, because the chance always exists for a method with a large upper bound on the error to actually converge very fast for a particular situation. For example, consider finding the zeros of the function $f(x) = x^2 - 4$ ($x_i = \pm 2$, for $i = 1,2$). If the quadratically convergent Newton iteration

$$x_{i+1} = x_i - \frac{f(x_i)}{f'(x_i)}$$

is used with $x_0 = 1.0$, then the solution $x = 2$ is never found exactly. A few iterations yield $x_1 = 2.5$, $x_2 = 2.05$, $x_3 = 2.000609756$ and $x_4 = 2.000000093$. However, if the simple bisection method is used with an initial bracketing of $x = 1.0$ and $x = 3.0$, the exact solution $x = 2.0$ is found exactly on the first try even though the convergence for this method is only guaranteed to be linear! Accordingly, we give upper bound results on the error, and use these bounds as heuristic support for the conjectures.

The importance of this work lies in connecting the convergence analysis to the convergence rates for identification procedures which use alternative structures. These results are important in active sonar target classification [36], adaptive equalization of communication channels [103], multipulse speech coding models [1,92,105] and seismic deconvolution [19]. Because the research also relates ways that individual parameters can influence overall system identification, the ideas can be incorporated into areas such as circuit testing and system fault detection [14]. More importantly, an analytical tool is presented which can be of aid in the design of systems with a twist towards improving the chances that a fault or construction error can be detected. Potential uses here include the detection of space-structure integrity [28].

We quote [28]

> **One of the key unanswered questions in parameter estimation is that of parameter sensitivity to changes in the input-output data and numerical accuracies. There has been very little work on this topic and yet the resolution of the question on which algorithm is the most effective in a numerical sense depends on the sensitivity. It would be foolish in system design work to select the design which is most sensitive to component changes or digital word length. ... Research on parameter sensitivity has been limited ... . The sensitivity question will be placed in the category of future research problems for the identification of large space structures.**

The original contribution of this research is simply the manner in which the parameter correlation matrix and its inverse, the Fisher information matrix, are used. Parameter sensitivity is

connected to estimate convergence, and we show that the numerical conditioning of the parameters strongly influences both parameter convergence and accuracy. We connect the two ideas in a proposed measure τ, defined

$$\tau \equiv \frac{\kappa_2(F)}{tr(F)}$$

where F is the Fisher information matrix of the chosen parameterization. The condition number $\kappa_2(F)$ has been connected to convergence rates in adaptive control, and it is proportional to the information disparity of the parameters of the chosen identification structure. The trace, tr(F), is the system sensitivity, and so it is connected to convergence rates encountered in the optimal input design problem of system identification.

Deterministic justifications for the measure τ can be found in the mathematical literature, specifically for Gauss-Newton optimization searches (one of the most commonly used parameter identification approaches). This measure is termed the **convergence time constant** since for smaller τ the convergence rate of the parameter estimates should be faster than for larger τ. This research extends the convergence results to stochastic identification algorithms, borrowing heavily from optimal input design as well as Lyapunov and Martingale convergence theory.

In the process, much of a general nature in identification algorithms and identification theory will be examined. The dissertation begins with a background review in Chapter 2. This section covers several seemingly disparate topics, among which are system theory (observability, controllability and system sensitivity), system identification theory and information theory. In Chapter 3, we discuss in detail the identification algorithms (Algorithms (A.1) and (A.2)) which are used in the exploration of the time constant τ. A complete description of the 3 single-input single-output structures used in the identifications is included. Chapter 4 connects the identification method to both the system parameter sensitivity and parameter information content. Chapter 5 and Chapter 6 give the details and results for two algorithmic implementations, a deterministic version and a stochastic version. Chapter 7 shows that the convergence analysis tool is not restricted to the PR problem, but can be used to explain the convergence of alternate structures in

the case of arbitrary input. Chapter 8 gives the conclusions and describes directions for further research effort. Appendices are included at the back to elaborate some details.

2.0 Previous Research and Related Work

This chapter is a collection of many ideas and results which are necessary for later understanding. As such, it may appear to the casual reader to be loosely organized. Hopefully, the relevance will become clear as we get into the problem particulars and the application results. Some motivation for each topic will be given as the opportunity arises. The first topic discussed is the parameter sensitivity and its connection to the system observability and controllability grammians, a connection which may be useful in explaining some convergence behavior. The next section discusses convergence and the identified system parameterization, which pertains directly to this research. The third and fourth topics concern areas of identification algorithm study which yield important results useful to the research. The next to last topic is a combination of directly related previous research and an alternative (and easy to implement) idea. Finally, we include some general discussion of research in partial realization theory and identification algorithms taken from the literature.

2.1 *Parameter Sensitivity*

To talk sensibly about the topic, we need to discuss first what is meant by parameter sensitivity. System parameter sensitivity is defined [4,23,24,98][1]

$$S = \sum_{i=1}^{NP} \frac{1}{2\pi j} \oint \frac{\partial H(z)}{\partial \theta_i} \frac{\partial H(z^{-1})}{\partial \theta_i} \frac{dz}{z} \tag{2.1.1}$$

where $H(z)$ is the (stable) system transfer function and NP is the number of system parameters θ_i. This sensitivity measure is an L_2 norm on the space of rational transfer functions. Motivation for this measure can be obtained in both a deterministic manner using Taylor's theorem and a stochastic manner using standard [91] quantization assumptions.

The sensitivity in equation (2.1.1) is strongly related to the quantization noise in digital filters [24]. Minimal sensitivity digital filters have minimal output quantization noise. Thus, a digital filter with low sensitivity is very desirable. A gradient-based optimization routine for the minimization of the sensitivity of a direct form II digital filter is given in Appendix G. The algorithm utilizes pole/zero cancellations to provide degrees of freedom over which minimal sensitivity filters can be found. The point here is to keep the filter transfer function invariant (and so the pole/zero cancellation pairs).

The system parameters θ_i can live anywhere, but if they are the state-space parameters, then (as noted in [23,24]) the observability and controllability grammians of the system are clearly and directly related to the sensitivity given in equation (2.1.1). To see this connection, some definitions are in order.

Let the parameters Θ be elements of the n-dimensional SISO state-space system

---

[1] The contour is along the unit circle of the z-plane in a counterclockwise direction.

$$x_{k+1} = Ax_k + Bu_k$$
$$y_k = Cx_k + du_k$$

where u_k is the system input, y_k is the system output and {A,B,C,d} describe the n-dimensional system whose transfer function $H(z)$ is given by

$$H(z) = C(zI - A)^{-1}B + d \tag{2.1.2}$$

Different parameterizations of the same system may be found via state transformations, i.e. the quadruple {$T^{-1}AT$, $T^{-1}B$, CT, d} also has transfer function $H(z)$ as long as T is an invertible matrix.

For the state-space parameters, we can now directly evaluate the partial derivatives needed for computing the sensitivity in equation (2.1.1). They are:

1. for the input vector parameters

$$\frac{\partial H(z)}{\partial b_i} = C(zI - A)^{-1}1_i \tag{2.1.3}$$

where 1_i is the i^{th} Euclidian basis vector, i.e. an (nx1) vector whose components are all zero except for the i^{th} one, which is equal to 1.

2. for the output vector parameters

$$\frac{\partial H(z)}{\partial c_i} = 1_i'(zI - A)^{-1}B \tag{2.1.4}$$

where the prime denotes transpose.

3. Slightly more difficult to determine are the partial derivatives for the state transition matrix parameters. Using the identity [41]

$$\frac{\partial A^{-1}}{\partial \alpha} = -A^{-1}\frac{\partial A}{\partial \alpha}A^{-1}$$

gives

$$\frac{\partial H(z)}{\partial a_{ij}} = - C(zI - A)^{-1} \frac{\partial (zI - A)}{\partial a_{ij}} (zI - A)^{-1} B$$

or,

$$\frac{\partial H(z)}{\partial a_{ij}} = C(zI - A)^{-1} 1_i 1_j' (zI - A)^{-1} B$$

Using equations (2.1.3) and (2.1.4), this is simply

$$\frac{\partial H(z)}{\partial a_{ij}} = \frac{\partial H(z)}{\partial b_i} \frac{\partial H(z)}{\partial c_j} \tag{2.1.5}$$

Notice that these sensitivity functions are rational functions with the same poles as the original transfer function $H(z)$. Thus, if the system is stable, the partial derivative system is also stable. This sensitivity measure (equation (2.1.1)) is an indication of the frequency response deviation caused by small changes in the system coefficients. The deviation is measured by changes in total system energy.

The state-space system has controllability grammian K and observability grammian W which are the solutions to the Lyapunov equations

$$K = AKA' + BB' \qquad W = A'WA + C'C \tag{2.1.6}$$

The well-known solutions to equations (2.1.6) are the infinite summations

$$K = \sum_{l=0}^{\infty} A^l BB' A'^l \qquad W = \sum_{l=0}^{\infty} A'^l C'C A^l$$

Alternatively, and most importantly to the sensitivity measure, the solutions to equations (2.1.6) may be computed [23,24] from the cross-correlations defined by

$$k_{ij} = \frac{1}{2\pi j} \oint \frac{\partial H(z)}{\partial c_i} \frac{\partial H(z^{-1})}{\partial c_j} \frac{dz}{z} \quad i,j = 1, \ldots, n$$
$$w_{ij} = \frac{1}{2\pi j} \oint \frac{\partial H(z)}{\partial b_i} \frac{\partial H(z^{-1})}{\partial b_j} \frac{dz}{z} \quad i,j = 1, \ldots, n \tag{2.1.7}$$

Note that from equation (2.1.4), the controllability grammian K is a function of only A and B, and not C. Similarly, the observability grammian W is a function of only A and C, and not of B. The scalar d does not affect the system controllability or observability. Under a state transformation T (T invertible), the grammians are transformed as $T^{-1}K(T^{-1})'$ and $T'WT$. These new grammians are not similar to the original grammians although the new grammian product $T^{-1}KWT$ is similar to the original product KW (similar meaning that the eigenvalues of both matrices are the same). Upon immediate comparison of equations (2.1.7) and equation (2.1.1), one can see that the diagonal elements of the grammians are specially related to the input and output vector parameters.

In fact, as used in [115-117], the grammians can be directly related to the sensitivity

$$S \leq \mathrm{tr}(K) + \mathrm{tr}(W) + \mathrm{tr}(KW) \tag{2.1.8}$$

where tr(•) denotes the trace of the argument matrix. In fact, an exact relationship is given [98]

$$S = \mathrm{tr}(K) + \mathrm{tr}(W) + \mathrm{tr}(K)\mathrm{tr}(W) - 2\sum_{n=1}^{\infty}\sum_{l=1}^{NP} W'_l A^n 1_l \sum_{j=1}^{NP} 1'_j A^n K_j \tag{2.1.9}$$

K_i and W_j are the i^{th} and j^{th} columns respectively of the grammians.

Generalized grammians are presented in [117]. The generalization is to frequency, and these new matrices are denoted K^{Φ} and W^{Ψ} respectively. The Φ and Ψ are continuous, integrable

weighting functions which determine the frequencies of interest. The generalized grammians thus have the elements

$$k_{ij}^{\Phi} = \frac{1}{2\pi j} \oint \frac{\partial H(z)}{\partial c_i} \frac{\partial H(z^{-1})}{\partial c_j} |\Phi(z)|^2 \frac{dz}{z} \qquad i,j = 1, \ldots, n$$

$$w_{ij}^{\Psi} = \frac{1}{2\pi j} \oint \frac{\partial H(z)}{\partial b_i} \frac{\partial H(z^{-1})}{\partial b_j} |\Psi(z)|^2 \frac{dz}{z} \qquad i,j = 1, \ldots, n$$

These generalized grammians provide the mathematical framework for the design of digital filters with low sensitivity in a particular frequency band of interest. In an identification context, the weighting functions would be used to reflect some prior knowledge about the frequency content of the system to be identified.

The connection between the sensitivity and the system grammians is expressed in equation (2.1.9), but what does this connection portend for a parameter identification procedure? The parameter sensitivity is directly related to system identifiability and controllability. What can be made of this connection from an identification standpoint? It is well known that to identify all the system parameters uniquely, all of the system modes must be both controllable and observable. Then, given a sufficiently rich input to the system whose parameters are to be determined, all of these system parameters can be identified. However, observability and controllability are not binary variables with one value for an observable (controllable) mode and another value for an unobservable (uncontrollable) one. Rather, the various modes of a general system are relatively (i.e. more or less) observable (controllable). Only in balanced [83] state-space coordinates are these measures the same for all system modes! The original hypothesis is that the more controllable and observable the modes of the system are, the "easier" it is to identify the system parameters. Later examples show this hypothesis to be a reasonable one. In this context "easier" translates into faster parameter convergence for the identification algorithm. Thus, the working hypothesis is that parameter sensitivity is related to the convergence rates for the parameter estimates in system

identification. Since the parameter sensitivity is not invariant to a state-space transformation T, one should then expect that different structures will have correspondingly different identification properties.

From the completely different perspective of function minimization, the parameter sensitivity would seem a logical property to examine when studying the parameter convergence of identification algorithms. Look back at equation (2.1.1) and reflect on what it is measuring. The sensitivity S is an indication of how much the system transfer function changes (in energy over all frequencies) in response to small parameter variations. In system identification, a parameter estimate adjustment scheme often used is one which matches the energy spectrums of the parameterized model and the true system.

2.2 Parameter Convergence and System Structure

2.2.1 Structure

The relationship, if any, between the assumed model structure in an identifier algorithm and the resulting parameter convergence is precisely the topic investigated in this dissertation. It appears that many in the research area overlook the importance of system structure (read parameter location) in the single-input, single-output (SISO) system identification. It is often stated, and (universally) believed, that for single-input, single-output (SISO) systems, the only structural parameter affecting convergence is the system order [107]. Consequently, research into system structure and identification has been limited to the identification of multiple-input, multiple-output (MIMO) systems. In these multivariable (MIMO) systems many structural parameters exist. Our premise is that while system order is a very important structural parameter, the existing different (canonical or otherwise) parameterizations of the same system elicit different identifiability

characteristics. As will be shown, this disagreement is not rhetorical, but in fact is well grounded in observation as well as numerical analysis and theory.

Recently, this notion of SISO systems and structure has been challenged by others as well. Lattice structures have been developed and used for their round-off properties [35], and now many Least-Square algorithms exist based on this structure. Stability of this structure is easily determined, as all reflection coefficient magnitudes must be less than 1. These reflection coefficients are the identified parameters of the structure, and the speed and accuracy of the identification is high. However, recent work has encompassed state-space structures of a more general nature [90,103,104]. The former examines the optimization by comparing the global and local minima of various parameterizations of the same system. This important point will be examined in Chapter 3. The latter two discuss gradient algorithms for use in IIR adaptive filtering and estimation. One interesting part of these papers is that adaptive identification of parallel, lattice and cascade systems is discussed briefly. The identification of the parameters belonging to the parallel structure for use in adaptive IIR filtering is further detailed by the author of these latter two papers [102]. We will examine this work more closely in Chapter 7. This method of identifying the parallel structure parameters is not easily extendable to a general state-space structure, but can be extended to cascade forms. Structural issues in the identification of MIMO systems will be briefly looked at next. These issues provide a basis with which SISO structure can be compared.

Some examples of research in MIMO identification are found in [58,60,61]. These papers describe techniques of state/parameter identification in which parametric, as well as structural, freedom is allowed. The identification methods are significant in that structural freedom is used for arbitrarily fast convergence of the estimated states. The convergence analysis follows that developed in [13,85] closely. The identification algorithms use conventional Luenberger observers. Valid solutions of the parameter estimates are assumed constant (identification of time-invariant systems). The model structure is determined by an a priori choice of error criterion. This prior restraint of the system structure is a limiting factor; one shared in the present investigation. In Chapter 5 and Chapter 6 a practical solution to this "fixed" a priori structure choice is proposed, and some brief examples are given to explain and verify the postulated solution. This solution involves the

monitoring of certain structural properties for several identifiable parameterizations. A switch to identifying the "best" structure is then suggested. A similar solution is presented for SISO systems [53] with a note that while computation requirements are severe, certain situations exist where only small changes in coefficients are expected so that the procedure could be used to advantage.

2.2.2 Observability and Controllability

The identifiability of any parameter is very important to an identification procedure since the chosen set of parameters must be identifiable [118], and the measure of identifiability can influence the identification. One book which discusses parameter identification from a structural viewpoint in state-space is [121]. This work is more closely related to the ideas presented in [118]. Many ideas about connectibility and structural observability (controllability) are explored in detail. Connections to Gauss-Newton gradient identification methods are given. Though the idea of input/output equivalence is mentioned and the existence of different parameterizations of the same system is noted, the authors do not indicate anywhere that they consider this to be a truly important point in an actual identification process. In some sense, [33] addresses the same issue, though low sensitivity and noise rejection are connected here instead of high sensitivity (high identifiability) and parameter estimation or identification. Also, from the other direction, a connection between parameter estimate convergence and controllability is examined in [93].

Finally, parameter sensitivity and identification are connected in the context of circuit testing [14]. An often used technique in circuit testing uses identification algorithms to identify the circuit under test from input/output data (which is often the only data to which the tester has ready access, e.g. in the case of integrated circuits). If the identified parameters are out of a specified range, then the circuit is rejected. In this examination, circuit parameters with high sensitivity are shown to be easy to identify. No proofs are given, yet the provided simulations back up the latter claim. A caution is in order here -- a quick jump to the reverse assumption should not be made. Parameters

which are easy to identify are not necessarily highly sensitive. As shown later, other factors enter in which affect the convergence rates for any particular parameter.

2.2.3 Numerical Stability of Structures

As further indication of a need for model structure choice in an identification procedure, the researcher is cautioned [120] against blindly choosing canonical structures (such as a direct II or controllable canonic form) for identification as these parameterizations are quite often a poor choice when numerical aspects are considered. Too often, the latter parameterizations are chosen for convenience of notation, with little or no thought of computational consequences [120]. In essence, the claim is that almost all near-term advances in identification methods will consist of improving the numerical accuracy of already defined identification algorithms; a fine tuning if you will. This then is exactly what we consider in this dissertation -- choosing the structure of the model to help improve the numerical behavior of the identification algorithm by hastening parameter convergence without sacrificing estimate accuracy.

2.3 Parameter Sensitivity and Optimal Input Design

Optimal input design for identification purposes is an idea that has been around since 1960 [106]. Essentially, the idea here is to determine an input so as to most efficiently excite (and therefore make most determinable) the system parameters. The notion of input design is also considered in [55,76] among many excellent texts. Optimal inputs are designed so that the sensitivity of the state variables to the unknown system parameters is maximized. It can be shown that the sensitivity of the parameter estimates to observation noise tends to be lowered for these optimal inputs [56]. This means that the optimal inputs must maximize the parameter sensitivity

as defined in equation (2.1.1) since the parameter estimates must not respond very much to noisy measurements. A way to look at it is this: If the estimated parameters possess a low sensitivity, they would actually have to change quite a lot to accommodate even relatively small fluctuations in the measurements. On the other hand, if the estimated parameters possess a high sensitivity, then relatively large fluctuations in the measurements would correspond to only minor parameter adjustments.

The design of optimal input signals entails the use of the system parameter correlation matrix R and its inverse, $F \equiv R^{-1}$, the Fisher information matrix. Under Gaussian assumptions (i.e. when the impulse response measurements are corrupted by additive independent Gaussian random variables with zero mean and unit variance), the ijth element of F is [118]:

$$f_{ij} = \sum_{k=1}^{N} \frac{\partial h_k}{\partial \gamma_i} \frac{\partial h_k}{\partial \gamma_j} \qquad i,j = 1, \ldots, NP \tag{2.3.1}$$

In the limiting case (as $N \to \infty$), we have [23]

$$f_{ij} = \frac{1}{2\pi j} \oint \frac{\partial H(z)}{\partial \gamma_i} \frac{\partial H(z^{-1})}{\partial \gamma_j} \frac{dz}{z} \qquad i,j = 1, \ldots, NP \tag{2.3.2}$$

A comparison of equations (2.3.2) and (2.1.1) shows that

$$S = \mathrm{tr}(F) \tag{2.3.3}$$

Also, by comparing equation (2.3.2) with equation (2.1.7), one can see that F has the form of a Grammian which includes all the system parameters γ_i (as opposed to the controllability grammian K which only includes the output vector C parameters or the observability grammian W which only includes the input vector B parameters.

If an efficient parameter estimator is used to estimate the NP system parameters, then three suitable measures of the optimality of the designed input are [106]:

1. $\mathrm{tr}(F) = \sum_{i=1}^{NP} \lambda_i(F) = \sum_{i=1}^{NP} \lambda_i(R^{-1})$

2. $\mathrm{Det}(F) = \prod_{i=1}^{NP} \lambda_i(F) = \prod_{i=1}^{NP} \lambda_i(R^{-1})$

3. $\mathrm{tr}(WR) = \sum_{i=1}^{NP} \lambda_i(WR) = \sum_{i=1}^{NP} \lambda_i(WF^{-1})$

where W is a nonnegative definite matrix and λ_i are the eigenvalues of the argumented matrix. Det(•) is the matrix determinant. Since the input is optimized, and the object is to identify the system parameters, the maximum amount of information in the system is desired. Thus, items 1 and 2 above are maximized, while item 3 is minimized. The information matrix F will be very important to later discussions.

The optimization of inputs for parameter identification purposes assumes that inputs can be assigned in a rather flexible way. This is a problem under many operational conditions where the inputs cannot be arbitrarily assigned. Another such situation (in a signal processing context) arises when the input cannot be observed (stochastic modeling). Many control systems do not have input flexibility either, as too much control variation would result, or too much input (control) energy would be used.

The design of the input signal best suited for identification entails determining the input which maximizes the gradient of the identification criterion near the solution [76]: "In general terms, we may say that the objective of experiment design is to choose an input that enhances interesting parameters and parameter combinations." Since the gradient should be steep near the stationary solution (zero gradient) point, the Fisher information matrix should also be large as shown later. The idea that an unidentifiable system has a Fisher information matrix with rank less than 2n is also noted here. Note that in item 2 above, if F is singular, Det(F) will be zero (which is not very large!).

An alternative approach is to consider the particular parameterization as variable (i.e. vary the system structure), and to leave the input alone. This situation is the dual to input optimization, and in fact is exactly the subject of the present investigation. In relation to the optimal input design problem, one is now required to pick a structure which requires low information (from the preset and not-optimal input signal) to accurately determine the system parameters in the chosen structure. Thus, a highly sensitive model structure needs to be chosen. In this dual problem then, the parameterization (structure) is chosen so that the maximum available amount of information is used to determine the parameters of the true system. The improvement of this dual approach over the optimal input design approach is that only the model is affected, and not the system itself. The model is affected by varying the internal structure (clearly the external input/output structure of the model is fixed by the input/output measurements of the true system). Note also that maximizing the system sensitivity increases the identifiability and controllability of the system, as can be seen from equations (2.1.9) and (2.1.8). This latter point will be more thoroughly examined in Chapter 4.

2.4 Convergence and Consistency of Recursive Least-Squares Algorithms

This sub-section begins with a brief discussion of convergence theory for identification algorithms. At this time, three basic approaches for convergence proofs of stochastic identification algorithms have been proposed [76]:

1. Associate a deterministic differential equation with the identification equations (Lyapunov Theory)
2. Martingale Theory (stochastic differential equations)

3. Summed Regression

Item 3 above has been used successfully in only special cases, none of which apply to the current problem under study. Thus, we look at the first two cases only. Later, in Chapters 4, 5 and 6, some details are provided which connect items 1 and 2 above, along with optimal input design, to the sensitivity S. These connections provide insight into the problem under study, and lead to significant results.

2.4.1 Lyapunov Theory Approach

Using Lyapunov theory, asymptotic exponential convergence of many identification algorithms can be shown (among very many [2,37,54,59]). Further, necessary (and sometimes sufficient) conditions can be derived relating input richness and parameter identification. An important fact [54] is that even with persistent (rich) input, any identification algorithm should incorporate data forgetting so that the identification algorithm never "goes to sleep". This point is considered later when a practical situation is at hand. The inherent problem with Lyapunov Theory comes directly from the asymptotic nature of the results which it provides. While these asymptotic results do directly indicate convergence (and exponential convergence at that), the interest here is at least as much in the transient convergence response. Since Lyapunov theory does not directly help with this point, item 2 above becomes very important. However, we will show later that the associated deterministic equations indicate useful data about the Fisher matrix.

2.4.2 Martingale Theory Approach

Another approach used in determining the convergence of parameter estimates comes from Martingale theory (the study of stochastic differential equations). Using this method, convergence

of the least-squares identification algorithm is studied in [15,16]. These results are used in the optimal adaptive control area [17,18,27]. The authors show that least-squares and stochastic gradient identification schemes consistently (in a probabilistic sense) converge asymptotically at an exponential rate if the eigenvalue spread of the approximation to the parameter correlation matrix R is not too great. As R is a positive definite symmetric matrix, the eigenvalue spread of $F = R^{-1}$ is exactly equal to the eigenvalue spread of R. The actual rate of exponential convergence is shown to depend inversely on the spread, i.e. the closer the minimum and maximum eigenvalues of R (or F) are to each other, the faster the convergence [16]. The ratio of maximum-to-minimum eigenvalue of R is also strongly tied to the idea of persistent excitation [59,74,84,109]. This notion of eigenvalue spread has an important meaning in the context of the information matrix F -- the structure should be required to have balanced information. In other words, if the chosen parameterization is skewed so that the information about 1 parameter is greatly increased (at the expense of the remaining parameters), then the identification procedure will typically converge much slower than would otherwise be the case. This is the same notion quoted in the optimal input design section (from [76]). The idea of balanced parameter information is strongly connected to the optimal input design goal of a large sensitivity, and this dissertation explores the connection thoroughly.

2.5 *Identifier Algorithm Robustness to Noise Outliers*

This research area is relatively old in the sense [76] that many identification algorithms have been proposed which alleviate problems due to probability densities being something other than the standard, often-designed-for Gaussian density. For example, it is well known that a standard least-squares identifier is biased in the presence of additive noise which is not Gaussian. The instrumental-variables approach eliminates this bias. However, recent work has been concentrated in two areas, which are now discussed briefly.

2.5.1 Insensitive Parameterizations

Since we often want to estimate a parametric model not for the identified parameters themselves, but for some combination of the parameters (e.g. pole frequencies), an identification model whose parameter sensitivity is low is desirable, since the desired parameter will not change very much as long as the identified parameters are "close" to the true values [45,86,89,97,112]. This is an often used, but not proven, heuristic. Insensitive parameterizations are good for noise rejection in the sense that a wrong parameter estimate will describe a model which is still close to the true system. Thus noise outliers affect identification schemes using these parameterizations less than other, more sensitive, parameterizations. It remains to be seen whether these low sensitivity parameterizations are good for fast, initial parameter convergence.

Using this heuristic, much work has been done in developing non-recursive identification algorithms [31,32,46,47,80,101] using a particularly insensitive parameterization: the balanced realization introduced in [83]. The balanced state-space form meets the necessary conditions given in [87] for minimum round-off noise filters, and was shown in [98] to actually exhibit low sensitivity. Also, as observability and controllability measures are balanced, the parameter information is also well-balanced. Further, the connection between minimum round-off noise and minimum sensitivity filters has been thoroughly explored [51,77,98,115,116]. The natural question is: Are these researchers justified in spending so much time and effort developing identification algorithms based on a model which may or may not be optimally suited for good, fast identification? Well, the answer may be "yes", but for reasons other than those related to robustness issues. Consider this (admittedly) heuristic argument: The parameter information matrix (and consequently the correlation matrix) has the characteristics of the system grammians. These grammians are "balanced", and so the ratio of maximum-to-minimum eigenvalue of these matrices is low (close to 1). From the Martingale theory in the previous sub-section, one might expect fast convergence. However, from the optimal input design method, one might expect slow convergence since the

balanced coordinate system is insensitive (minimum sensitivity) to its parameters. Which structural property dominates will be considered later.

2.5.2 Statistical Improvements

As for statistical improvements, the design choice in these algorithms is to optimally adjust a data weighting factor to account for noise outliers [95,96]. Here, the idea is that the noise outliers cause the error between the true system output and the identified system output to be a non-Gaussian sequence. Since the choice of data weighting factor is often made arbitrarily, the freedom exists to choose it so that wide variations in output are rejected via scaling with a low weight. This scaling is an alternative to using other norm measurements such as a 1-norm scaling in a median filtering context. Of course, the arbitrary weighting slows convergence since some data are discarded, but the resulting parameter estimates are less sensitive to noise outliers. The data weighting factor is also often used to "forget" past data when the identifier is tracking slowly varying non-stationary processes.

In a least-squares problem, a weight of zero means that there is absolutely no confidence in a measurement sample, and so the equation is discarded (not used). A weight of 1 indicates complete measurement confidence, and so the resulting equation is used to estimate the parameters. Weights between 0 and 1 indicate the relative reliability of the measurement. The implementation is simple, and so it could be incorporated in conjunction with an optimal structure for faster, more reliable convergence.

2.6 *Partial Realization*

Partial realization (stochastic partial realization) entails the use of an initial, partial set of an infinite sequence of impulse (covariance) values. Two different approaches have been proposed to solve the problem; one off-line (and so non-recursive) and the other on-line (and recursive). The off-line method is matrix based and thus not applicable to real time implementation at this time, and consists of eigen- or singular-value decompositions of a Hankel-type matrix. Real time use of these methods will require fast algorithms for these decompositions which take the matrix structure into account. Systolic (or wave-front) arrays or some other parallel computer architecture may also help move these algorithms into real time use. We look at a particular on-line (recursive) method, and so will defer the details until Chapter 3. A recent collection of papers in this area is [30]. This text provides a good survey of the modeling/identification areas.

2.6.1 Ho-Kalman (type) Algorithms

These algorithms were initially a noiseless identifier (PR) based on a singular value decomposition of the system Hankel matrix [43,57,62-67,81,82,100,110]. Gradually (from naively at first to sophisticated later), the algorithms were altered to improve the estimates in the noisy case (APR) [20,21,44]. Variations to the Hankel matrix, and the adoption of balanced state-space coordinates helped reduce the effects of noise. An estimate for the system order can be determined in a straightforward manner from the rank of the Hankel matrix or its variation and so these methods have application to reduced order modeling. An important concept to note here is that since these methods involve decomposing the Hankel matrix, a rigid trapezoidal "weighting" is imposed on the sequence elements used in the partial realization. This weighting has an undesirable effect on the high and low frequency components of the estimated system since the first and last few measurements do not appear in the Hankel matrix as often as the middle measurements! The

appearance of these measurements in the Hankel matrix has the effect of rigidly locking a trapezoidal weighting function on the measured data.

One also needs to recognize that a canonical state-space representation arises in the context of partial realizations, namely the dual generalized Hessenberg representation [68]. The connection flows out of [42,57]. This canonical representation has usefulness in reduced order modeling [69-71] as well as a strong connection with controllability and observability [72,73]. Due to its connection to the partial realization problem and its parameter sensitivities, this structure will be examined in detail later.

2.6.2 Recursive Algorithms

On the other hand, recursive algorithms have been around much longer, and are specifically designed for the fast implementation required in real time processing. Also, these algorithms have great flexibility in the choice of the data weighting factor (in fact, as discussed above, one idea for minimizing the effects of noise is based on the adjustment of these weights). The recursive methods have the ability to handle noisy data in a more appropriate manner than the Ho-Kalman type matrix methods given above. In particular, the Recursive Prediction Error Method will be examined in Chapter 3. Related papers include [5-8,11,79,88,119]. These papers discuss recursive algorithms as they are used in robust identification.

3.0 The Structure-Dependent Output Error Identification Algorithms

This section presents a general recursive prediction (output) error method (RPEM) algorithm for identification, and then considers some global convergence issues of the RPEM on ARMA models. Alternative algorithmic computational implementations are included for later use. The direct formulations necessary for this research are made and the exact identification algorithms as used in [25] are presented. A confirmation that the subject of investigation is worthwhile is given next under the title "Why Use Recursive Prediction Error Methods?" (and not some other kind of partial realization algorithm). Some discussion and results which answer this question are included.

3.1 RPEM for System Identification from Impulse Response Data

In this section, a gradient algorithm [5,6,76] is discussed which is suitable for identifying the system parameters of a stable, but otherwise arbitrary, state-space structure from either a (noisy) impulse response measurement or a set of (noisy) impulse response measurements. These two measurement requirements actually determine which of the two different algorithms will be implemented. Denote as **deterministic** the algorithms which use only a single set of measurements. The implementation of these algorithms is discussed in Chapter 5. Those algorithms which use many sets (or realizations) of measurement data are termed **stochastic**, and are discussed in Chapter 6. A numerically superior algorithm is also given. The equations required for specific implementation in identifying the Direct Form II (DII), the Parallel (PRLL) and the dual generalized Hessenberg representation (DGHR) forms respectively are given later in this Chapter. First, define:

1. y_n, the noisy impulse response measurements at time n
2. $h_n(\Theta)$, the impulse response at time n corresponding to parameterization Θ
3. w_n, a positive weight at time n $(0 < w_n \leq 1)$
4. $e_n \equiv y_n - h_n(\Theta)$, the impulse response error at time n
5. the error criterion:

$$J_N = \frac{1}{2} \sum_{n=0}^{N} w_n e_n^2$$

6. Θ_n, the vector of identified parameters at time n
7. Φ_n, the vector of parameter gradients at time n (also called the "information vector" [102])

Noting that

$$h_n(\Theta) = \frac{1}{2\pi j} \oint H(z;\Theta) z^n \frac{dz}{z}$$

(assuming stable causal systems) we have the following Gauss-Newton algorithm [76]:

Algorithm (A.1)

1. $\Theta_k = \Theta_{k-1} + L_k[y_k - h_k(\Theta_{k-1})] \equiv \Theta_{k-1} + L_k e_k$

2. $L_k = \dfrac{P_{k-1}\Phi_k}{\Phi'_k P_{k-1}\Phi_k + \dfrac{1}{w_k}}$

3. $P_k = P_{k-1} - \dfrac{P_{k-1}\Phi_k\Phi'_k P_{k-1}}{\Phi'_k P_{k-1}\Phi_k + \dfrac{1}{w_k}}$

4. $\Phi_k = \dfrac{\partial h_k(\Theta_{k-1})}{\partial\Theta} = \dfrac{1}{2\pi j}\oint \dfrac{\partial H(z;\Theta_{k-1})}{\partial\Theta} z^k \dfrac{dz}{z}$

The integration

$$r_l = \frac{1}{2\pi j}\oint H(z)G(z^{-1})z^l \frac{dz}{z} \tag{3.1.1}$$

can be determined efficiently and in closed form [10,23,26] by recognizing it as an ARMA cross covariance. Thus the needed gradients (4 above) can be computed easily.

Alternatively, the gradients can be computed by running partial derivative systems driven by impulse functions, since they are just the k^{th} sample of the corresponding impulse response. Computing the gradients in this manner has the advantage of using the identified parameter vector Θ_k directly (as opposed to the indirect manner required by equation (3.1.1)). However, this numerical accuracy is counterbalanced by the fact that computing the gradients from equation (3.1.1) has a speed advantage. This method is also general enough that it can be easily used in implementing an identification scheme from covariance information [5].

Under Gaussian assumptions, the Hessian is equal to F, and the estimate of the Hessian P_k^{-1} is thus an approximation to the Fisher information matrix F [76,103]. Recall that the Martingale convergence results, referred to at the end of Chapter 2, are based on the Fisher information matrix. As shown in a Chapter 6, F appears in Lyapunov convergence theory as well. The second

derivative information (contained in the Hessian) is important to understanding and explaining the algorithm convergence performance.

Now consider another numerical aspect of the above algorithm. In Algorithm (A.1) above, a straightforward manner for computing both the gain vector L_k and the Hessian approximation P is given in steps 2 and 3. In practice however, these equations may not define the best procedure numerically. To improve numerical performance, a factorization of the P matrix is carried along instead -- the components of the factorization are then updated [76]. The most commonly used such factorization is the Cholesky factorization of P, so that $P = QQ'$. The matrix Q is termed the square root of P, and the new algorithm is due to Potter [76]. Since Q is the square root of P, computations involving it will have twice the precision of those involving P. Another advantage of updating Q is that P is guaranteed to be nonnegative definite (since it is the square of the updated Q). Note that in Algorithm (A.1), there is no check on the definiteness of P! As shown later in the example sections, the improvement afforded by this factorization of P may be necessary. This algorithm requires, however, slightly more computations than Algorithm (A.1). The square root version of the algorithm then becomes:

Algorithm (A.2)

1. $\Theta_k = \Theta_{k-1} + G_k[y_k - h_k(\Theta_{k-1})] \dfrac{1}{\sqrt{w_k}} \equiv \Theta_{k-1} + G_k \dfrac{e_k}{\sqrt{w_k}}$
2. $f_k = Q'_{k-1}\Phi_k$
3. $\beta_k = w_k + f'_k f_k$
4. $\alpha_k = \dfrac{1}{\beta_k + \sqrt{\beta_k w_k}}$
5. $G_k = Q_{k-1} f_k$
6. $Q_k = Q_{k-1} - \alpha_k G_k f'_k$
7. $\Phi_k = \dfrac{\partial h_k(\Theta_{k-1})}{\partial \Theta} = \dfrac{1}{2\pi j} \oint \dfrac{\partial H(z; \Theta_{k-1})}{\partial \Theta} z^k \dfrac{dz}{z}$

The algorithm is simplified somewhat when the weighting factor w_n is 1 for all time samples n. Also, the G_k vector is a just the old gain vector L_k normalized by the scalar β_k. Another popular

factorization is the U-D factorization (or Square-Root free Cholesky factorization) where the matrix P is factored into $P = UDU'$. U is an upper-triangular matrix and D is diagonal (thus the square-root free, as the $\sqrt{d_{ii}}$ is not needed to pull D apart to form the Q matrix in Algorithm (A.2)). This factorization is due to Bierman, and the update algorithm is provided in [76] also. Its complexity is roughly the same as for the Potter square root algorithm (Algorithm (A.2)).

3.2 *Global Convergence Issues of ARMA Models*

As with most nonlinear estimators, convergence of the estimates to the global minimum is not always guaranteed [113,114]. Local minima may exist which can trap the estimates away from the global minimum. A fact that is not universally known (or accepted) is that the optimization criterion J_N may have local minima for a standard ARMA model [34,108]. These 2 latter papers provide examples which violate the Stearns Conjecture [111]: "If the input excitation is a white process and if the adaptive filter has a sufficiently high order with respect to the unknown linear system, then the error surface will have no local minima." A sufficient condition for validity is that the degree of the numerator plus 1 must be greater than or equal to the denominator degree. In fact, it can be shown [103] that no local minima exist if:

1. the model set encompasses the true system
2. the input is a white-noise sequence, and
3. the order of the model numerator exceeds that of the denominator of the unknown system

Note that both the Stearns Conjecture and the above require white-noise input, a condition not present in the investigated problem.

One other important point about convergence that needs to be addressed is whether the different structures (describing the same system) have different global and local minima. One would

assume that the global minima are unchanged since the optimization criterion J_N depends only on the impulse response and the measurements -- and while the parameters are different for the different structures, the impulse response is not. To examine the question of the creation (or deletion) of locations in parameter space which have gradient = 0, a more detailed analytic proof of the global minima is required (based on ideas presented in [90,103]). Consider two canonical structures, $S^{(1)}$ and $S^{(2)}$ with parameterizations $\theta^{(1)}$ and $\theta^{(2)}$ respectively, each parameter vector an element of R^n (i.e. each is an (nx1) vector). There is a continuous mapping f from $\theta^{(1)}$ onto $\theta^{(2)}$ [90]. Thus, f maps a vector $\theta^{(1)}$ in R^n to a vector $\theta^{(2)}$ also in R^n . At a point of ***equivalency***, the 2 parameterizations describe the same system with respect to the optimization criterion J_N, i.e.

$$J_N(\theta^{(1)}) = J_N(\theta^{(2)})$$

Note that this merely implies that the impulse response of structure $S^{(1)}$ is equal to that of $S^{(2)}$, at least for the first N samples. An alternative way to view equivalency is that $\theta^{(1)}$ and $\theta^{(2)}$ are equivalent with respect to J_N if they are different parameterizations of the same system.

If f is differentiable (the partial derivatives of f are continuous) then by the chain rule,

$$\frac{\partial J_N(\theta^{(1)})}{\partial \theta^{(1)}} = \frac{\partial J_N(\theta^{(2)})}{\partial \theta^{(1)}} \quad \text{by equivalency}$$

$$= \frac{\partial \theta^{(2)}}{\partial \theta^{(1)}} \; \frac{\partial J_N(\theta^{(2)})}{\partial \theta^{(2)}}$$

The partial derivatives of J_N are (nx1) vectors (in fact the gradient Φ), and the Jacobian of the mapping f is (nxn). Clearly then, a stationary point of $J_N(\theta_+^{(2)}) = 0$ implies that $\theta_+^{(1)} = f(\theta_+^{(2)})$ is also a stationary point, i.e.

$$\frac{\partial J_N(\theta^{(2)})}{\partial \theta^{(2)}} \Big|_{\theta_+^{(2)}} = 0 \rightarrow \frac{\partial J_N(\theta^{(1)})}{\partial \theta^{(1)}} \Big|_{\theta_+^{(1)}} = 0$$

The second derivatives are quadratically related (positively) to each other, and so the points are analogous -- a minimum for one structure is also a minimum for the second structure, and similarly

for any maxima. Thus, a minimum of structure $S^{(2)}$ is also a minimum of structure $S^{(1)}$. The solution $\theta_*^{(1)}$ exists since f is onto.

Now, suppose that $\theta_*^{(1)}$ is a solution so that $J_N(\theta_*^{(1)}) = 0$. If f is differentiable, then $J_N(\theta_*^{(2)}) = 0$ and minimums of structure $S^{(1)}$ are also minimums of $S^{(2)}$. However, if f is not differentiable, then the chain rule does not hold and a point $\theta_*^{(2)}$ such that $J_N(\theta_*^{(2)}) = 0$ may not imply that $J_N(\theta_*^{(1)}) = 0$. Thus, the function f cannot be differentiable at any newly formed stationary point of $J_N(\theta^{(2)})$. Because f is continuous and onto, any of these newly formed stationary points must be saddles [90]. The implications of these statements are simple: Changing the structure does not change the global minimum, and any new stationary points are unstable saddle points. Thus, if the DII structure will converge, the PRLL and DGHR structures will also converge if inexact arithmetic is used (so that the identifier is not caught on a saddle).

We need to keep this convergence problem (global vs. local) in mind, although it apparently does not matter in a great many identification processes. Some examples are shown in later chapters which will help clarify this statement. Note that in the deterministic algorithms where the same noisy impulse response record is used repeatedly, convergence is to that set of system parameters which represents minimization of J_N [74]. In the presence of Gaussian noise, the convergence of the stochastic algorithms is to the true parameters [76] since the noise is averaged out.

3.3 The Use of Recursive Prediction Error Methods over Off-Line Methods

In general, one may be inclined to ask why one should even consider recursive prediction error methods when off-line methods based on the Ho-Kalman Algorithm yield adequate results. One reason is that the off-line methods do not handle noisy measurements well [21]. Secondly, the

off-line matrix methods are more susceptible to numerical noise, with possibly disastrous results for the more interesting, ill-conditioned problems. "In an off-line situation it might consequently be a good idea to pass the data through the recursive algorithm a couple of times [to improve the numerical accuracy of the result]" [75]. As noted in the experiments, many of the SVD-type algorithms do not handle measurement noise well, as the algorithms are adaptations of perfect (no-noise) theoretical arguments [21]. Also, again as previously noted, the Hankel matrix fixes some strict weighting on the data, a limitation that the recursive algorithms do not have (in fact, the w_n is left arbitrary within (0,1]). Also, the amount of computation may be of importance, as the recursive methods have a fixed required effort per iteration, while the off-line methods based on eigen- or singular-value decompositions are of necessity iterative in nature, with an indeterminate computation time until any results become available.

3.4 The Parameterization Structures Under Study

In particular, three SISO structures are examined: the direct II (DII), the parallel (PRLL) and the dual generalized Hessenberg representations (DGHR). The identification method used is derived from [6]. The direct II parameters are simply the commonly identified ARMA parameters and this system structure is typically very sensitive to these parameters. The parallel form was chosen for its simple structure (2^{nd}-order direct II sub-filters) and it is typically insensitive to its parameters. The DGHR structure is connected to continued fractions [57], and it exhibits both input and output structure in its state matrix [69]. Since all the pole/zero information resides in the DGHR state matrix, this form can be particularly useful in reduced order modeling based on partial realizations [42,57,100]. We have also observed that the DGHR structure parameter sensitivity varies widely [24]. A more detailed description of the structures, and their attendant Θ and Φ is given next.

3.4.1 The Direct II Structure

3.4.1.1 The DII Parameterization

In the Direct II form the identified parameters are the difference equation parameters. Thus, we have the system

$$H(z) = \frac{b_1 z^{-1} + b_2 z^{-2} + \cdots + b_m z^{-m}}{1 + a_1 z^{-1} + a_2 z^{-2} + \cdots + a_n z^{-n}} \equiv \frac{B(z)}{A(z)} \tag{3.4.1}$$

The difference equation parameters appear directly in state-space, with the a_i's in the state matrix and the b_i's in the output vector. Since the state-space form of the Direct II structure provides no insight into the problem at hand, it will not be included here.

3.4.1.2 The DII Identification Algorithm

For the Direct II model, defining the parameter vector from equation (3.4.1) as

$$\Theta_t = [a_1 \quad a_2 \quad \cdots \quad a_n \quad b_1 \quad b_2 \quad \cdots \quad b_m]'$$

the gradient $\Phi_t(k)$ can be evaluated from

1. For $1 \le k \le n$

$$\Phi_t(k) = \frac{-1}{2\pi j} \oint \frac{B(z) z^{t-k}}{A^2(z)} \frac{dz}{z}$$

2. For $n+1 \le n+k \le n+m$

$$\Phi_t(n+k) = \frac{1}{2\pi j} \oint \frac{z^{t-k}}{A(z)} \frac{dz}{z}$$

Note that these equations are actually inverse z-transform computations.

Alternatively, the gradients are:

1. For $1 \leq k \leq n$

$$\Phi_t(k) = h_{t-k} \text{ of the system } -\frac{B(z)}{A^2(z)}$$

2. For $n+1 \leq n+k \leq n+m$

$$\Phi_t(n+k) = h_{t-k} \text{ of the system } \frac{1}{A(z)}$$

These impulse response values can be directly computed by running the difference equation, or in fact by any other equivalent parameterization (with proper combinations)![2]

3.4.2 The Parallel Structure

3.4.2.1 The PRLL Parameterization

The PRLL structure consists of 2^{nd}-order DII sub-filters, i.e.

$$H(z) = \sum_{i=1}^{p} \frac{\xi_{i1} z^{-1} + \xi_{i2} z^{-2}}{1 - \nu_{i1} z^{-1} - \nu_{i2} z^{-2}} \tag{3.4.2}$$

In state-space, we write

[2] The notation "h_{t-k} of the system" means that the difference equation of the system given by the transfer function or state-space triple {A,b,c} is run with input δ_n to compute the impulse response h_{t-k}

$$x_{k+1} = \begin{bmatrix} A_1 & 0 & & 0 \\ 0 & A_2 & & 0 \\ 0 & 0 & & 0 \\ \cdot & \cdot & & \cdot \\ \cdot & \cdot & \cdots & \cdot \\ \cdot & \cdot & & \cdot \\ 0 & 0 & & 0 \\ 0 & 0 & & A_p \end{bmatrix} x_k + \begin{bmatrix} B_1 \\ B_2 \\ B_3 \\ \cdot \\ \cdot \\ \cdot \\ B_{p-1} \\ B_p \end{bmatrix} u_k \equiv F_{//} x_k + G_{//} u_k \quad (3.4.3)$$

$$y_k = \begin{bmatrix} C_1 & C_2 & \cdots & C_p \end{bmatrix} x_k \equiv H_{//} x_k$$

where the triple $\{A_i, B_i, C_i\}$ for $i = 1, \ldots, p$ is the 2^{nd}-order DII implementation of the i^{th} partial fraction, i.e.

$$A_i = \begin{bmatrix} 0 & 1 \\ \nu_{i2} & \nu_{i1} \end{bmatrix} \qquad B_i = \begin{bmatrix} 0 \\ 1 \end{bmatrix} \qquad C_i = \begin{bmatrix} \xi_{i2} & \xi_{i1} \end{bmatrix}$$

p is the largest integer so that $p \leq \frac{n+1}{2}$. If n is odd, then the 1^{st}-order subfilter is assigned to the p^{th} partial fraction.

3.4.2.2 The PRLL Identification Algorithm

Define the parameter vector from equation (3.4.3) as

$$\Theta_t = \begin{bmatrix} \nu_{12} & \nu_{11} & \cdots & \nu_{p-1,2} & \nu_{p-1,1} & \{\nu_{p2}\} & \nu_{p1} & \xi_{12} & \xi_{11} & \cdots & \xi_{p-1,2} & \xi_{p-1,1} & \{\xi_{p2}\} & \xi_{p1} \end{bmatrix}'$$

where $\{\cdot\}$ are only included if the system order is even. Let ki be the largest integer such that $ki \leq \frac{k+1}{2}$. Then the gradient is:

1. For $1 \leq k \leq n$, n even, or for $1 \leq k \leq n-1$, n odd

$$\Phi_t(k) = \frac{1}{2\pi j} \oint H_{//}(zI - F_{//})^{-1} 1_{ki} 1_k'(zI - F_{//})^{-1} G_{//} z^t \frac{dz}{z}$$

2. If n odd

$$\Phi_t(n) = \frac{1}{2\pi j} \oint H_{//}(zI - F_{//})^{-1} 1_n 1_n'(zI - F_{//})^{-1} G_{//} z^t \frac{dz}{z}$$

3. For $n + 1 \leq n + k \leq 2n$

$$\Phi_t(n + k) = \frac{1}{2\pi j} \oint 1'_k(zI - F_{//})^{-1} G_{//} z^t \frac{dz}{z}$$

where again 1_k is the k^{th} Euclidian basis vector. The latter is easily adapted for arbitrary state-space structures [23].

Alternatively, note that from equation (2.1.4) the gradients can be computed as follows:

1. for $n + 1 \leq n + k \leq 2n$

$$\Phi_t(n + k) = h_t \text{ of the system defined by the state-space triple } \{A, b, 1_k\}$$

2. The remaining gradients may be computed by running the cascaded system defined in equation (2.1.5) and shown in Figure 1. The ki and k are appropriate for the above complex integral items. This impulse response may be computed by running the state-space filter

$$x_{k+1} = \begin{bmatrix} F_{//} & 0 \\ G_{//}H_{//} & F_{//} \end{bmatrix} x_k + \begin{bmatrix} 1_{kl} \\ 0 \end{bmatrix} \delta_k$$
$$h_k = [0 \qquad 1'_k] x_k$$

Another way to compute the gradients is to actually form the impulse response from the relationship

$$h_t = c' A^{t-1} b$$

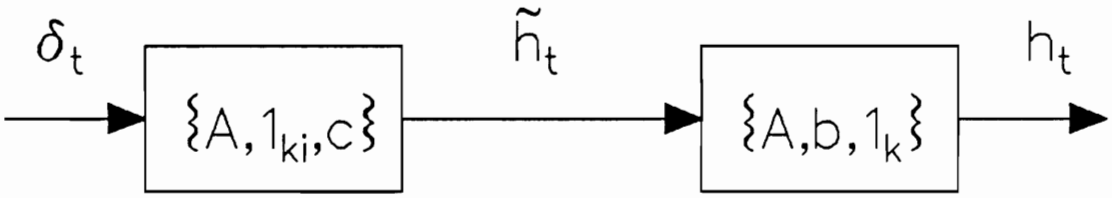

Figure 1. The partial derivative system for state matrix components

The triple {A,b,c} is the state-space formulation which defines the system whose impulse response is h_t. We do not choose to perform the computation this way, but merely note that this procedure could be used.

3.4.3 The Dual Generalized Hessenberg Representation

3.4.3.1 The DGHR Parameterization

The DGHR was noticed in previous work [24] to exhibit high parameter sensitivity for certain system dynamics. A generic [57] SISO system has the state-space representation:

$$x_{k+1} = \begin{bmatrix} \alpha_1 & \gamma_2 & & 0 & 0 \\ 1 & \alpha_2 & & 0 & 0 \\ 0 & 1 & & 0 & 0 \\ \cdot & \cdot & & \cdot & \cdot \\ \cdot & \cdot & \cdots & \cdot & \cdot \\ \cdot & \cdot & & \cdot & \cdot \\ 0 & 0 & & \gamma_{n-1} & 0 \\ 0 & 0 & & \alpha_{n-1} & \gamma_n \\ 0 & 0 & & 1 & \alpha_n \end{bmatrix} x_k + \begin{bmatrix} \gamma_1 \\ 0 \\ 0 \\ \cdot \\ \cdot \\ \cdot \\ 0 \\ 0 \\ 0 \end{bmatrix} u_k \qquad (3.4.4)$$

$$y_k = [1 \quad 0 \quad \cdots \quad 0 \quad 0]x_k$$

-----or-----

$$x_{k+1} \equiv F_D x_k + G_D u_k$$
$$y_k \equiv H_D x_k$$

The zeros of the system can be determined from the state matrix by deleting the first column and row, and then computing the eigenvalues of the resulting (n-1) dimensional matrix. The constant

gain γ_1 has no effect on the system poles or zeros. The DGHR structure is unique in this placement of the pole and zero information.

3.4.3.2 The DGHR Identification Algorithm

Define the parameter vector from equation (3.4.4) as

$$\Theta_t = [\alpha_1 \quad \alpha_2 \quad \cdots \quad \alpha_n \quad \gamma_1 \quad \gamma_2 \quad \cdots \quad \gamma_n]'$$

Then the gradient is:

1. For $1 \le k \le n$

$$\Phi_t(k) = \frac{1}{2\pi j} \oint H_D(zI - F_D)^{-1} 1_k 1'_k (zI - F_D)^{-1} G_D z^t \frac{dz}{z}$$

2. For $k = n + 1$

$$\Phi_t(n+1) = \frac{1}{2\pi j} \oint H_D(zI - F_D)^{-1} 1_1 z^t \frac{dz}{z}$$

3. For $n + 2 \le n + k \le 2n$

$$\Phi_t(n+k) = \frac{1}{2\pi j} \oint H_D(zI - F_D)^{-1} 1_{k-1} 1'_k (zI - F_D)^{-1} G_D z^t \frac{dz}{z}$$

As in the PRLL structure, the gradients can be evaluated by running the corresponding partial derivative systems with an impulse function as input. Then the gradients are found as follows:

1. For $1 \le k \le n$

$$\Phi_t(k) = h_t \text{ of the state-space triple } \left\{ \begin{bmatrix} F_D & 0 \\ G_D H_D & F_D \end{bmatrix}, \begin{bmatrix} 1_k \\ 0 \end{bmatrix}, \begin{bmatrix} 0 \\ 1_k' \end{bmatrix} \right\}$$

2. For $k = n + 1$

$$\Phi_t(k) = h_t \text{ of the triple } \{F_D, 1_1, H_D\}$$

3. For $n + 2 \le n + k \le 2n$

$$\Phi_t(n+k) = h_t \text{ of the triple } \left\{ \begin{bmatrix} F_D & 0 \\ G_D H_D & F_D \end{bmatrix}, \begin{bmatrix} 1_{k-1} \\ 0 \end{bmatrix}, \begin{bmatrix} 0 \\ 1_k' \end{bmatrix} \right\}$$

4.0 The Error Criterion, System Sensitivity and Parameter Information

In this chapter, we first explore the special way in which the error criterion J_N and the system parameter sensitivity are related. This relationship was the starting point to connecting sensitivity to convergence rates [9]. Some very encouraging results suggested the appropriateness of this approach, especially in the initial steps of identification, as we will show in Chapter 6. However, in an attempt to explain behavior after an initial rough convergence has occurred, we need to introduce another structural property. This new property (the conditioning of the parameter set) is introduced, and a measure that combines it with the system sensitivity is proposed. Sensitivity is connected to the steepness of the function J_N, and J_N , near the solution set of parameters, is shown to be quadratic in the Fisher information matrix. Convergence proofs are not provided in this chapter, but rather are given in the appropriate context of examples and discussion in Chapters 5 and 6.

4.1 The Sensitivity-Error Gradient Relationship

Using our previously developed sensitivity (see equation (2.1.1)), the sensitivity of the parameterization with respect to the i^{th} parameter (i.e. $\Theta(i) = \gamma_i$) is [23][3]

$$S(i) = \frac{1}{2\pi j} \oint \left| \frac{\partial H(z)}{\partial \Theta(i)} \right|^2 \frac{dz}{z} = \sum_{n=1}^{\infty} \left| \frac{\partial h_n(\Theta)}{\partial \Theta(i)} \right|^2 \tag{4.1.1}$$

Now, the i^{th} gradient of our cost function J_N is (for $w_n \equiv 1$ for all n)

$$\frac{\partial J_N}{\partial \Theta(i)} = -\sum_{n=1}^{N} (y_n - h_n(\Theta)) \frac{\partial h_n(\Theta)}{\partial \Theta(i)} \tag{4.1.2}$$

As N gets large and the identified system gets "close" to the true system, a Taylor series approximation of y_n about $h_n(\Theta)$ shows that the gradient of the error criterion (equation (4.1.2)) and the sensitivity S(i) (equation (4.1.1)) become positively correlated: a high error gradient for J_N implies high sensitivity and vice versa.

An alternative relationship between the sensitivity and the cost function J_N can be obtained via linear system theory. Consider the output error covariance

$$\sigma_e^2 = \sum_{n=1}^{\infty} e_n^2 \tag{4.1.3}$$

---

[3] The summation index can run from sample 0 if desired. We have only considered the identification of systems with no direct feed through, and so the impulse response at sample 0 is identically 0 since the system has at least one unit-delay.

A quick comparison of equation (4.1.3) and the defining equation of J_N (5. in Chapter 3) shows that for $w_n = 1$ and neglecting the ½ term, J_N is a finite approximation to σ_e^2! For small parameter variations (i.e. when the estimated parameters are close to the true parameters), S defines a linear lower bound to σ_e^2 [52]

$$\sigma_0^2 S \leq \sigma_e^2$$

where σ_0^2 is a constant.

In fact, this leads to an alternative form for the optimization criterion (see Figure 2)

$$J_N = \frac{1}{2}\frac{1}{2\pi}\int_{-\pi}^{\pi}\left[\left[H(e^{jw}) - \hat{H}(e^{jw})\right]\otimes F(e^{jw})\right]\left[\left[H(e^{-jw}) - \hat{H}(e^{-jw})\right]\otimes F(e^{-jw})\right]dw$$

where H is the transfer function of the true system and $\hat{H}$ is the transfer function of the model. Also, $F(e^{jw})$ is the Fourier-transform of the sequence $f_n = u_{N-n}u_n$ and u_n is the unit step sequence ($u_n = 1$ if $n \geq 0$ and is zero elsewhere). The symbol $\otimes$ denotes periodic convolution. This characterization of J_N may prove useful in digital filter design.

In order to provide some physical support for the above statement connecting the sensitivity S and the optimization criterion J_N, 7 example systems are introduced. The pole/zero specifications are given in Table 1. These systems are all 3rd-order except for the last two which are 4th-order; 3 are low-pass, 1 is high-pass, the next 2 are band-pass, and the last system does not fall into any category. This last system [104] will be discussed extensively in Chapter 7. All of the systems have a zero at $+\infty$.

For the LP2 DGHR system, the behavior of the error criterion vs. the normalized parameter deviation of the LP2 DGHR system one parameter at a time (keeping all other parameters at their true value) is shown in Figure 3 and Figure 4. Note the ERROR scale differences between the 2 figures. The steepness of J_N (i.e. the gradient) is seen to be related to the parameter sensitivity. In Figure 3, the error depends on the first 10 samples of the impulse response, while in Figure 4, the error depends on the first 25. Comparing the sensitivities and the corresponding error curves, one

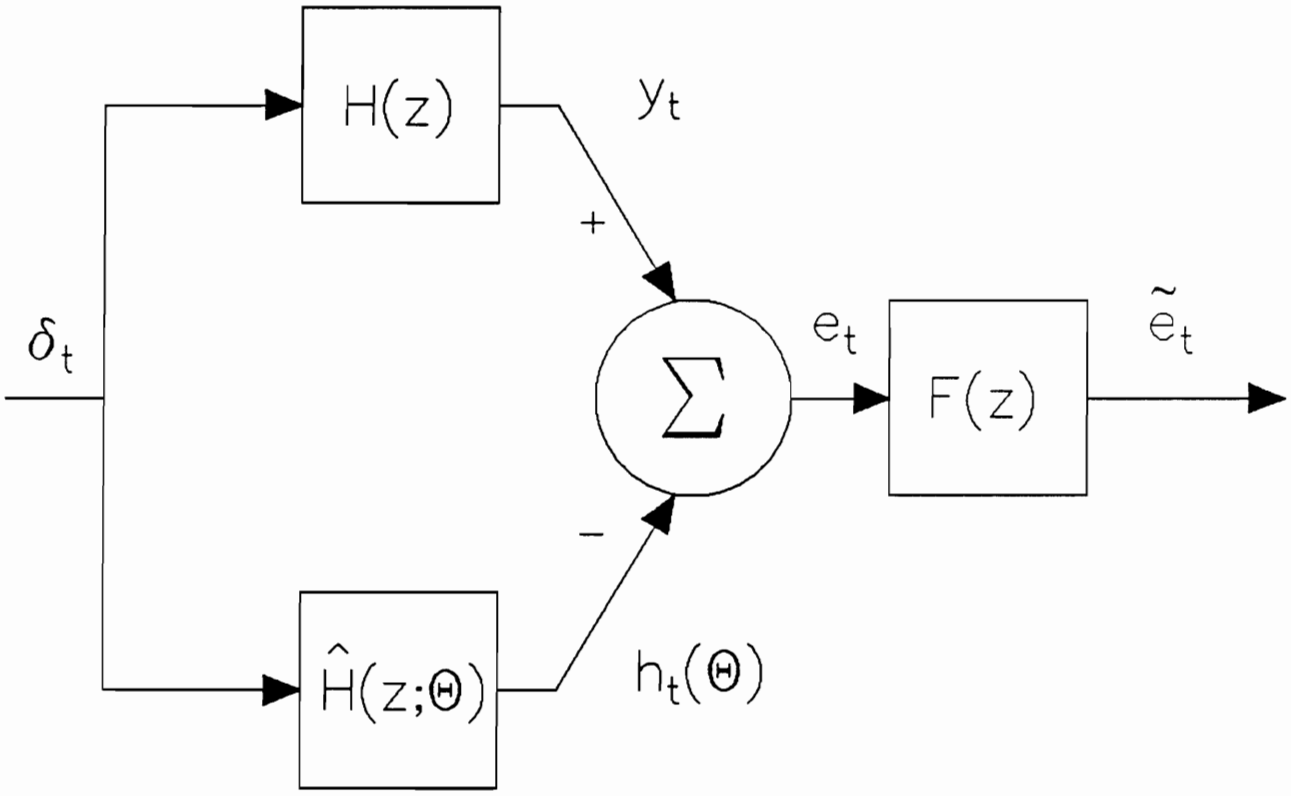

Figure 2. Block Diagram Relating J and Output Error Power

Table 1. The systems under examination

	Zeros	Poles	
LP1	$0.5^{\pm j\frac{\pi}{3}}$	$0.707^{\pm j\frac{\pi}{2.6}}$	0.5
LP2	$0.925^{\pm j\frac{\pi}{6}}$	$0.95^{\pm j\frac{\pi}{9}}$	0.9
LP3	$0.85^{\pm j\frac{\pi}{3}}$	$0.8^{\pm j\frac{\pi}{4}}$	0.7
HP1	$0.95^{\pm j\frac{\pi}{2}}$	$0.8^{\pm j0.8\pi}$	-0.5
BP1	± 1	$0.825^{\pm j}$	0.2
BP2	$0.8,\ 0.55^{\pm j0.375\pi}$	$0.7^{\pm j\frac{\pi}{3}}$	$0.48^{\pm j0.1\pi}$
SHY	$\pm j0.9,\ 0.9$	$0.8e^{\pm j\frac{\pi}{4}}$	$0.9e^{\pm j\frac{2\pi}{3}}$

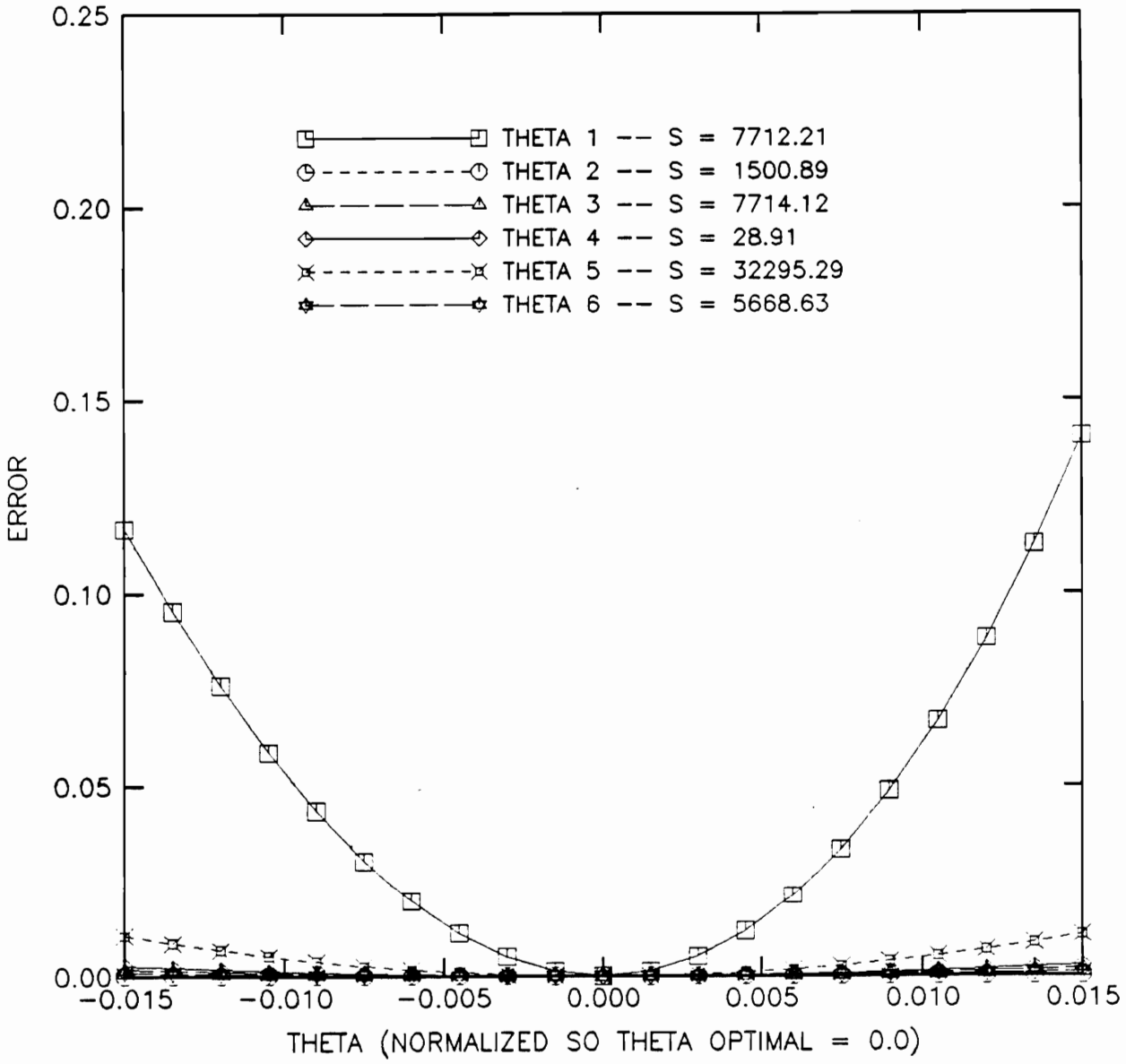

Figure 3. LP2, Error criterion for DGHR parameters (N = 10): J_{10} slightly correlated to S.

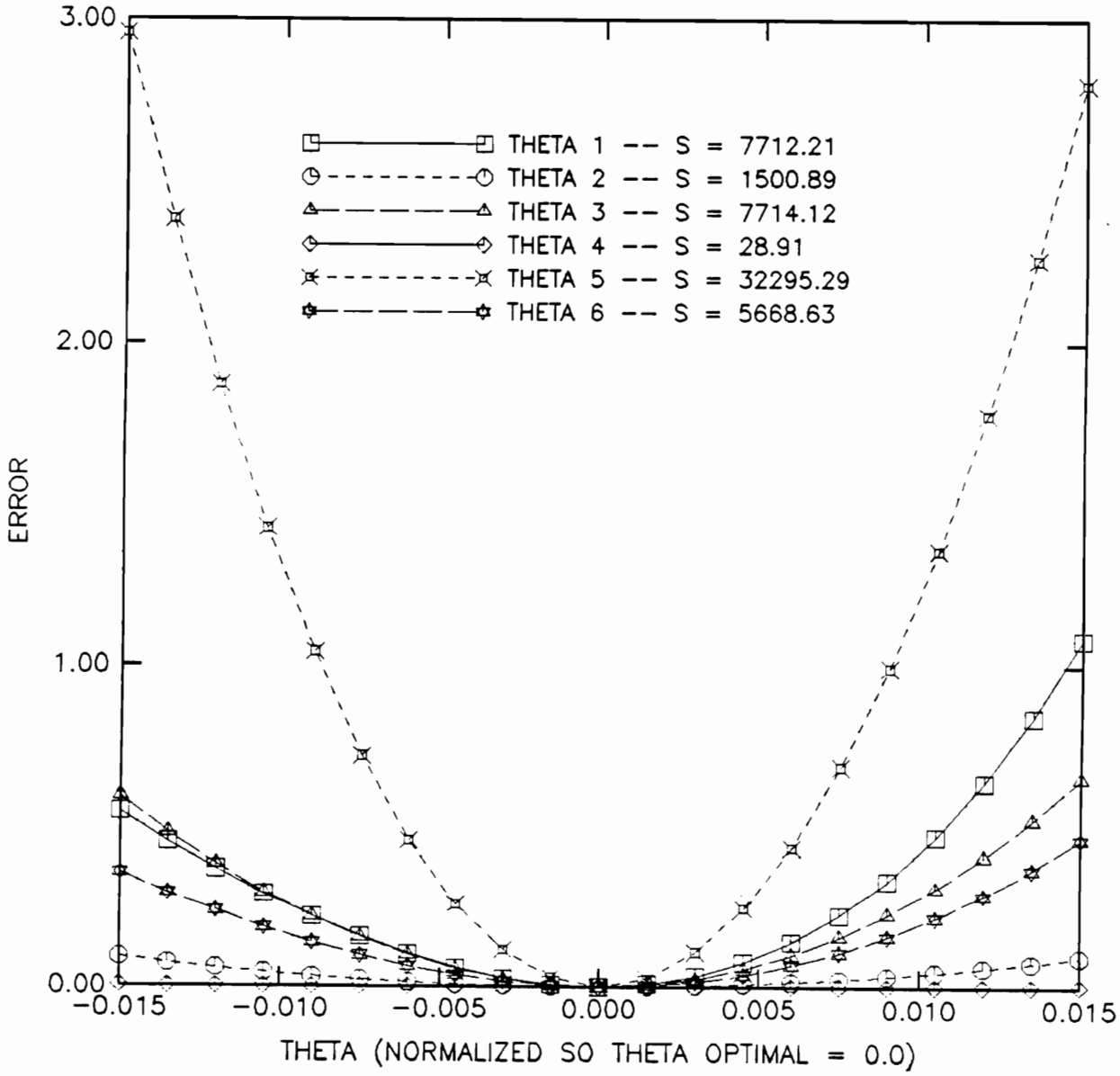

Figure 4. LP2, Error criterion for DGHR parameters (N = 25): J_{25} strongly correlated to S.

can notice that the slopes in Figure 4 correspond much better with the sensitivities than do those in Figure 3.

The equivalent plots for all of the systems are included in Appendix B. An important observation to make from these plots is that a large enough N may be found so that the error criterion J_N is directly related to the sensitivity. These values of N are subsequently used in the identification simulations which follow in the next two chapters. Furthermore, an example is provided in Chapter 5 which will illustrate the necessity of N large for an accurate S - J_N comparison. Finally, note that the S - J_N relationship is **not** structure or system dependent; if a parameter in one structure or system has a higher system sensitivity than that of another parameter belonging to a different structure or system, then the J_N curves are correspondingly steeper.

4.2 The Error-Information Relationship

An alternative view of parameter convergence, based on the optimal input design approach [94,99], also leads to a numerical reason for exploring the Fisher information matrix. To do this, we show that the error criterion J_N is nearly quadratic in the parameters, and that the ellipsoid of the quadratic function is defined by the Fisher information matrix F.

Proof: Write the Taylor series of the criterion J_N about the true parameters

$$J_N(\Theta + \Delta\Theta) = J_N(\Theta) + \sum_{i=1}^{NP} \frac{\partial J_N}{\partial \theta_i} \Big|_{\Theta} \delta\theta_i + \frac{1}{2} \sum_{i=1}^{NP} \sum_{j=1}^{NP} \frac{\partial^2 J_N}{\partial \theta_i \partial \theta_j} \Big|_{\Theta} \delta\theta_i \delta\theta_j + \text{h.o.t.}$$

From the following:

1.

$$\frac{\partial J_N}{\partial \theta_i} = \sum_{i=1}^{N} (h_n(\Theta) - y_n) \frac{\partial h_n}{\partial \theta_i}$$

2.

$$\frac{\partial^2 J_N}{\partial\theta_i\partial\theta_j} = \sum_{i=1}^{N} (h_n(\Theta) - y_n) \frac{\partial^2 h_n(\Theta)}{\partial\theta_i\partial\theta_j} + \frac{\partial h_n(\Theta)}{\partial\theta_i} \frac{\partial h_n(\Theta)}{\partial\theta_j}$$

3. $h_n(\Theta) = y_n$ at the true parameters Θ (no noise)

one has

$$\Delta J_N = \frac{1}{2} \Delta\Theta' F \Delta\Theta + \text{h.o.t.}$$

Thus, J_N is nearly quadratic in the parameters where the higher order terms are negligible:

$$\Delta J_N \simeq \frac{1}{2} \Delta\Theta' F \Delta\Theta \tag{4.2.1}$$

with

$$f_{ij} = \sum_{n=1}^{N} \frac{\partial h_n(\Theta)}{\partial\theta_i} \frac{\partial h_n(\Theta)}{\partial\theta_j} \tag{4.2.2}$$

F is the Fisher information matrix (as can be seen by a direct comparison of equations (4.2.2) and (2.3.1)).

As N gets large, F becomes the parameter correlation matrix inverse. The result (equation (4.2.1)) should come as no surprise, as a simple glance at Figure 4 (and at Appendix B) strongly suggests that the error criterion is close to being quadratic-in-the-parameters in a neighborhood of the optimal "true" parameters Θ. Also, a Gauss-Newton algorithm uses a 2^{nd}-order (quadratic) polynomial fit of the data.

4.3 *Connecting Convergence to Sensitivity and Information -- τ*

Now, we claim that the local convergence properties of the identification procedure given in Algorithm (A.1) (and Algorithm (A.2) as well) depend on the Fisher information matrix -- a matrix which depends on the particular structure being identified. Furthermore, this convergence depends upon two properties of the matrix:

1. tr(F) -- the sensitivity
2. $\kappa_2(F)$ -- the condition number (which is the ratio of its maximum-to-minimum eigenvalues since F is a positive semi-definite symmetric matrix)

When the condition number is small (near 1), the isoclines of J_N are nearly circular. When the condition number is large (i.e. F is ill-conditioned), the isoclines are elongated hyperellipsoids. When the trace is high, the "valleys" of J_N are steep, while if the trace is low, the "valleys" are broad. If the trace is large (high sensitivity), but the structure is also ill-conditioned (high κ_2), an undesirable situation arises. In the latter situation, an algorithm like the Output Error Method bounces across and down a valley rather than just down the valley [41]. The new idea here is to combine these two measures into one, creating what is termed the structural **algorithm time constant, τ**

$$\tau \equiv \frac{\kappa_2(F)}{\mathrm{tr}(F)} \tag{4.2.3}$$

When τ is small, the convergence should be quite fast, while for large τ the convergence is slow. As a result, τ is truly a time constant! The measure τ connects the idea of high sensitivity from optimal input design to the eigenvalue spread constraint from Martingale theory.

5.0 The Deterministic Algorithms

In this chapter, Algorithms (A.1) and (A.2) are considered as used in a deterministic sense. The same noisy impulse response record is used repeatedly in this method, so that convergence is to a set of system parameters which represents a minimum of J_N [74]. These algorithms are termed "deterministic" because no attempt is made to average out the noise which is inherently a part of any measurement. A look at this case is imperative for any understanding of the stochastic version of the algorithms, which are discussed in Chapter 6. In addition, in many practical situations there is no opportunity for repeated measurements of the impulse response. In this section, many results from the numerical analysis literature are used. On the other hand, some problems (from no noise) are immediately relieved by the presence of noise. Comments are made appropriately.

5.1 A Conjecture for Parameter Convergence

Formally, for the deterministic case, the following conjecture is advanced.

Conjecture (C.1)

> Let S_1 and S_2 be two different parameterizations of the same system of known order. The Gauss-Newton algorithm presented is used to identify the corresponding parameters of both S_1 and S_2 , and the optimization criterion J_N possesses no local minima and N is large enough. Then for the same measurement data and equivalent local parameter covariance and initializations, the parameters of S_1 will converge to the true parameters before those of S_2 if and only if $\tau_1 < \tau_2$.

How local to the true system the initial guess must be is still an open question. Later examples will explore this point.

Prior to exploration of the example identifications, we first discuss some convergence results with direct bearing on the above conjecture (C.1) [48]. Let $C^{(2)}$ be the class of continuous functions with continuous derivatives of orders 1 and 2. Since the identification procedures use a Gauss direction, the convergence is superlinear if J_N is not in $C^{(2)}$, and quadratic otherwise. The convergence rate is bounded above by the condition number of the Hessian approximation (i.e. by $\kappa_2(F)$ as $N \to \infty$) [78]. In fact, the bound is

$$||\Theta_{k+1} - \Theta_{\text{true}}||^2 \leq \frac{4}{\lambda_{\min}(P_k^{-1})} J_N(1) \left(\frac{1 - \sqrt{\kappa_2(F)}}{1 + \sqrt{\kappa_2(F)}} \right)^{2k} \tag{5.1.1}$$

The error tends to zero in dim(Θ) steps. Note that as the condition number κ_2 gets large, the ratio involving κ_2 is nearly 1. The error bound can be large when the minimum eigenvalue of P_k^{-1} is small, and then decreases in the error occur only very slowly. Thus, in this case, the higher the condition number, the higher the error bound, implying that slower convergence may occur. On the other hand, if the conditioning were ideal ($\kappa_2 = 1.0$), then the error bound would be 0! Extremely quick convergence should result. Ideally conditioned parameter sets would have diagonal Fisher information matrices which are scalings of the identity matrix. We speculate that such parameter sets do not exist. This bound is of limited use in a practical sense, though, since the right-hand side (the bound) goes to zero. As we shall see later in the example section, the error does not go to zero, and this is expected since the computer does not operate with infinite precision arithmetic. Hence, the utility of computing this bound in the simulations is questioned.

Another upper bound on the convergence rate of the estimated parameters can be found by examining the rate at which the Hessian approximation converges to the true Hessian [48]. Suppose that the sequence Θ_k generated by algorithm (A.1) converges to the true parameters Θ_{true}. If the Hessian approximations P_k^{-1} are neither singular nor infinite (i.e. both P_k and P_k^{-1} exist for all k and are bounded), then

$$\underset{k \to \infty}{limsup} \frac{||\Theta_{k+1} - \Theta_{true}||}{||\Theta_k - \Theta_{true}||} \leq \underset{k \to \infty}{limsup} ||I - kP_kF|| \tag{5.1.2}$$

In this case, the faster the Hessian approximation converges to the true Hessian, the lower the upper error bound on the parameter estimates, implying that faster convergence may occur. An examination of the identification algorithms shows that for the P_k to converge, the matrix P_k^{-1} should be large (but bounded) in all directions [76]. Again, as $N \to \infty$, P_k^{-1} approximates the Fisher information matrix (Hessian) F, and a suitable measure for the largeness of F is its trace, tr(F). This is exactly the sensitivity. We can compute the convergence of the Hessian approximation P_k^{-1} to the true Hessian. Since the Hessian approximation is not required to converge to the true Hessian for the estimates to converge, a better convergence result is to check the [29]

$$\underset{k \to \infty}{limsup} \frac{||kP_kFL_k - L_k||}{||L_k||} \tag{5.1.3}$$

This measure checks that the Hessian estimate provides proper directional information, i.e. it checks whether the parameter estimate update is in the direction which properly minimizes the criterion J_N. If the limit is 0, the convergence rate of the estimate is superlinear. If the limit is nonzero, the convergence rate is linear, assuming the iterations converge at all [29]. This measure is observed later in the example section, where we will see that it generally agrees with Conjecture (C.1).

Since these results are based on upper bounds for the errors, we cannot make a quantitative statement about the conjecture; however, these ideas strongly suggest that we are looking at the convergence issue in an appropriate manner.

5.2 *Deterministic Examples*

For some experimental confirmation of the conjecture, we look at the systems described in Table 1. These systems are all 3^{rd}-order except for the last two which are 4^{th}-order; 3 are low-pass, 1 is high-pass, the next 2 are band-pass, and the last system does not fall into any category. This last system [104] will be discussed extensively in Chapter 7. All of the systems have a zero at $+\infty$. The Fisher information matrix data is given in Appendix A. From the tabular data, one can see that the example systems possess wide ranges in both sensitivities S and condition numbers κ_2. No one structure is always a better choice from a τ viewpoint. Also, no one structure is always the most sensitive, or the most ill-conditioned. In practice, this means that upon implementation, τ should be monitored for various structures, and a choice as to the best structure for identification should be made adaptively.

We have briefly considered also the balanced state-space representation (BSSR) for identification. In this non-canonical structure, all but 2n (system order n) of the eigenvalues of F, which is here a large $(n^2 + 2n)$ by $(n^2 + 2n)$ matrix, are identically zero. Defining κ_2 then as the ratio of the largest to the smallest non-zero eigenvalue, τ is always the smallest for this structure. This suggests that the fastest identifier structure would be the balanced state-space form except for the fact that the structure is not canonical (and therefore this structure is difficult to enforce). It would require minimizing the system sensitivity along with the identification of the parameters in order to yield a unique result. Such an approach remains to be investigated.

We begin by looking at LP1, a system with poles well within the unit circle. The number of impulse response samples was chosen to be 6 since J_6 is strongly correlated to S, even at this low number of samples. The plot (see Figure 5) shows that the time constant accurately predicts the relative convergence rate! Note that while the DII structure is more ill-conditioned than the PRLL structure, the sensitivity overcomes the conditioning to the point that the DII structure actually converges faster than the PRLL structure. Also, the sensitivity by itself is not enough to predict the convergence, as the DII structure has a higher sensitivity than the DGHR structure, and yet the

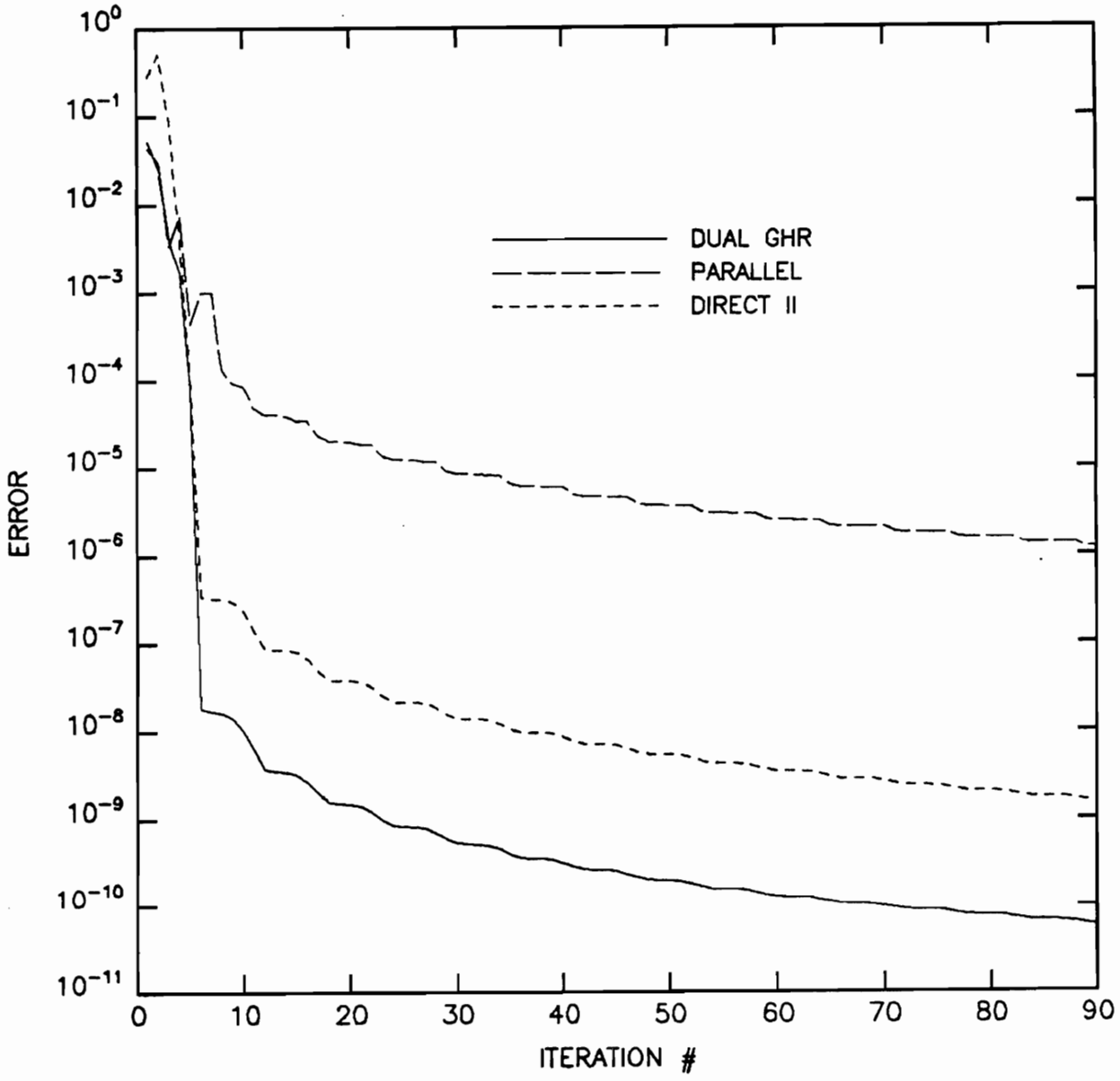

Figure 5. LP1, Absolute error for 90 iterations (N = 6)

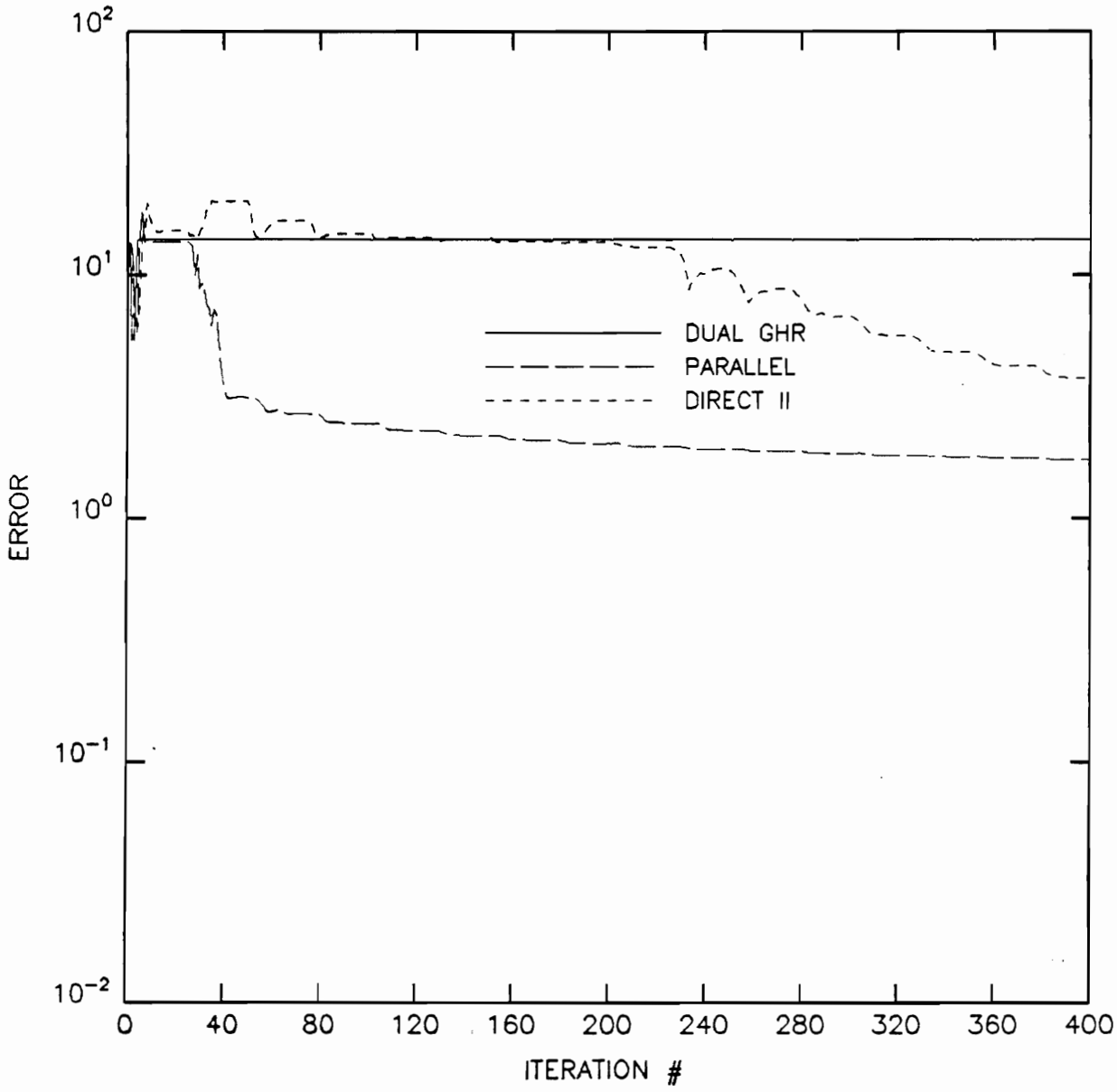

Figure 6. LP2, Absolute error for 400 iterations (N = 25)

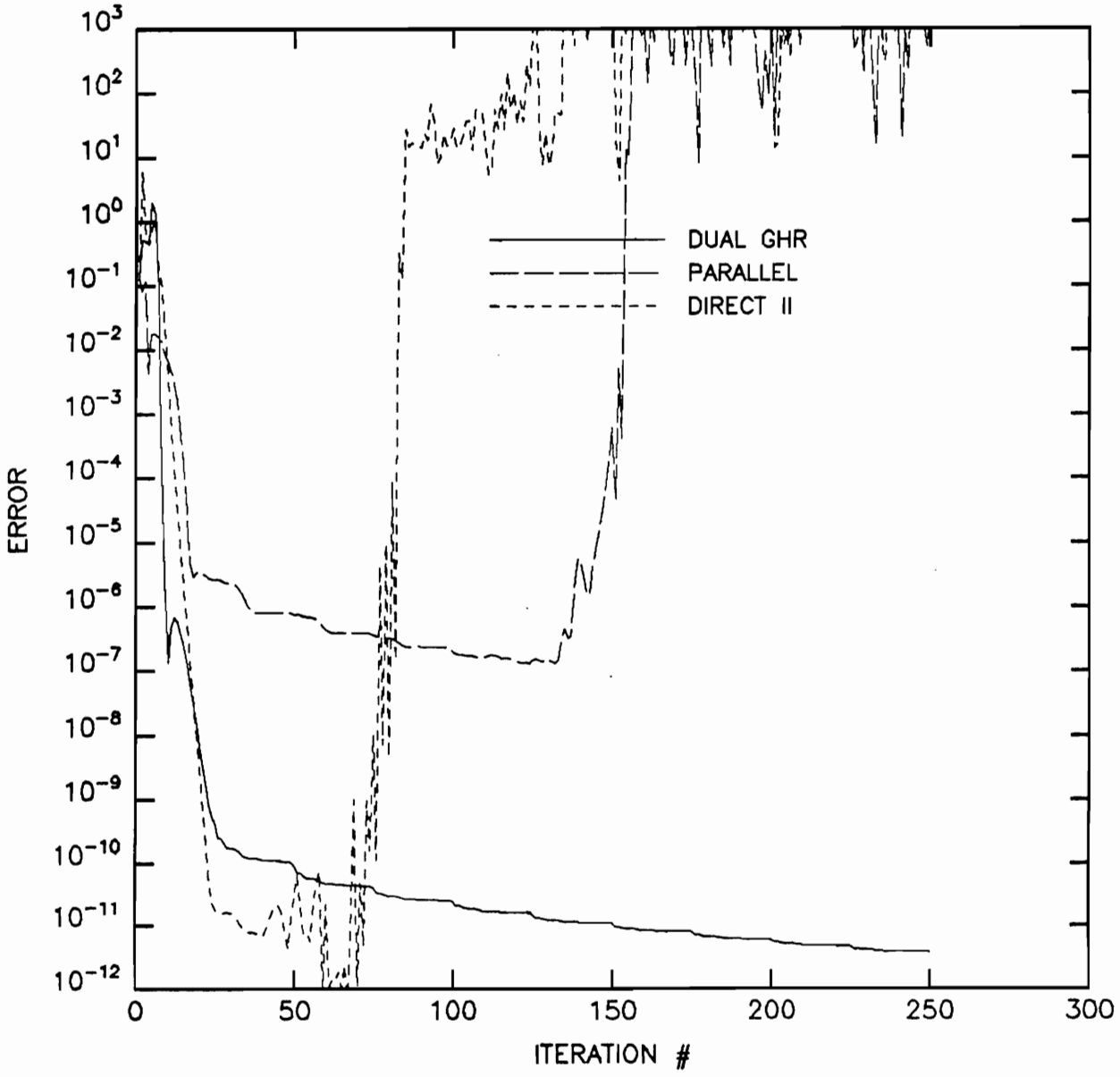

Figure 7. LP2, Absolute error for 250 iterations (N = 25): Pole/zero projection factor is 0.95 in Algorithm (A.1).

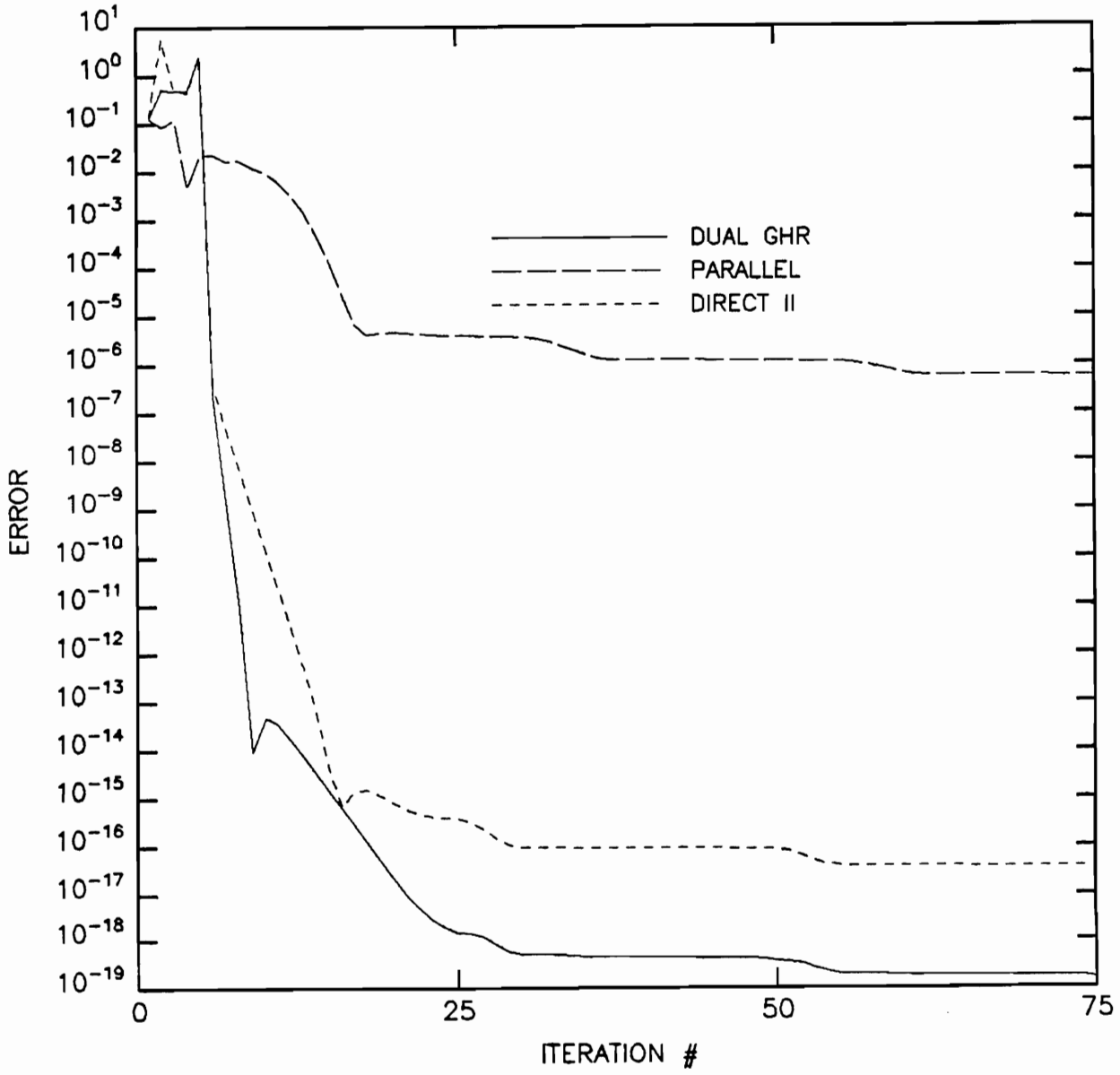

Figure 8. LP2, Absolute error for 75 iterations (N = 25): The μ projection is used in Algorithm (A.2).

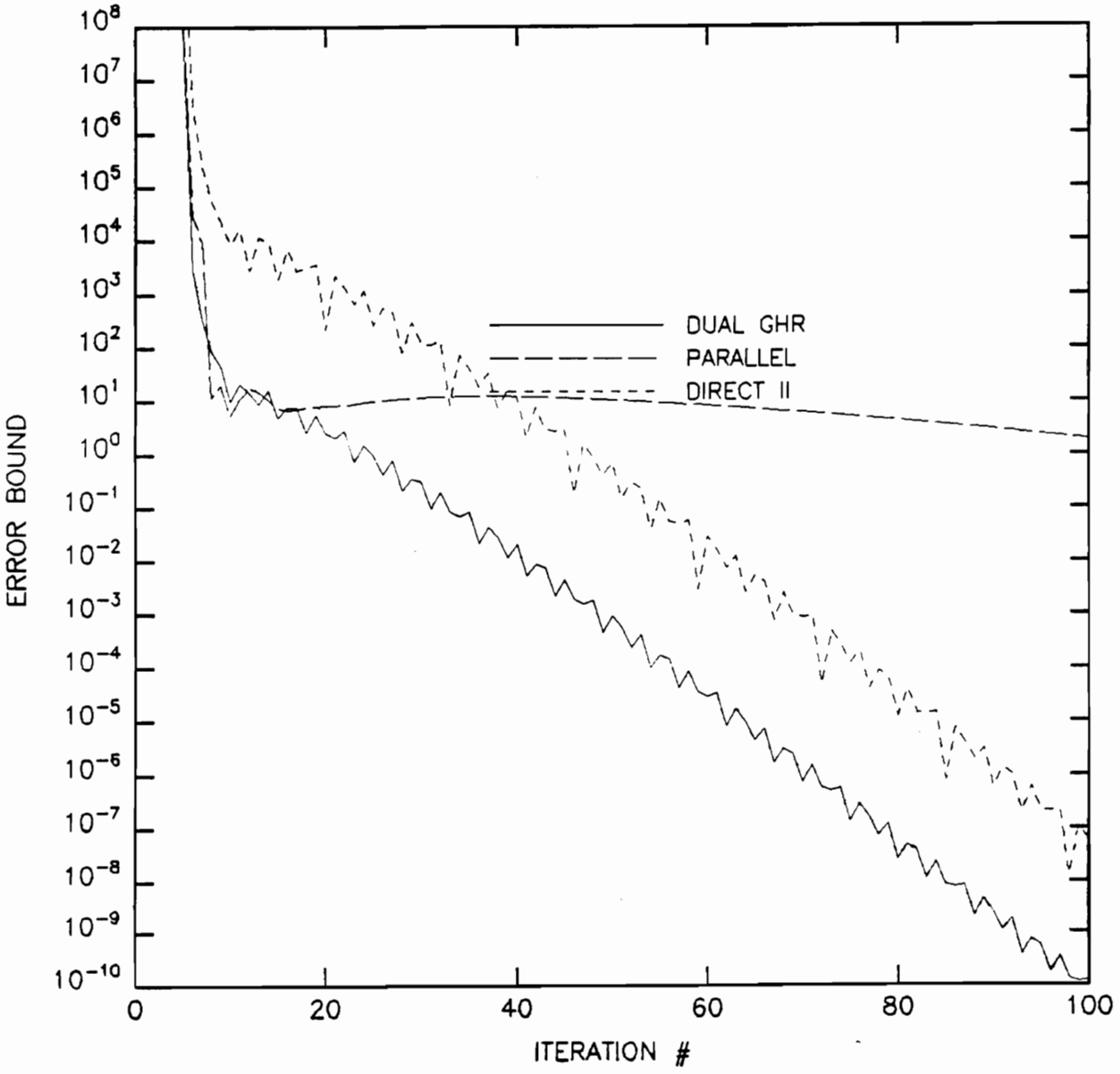

Figure 9. LP1, The Hessian approximation convergence with N = 100

DGHR structure is so well conditioned that it overcomes its low sensitivity to converge faster than the DII structure. This isolation of τ as the only (of S, κ_2, and τ) good predictor of convergence is present in all the example systems. The initial parameter estimates Θ_0 are reasonably close (meaning local) to the true parameters Θ_{true}. Also, note that the Hessian approximations converge well for the DII and DGHR structures, but not so well for the PRLL structure (see Figure 9). The plot shows the measure given in equation (5.1.3) for each k. In the plot, the fact that the PRLL structure Hessian approximation does not converge is also reflected in the fact that for this choice of N, the PRLL structure parameters do not converge.

The identifier performance for LP2 is shown in Figure 6. The system is close enough to being unstable that the projection operator (necessary since the identified system must be stable) is used extensively. The DGHR structure seems particularly susceptible to the chosen projection operator. At first, we chose to scale down the identified system pole and zero radii as this is relatively simple to accomplish for all three identifier structures. However, for the DGHR structure, this scaling has the effect of trapping the model in a neighborhood of the origin of parameter space. Another, even simpler projection was therefore used [76]. Here, if the parameter estimate update moves the estimates out of the stability region, the parameter update vector is set to zero. Thus, the old parameter estimates are kept. We will term this stability projection the μ projection[4] . Figure 7 shows a run with the initial conditions moved closer to the true values. Notice that the DII and PRLL structure identifiers "blow up". This numerical problem can be alleviated by running Algorithm (A.2), whose run is shown in Figure 8. Here the μ projection is also used. However, τ predicts the convergence incorrectly!

From the numerical problems previously encountered (and discussed), it is surmised that the round-off noise is adversely affecting the convergence behavior of the PRLL identifier. By injecting a slight amount of noise (so that a SNR[5] of 67dB exists), the convergence is as expected (see Figure 10). By increasing the SNR in small steps, one can see that adding more noise merely alters

---

[4] See Appendix E for more details about the stability projections.

[5] For more information on what is meant by SNR in this context, and how it is computed, see appendix F

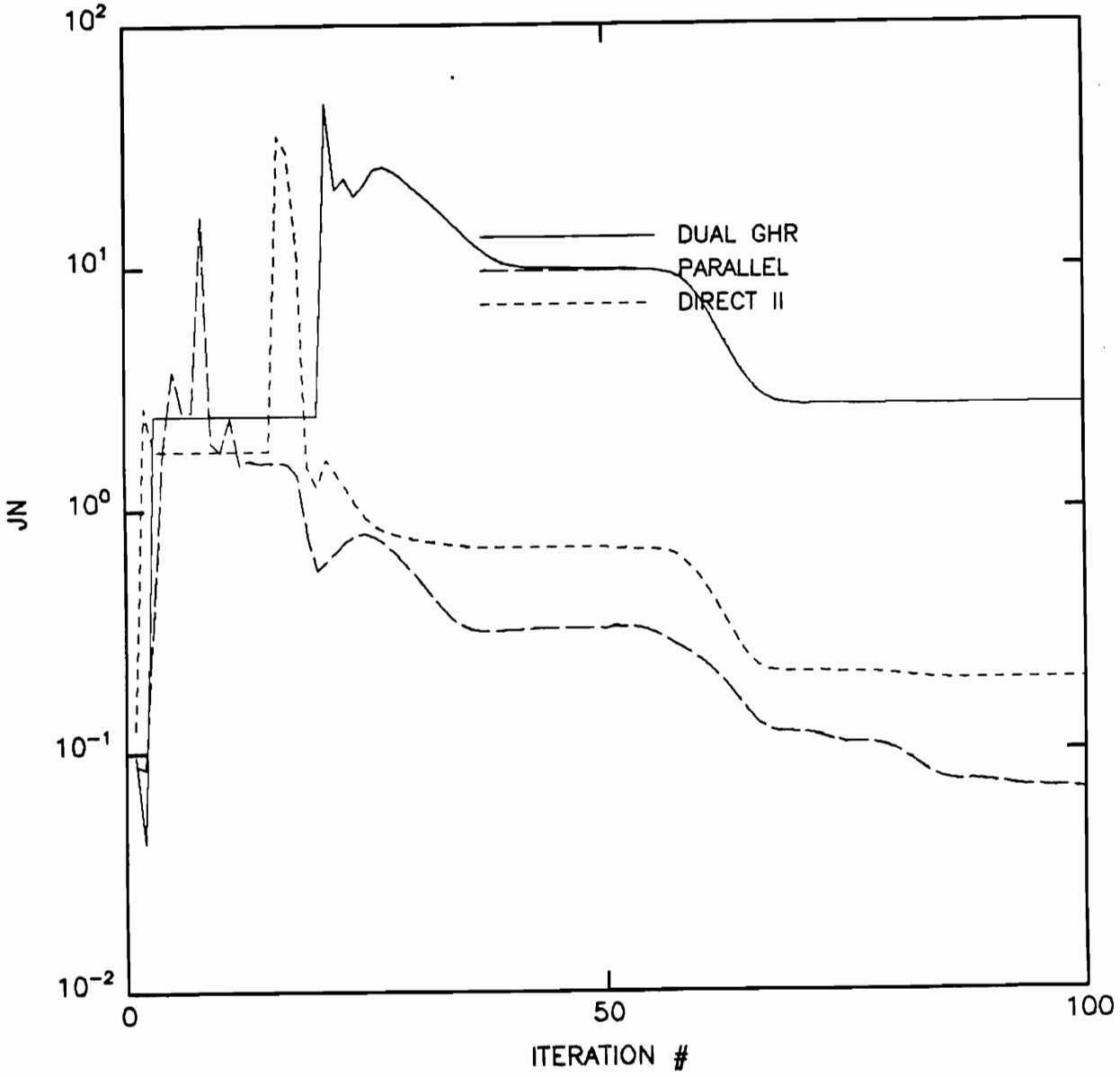

Figure 10. LP2, Absolute error with a 67 dB SNR: The μ projection is used in Algorithm (A.2).

the absolute error levels, leaving the convergence as τ predicted. Subtracting noise from this level alters the relative convergence rates so that the convergence is not τ predicted. This is consistent with the idea of numerical noise being the causative agent, but it is not proof. Note that noise is inherently present in all practical applications. Also, since the impulse response of all stable systems approaches zero for large k, increasing N may actually impede good parameter identification, rather than improve convergence performance. To put it another way, for a fixed SNR, adding samples to the identification criterion J_N may mean that the measurement samples near sample N are almost all noise. Therefore, using these measurements in the identification would result in a worse identification than using fewer samples.

System LP3 is run with N = 10, which is not quite enough samples for the identification criterion to be strongly correlated to the sensitivity. However, enough samples are used to perform the identification. We see that the DGHR structure identifier is not converging (Figure 11). This is due to the stability projection problem mentioned earlier. However, here we also see that the PRLL structure is apparently converging to the "wrong" system. A check of these "converged" parameters shows that the PRLL structure is in a region of parameter space that represents a 1^{st} -order approximation to the true 3^{rd}-order system. In other words, the identified PRLL parameters correspond to 2 pairs of near pole/zero cancellations, with only 1 pole left to fit the measured data. These "converged" parameters also correspond to a region of parameter space which is very ill conditioned -- these parameters of the PRLL structure have $\kappa_2 = 5.38 \times 10^6$ as opposed to the true PRLL system conditioning of 1163.3 (three orders of magnitude less!). The sensitivity is decreased by a factor of 2, and so we see that the PRLL identifier has wandered into a "bad neighborhood" of parameter space. When we start the identification of the PRLL parameters from here, the parameter estimates move only slightly. If we start the identification with initial parameter guesses near the true parameter values, then the identification algorithms succeed easily, with convergence according to the time constant τ as conjectured. Therefore, we believe that with enough iterations, the PRLL parameter estimates will eventually "escape". We check this in Figure 12 and Figure 13. In Figure 12, pole/zero scaling is used with the initial conditions close to Θ_{true}. The DGHR structure still does not converge. However, if the μ projection is used as shown in

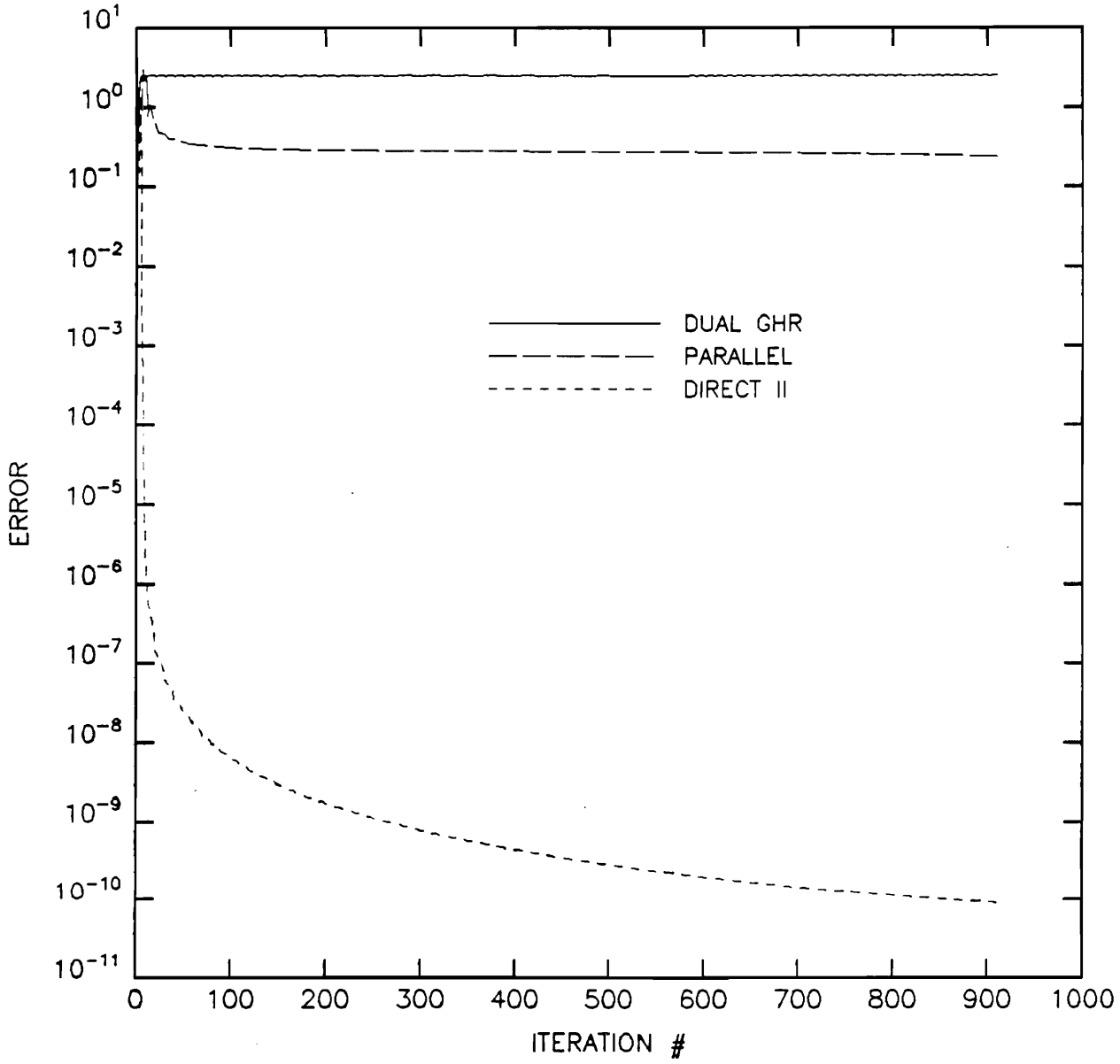

Figure 11. LP3, Absolute error, nonlocal initial conditions (N = 10)

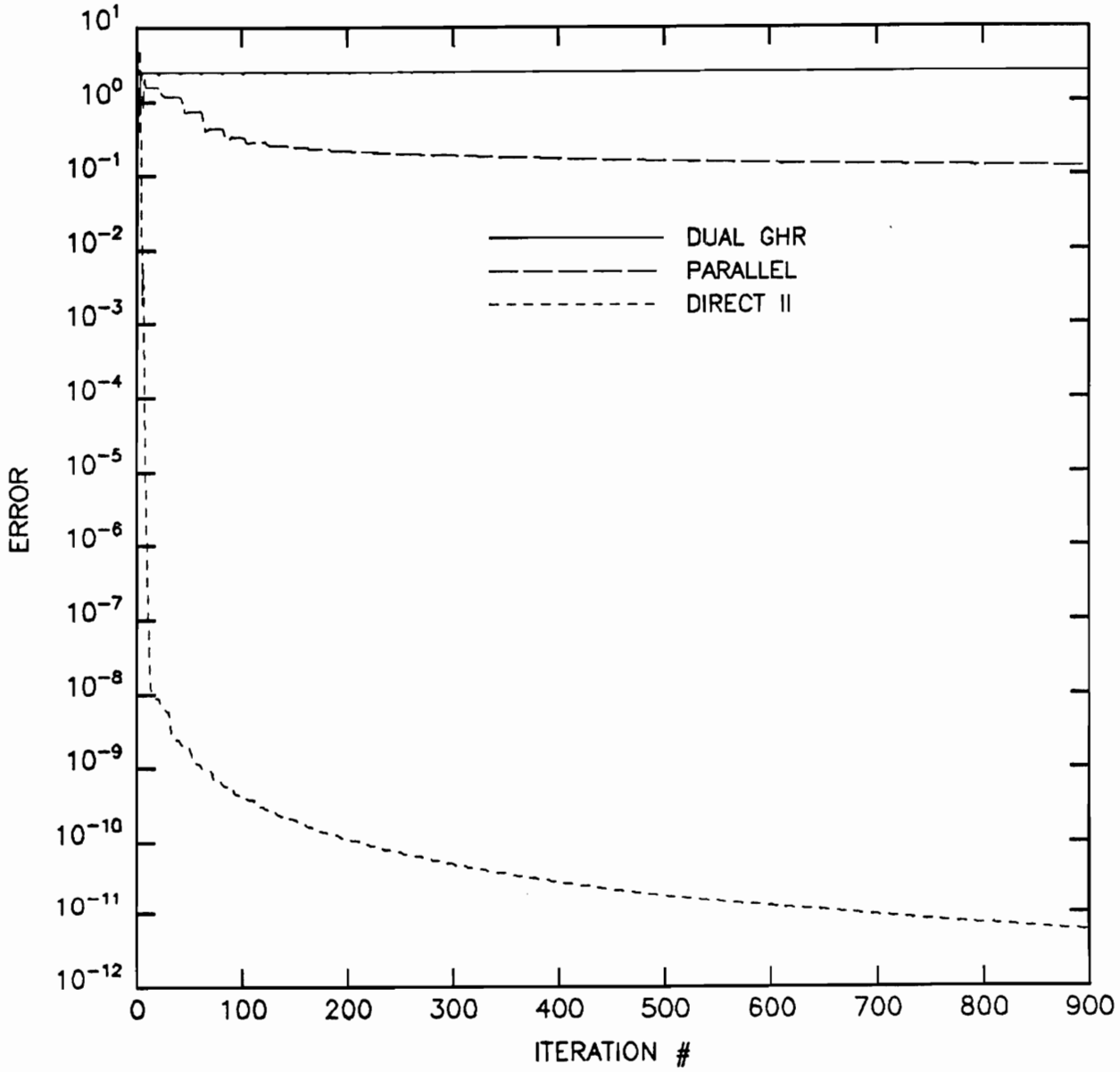

Figure 12. LP3, Absolute error, local initial conditions and pole/zero projection used (N = 20): Pole/zero projection factor is 0.90 in Algorithm (A.1).

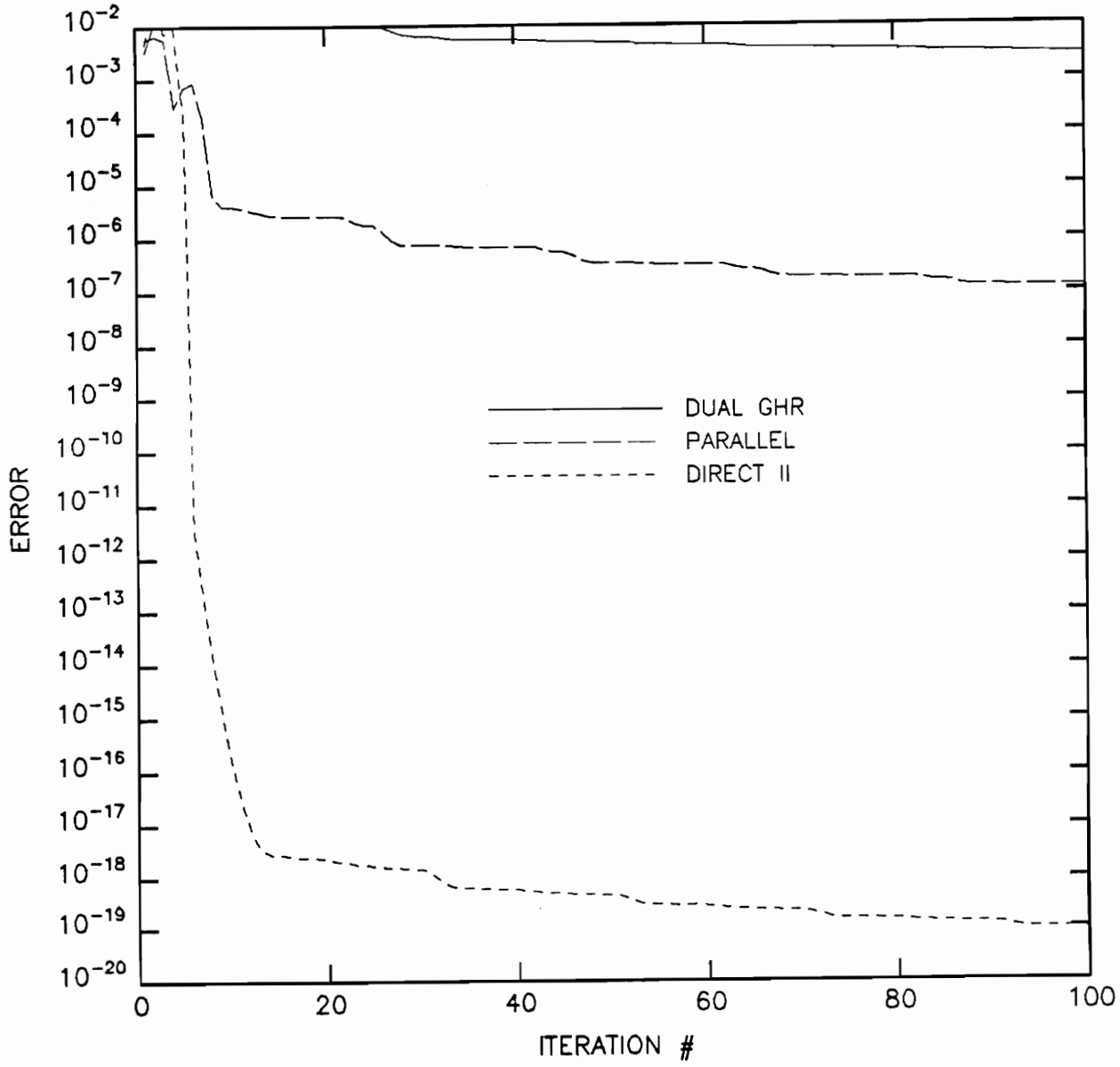

Figure 13. LP3, Absolute error, local initial conditions and μ projection used (N = 20): Algorithm (A.2)

Figure 13, all convergence is τ predicted (i.e. as conjectured). Note that the Algorithm (A.2) is used here for numerical reasons, as the PRLL identifier requires it for numerical stability.

System HP1 also illustrates how the convergence results can be influenced by the stability projections. We see the effects of the stability projection in Figure 14 (μ scaling) and in Figure 15 (pole/zero scaling). With the μ projection, the DGHR structure converges slowly (since the update vector is discarded many times). This is an improvement over the pole/zero radii scaling, as the DGHR structure parameter estimates do not converge at all in that case (as seen in Figure 15). Figure 16 shows the J_N curves for the final DGHR structure identifier parameters of Figure 15. All parameters are trapped in a "flat" region of parameter space except for θ_4, which is only a scale factor, affecting neither the system poles nor zeros. The staircase visible in the convergence plots is directly connected to the value of N. Most of the error improvement (after the initial few passes through the data) comes with the first sample or two of each pass. The remaining data in each pass affect the system only slightly, thus creating the step changes in the error versus iteration plots. This phenomenon is not due to the projection operator.

The bandpass system BP1 gives an indication of the necessity of placing a local neighborhood requirement on the Conjecture (C.1). In Figure 17, one can see that the convergence paths do not follow τ. The DGHR structure has the lowest τ, and yet the DII structure (with the middle τ value) actually outperforms it. If the identification of all three structures is started with an arbitrary initial parameter choice, a change to the structure whose $\tau(\Theta_k)$ is smaller yields the fastest convergence rate. This point is illustrated by computing τ for the 3 structures corresponding to the end DII system of Figure 17, and then reinitializing all 3 identifiers at that point in system space (see Figure 18). The DGHR structure now outperforms the DII structure, and they both outperform the PRLL structure, as conjectured.

We also note that the choice of N can be important in the τ predicted convergence. Examine Figure 19 and Figure 20. When $N = 20$, the convergence of the DII structure is not τ predicted! However, when $N = 50$, the convergence is τ predicted. Since the impulse response of BP2 is below 10^{-3} after $N = 20$, and the total energy in the impulse response is 1.61, one might have naturally thought that $N = 20$ is sufficient, but it is not. We know that the identifiers have converged to

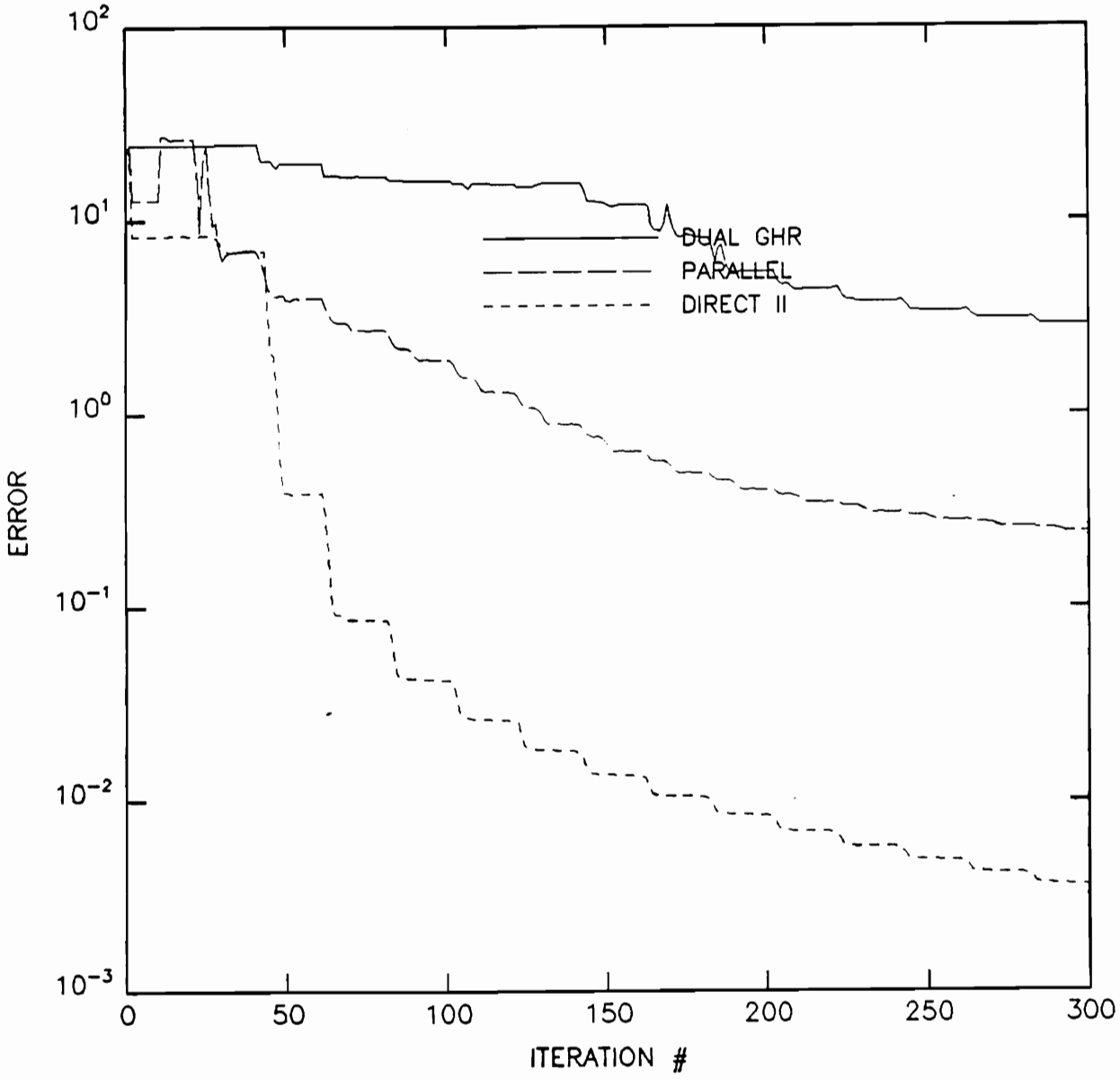

Figure 14. HP1, Absolute error with μ scaling (N = 20): Algorithm (A.1)

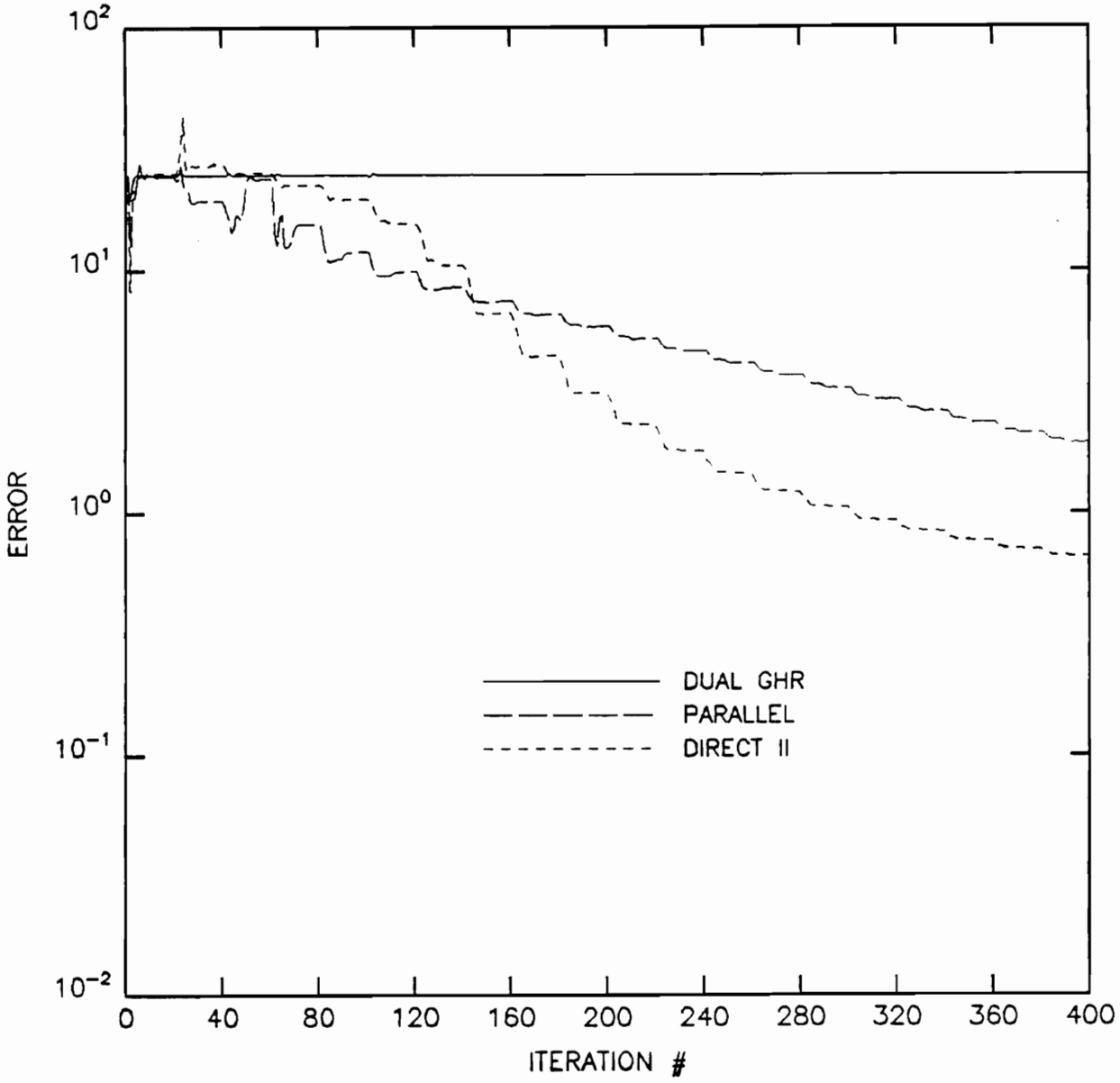

Figure 15. HP1, Absolute error with pole/zero scaling (N = 20): Algorithm (A.1)

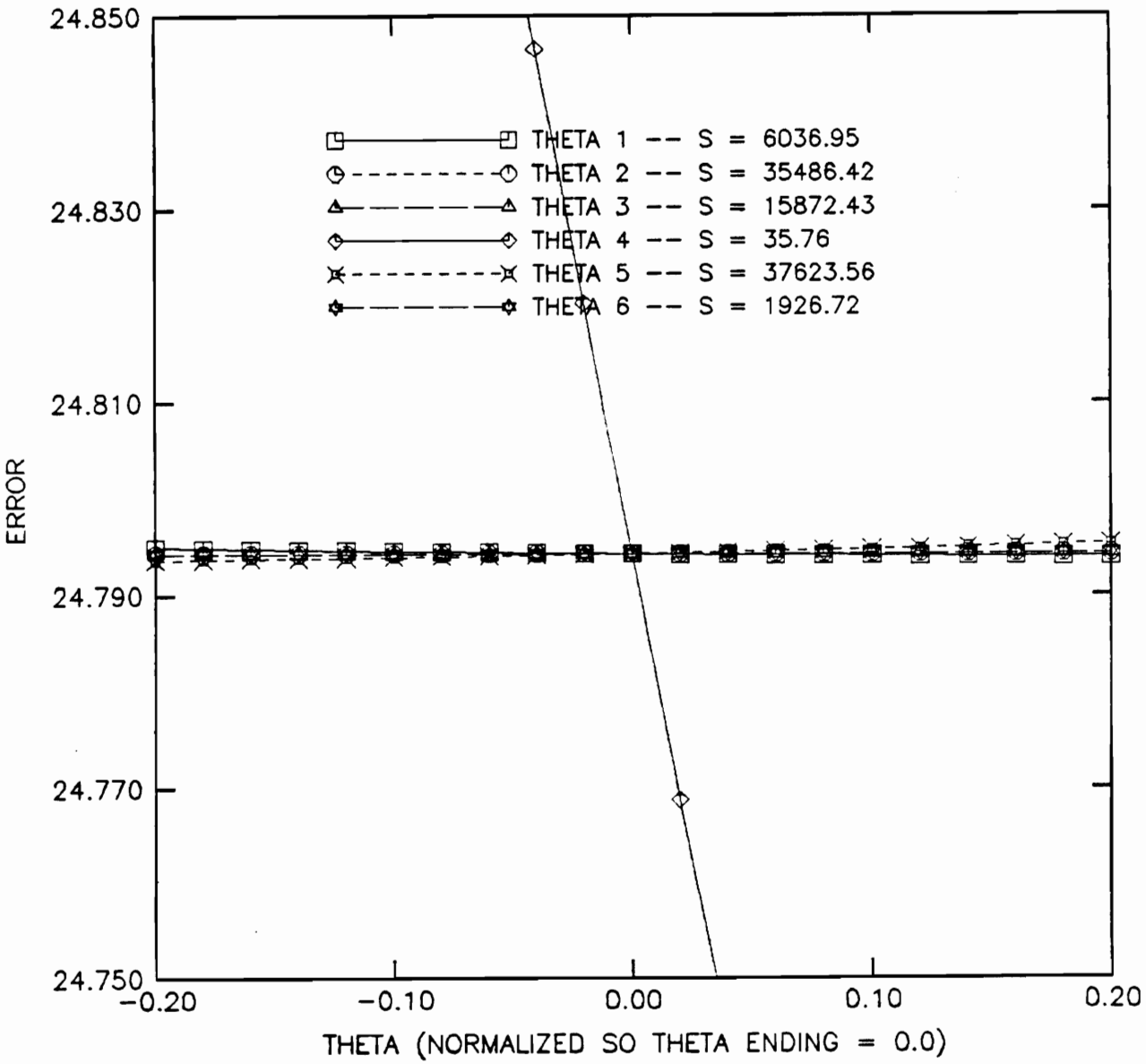

Figure 16. HP1, Error versus deviations about theta ending: The parameters are the DGHR structure identifier results.

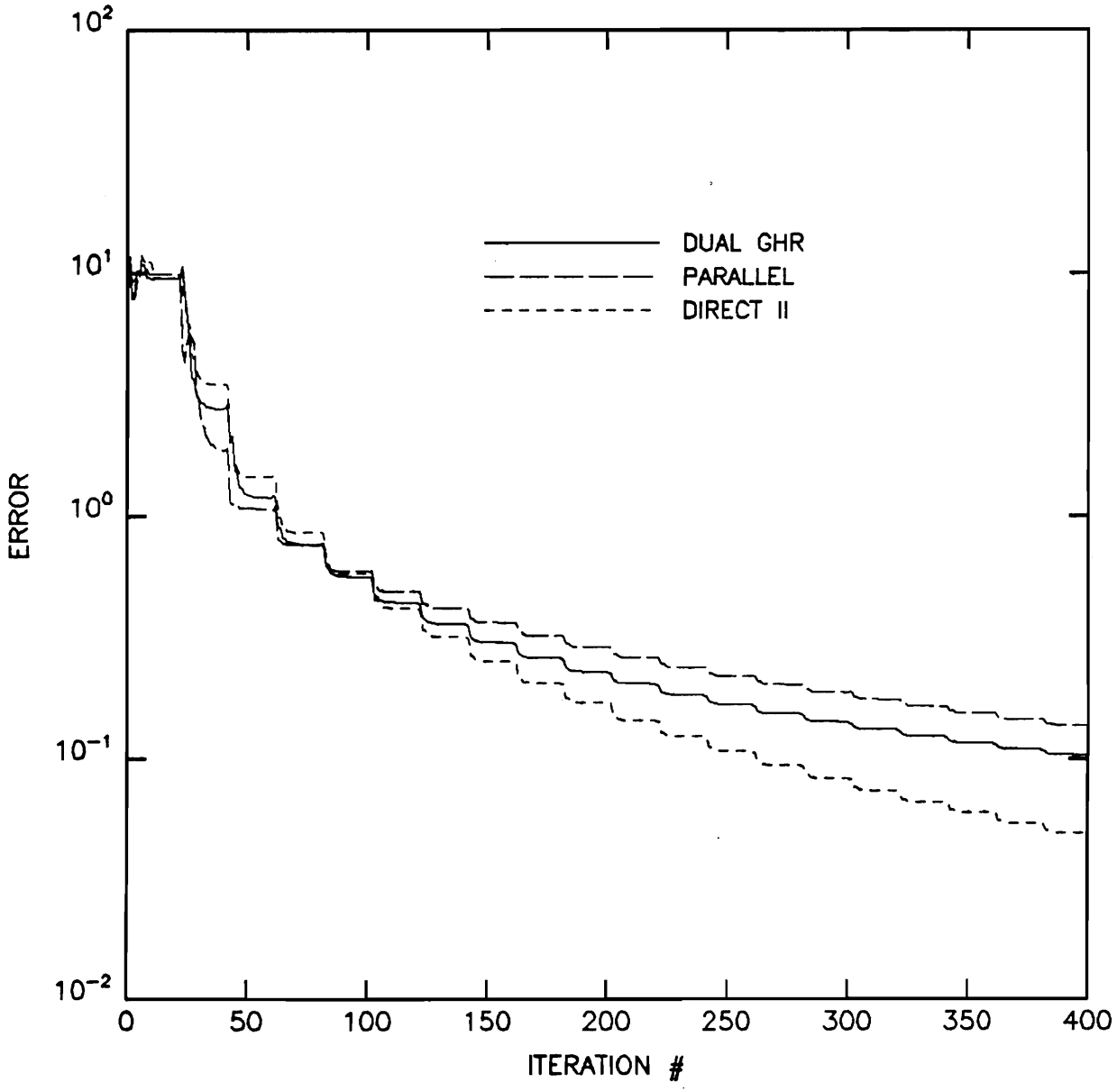

Figure 17. BP1, Absolute error, non-local initial conditions (N = 20)

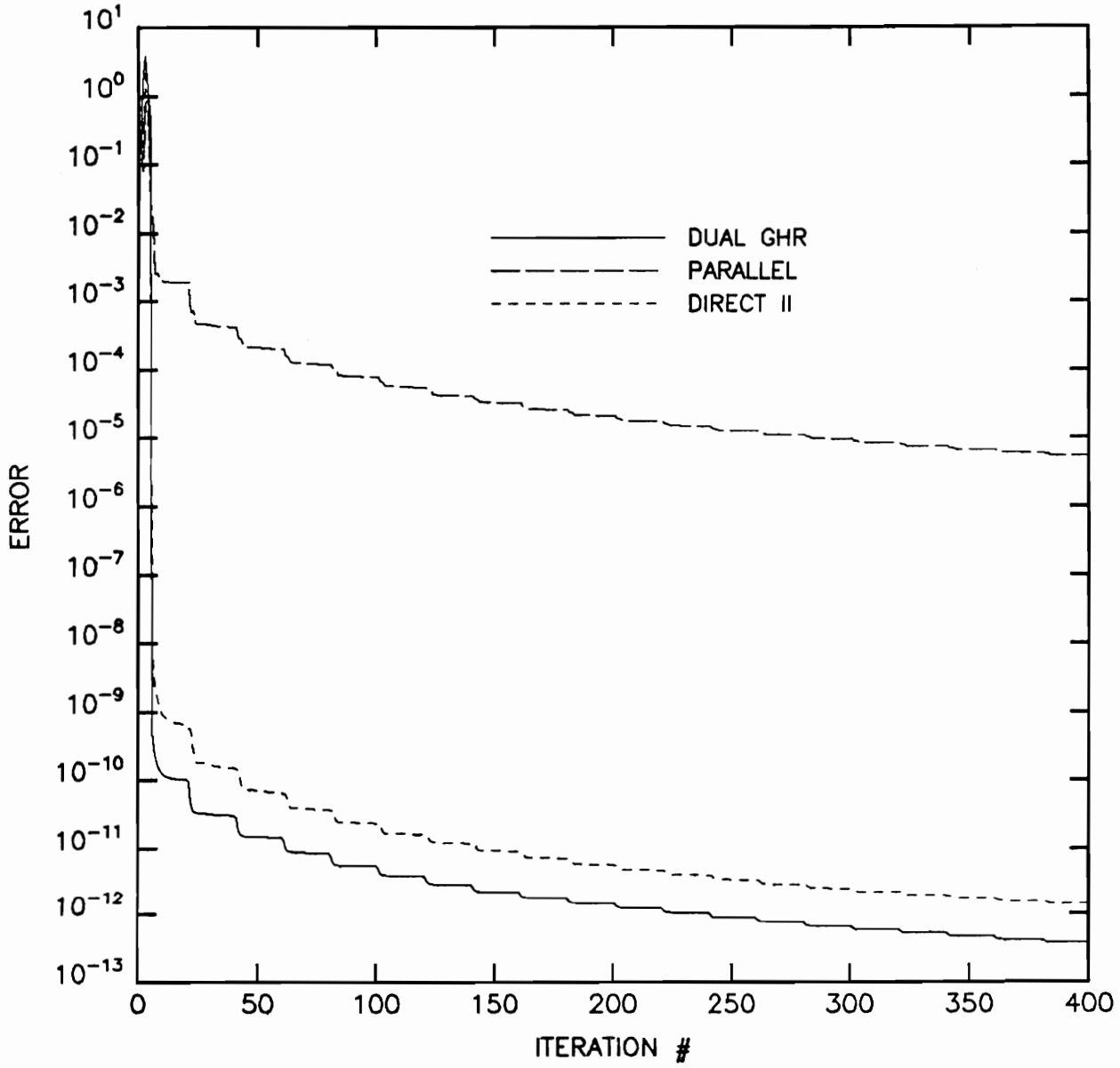

Figure 18. BP1, Absolute error with local initial conditions (N = 20)

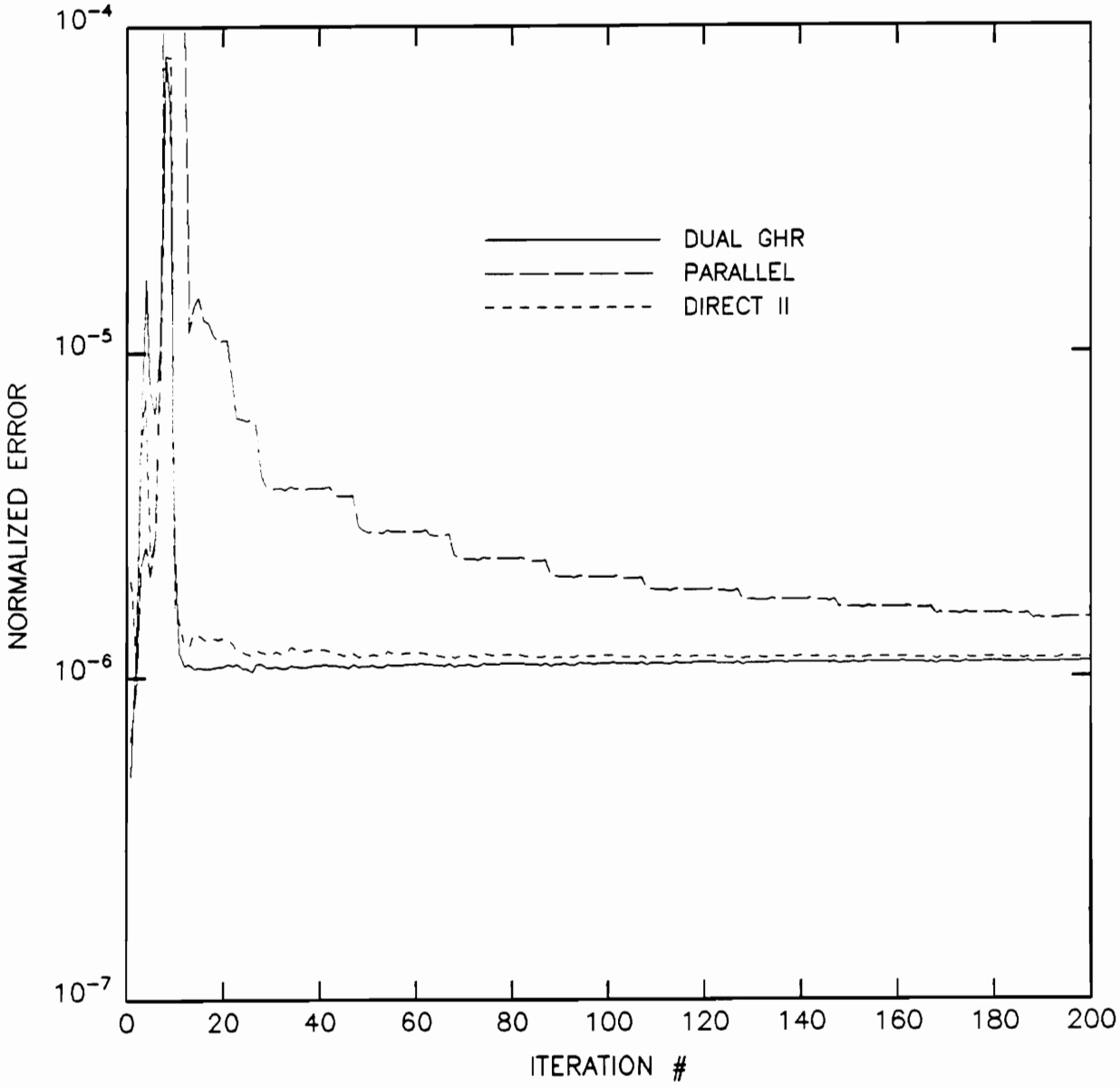

Figure 19. BP2, Normalized error (N = 20)

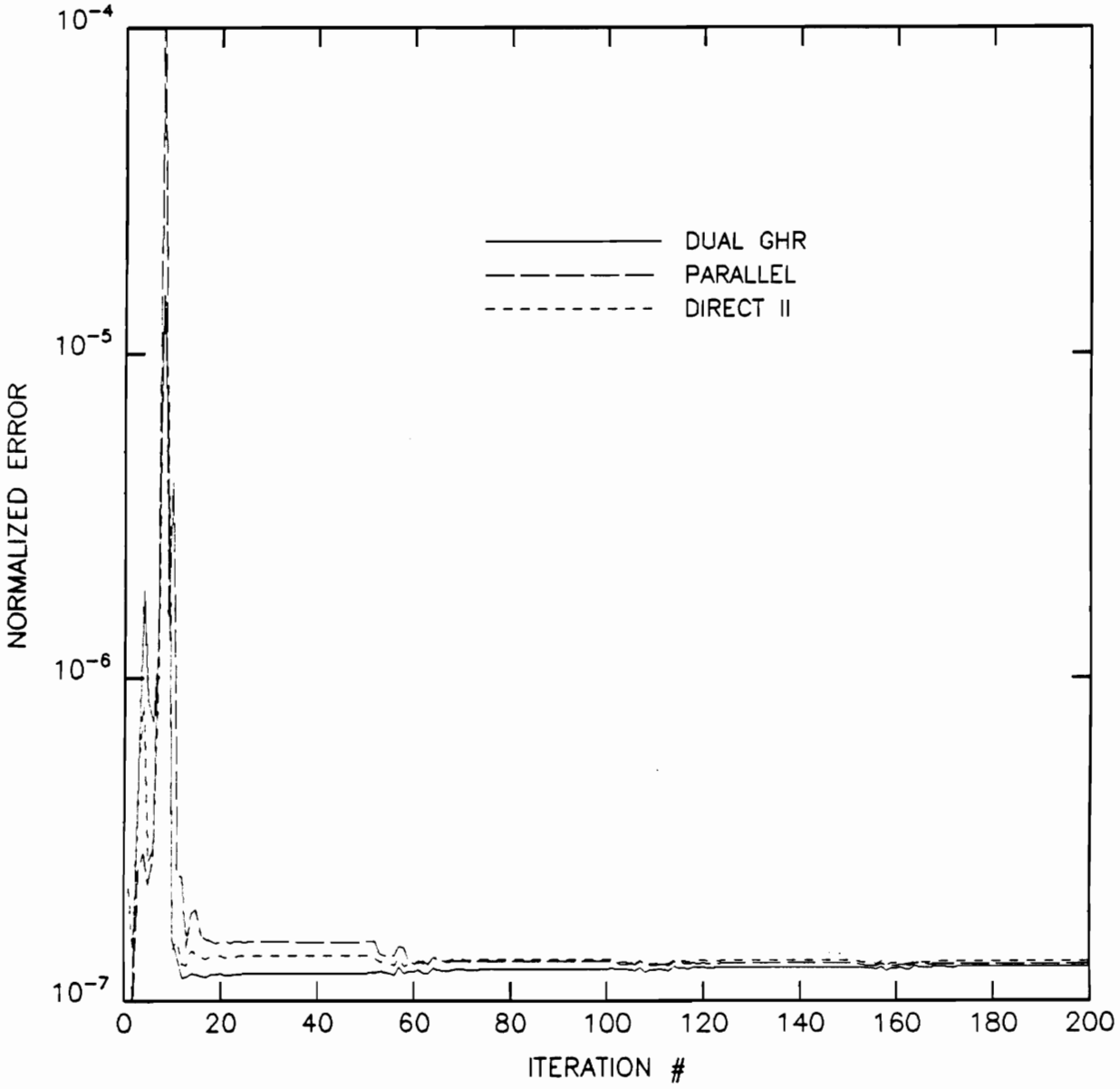

Figure 20. BP2, Normalized error (N = 50)

minima by examination of the J_N versus Θ curves. Looking in Appendix B, one can see that even though the error curves for $N = 20$ are related to the sensitivity S, some improvement could be gained.

We close this example section by noting that the results given so far were for impulse response data without noise, i.e. with infinite signal-to-noise ratios. We have thus concentrated on proposing and validating our analysis tool, rather than on the many practical considerations which must be taken into account before actually using this tool in an identification context. However, on a more practical note, we have considered the use of the chosen algorithms for identification from noisy measurements with large signal-to-noise-ratios (SNR). Figure 21 and Figure 22 show composites of the error (J_6) for 90 iterations. In Figure 21, the impulse response of LP1 has been corrupted by 5 different noise realizations, each 60dB below the impulse response power level. In Figure 22, the noise power levels are only 40dB below the impulse response power level. While for different noise realizations the 40dB SNR composite plot shows some identifications of the DII parameters to converge faster than some identifications of the DGHR parameters, the convergence is consistent with the conjecture for each individual noise realization. In both figures, the different realizations are indicated by different point markers. It appears therefore that our conjecture for convergence results still holds in a neighborhood of the true parameters, and in fact, this argument was used to help explain some numerical experiences observed in studying system LP2.

5.3 Order and the Model Set

So far, we have looked into the situation where the model set contains the true parameters exactly. What happens when the model set is overparameterized? What happens when the model set is underparameterized? We explore these two questions in this section. The work presented here is preliminary. Note that the underparameterized case is of great interest, since reduced-order

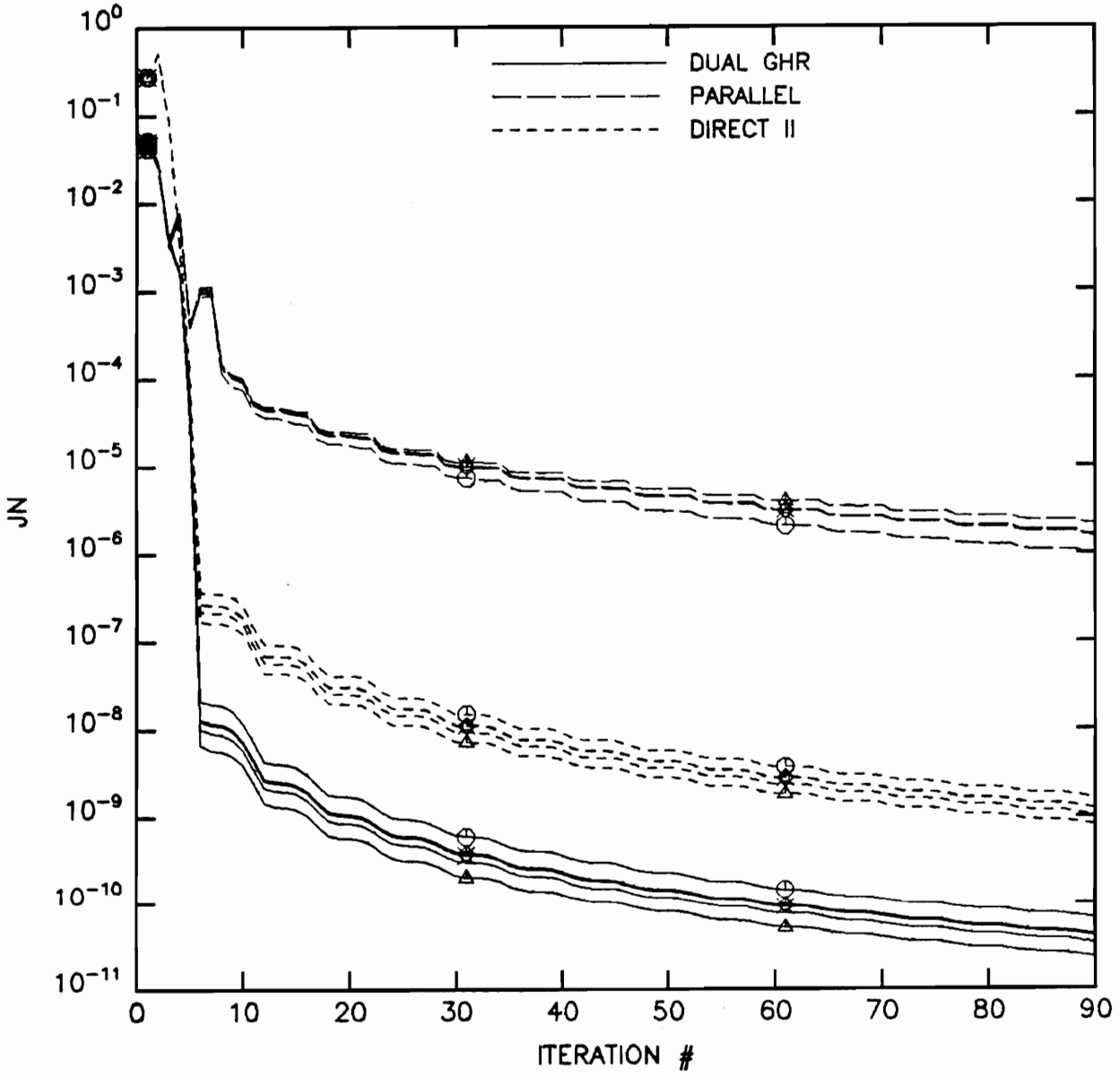

Figure 21. LP1, Absolute error for 90 iterations, 60 dB SNR (N = 6)

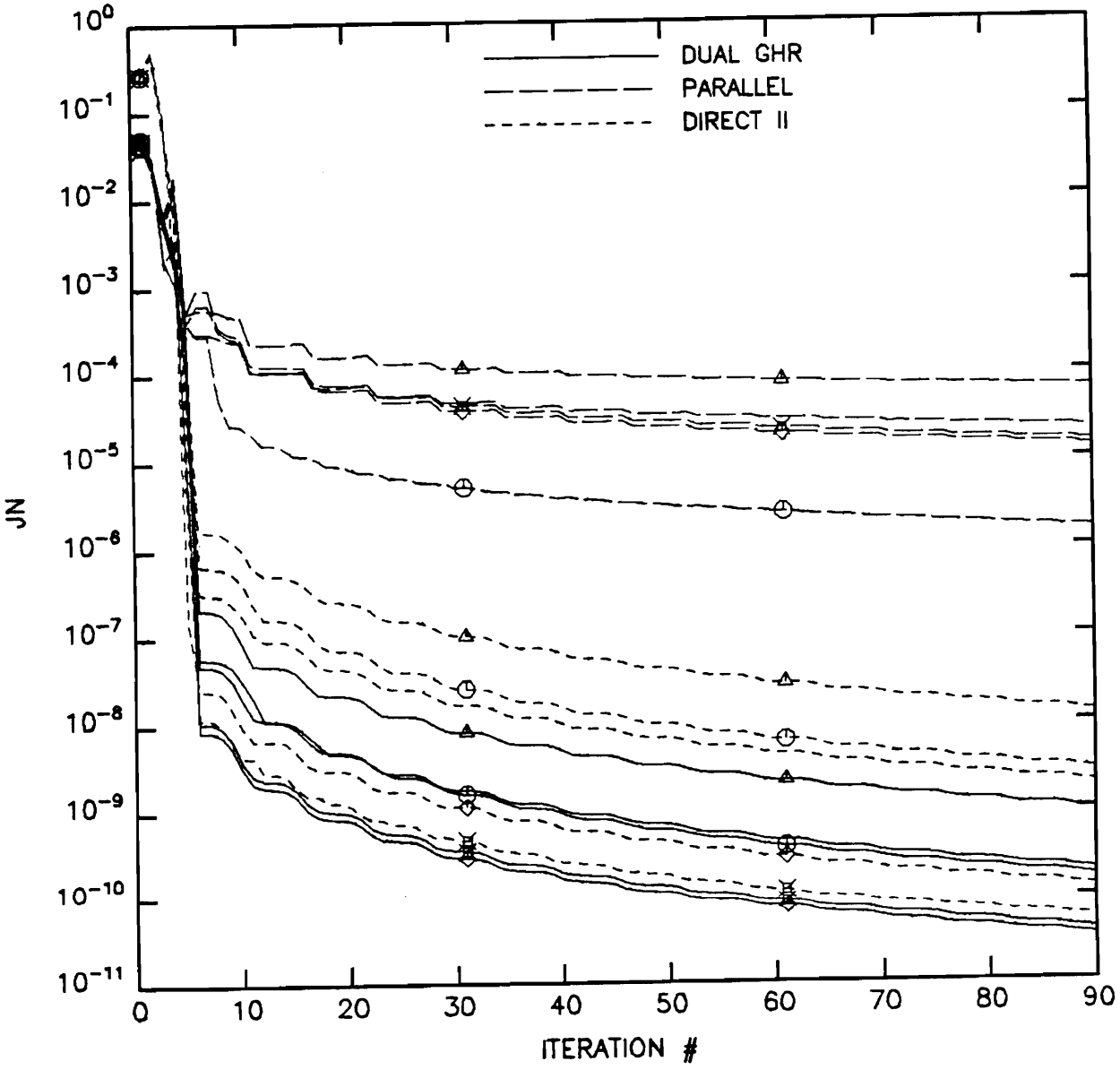

Figure 22. LP1, Absolute error for 90 iterations, 40 dB SNR (N = 6)

modeling is of great importance in the general research community. Most of the work presented here is at an observation level, i.e. we are making statements based primarily on observed behavior.

5.4 *The Overparameterized Model*

The Hessian matrix of an overparameterized identifier structure is singular at the convergence point [76]. Thus, the matrix kP_k in Algorithm (A.1) will grow without bound as the sequence converges to F^{-1} (as will the square root matrix Q in Algorithm (A.2)). Note that the bound in equation (5.1.1) will be quite large, since $\lambda_{\min}(P_k^{-1})$ approaches 0. More importantly, the bound in equation (5.1.2) is no longer valid, and so the justification for τ no longer exists. In fact, if F is singular, J_N may either fail to have a minimum point, or it may have an infinite number of minimum points [48]! However, in the algorithms presented here, a minimum point always exists, and the converged-to system should be the least-square solution. Note, however, that since the true system parameters belong to the model set of parameters, an exact identification (up to a pole\zero cancellation) is possible.

For example, if LP1 is identified as a 4^{th} -order system, the DII system accurately finds the 3 poles and 2 finite zeros belonging to LP1. The model also has a pole\zero cancellation pair at $z = 0.66168346$. Neither the PRLL nor the DGHR structure identifiers converge to the global minimum. The convergence is shown in Figure 23. However, these two structures do converge to something -- but what? First, neither structure has an end model estimate with the poles and zeros of the true system. Neither structure has a pole/zero cancellation pair, though some poles and zeros are close to each other. To further explore this situation, we compute the error criterion vs. parameter deviation curves for the DGHR structure about Θ_{125}. These curves are shown in Figure 24. They clearly show that the identifier has found a local minimum! Although it is difficult to tell from the plots, the error criterion J_N is approximately 0.0005 at the minimum, rather than the J_N of 0.0000 which occurs at the global minimum. The same situation is found for the PRLL

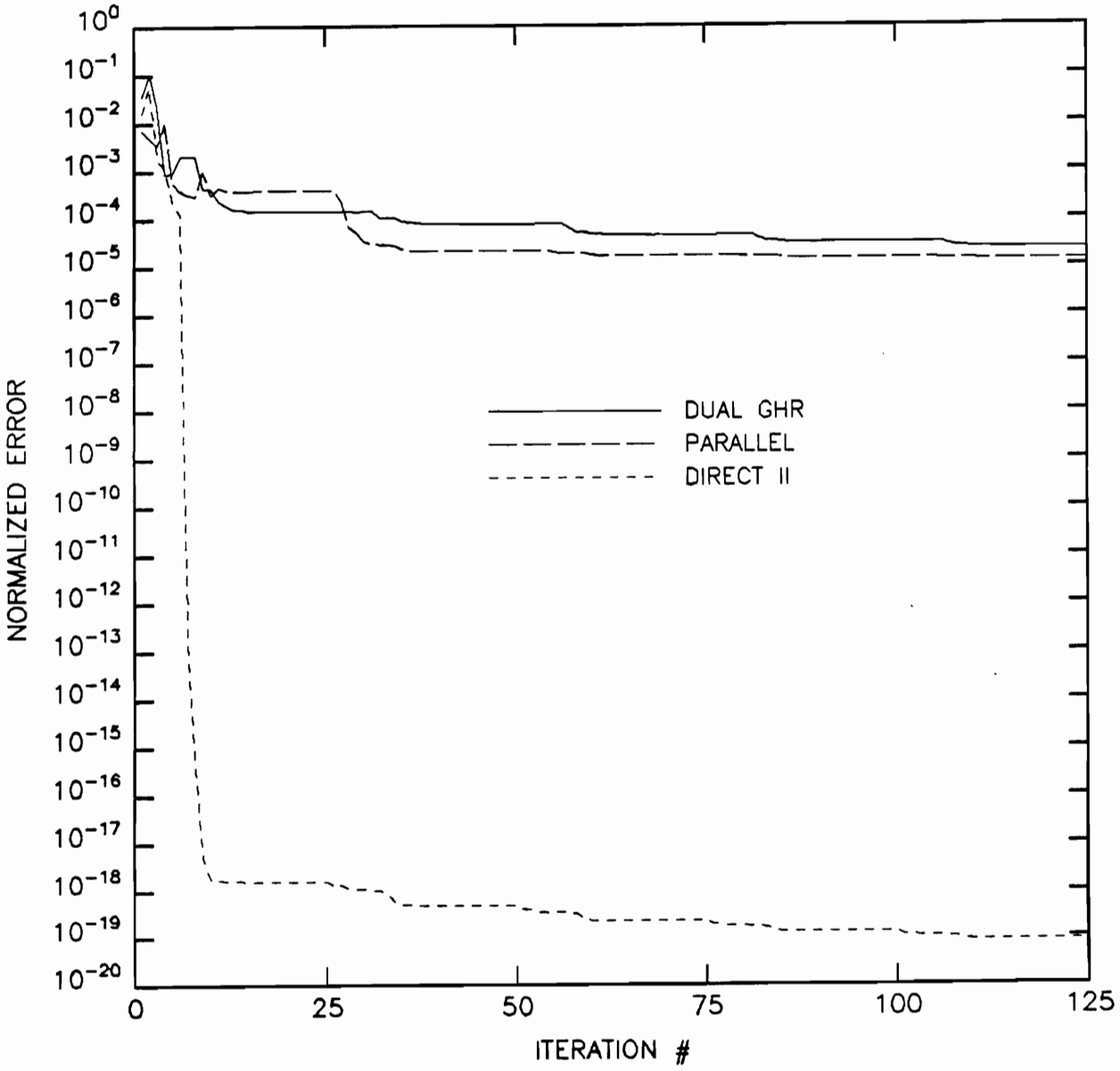

Figure 23. LP1, Overparameterized model

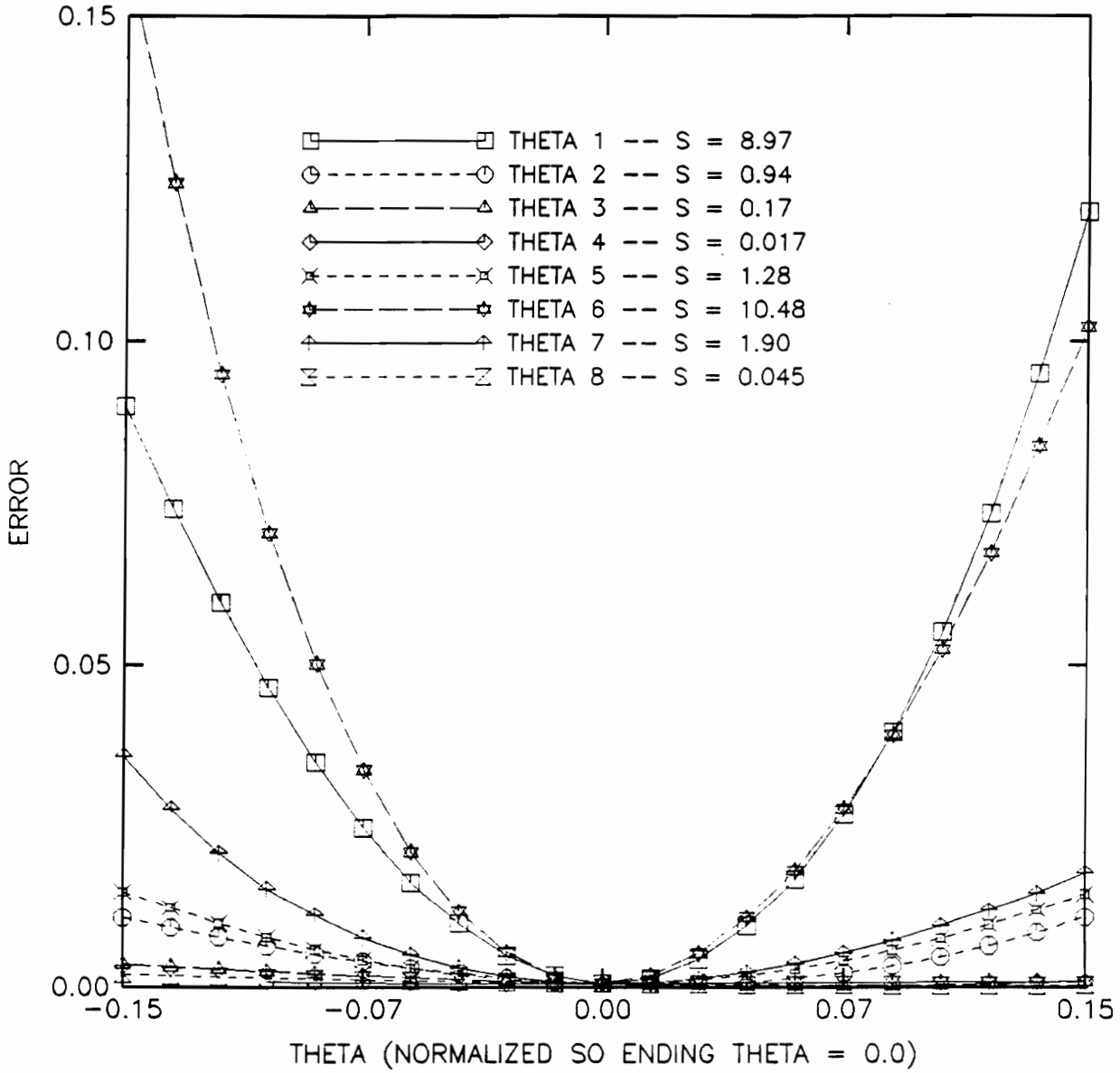

Figure 24. LP1, Error criterion vs. Θ

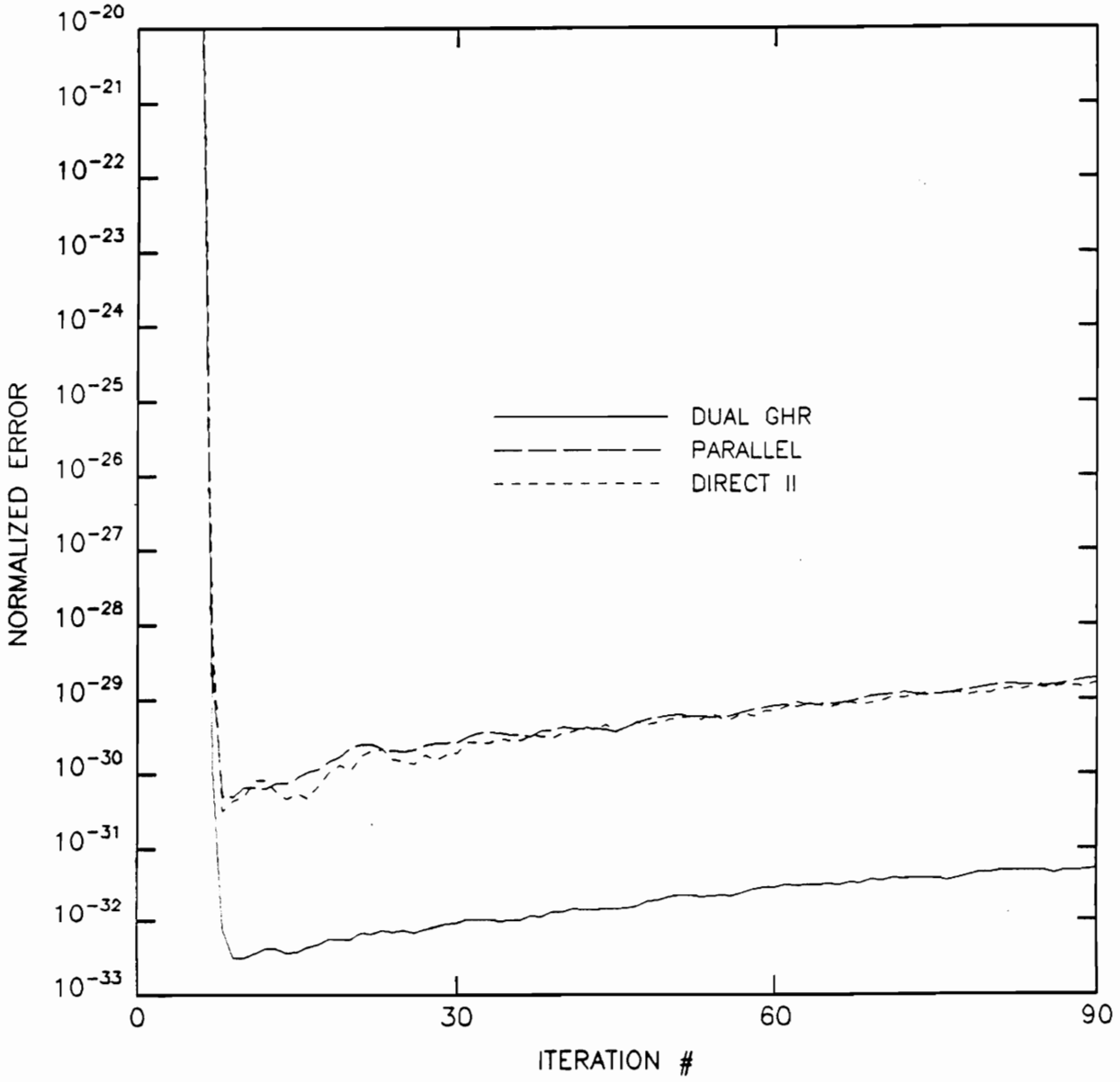

Figure 25. LP1, Overparameterized model with local Θ_0

structure. Now, suppose we take as the initial parameter guesses the end system from the DII identifier shown in Figure 23. The new identification convergence is shown in Figure 25. The structures now converge at the τ predicted rate, i.e. with the DGHR performing the best, the PRLL the worst and the DII in the middle. Apparently, τ is still meaningful for this overparameterized situation.

5.5 *The Underparameterized Model*

Here, the model set does not encompass the true system. Thus, the true system looks "noisy" to the reduced-order model, even when the measurements are exact. One does not expect that the different structures will converge to equivalent systems. Since all convergence results given previously are based on the converged-to system, the τ of interest will correspond to different systems! Thus, a natural question to ask is: Is Conjecture (C.1) system dependent? As we shall see, the answer to the question with respect to 3^{rd}-order modeling of system BP2 is no. To explore this area, we examine system BP2. We start the examination of this system by commenting on the system order.

System BP2, while a 4^{th}-order system, is close to a 2^{nd}-order system. That this is so can be seen by noticing that the pole frequencies lie between the zero frequencies (thus creating the bandpass characteristic in the first place). The magnitude of the transfer function has a peak between the real pole frequencies, and it falls off on both sides. Of course, this general shape can be achieved with one conjugate pair of pole frequencies and adequately placed zero frequencies.

We naively want to identify this system BP2 by using a 3^{rd}-order model with no noise in the measurements. Of course, since the true system is of higher order, no 3^{rd}-order model is going to have an impulse response which exactly matches the measured impulse response, so that we have in effect a "noisy" measurement. Since the true system BP2 is close to a 2^{nd}-order system, we should be able to identify a model with an impulse response which is fairly close to the measured

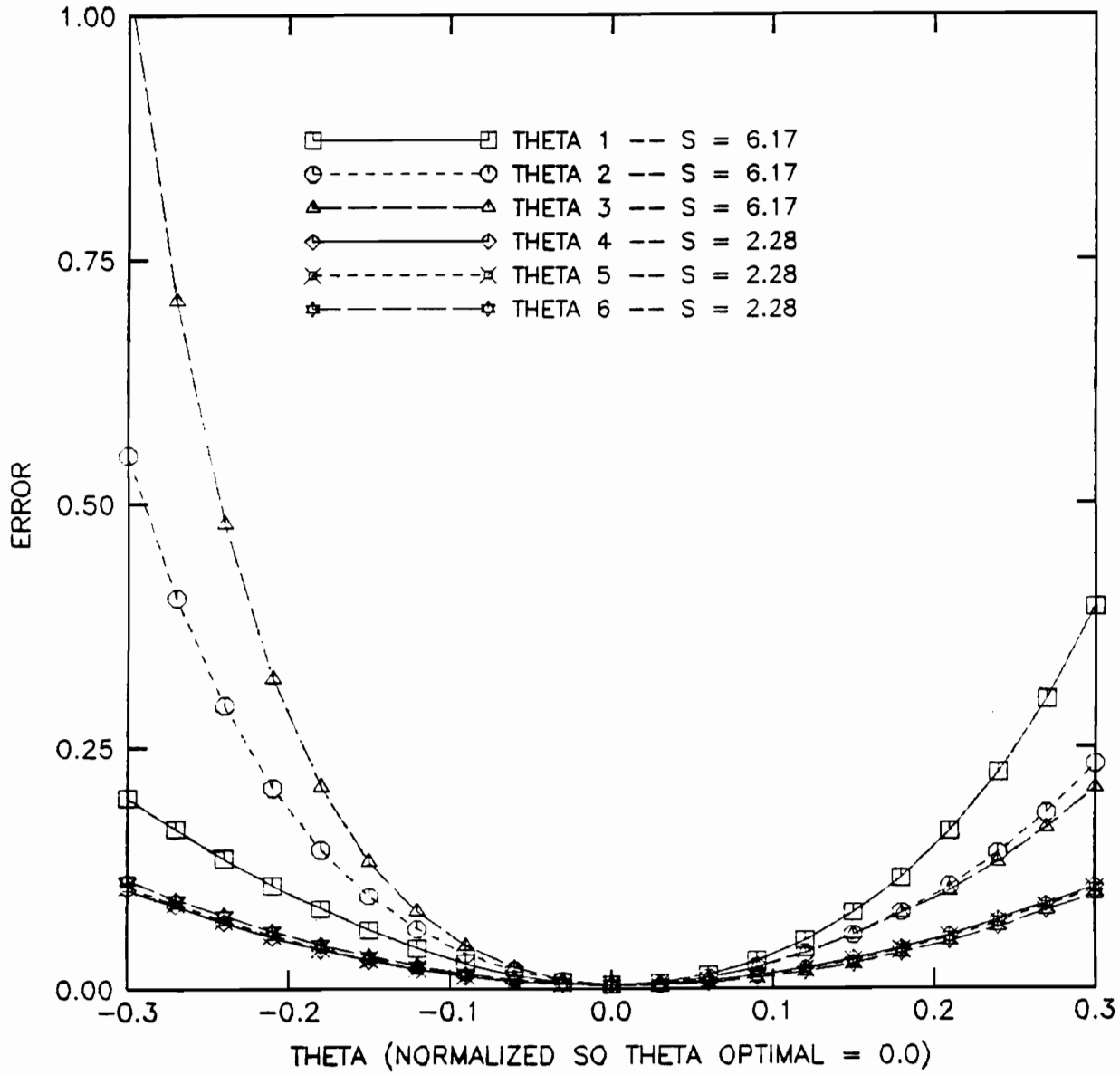

Figure 26. BP2, Reduced-order model DII local minimum (N = 20)

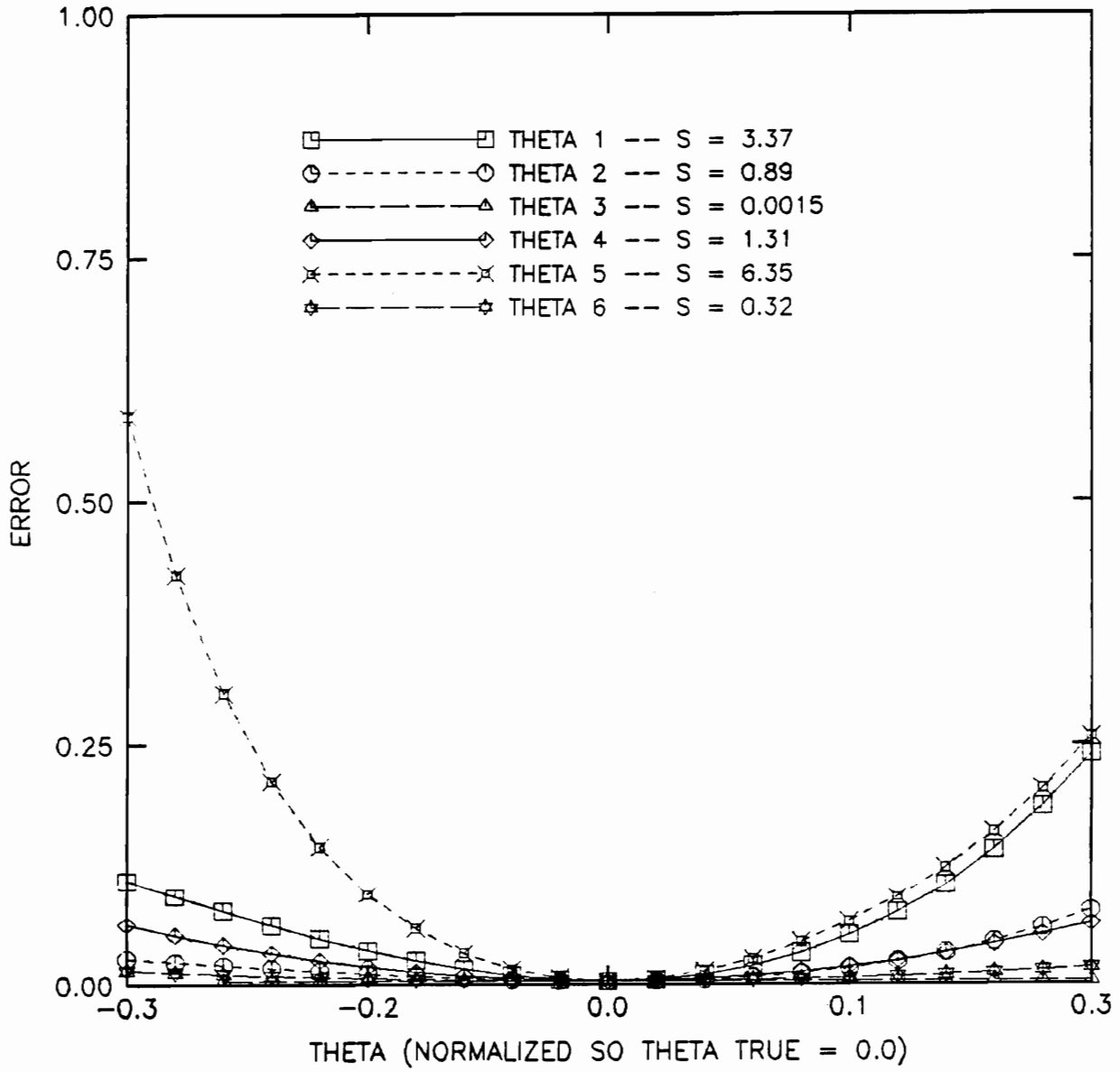

Figure 27. BP2, Reduced-order model DGHR global minimum (N = 20)

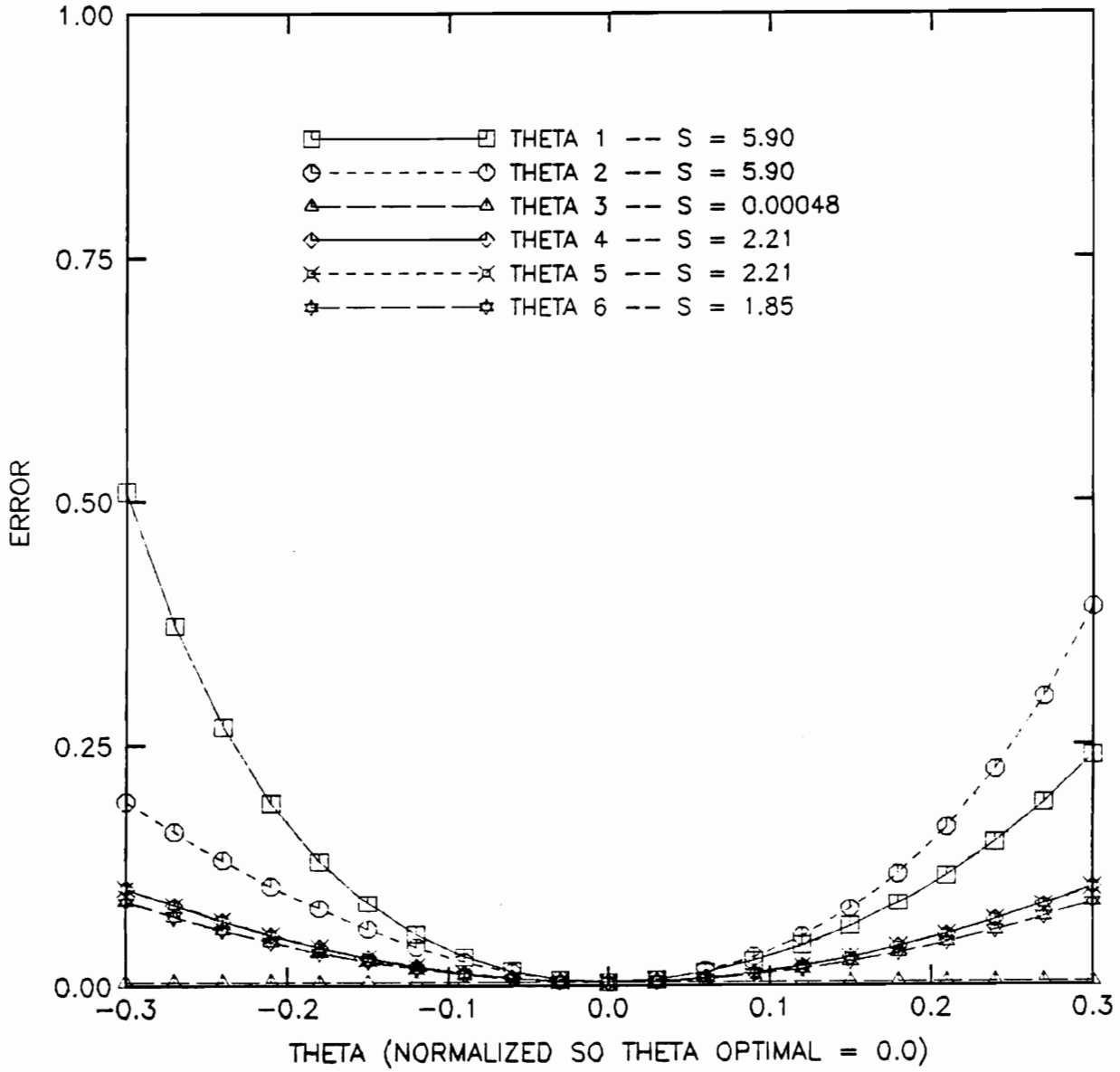

Figure 28. BP2, Reduced-order model PRLL global minimum (N = 20)

impulse response. We begin the identification for all 3 structures at a randomly determined initial system. We allow each structure to converge. This convergence may entail the restarting of the identification algorithm (Algorithm (A.2)) so that a very good estimate of the solution point is achieved. **This end system is different for the 3 structures** (see Table 2). We actually check to see that the converged-to system is a minima of J_N by computing the error curves shown in Figure 26 through Figure 28. The τ corresponding to each solution point is:

1. DII -- τ = 4611.71
2. DGHR -- τ = 777.53
3. PRLL -- τ = 3832.09

The normalized error ($\frac{1}{20} J_{20}$) is inversely proportional to τ.

We know that the solution point for the DII structure is a local minimum because if we start the identification at a different location the structure converges to the point in parameter space shown in Figure 29. The corresponding τ for this DII structure is only τ = 209.35. By starting the identifications for each structure at a point in parameter space near the global minima (a point such that J_{20} is the same for all structures), we see that the identification follows Conjecture (C.1) (see Figure 30). The DII structure converges fastest (and to the lowest error), followed by the DGHR structure and finally by the PRLL structure. We also note that τ appears to be connected to the absolute minimum of the criterion J_N. The local minimum of the DII structure has the highest τ, and it also has the largest non-zero minimum of all the minima found in this section. The global minimum of the DII structure has the lowest τ, and it also has the smallest value for J_{20} found in this section. The DGHR and PRLL structure have minima which are extremely close to each other, but still the DGHR structure has both a lower τ and smaller minimum J_{20} than the PRLL structure has. While the heuristic support for considering the measure τ is based on convergence rates, this data suggest that τ is also positively correlated to the closeness of J_N to 0.

We also note that in the above cases, the minima correspond to systems which have near pole/zero cancellations (see Table 2). The local minimum for the DII structure contains its near pole/zero cancellation at the origin, while the global minimum has its near cancellation on the

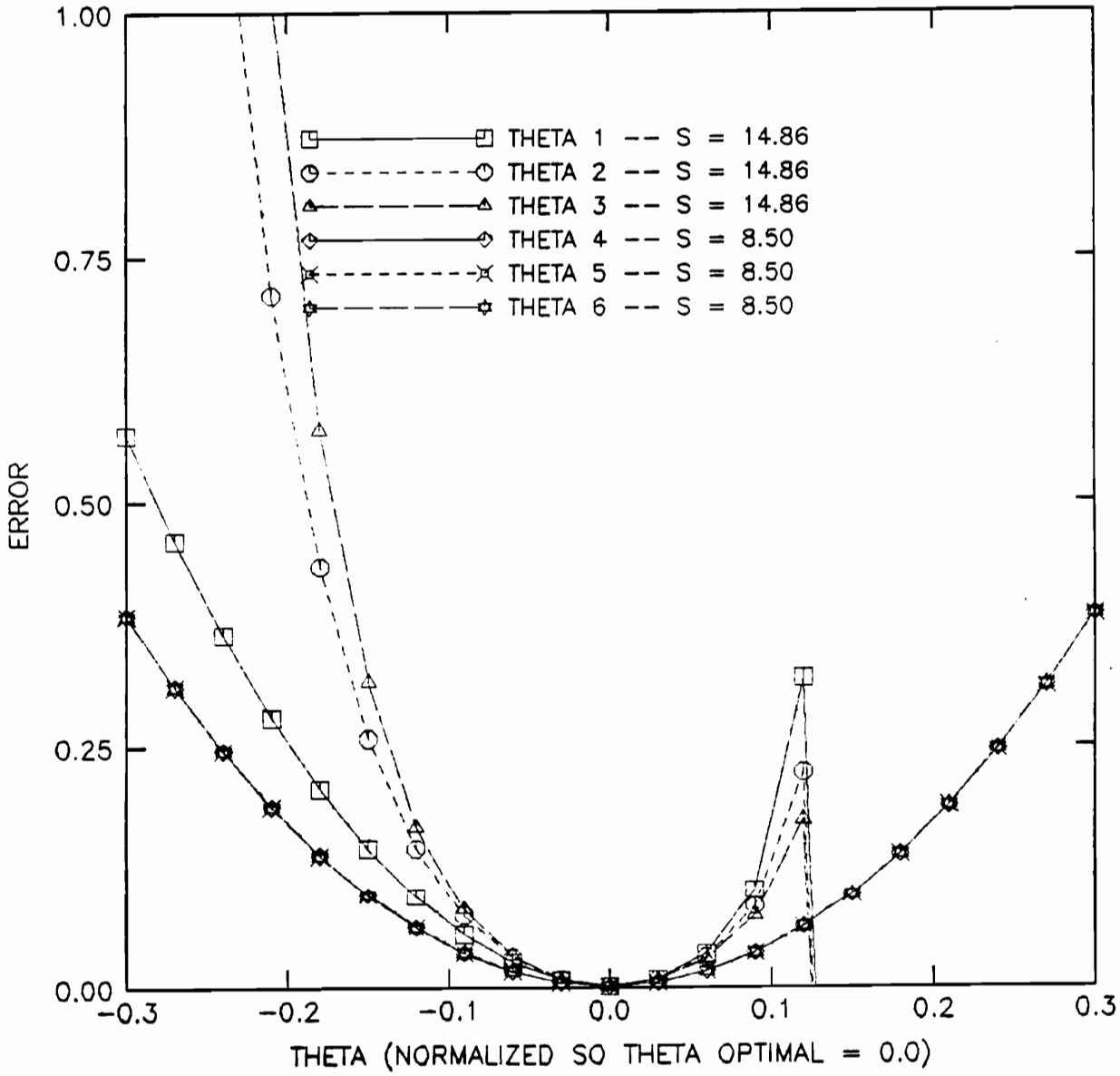

Figure 29. BP2, Reduced-order model DII global minimum (N = 20)

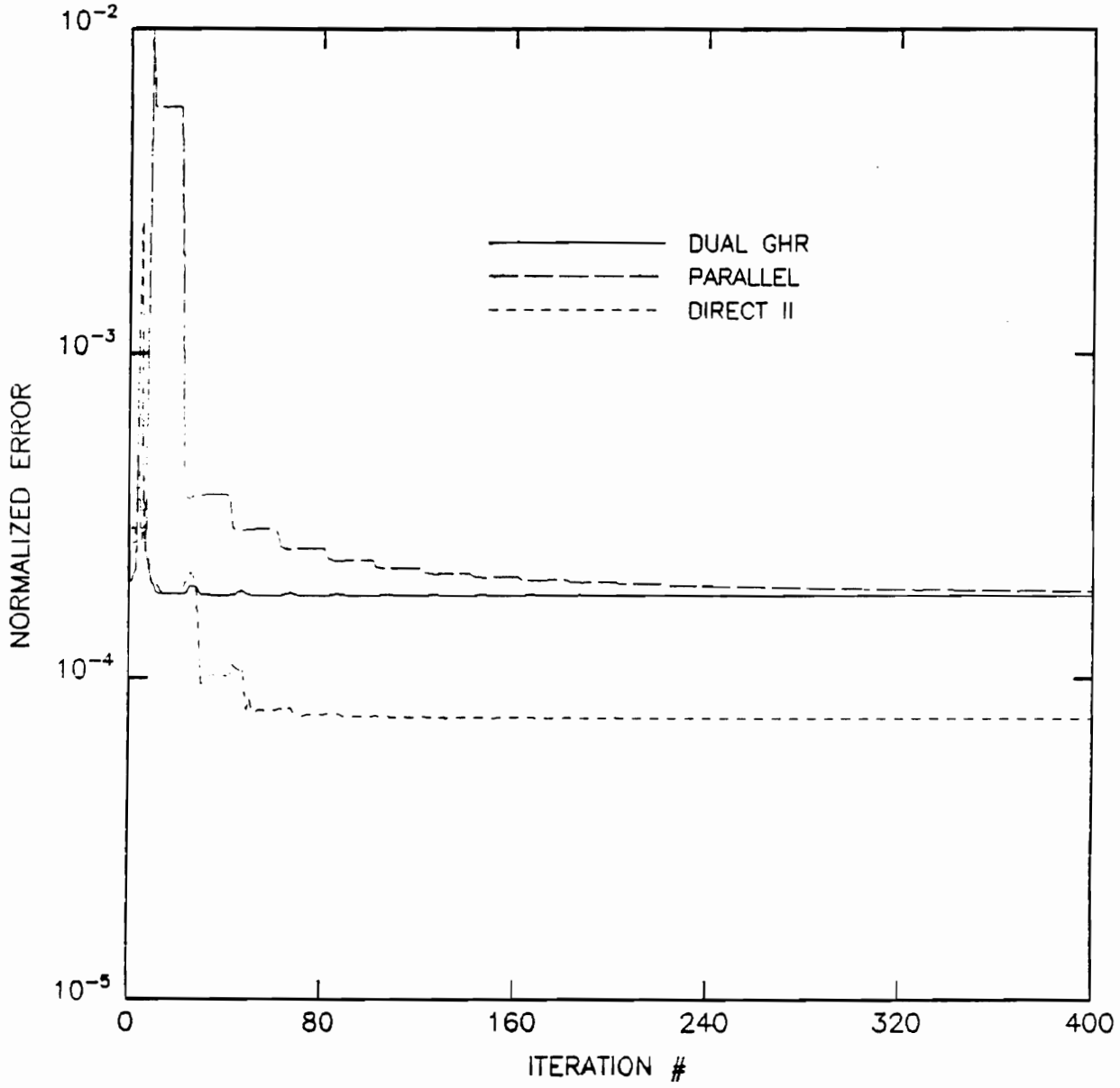

Figure 30. BP2, Reduced-order model normalized error convergence (N = 20)

Table 2. Pole/zero information for BP2 converged-to systems

	Zeros	Poles	
DII (local)	0.6054, -0.0432	$0.6859^{\pm j0.255\pi}$	0.0203
DII (global)	0.3784, 0.8618	$0.6628^{\pm j0.272\pi}$	0.7810
DGHR	0.5470, -0.7284	$0.6934^{\pm j0.260\pi}$	-0.7392
PRLL	0.5486, -0.6696	$0.6928^{\pm j0.259\pi}$	-0.6696

positive real axis (at 0 frequency). Both the DGHR and PRLL structures place theirs on the negative real axis (at half the sampling frequency).

Finally, we note that if the identification of all 3 structures is run in parallel (i.e. if all 3 structures are identified simultaneously), the structure with the smallest τ is again the single best structure to identify. This fact suggests that monitoring τ can lead to better identification in a shorter amount of time. As we have seen, this situation has occurred in all cases -- when the model order is too high, too low or exactly correct. This is important in a practical situation.

5.6 Deterministic Algorithm Conclusions

For single-input single-output systems, the identifier structure has been shown to make a difference in the convergence rates of the identified parameters. The influence of the structure comes through observation of the parameter correlation matrix or its inverse, the Fisher information matrix. One influence is the sensitivity of the system to its parameters. This system measure indicates the degree to which the individual parameters of the system are identifiable. However, by itself, the sensitivity measure is not enough to predict convergence behavior, as the parameters of the system are not isolated from each other, but rather are connected in a nontrivial manner. This interconnection between parameter vector elements is measured by the condition number of its Fisher information matrix. Examination of these system measures was motivated by numerical arguments on the shape of the optimization criterion J_N. As we shall see in Chapter 6, motivations for examining these measures come also from optimal input design as well as Lyapunov and Martingale convergence theory. Based on observation, a measure τ was introduced and a conjecture based on this time constant was offered. The inadequacy of the conjecture is that all convergence results are connected with upper bounds on the errors, and for relative convergence rates a lower bound on the error is also required. As noted in the introduction, Chapter 1, no lower

bound exists, since convergence might be arbitrarily fast for any given initial condition specifications.

6.0 The Stochastic Algorithms

In this chapter, Algorithms (A.1) and (A.2) as used in a stochastic sense are considered. Repeated noisy impulse response measurements are made and used in this implementation, so that convergence is to a set of system parameters which represents a minimum of J_N over **all** runs used. For output error methods in the presence of additive Gaussian noise, these converged-to-parameters are the true system parameters, and so the noise is averaged out in this case [75].

6.1 Analyzing Stochastic Convergence

As noted in Chapter 2, Lyapunov theory does not attempt to quantify transient convergence speed. Lyapunov functions can guarantee asymptotic convergence, but whether that convergence is 10^{-t} or even 10^{-10t} can not truly be determined. However, an interesting coincidence occurs in RPEM algorithms. The optimization criterion J_N is in this case a truncated version of the natural Lyapunov function ($\sigma_e^2(\Theta)$) used in convergence analysis. We noted this in Chapter 4, equation (4.1.3). From [76,103], the following deterministic differential equation is related to the RPEM algorithm:

$$\dot{\Theta}_D = -F_D^{-1} \frac{\partial J_\infty(\Theta_D)}{\partial \Theta}$$
$$\dot{F}_D = G(\Theta_D) - F_D \tag{6.1.1}$$

where $G(\Theta)$ is the correlation matrix of Φ. Here, the subscript D refers to the deterministic versions of the parameters Θ and Fisher information matrix F. These equations, while difficult to analyze, do immediately trigger the notion that the Fisher information matrix directly affects the convergence rate of the parameter vector Θ, through the inverse relationship F_D^{-1}. In fact, as seen from Martingale theory, at the very least the ratio of the maximum-to-minimum eigenvalue of this matrix has a lot to do with the convergence rate. Also, the duality with optimal input design suggests maximizing the trace of F. Note that at the solution to (6.1.1), the Hessian approximation must have converged to F, and that if F is "large", the parameter gradient $\dot{\Theta}$ is small. Thus convergence of the Hessian approximation ties directly into the convergence of the parameter estimates by Lyapunov convergence theory. We want to examine the Conjecture (C.1) in this context.

6.2 *Stochastic Examples*

Let's now look at system LP1. Since we are only considering structural differences, the identification algorithms of the DII, PRLL and DGHR structures are started with the same initial systems, though the parameterizations are quite different, of course. In this case, 6 impulse response samples are used to recursively identify the system (60 cycles of 6 samples = 360 iterations) with a 40 dB SNR. Figure 31 shows the relative convergence of the three models. After 70 iterations the DGHR model clearly outperforms the DII model, while both of these structures have identified the system better (in the J_N sense) than the PRLL model. However, in the first 20 iterations or so, the DII model structure is as good as, or better than, the DGHR structure (see Figure 32).

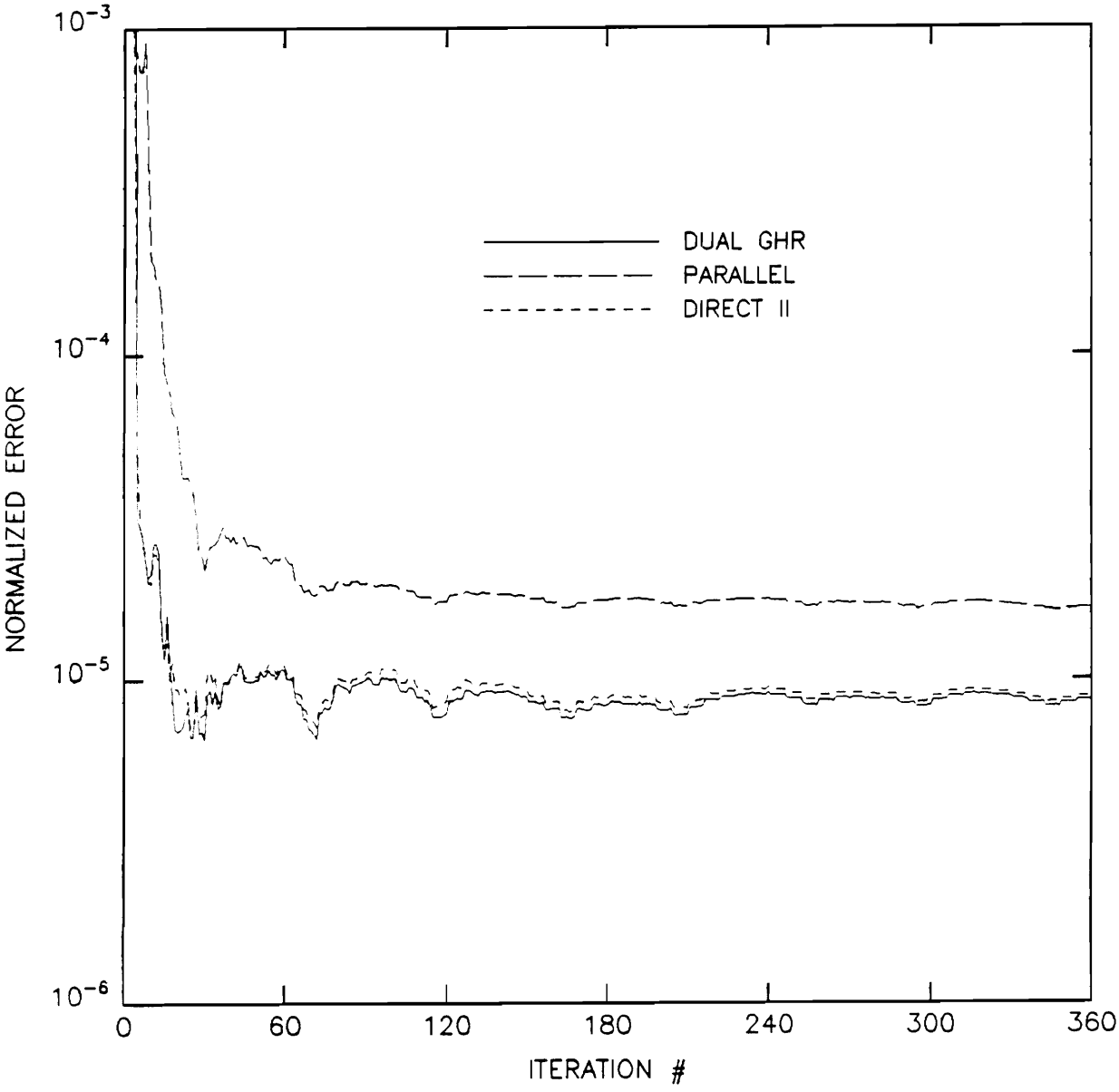

Figure 31. LP1, Normalized error for 360 iterations, 40 dB SNR (N = 6)

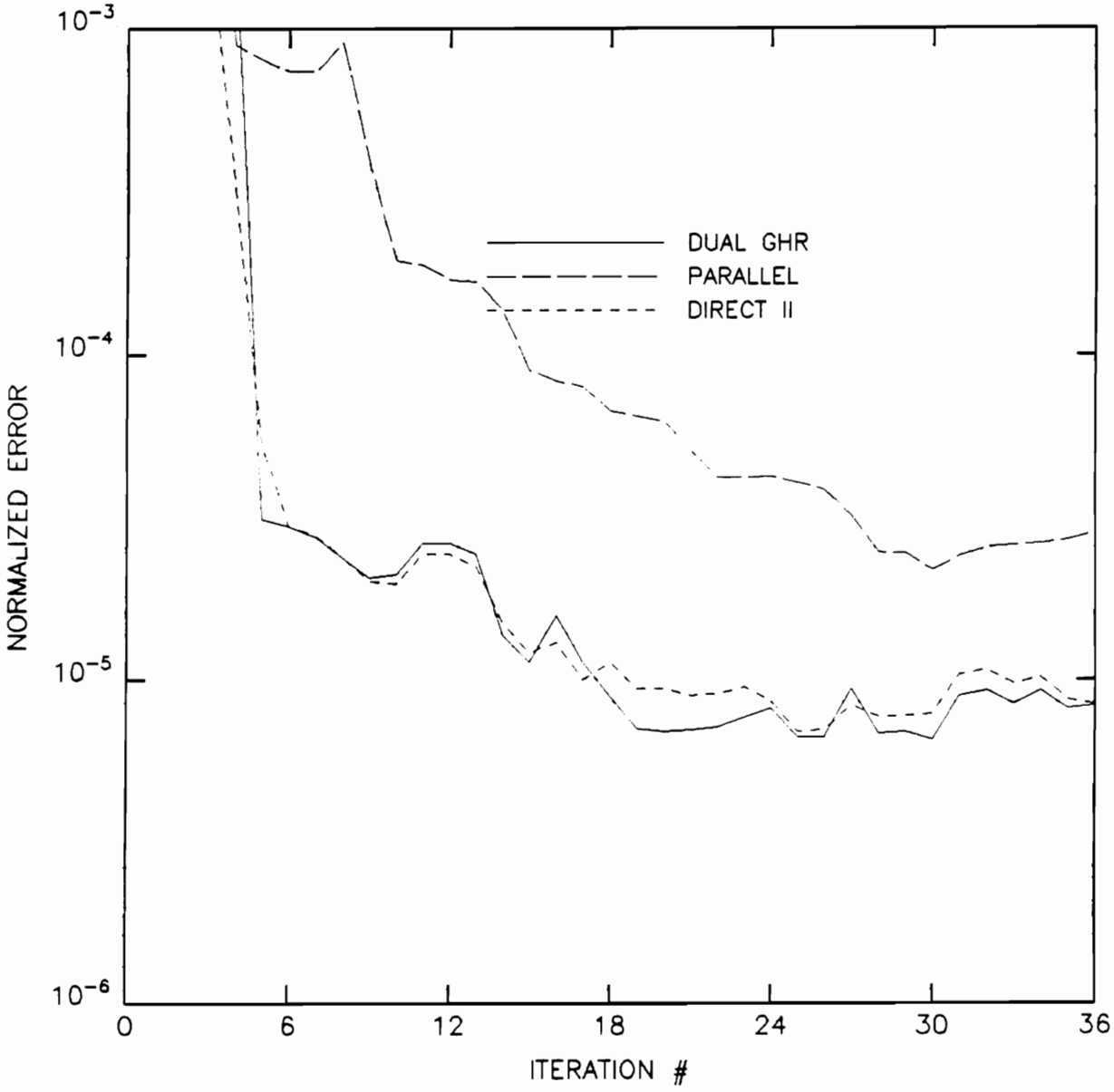

Figure 32. LP1, Detailed normalized error (first 36 iterations), 40 dB SNR

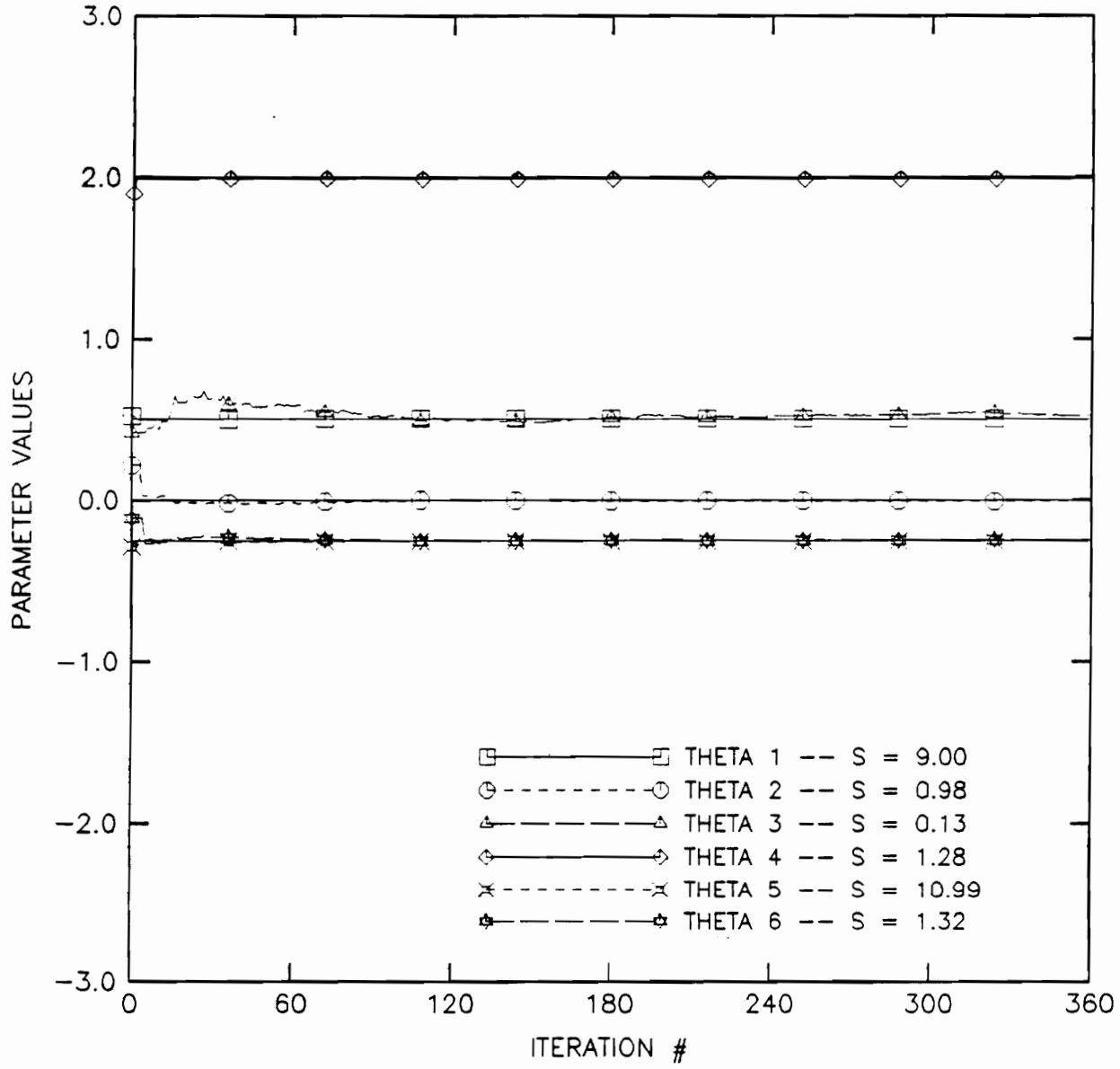

Figure 33. LP1, DGHR parameter convergence

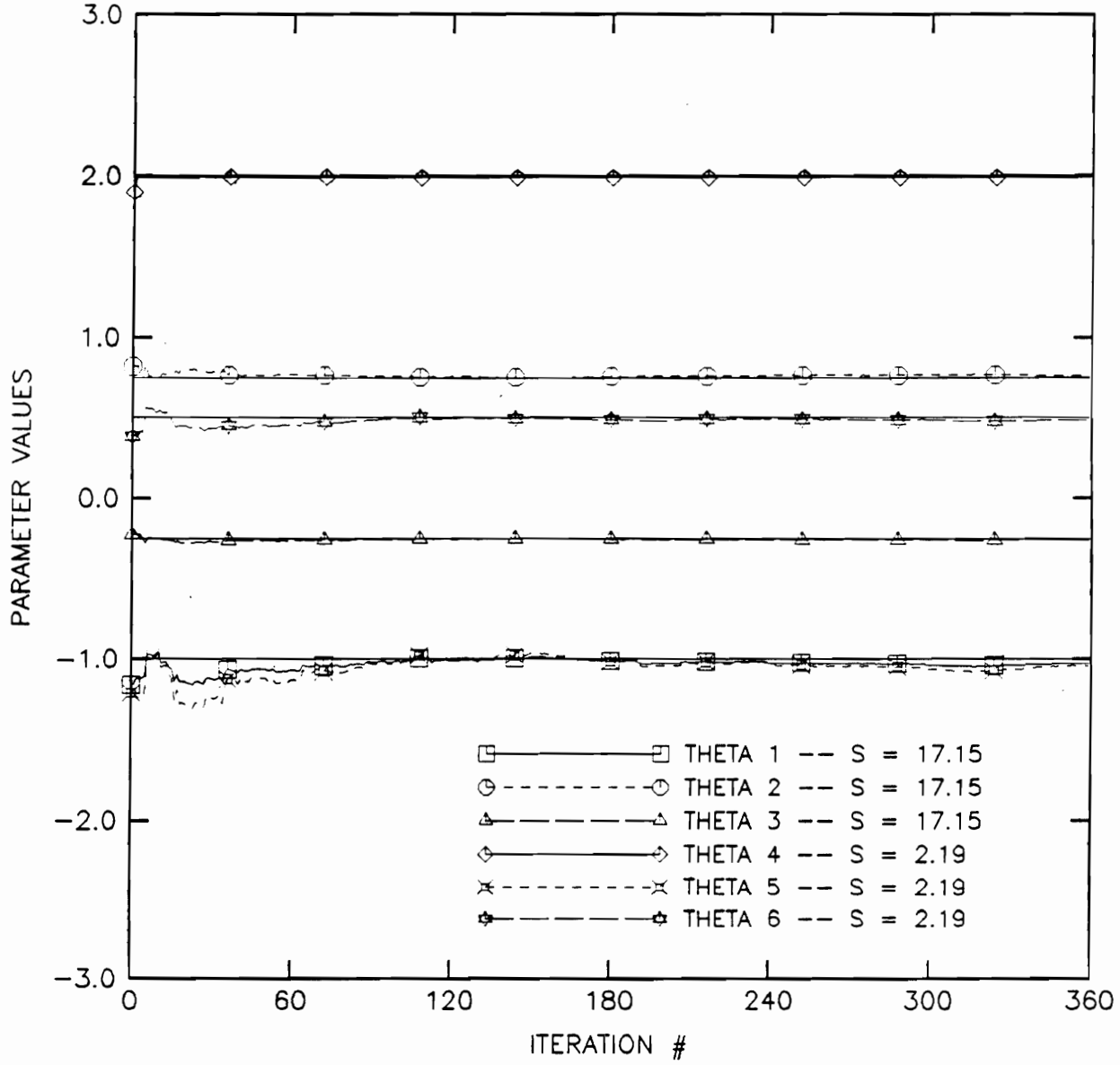

Figure 34. LP1, DII parameter convergence

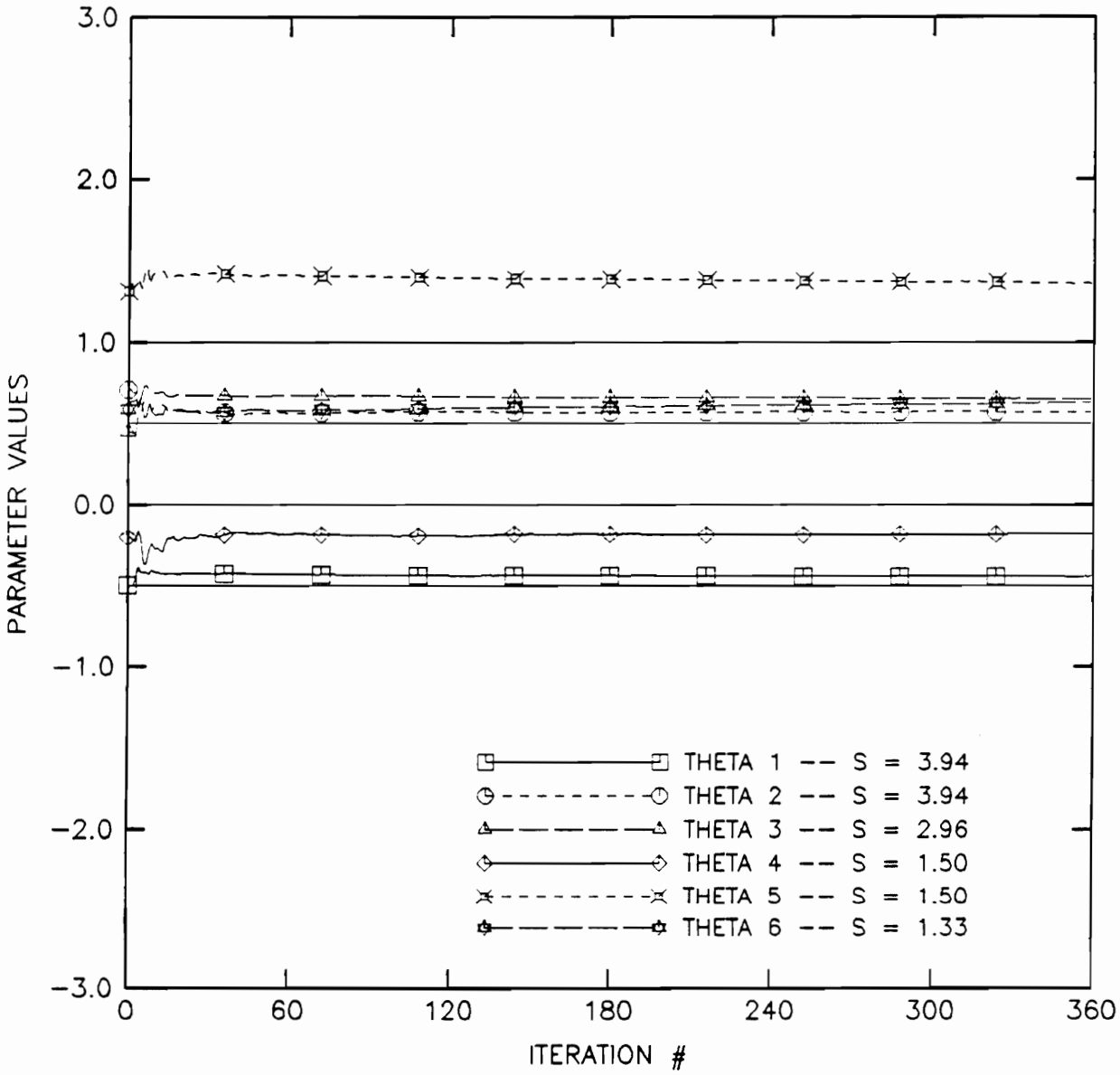

Figure 35. LP1, PRLL parameter convergence

To help explain these occurrences, we need to refer to Figure 33 through Figure 35. From the first of these figures, Figure 33, one can easily see that all the estimated parameters are fairly close to their true value (the solid lines without symbols) after 20 iterations, except for $\Theta(3)$. This parameter has the lowest sensitivity of all the parameters, and a look at the error curves in appendix B shows that this parameter has a very flat error curve indeed! Consequently, this parameter is free to wander around without significantly affecting the optimization criterion J_6. On the other hand, Figure 34 shows that the DII parameter estimates wander a little more than the DGHR parameter estimates do. Finally, Figure 35 shows that the PRLL estimates seem to be turned off after the 50^{th} iteration or so. Examination of the parameter gains (the L_k in Algorithm (A.1) or G_k in Algorithm (A.2)) reveals that the algorithm has indeed quit identifying the system parameters, as these gains are rapidly approaching zero. A reinitialization of the PRLL identifier at this end system proves that the algorithm works, as the identified parameters quickly converge to their true values; however, the parameters again start to drift away, the gains again approach zero, and the noise effects begin to play a relatively important part. It seems that the PRLL parameterization is ill-suited for the identification of this system. Look at the error curves for the PRLL structure in Appendix B. Large changes in the parameters can (and will) have relatively little effect on the system output. Notice that the end convergence behavior is according to τ as predicted from Conjecture (C.1).

Now, how do these plots explain the convergence? We conjecture that the steep error curves of the more sensitive DII model allow a quicker convergence to a neighborhood of the true system, but that the less sensitive DGHR structure has inherently better noise rejection. The PRLL structure not only has flat error surfaces (low sensitivity), but it also has relatively poorly conditioned parameters at that. Note also that neither the conditioning κ_2 nor the sensitivity S predict the convergence, only τ does!

With initial guesses which are much further away (outside the region in parameter space for which J_N is quadratic in the parameters), the convergence behavior is not as τ would indicate. For example, Figure 36 shows that the PRLL structure can have good performance. However, with a 200 dB SNR, Figure 37 shows clearly that the convergence is now τ predicted (which one would

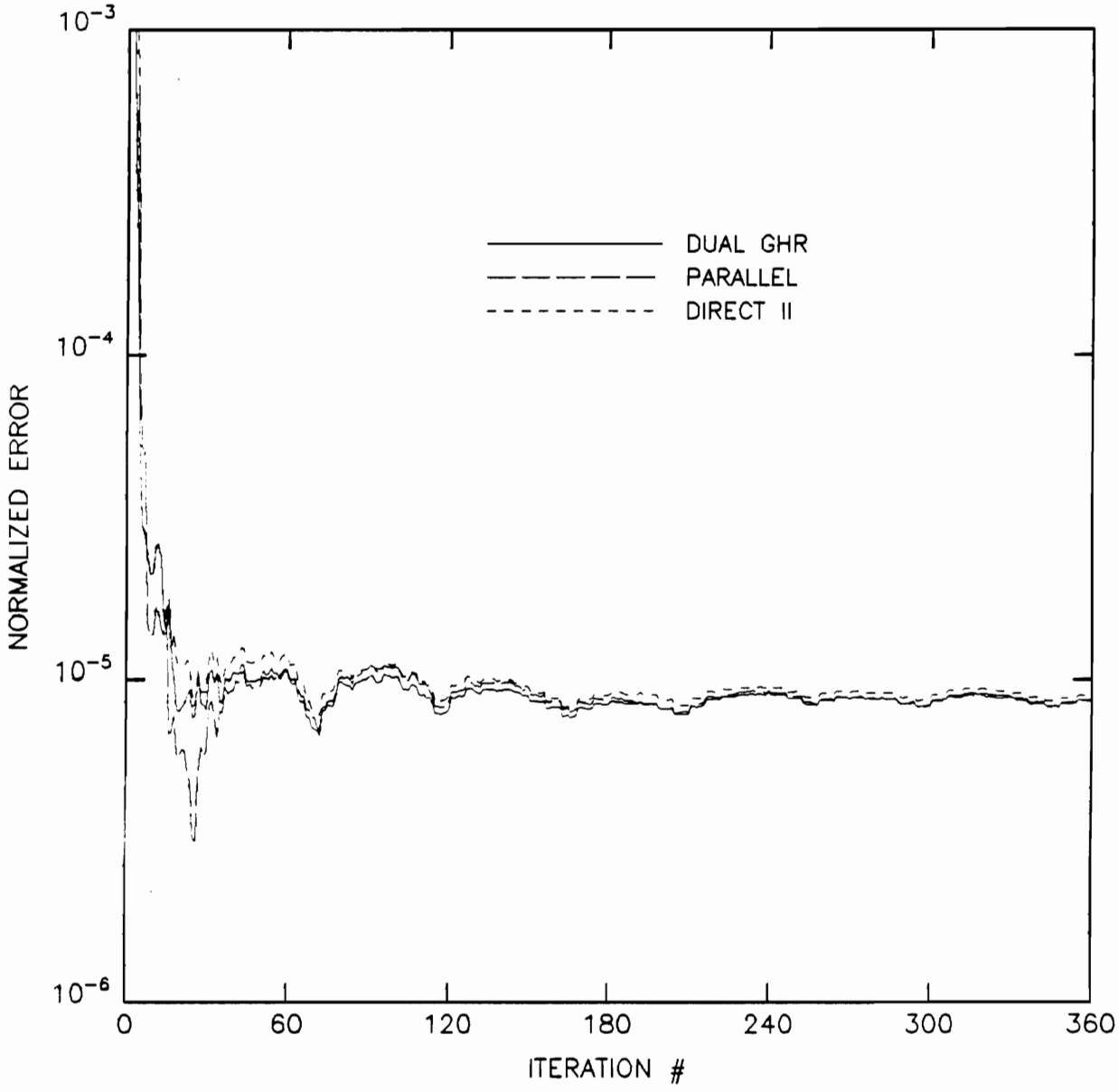

Figure 36. LP1, Normalized error (IC far away), 40 dB SNR

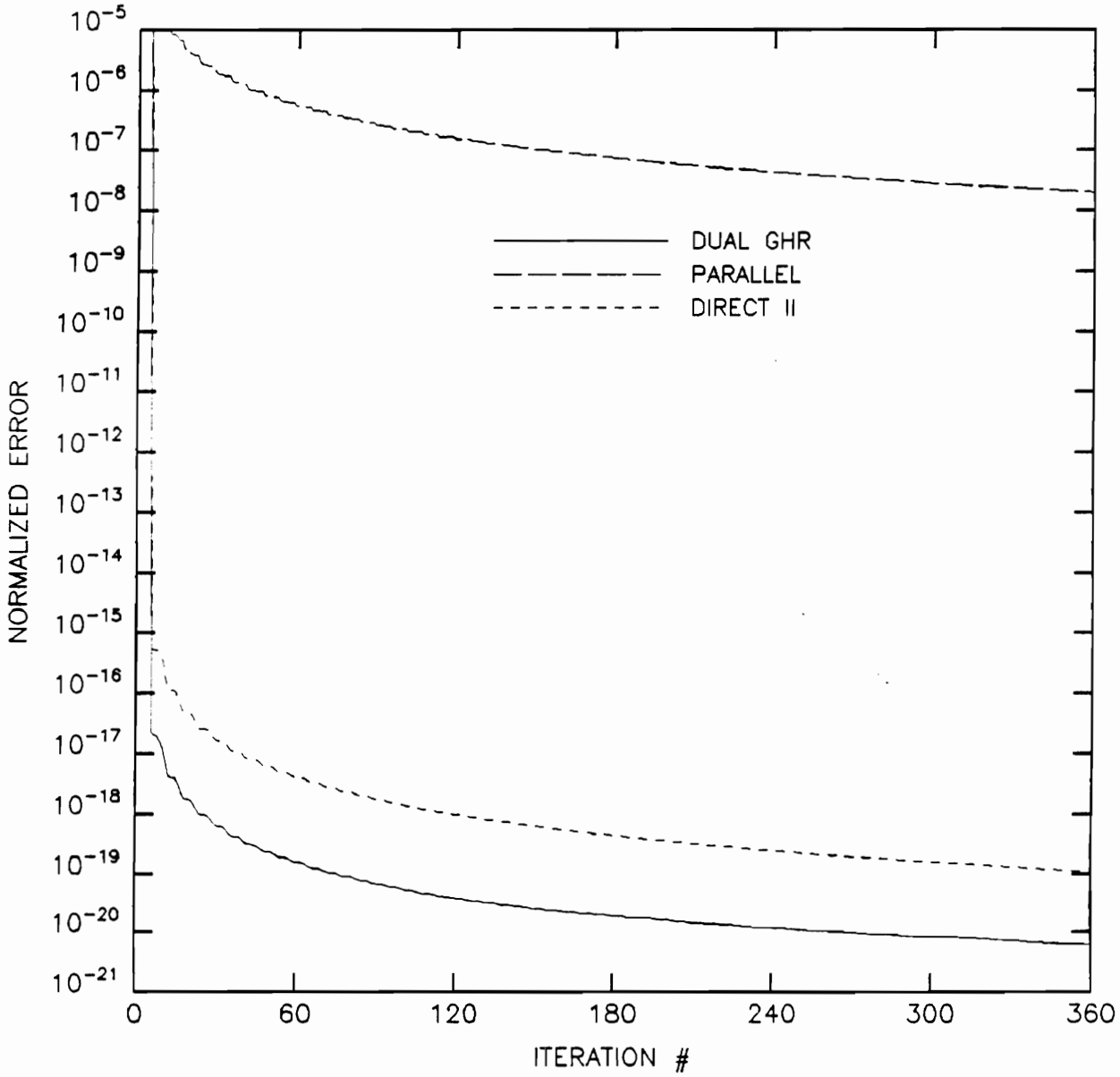

Figure 37. LP1, Normalized error (IC far away), 200 dB SNR

expect from looking at the simulation in Chapter 5). The PRLL algorithm cannot handle any more noise, as a few less dB in SNR dramatically increases the normalized error. In fact, a few more dB in SNR also dramatically increases the normalized error. If one looks at Figure 36 carefully, a deep drop in the error is noticeable at about the 20^{th} iteration. Apparently, the noise realization is such that the PRLL structure just happens to converge quickly. To test this hypothesis, the exact same simulation was run with different noise realizations. In this case, the PRLL structure performs markedly worse, with a final error around 7×10^{-4}.

For LP2, Figure 38 shows the estimate convergence for one simulation. Notice that the DII structure hardly converges at all. Also, note that the PRLL and DGHR convergence is as expected. This may be explained by the noise realization used to create the simulated impulse response measurements. By picking a different realization with a higher SNR, we can get the conjecture (C.1) predicted convergence: PRLL best, DII middle and DGHR worst of all. This is shown in Figure 39 and Figure 40. Note the dip in the DII and DGHR errors within the first 5 iterations. The PRLL structure overcomes this initial disadvantage, however, and actually outperforms the other 2 by the 11^{th} iteration. Since $N = 25$, not all of the samples have been used even once. More importantly, the system order is 3, so that 6 samples minimum are required to fully identify the system (at least in a no noise situation). Thus, these initial error advantages for the DGHR and DII structures do not carry on throughout the identification. Note also that these 2 structures have sensitivities 1 and 2 orders of magnitude higher than the PRLL structure. This may help explain the initial convergence results. However, the conditioning of the PRLL structure helps it to overcome the sensitivity disadvantage and ultimately to outperform the other 2 structures. One idea is that the sensitivity advantage may be sufficient to propel the parameter estimates into a neighborhood of the solution point, and thus a structure starting from a nonlocal initial parameter guess may overcome other parameterizations with a smaller τ. We want to stress that this does not invalidate Conjecture (C.1) since the conjecture depends on local initial conditions.

That the amount of noise can affect the convergence rates is also detailed in the simulation of LP3. Figure 41 shows that the DGHR and PRLL convergence is unexpectedly reversed, since the DGHR structure has a much higher τ than the PRLL structure. However, if the SNR is

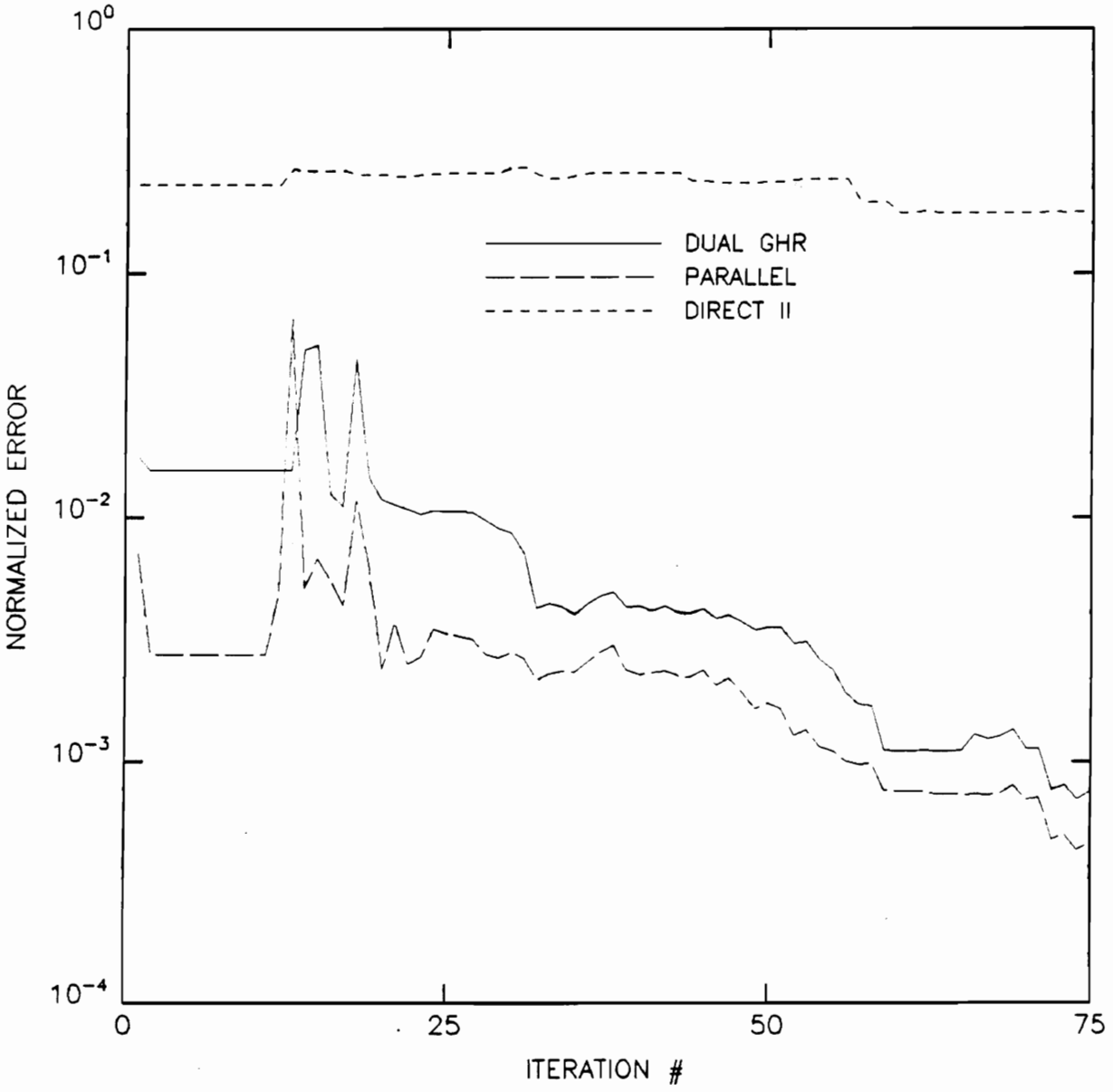

Figure 38. LP2, Normalized error (N = 25), 20 dB SNR

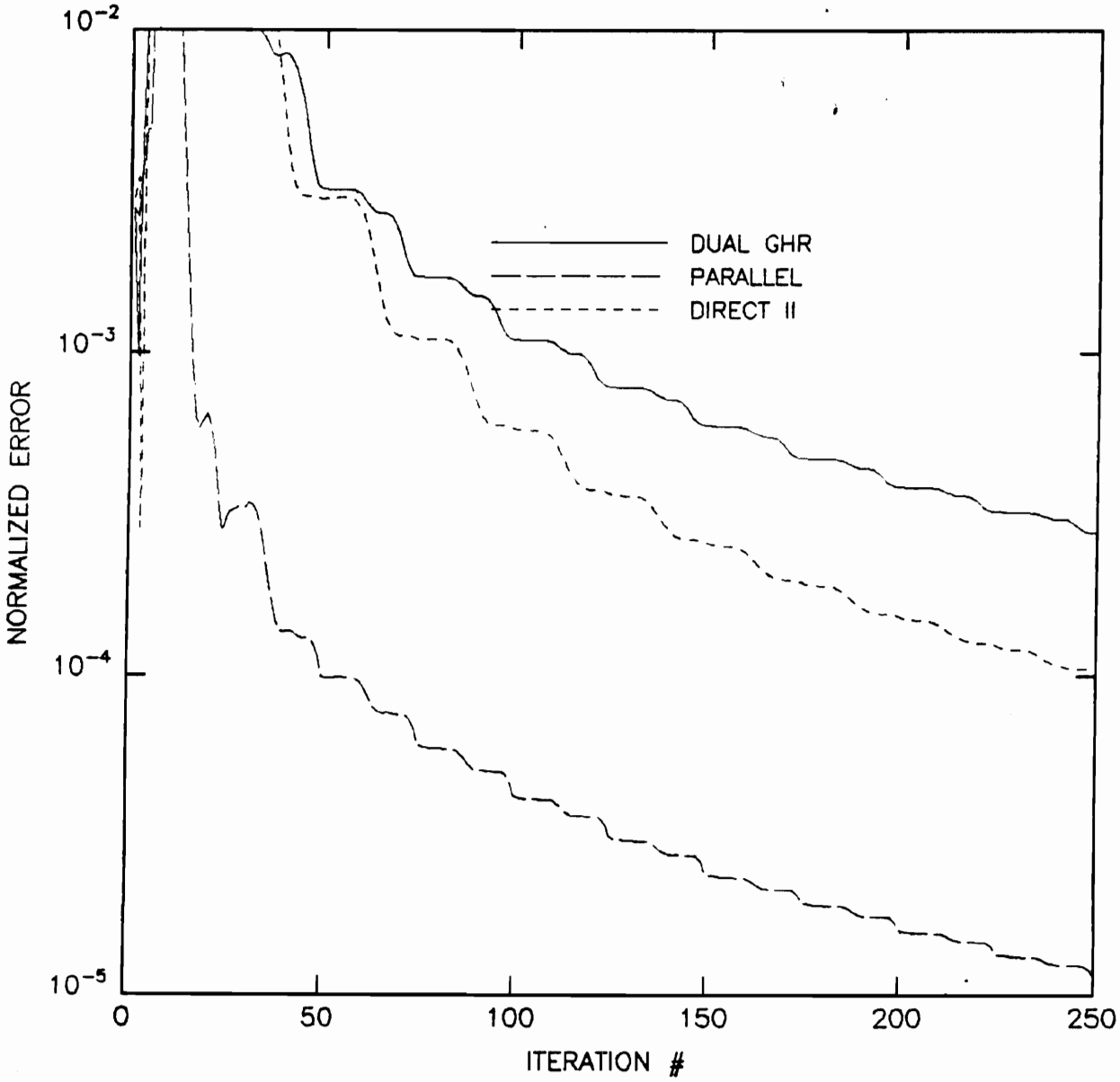

Figure 39. LP2, Normalized error (N = 25), 60 dB SNR

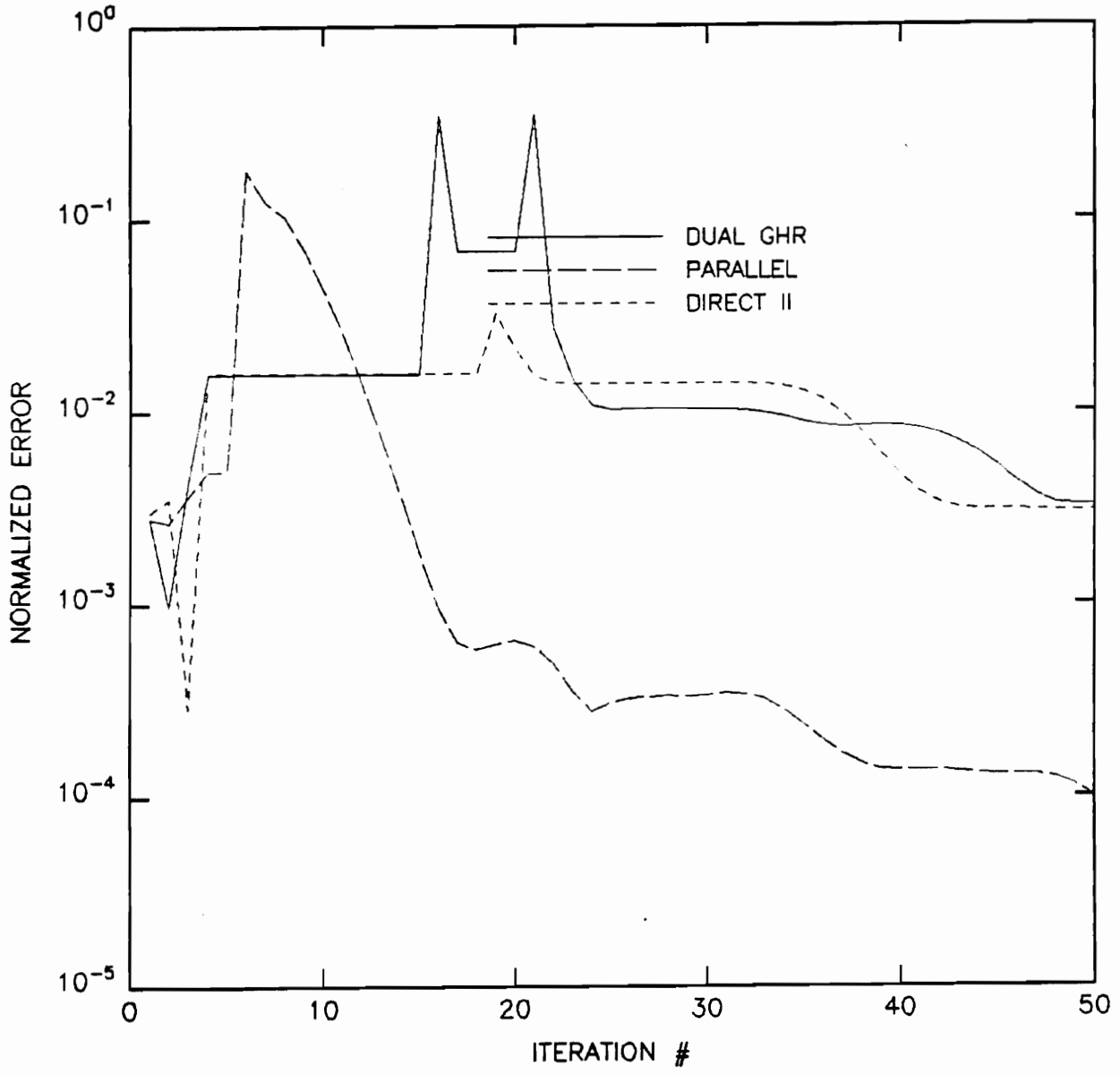

Figure 40. LP2, Normalized error for first 50 iterations (N = 25), 60 dB SNR

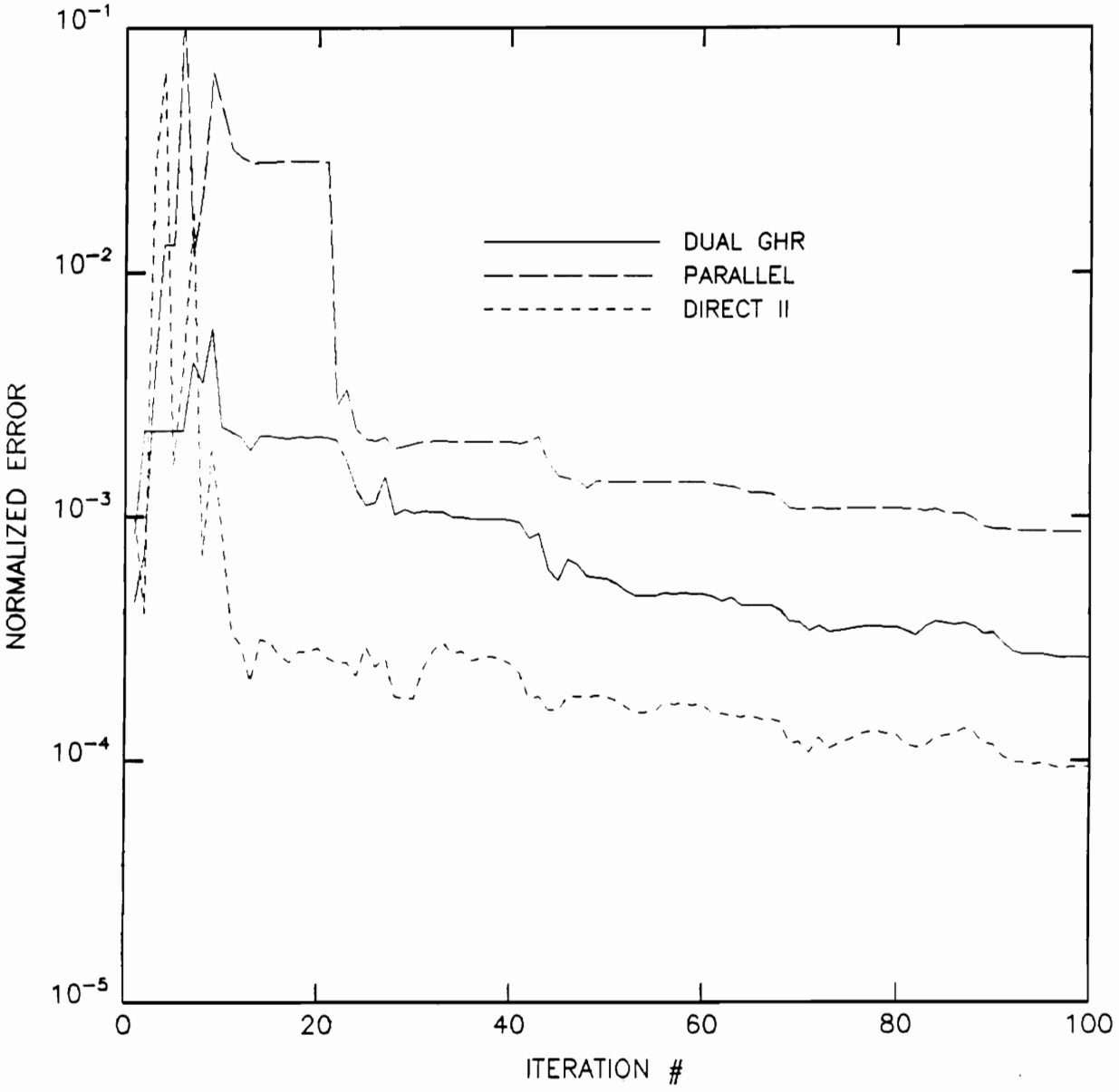

Figure 41. LP3, Normalized error (N = 20), 20 dB SNR

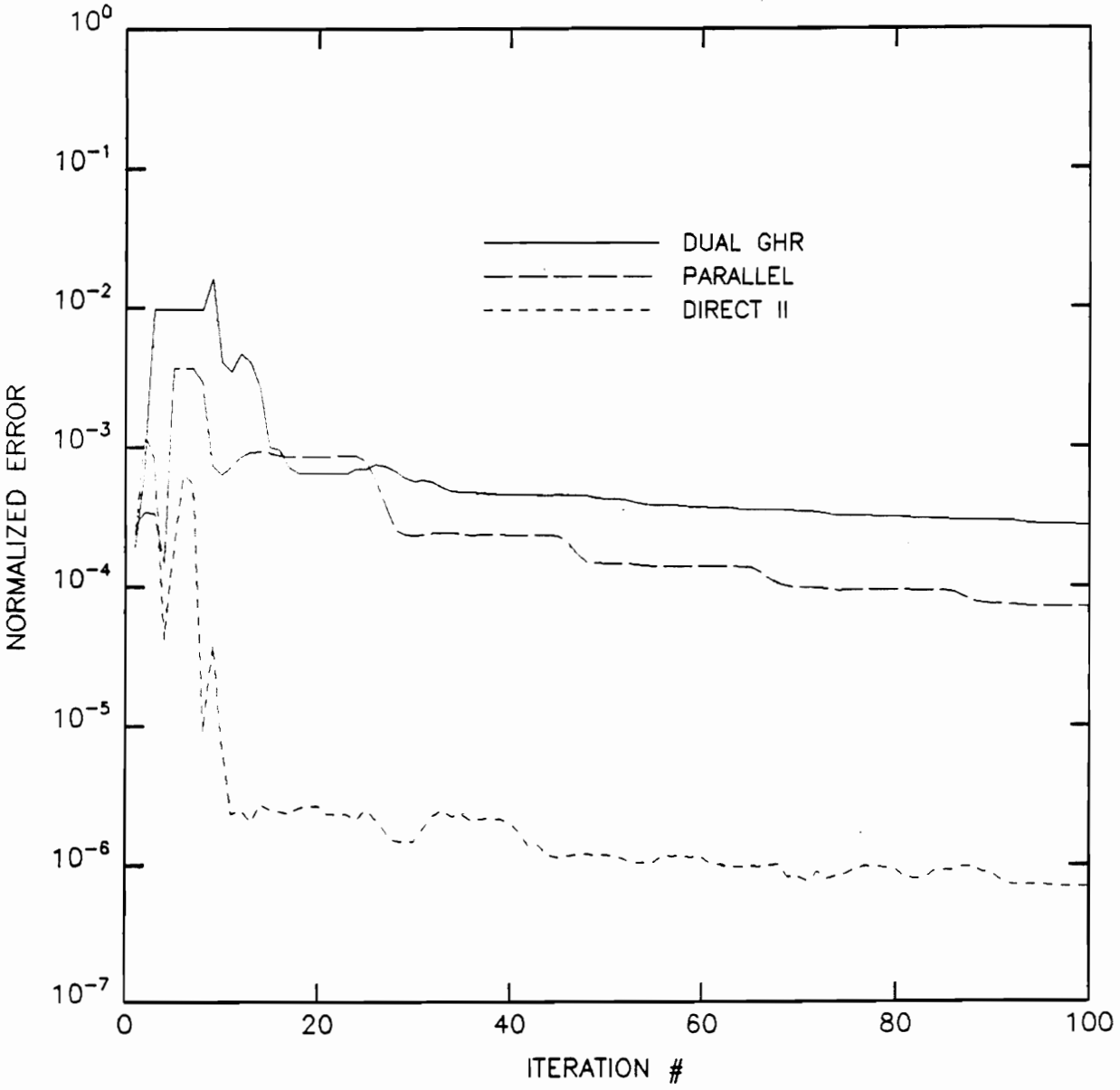

Figure 42. LP3, Normalized error (N = 20), 40 dB SNR

increased to 40 dB as in Figure 42, the convergence reverts back to the τ predicted order. Notice also in these two error vs. iteration plots that the DGHR structure has almost exactly the same error, i.e. the DGHR structure did not respond to the 20 dB increase in noise. Both the PRLL and DII structures have errors which changed by an order of magnitude or more!

An example run for HP1 is shown in Figure 43. Here the convergence is consistent with our Conjecture (C.1). However, if we run the identification using the systems equivalent to the ending DII structure as the initial conditions, we see that the convergence is not explained by τ (see Figure 44). This behavior may be explained by noting that the DII structure parameter estimates get quite far away initially (as compared to the PRLL and DGHR structure identifiers). As the early estimates depend on the initial Hessian approximation (which may not be a very good estimate at all), this behavior cannot be characterized by τ at all.

The plot for BP1 is shown in Figure 45. The convergence here is also consistent with the Conjecture (C.1). Note that early in the identification the DII structure identifier performs slightly better than the DGHR structural identifier. This is consistent with the idea that a highly sensitive structure will have better initial convergence. The conditioning becomes important only later in the estimation process, when the parameter estimates are near the solution.

6.3 Conclusions

We have seen that the convergence of the stochastic algorithms is a natural extension of the deterministic case. As the SNR is increased, the convergence behavior becomes more and more like the deterministic algorithm convergence behavior. This is as expected.

We have also seen that the particular realizations affect the convergence, and that by adjusting the noise energy level or the particular noisy realization, the overall convergence behavior can be different than predicted by the conjecture (C.1). It appears that the structure sensitivity has a strong

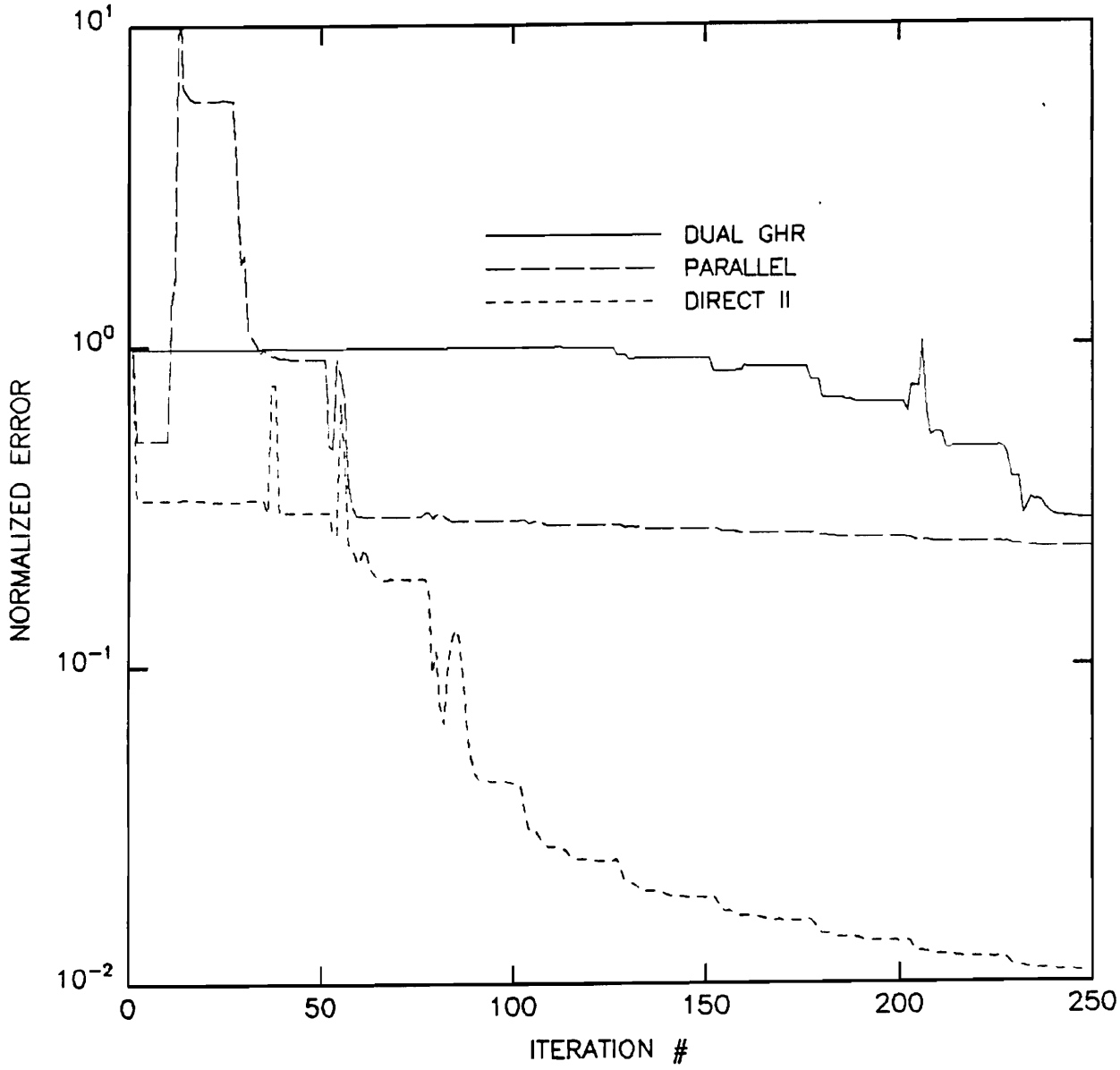

Figure 43. HP1, Normalized error with arbitrary IC (N = 25), 80 dB SNR

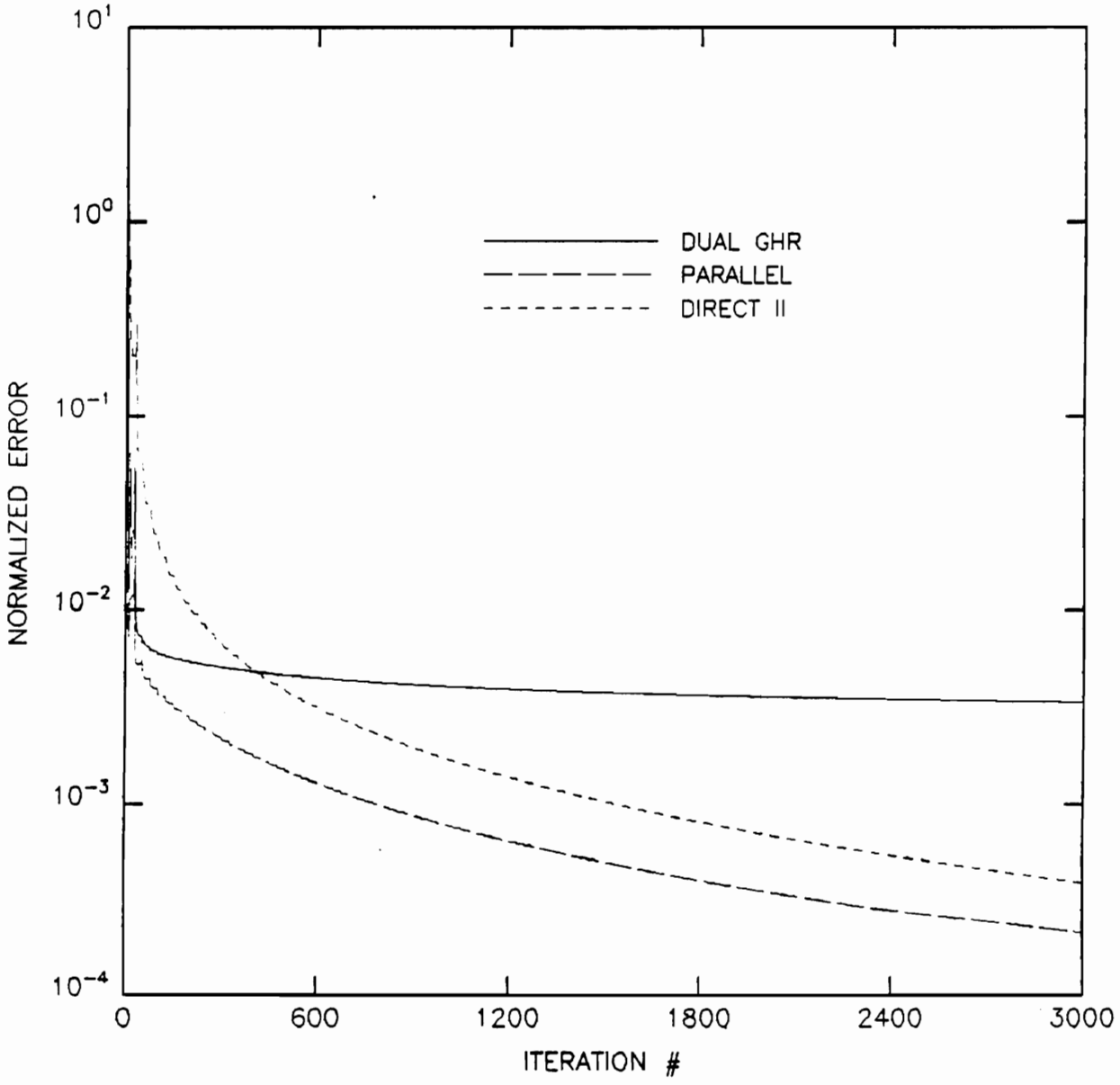

Figure 44. HP1, Normalized error with local IC (N = 25), 80 dB SNR

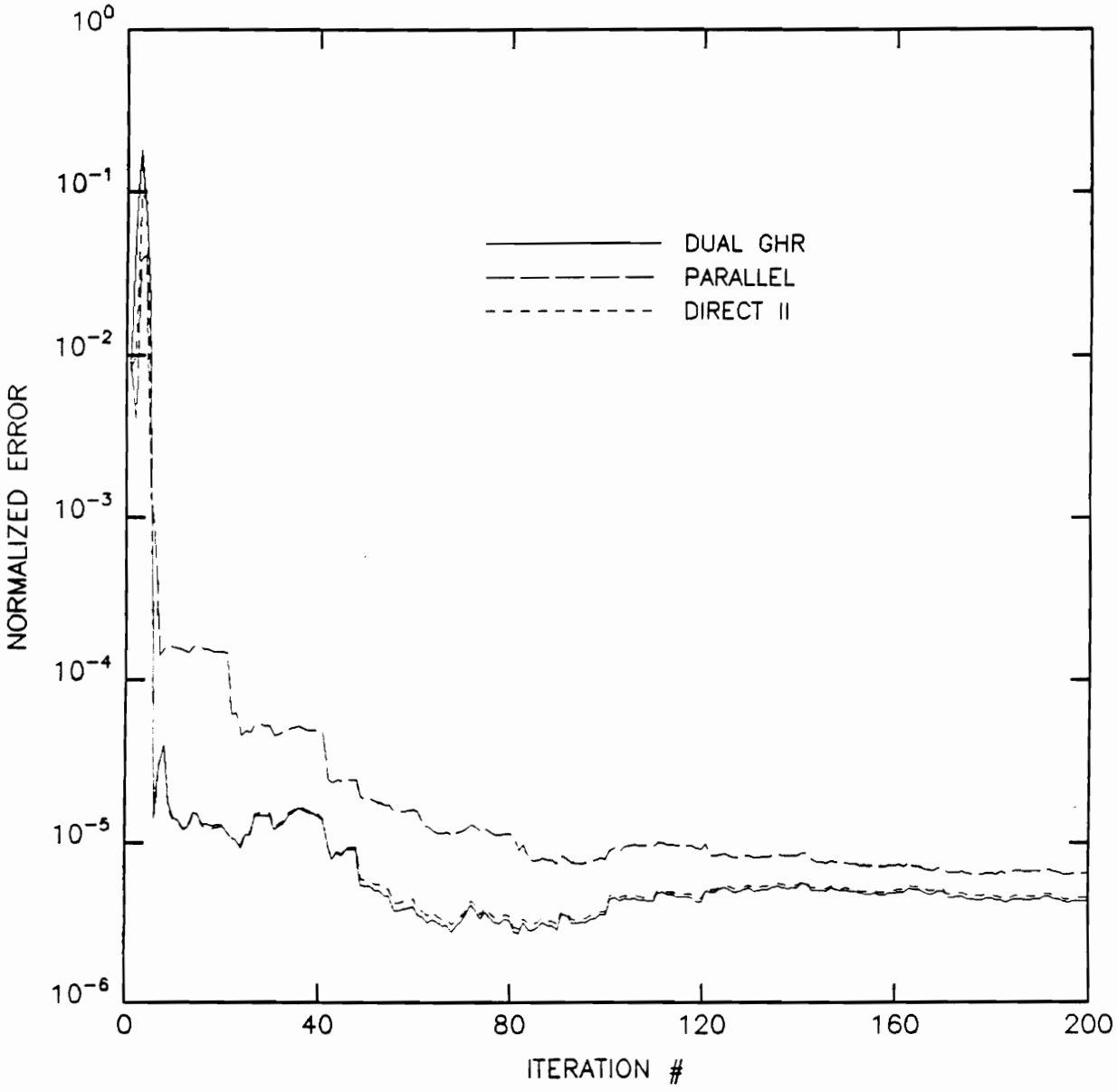

Figure 45. BP1, Normalized error (N = 20), 40 dB SNR

influence in the stochastic case when the initial parameter guesses are quite far from the solution. This does not invalidate Conjecture (C.1).

7.0 Arbitrary Input IIR Adaptive Filtering and Structure

In this chapter, we briefly explore the application of different structures in identification algorithms for the identification of systems from arbitrary input/output measurements. This application has only recently been explored [102-104]. The proposed measure τ apparently explains some of the convergence behavior seen in [104]. Consequently, we include an extensive review of this paper.

In this paper [104], the estimation/convergence performance of DII, PRLL, lattice and cascade (CSCD) structures are examined and compared. The primary motivation for this comparison was to optimize the speed of convergence by reducing both gradient computation complexity and stability monitoring. The DII structure is, as was previously noted in Chapter 2, the most commonly identified adaptive filter structure. However, the stability of the DII structure is relatively more difficult to determine than for the cascade or PRLL structures. Of course, the lattice structure contains the stability information directly in the reflection coefficients, parameters which appear as structure parameters. The stability of the DII structure may be determined quickly via the Levinson algorithm on the AR portion of the transfer function; however, the exact pole locations will not be available. To get the exact pole locations, a root-finding algorithm must be

used, which is computationally expensive in both time and power. Knowing the exact locations of the unstable poles is very useful in performing the stability projections required by Gauss-Newton identification algorithms. Stability monitoring for the PRLL and cascade structures is simple since only 2^{nd}-order polynomials need to be factored to exactly determine the poles. A square-root operation is required, but the computation is otherwise very simple (and closed-form, too).

Another reason for choosing to identify structures other than the DII structure is that the DII structure is inherently very sensitive [4,22-24]. Consequently, this structure is not typically used in fixed digital filtering applications. In adaptive equalization, one would most likely not want to use the DII structure either, so that a transformation to the desired, less-sensitive structure would be required at every iteration. The PRLL and cascade systems are typically much less sensitive than the DII structure [24], and so identifying the parameters of one of these structures would eliminate this transformation.

7.1 Gradient Computation in the General Input/Output Configuration

The main problem with the formulations required for the identification of systems with general input is in the complexity of the gradient calculations [38][6] . In general, we can run the partial derivative systems described in Chapter 3 with an arbitrary, but measured input. The needed gradients are then the outputs of these systems at a particular sample time. In practice, the complexity of such an approach precludes this direct computation. For instance, if the system model is 3^{rd}-order, the partial derivative system is of order 6. Then, this filter must be run from time

[6] See appendix H for DII and PRLL gradient details in the arbitrary input case.

0 to get just one gradient. Worse, since the estimates vary with time (hopefully converging to the optimal solution), a new filter must be run from time 0 for every identification step. For certain parameterizations, the exact gradient computation load may be reduced, but this is not true in general, and the amount of computational savings can vary quite a lot from structure to structure.

The gradients for the DII structure can be simplified by recognizing that the gradients are recursive in the identified parameters [33,76], and so the gradients for this form now require $2n^2$ multiplications and $2n^2$ additions [104]. However, this number can be further reduced by approximating some of the parameter gradients. These approximate gradients are found by noting that some of the gradient components (i.e. some of the elements of the 2n-dimensional gradient vector Φ_t) are just delayed versions of each other [49]. Then, certain elements of the gradient can be approximated by saving previous elemental gradients (not the same element, however). Since the estimated parameters change at every measurement time, these old gradients are not valid per se, but if the iteration is near convergence, then the estimates will be quite close. As a practical matter, a gradient estimate which is not too far wrong can lead to acceptable convergence rates [41]. This approximation results in a computational savings, so that the gradients can be found with only $2n$ multiplies and $2n$ adds [104]. This approximation slows the rate of convergence, but apparently provides satisfactory performance [49].

Since the PRLL and cascade structures are parallel and series interconnections of 2^{nd}-order DII sub-sections, the gradient computations follow directly from the DII structure. However, the gradients are only delayed versions within each subfilter, so that the computational complexity can only be reduced by 2 (see Figure 46). The computational complexity of the exact gradient computations for the PRLL structure is only $4n$ multiplies and $4n$ adds, so that the approximated gradients are equal in required computational effort to the approximated DII gradient and the exact gradients (faster convergence) are much simpler to compute for the PRLL structure. On the other hand, the cascade structure has complexity of order n^2 for the exact gradient computation ($2n^2$ multiplies and $2n^2 - 2n + 4$ adds per iteration) since the 2^{nd}-order structures are not independent of each other like the PRLL sub-sections are. The approximate gradients reduce the computational complexity by a factor of 2.

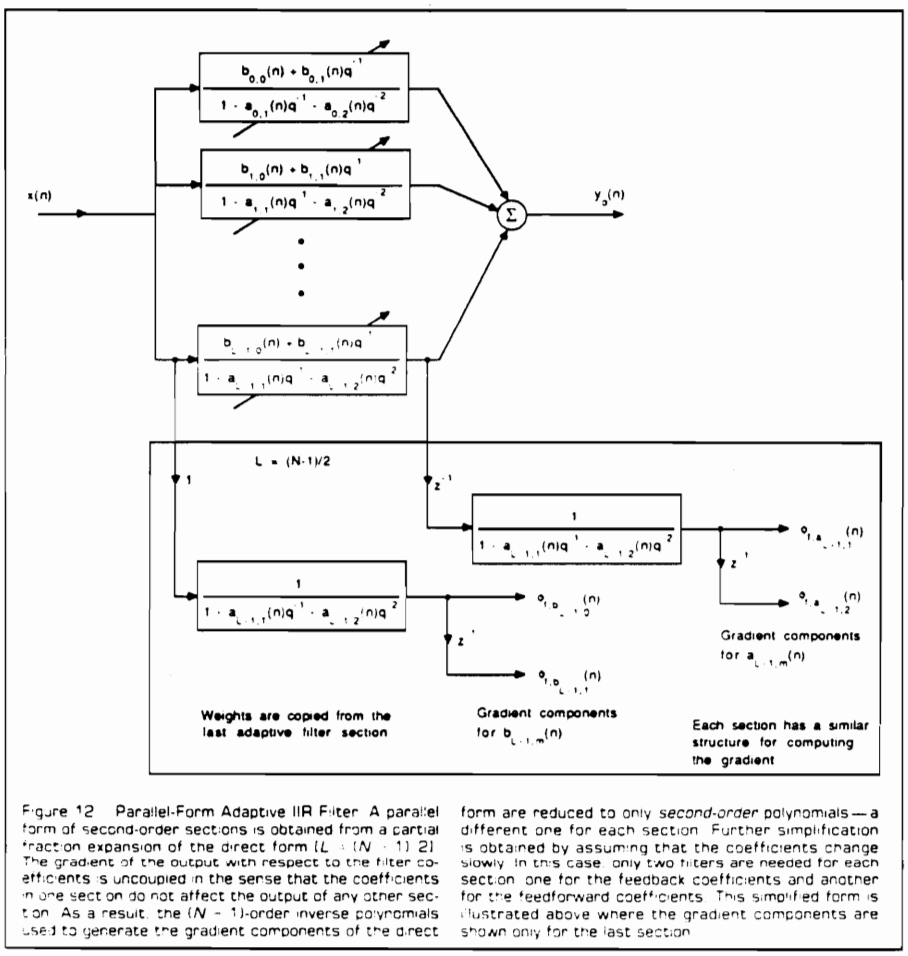

Figure 12 Parallel-Form Adaptive IIR Filter A parallel form of second-order sections is obtained from a partial fraction expansion of the direct form ($L = (N - 1)/2$). The gradient of the output with respect to the filter coefficients is uncoupled in the sense that the coefficients in one section do not affect the output of any other section. As a result, the $(N - 1)$-order inverse polynomials used to generate the gradient components of the direct form are reduced to only *second-order* polynomials — a different one for each section. Further simplification is obtained by assuming that the coefficients change slowly. In this case, only two filters are needed for each section: one for the feedback coefficients and another for the feedforward coefficients. This simplified form is illustrated above where the gradient components are shown only for the last section.

Figure 46. PRLL approximate gradient computations [102]

No such approximation is currently available for the lattice structure. The gradients for the lattice structure require $2n^2$ multiplies and $4n^2$ additions. We have not investigated the DGHR gradient computations at this time, leaving it for further research. Some recent work in the efficient generation of gradients for parameters arbitrarily located in the state-space model may be found [12].

7.2 *Convergence and Local/Global Minima*

Since the input in this case can be continuously and informationally exciting to the system parameters and modes, all convergence results cited in Chapters 2 and 3 are potentially useful. As noted in Chapter 3, the global minima are unaffected by the state transformation.

However, zero gradient locations can be created. These new stationary points are created by the fact that neither the PRLL nor the cascade structure is unique for any system, i.e. these structures are unique in pole/zero specifications, but not in order. For example, a 4^{th}-order system has 2 sub-sections in the PRLL structure. These two sub-sections operate relatively independently of each other, and so which sub-section corresponds to which block of the identifier model is not in general known beforehand. These stationary points are saddles of parameter space [90], and so are not considered to be a problem here.

The simulations shown in Chapters 5 and 6 seem to bear out the fact that local minima do not create problems. This area needs to also be further explored, so that good adaptive algorithms can be implemented in practical situations, but we do not foresee any real problems in this area.

7.3 *Arbitrary Input Example*

To examine identification in this context, we look at the examples in [104]. Here, the author uses Algorithm (A.1) with weights w_k which are not quite equal to 1. This choice of the w_k keeps the identifier alert [76]. The test system is SHY in Table 1. All structures were started with parameters corresponding to the same initial condition system (initial poles were at radius 0.1 and angle 45°, 90°, 135° and 180°). P_0 is the identity matrix, and $w_n = 0.99$ for all n.

In the first run (see Figure 47), no noise was added (so that the run is the deterministic version of Algorithm (A.1)). The DII structure outperformed the PRLL and cascade structures in the sense that the DII structure converged to the true system faster than the other 2. Also, the PRLL structure outperformed the cascade structure (As an aside, the lattice structure converged slightly faster than the DII structure.). The author here theorizes that the " [relative convergence] may be related to their [PRLL and cascade] performance-surface manifolds ... ." Further, the author states that "Although it is difficult to accurately predict the performance of these realizations (there are very few analytical results) ... ." The proposed Conjecture (C.1) appears to explain the performance here quite readily. By examining the tabulated Fisher information matrix data in Appendix A, one can see that the convergence is consistent with τ, i.e. the DII structure has the lowest τ, followed by the PRLL structure, with the cascade structure having the highest τ of all.

Changing the initial condition pole radii to $r = 0.01$ does affect the rate of convergence for all structures, but not their relative rate. The addition of zero mean white Gaussian noise with variance 0.001 again affects the rate of convergence for all of the identified structures, but not their convergence relative to each other.

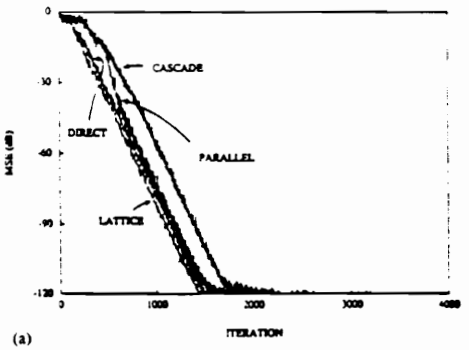

(a)

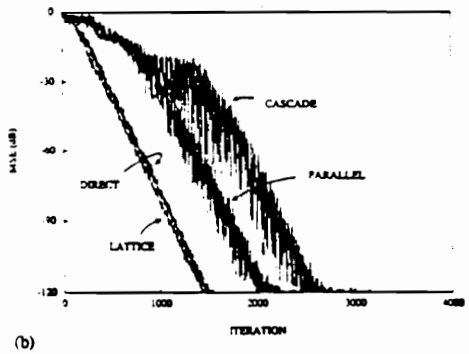

(b)

Fig. 2. MSE learning curves. (a) $r = 0.1$. (b) $r = 0.01$.

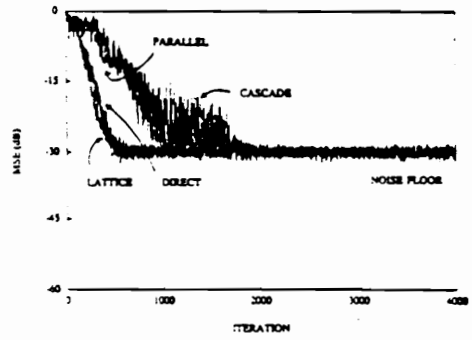

Fig. 3. MSE learning curves for simulations with noise.

Figure 47. Arbitrary input examples [104]: 3 figures

7.4 Conclusions about Identification from Arbitrary Input

The author in [104] jumps to the hasty conclusion that "Its [The PRLL structure] convergence is generally slower than that of the direct form [DII] ... ." As we have seen in previous chapters, this statement is not necessarily true, and the convergence time constant τ seems to provide the information necessary for analytically deciding on the proper structure to identify if fast convergence is desired. Of course, any implementation must take into account the amount of computation required in the gradient computation as well as in checking the system stability.

8.0 Conclusions and Directions for Further Research

First, we have shown that structure affects the convergence rates of the RPEM identifier algorithm when used to identify systems from an impulse response record. These algorithms use a Gauss-Newton search direction. The effects were explained by using the parameter correlation matrix inverse, called the Fisher information matrix. The trace of this matrix is shown to be the sensitivity of the structure. The condition number of the Fisher information matrix relates the disparity of information available for the individual parameters for a particular parameterization. It was conjectured that the parameter estimate convergence of any structure is directly related to the ratio of the conditioning over the sensitivity. We defined this ratio as the **convergence time constant, τ.**

This analysis tool τ is supported by absolute error bounds for the deterministic algorithms presented in Chapter 5 and by probabilistic arguments for the stochastic algorithms as given in Chapter 6. We have also seen (Chapter 7) that the conjecture may explain convergence behavior for identification from arbitrary input. The measure τ ties identification theory directly to information theory. A heuristic argument is given for a fast identification method which employs τ to indicate when switching from structure to structure will be advantageous. In stochastic

versions of the algorithms (A.1) and (A.2), the system sensitivity also seems to affect initial convergence. If this initial convergence is substantially affected early on relative to the other structures, the structure may perform best because Conjecture (C.1) holds only when the estimated parameters are close to the solution set of parameters, i.e. when the estimated parameters Θ_t are within the quadratic neighborhood (with respect to J_N) of Θ_{true}.

Other researchers are beginning to examine the identification of structures other than the DII structure. This dissertation has begun the task of comparing these structures in an information theoretic manner. In fact, the Conjecture (C.1) based on τ appears to explain the convergence behavior seen in [104] and explored in Chapter 7. More work on gradient computation for general state-space structures is needed in this context. However, it is very interesting to note that this work seems to extend into procedures which identify the system from an arbitrary input. While this work is not complete, a solid basis has been formed upon which further work can be based.

An important outcome of this research is that the commonly identified DII structure (ARMA parameters) is **not always** the best structure to identify. In fact, the examples presented do not indicate that any one structure is vastly superior to another -- thus implying that τ needs to be considered in all situations.

Some of this further work is in the effects of model order errors. We have loosely shown that overparameterization is not fatal to τ. Underparameterization (reduced order modeling) has also been considered, but only briefly. In this situation, the different structures do not converge to equivalent systems. However, an examination of τ for these different ending systems indicates that a connection between τ and the rates of convergence (as well as the minimum value of J_N) exists. This fact is important in that τ can be monitored for different structures. The model structure for the best identification is then easily decided upon.

Also, an identification algorithm based on the balanced state-space coordinate system should converge fastest of all, since its τ was noticed to indicate the best convergence in all the example systems (and more). However, this structure is not canonical, and so many questions remain as to its use in an identification procedure. This question was detailed further in Chapter 5.

The effects of noisy (outlier) measurements on the identification also need to be explored. Are more sensitive structures better or worse than low sensitivity structures? More detailed work is in order to fully answer this important question. Finally, what modifications are necessary to use τ to predict the identification performance for the case of covariance sequence modeling.

To reiterate the areas for needed further research, we include the following list:

1. Relating sensitivity to initial convergence in stochastic versions of Algorithm (A.1) and (A.2)
2. Investigating the effects of noisy measurements
3. Investigating the effects of model order errors
4. The identification of balanced state-space coordinate structures
5. A tighter formulation for system identification from arbitrary input/output measurements
6. Formulating a conjecture for covariance sequence modeling (the (A)SPR problem)

While much work remains to be done, the groundwork for all of these further explorations has been laid. Each of these areas represents a significant effort in its own right.

Appendix A. Fisher Information Matrix Data Tables

This appendix contains the tabulated Fisher information matrix data for the example systems described in Table 1. The high sensitivities correspond to systems with poles near the unit circle, and to systems with a narrow bandpass frequency characteristic. The conditioning is not so easily characterized. For example, look at the conditioning and sensitivity of the DGHR structure. One might think that its conditioning is strongly related to its sensitivity, until τ for system LP3 is noticed. While the other structures do not display such varied behavior, care must be taken so as not to jump to any conclusions.

In the system from Shynk [104], CSCD denotes the cascaded (or series) version of the system. As this structure is not canonical, we use only the non-zero eigenvalues of the information matrix in computing κ_2, and ultimately τ.

Table 3. LP1 Fisher information matrix data

	S	κ_2	τ
DII	58.03	1623.75	27.98
PRLL	15.17	579.06	38.17
DGHR	23.66	271.10	11.46
BSSR	1160.04	143.78	0.12

Table 4. LP2 Fisher information matrix data

	S	κ_2	τ
DII	4.58×10^5	1.68×10^6	3.66
PRLL	7.84×10^3	1.18×10^4	1.51
DGHR	5.50×10^4	7.73×10^5	14.05
BSSR	3.45×10^3	1.61×10^2	0.05

Table 5. LP3 Fisher information matrix data

	S	κ_2	τ
DII	545.7	4958.1	9.1
PRLL	63.7	1163.3	18.3
DGHR	442.2	1.43×10^6	3232.1
BSSR	80.03	107.15	1.34

Table 6. HP1 Fisher information matrix data

	S	κ_2	τ
DII	6.12×10^3	3.65×10^4	5.96
PRLL	1.14×10^3	4.66×10^4	40.77
DGHR	9.70×10^4	4.90×10^9	50517
BSSR	1.18×10^3	1.96×10^2	0.17

Table 7. BP1 Fisher information matrix data

	S	κ_2	τ
DII	415.49	1164.62	2.80
PRLL	441.24	2687.16	6.09
DGHR	981.71	1922.94	1.96
BSSR	635.83	106.59	0.17

Table 8. BP2 Fisher information matrix data

	S	κ_2	τ
DII	75.81	9.14×10^4	1206.1
PRLL	13.56	1.28×10^4	944.64
DGHR	13.81	3.62×10^3	261.88
BSSR	12.47	9.11×10^2	73.00

Table 9. SHY Fisher information matrix data [104]

	S	κ_2	τ
DII	8.09×10^3	1.03×10^4	1.28
PRLL	1.58×10^4	4.00×10^4	2.54
DGHR	8.49×10^4	5.39×10^5	6.35
BSSR	2.11×10^4	2.71×10^2	0.013
CSCD	1.61×10^4	8.53×10^4	5.29

Appendix B. The Error Versus Normalized Parameter Curves

This appendix discusses the error criterion J_N as a function of the change from Θ_{true}. If the system is unstable for a particular set of parameters, then we have plotted the error J_N as a -1.0. On each corresponding plot, the system sensitivities to each individual parameter are included for reference. When looking through the plots, notice that the sensitivity not only corresponds to the slopes of the error curves within an individual system, but actually are independent of the system. For example, if one parameter is more sensitive in system 1 than another parameter in system 2, then its error curve is correspondingly steeper. Thus, systems with large parameter sensitivities have steep J_N curves and vice versa.

Looking at Figure 48 through Figure 50, one can get a strong sense of the connection between sensitivity and the error curve slopes. The structure parameters which are most sensitive in LP1 are the DII parameters θ_1, θ_2 and θ_3. These parameters also have the most steeply-sloped error curves. The curves belonging to the PRLL structure are very flat, reflecting its low parameter sensitivities. Note also that the error curves are nearly parabolic.

Figure 51 and Figure 52 complete the set of error curve plots started by Figure 4 given in Chapter 4. Notice that since the sensitivities are large, the $\Delta\Theta$ (the x-axis) varies only by 0.03, as

opposed to the 0.3 of the plots for LP1. The plots for the DGHR and PRLL parameters are not very interesting, but Figure 51 indicates that the DII structure is not well behaved. The curves are not nearly as parabolic across the whole range as those for the other two structures. Also, this structure goes unstable for slight parameter deviations.

One can see this same kind of behavior in Figure 53 through Figure 55. These plots indicate that the parabolic nature of the error criterion J_N is a local property. It was shown in Chapter 5 how this local behavior of the criterion actually affects the convergence rates of the structure parameters.

The error curves of system HP1, shown in Figure 56 through Figure 58, are parabolic for $\Delta\Theta$ in the interval from -0.15 to 0.15. The error curves of system BP1 are given in Figure 59 through Figure 61. Notice that these curves deviate slightly from parabolic, but not nearly to the extent seen in Figure 51. The error curves of system BP2 are given in Figure 62 through Figure 64. Notice that these curves also deviate slightly from parabolic, but again not nearly to the extent seen in Figure 51.

Finally, the parameter error curves for the system SHY [104] are given in Figure 65 through Figure 67. Note that at N = 25, all curves are strongly correlated to the sensitivities, except for θ_7 and θ_8 in the DII structure (as shown in Figure 66). Apparently N is not large enough for the sensitivity connection in these two parameters, though their steepness is not too far off the expected.

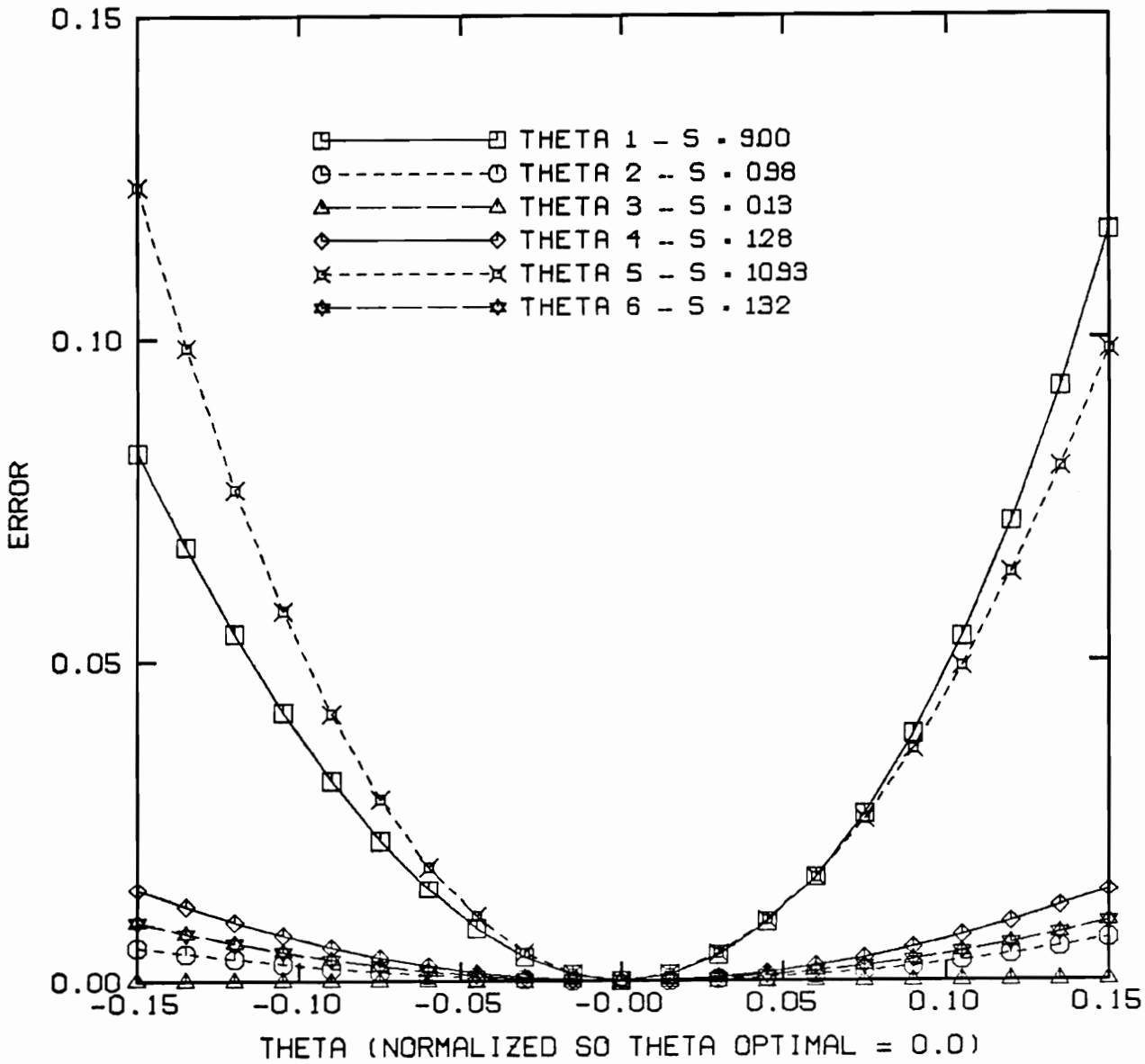

Figure 48. LP1, Error criterion for DGHR parameters (N = 6)

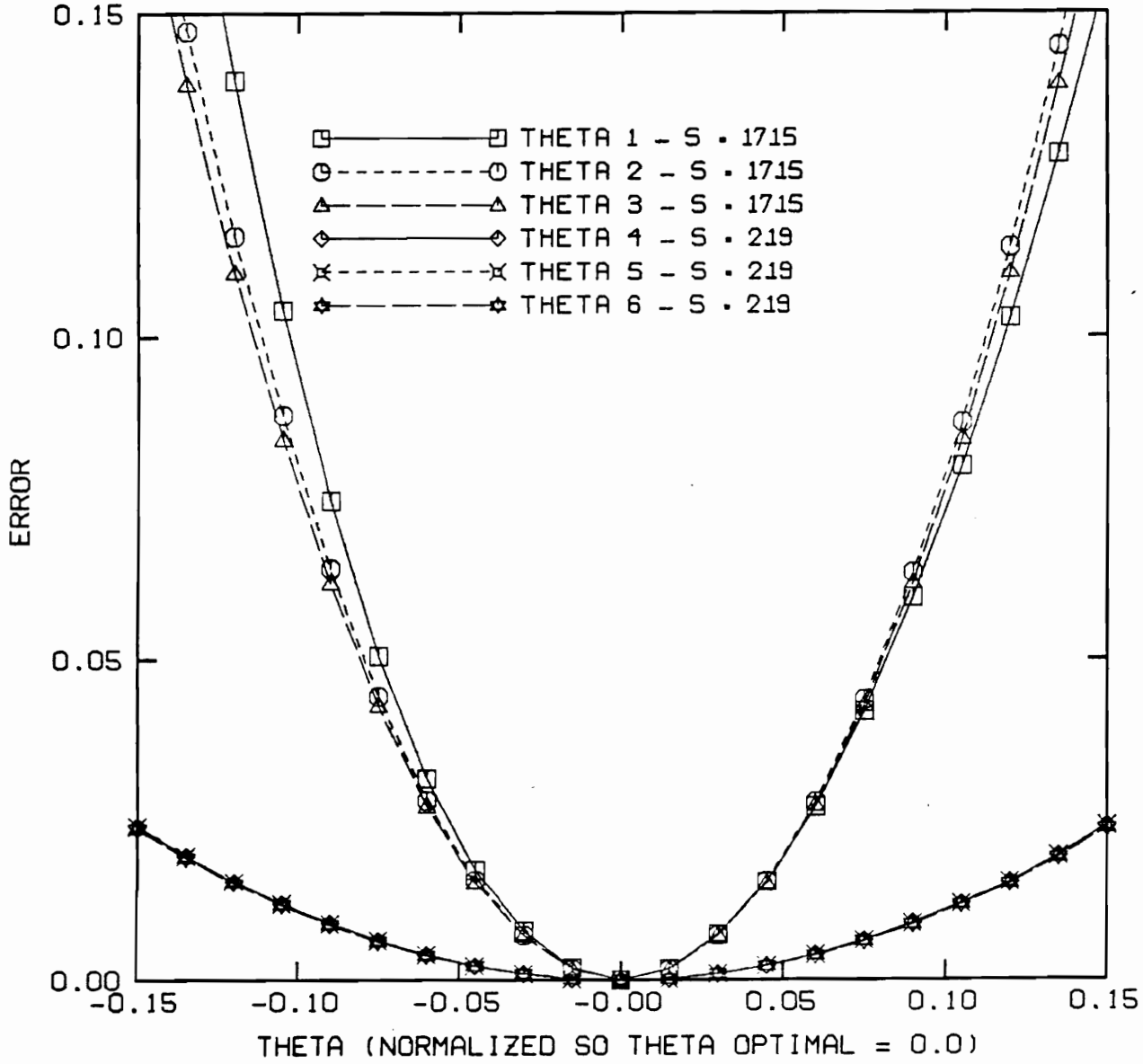

Figure 49. LP1, Error criterion for DII parameters (N = 6)

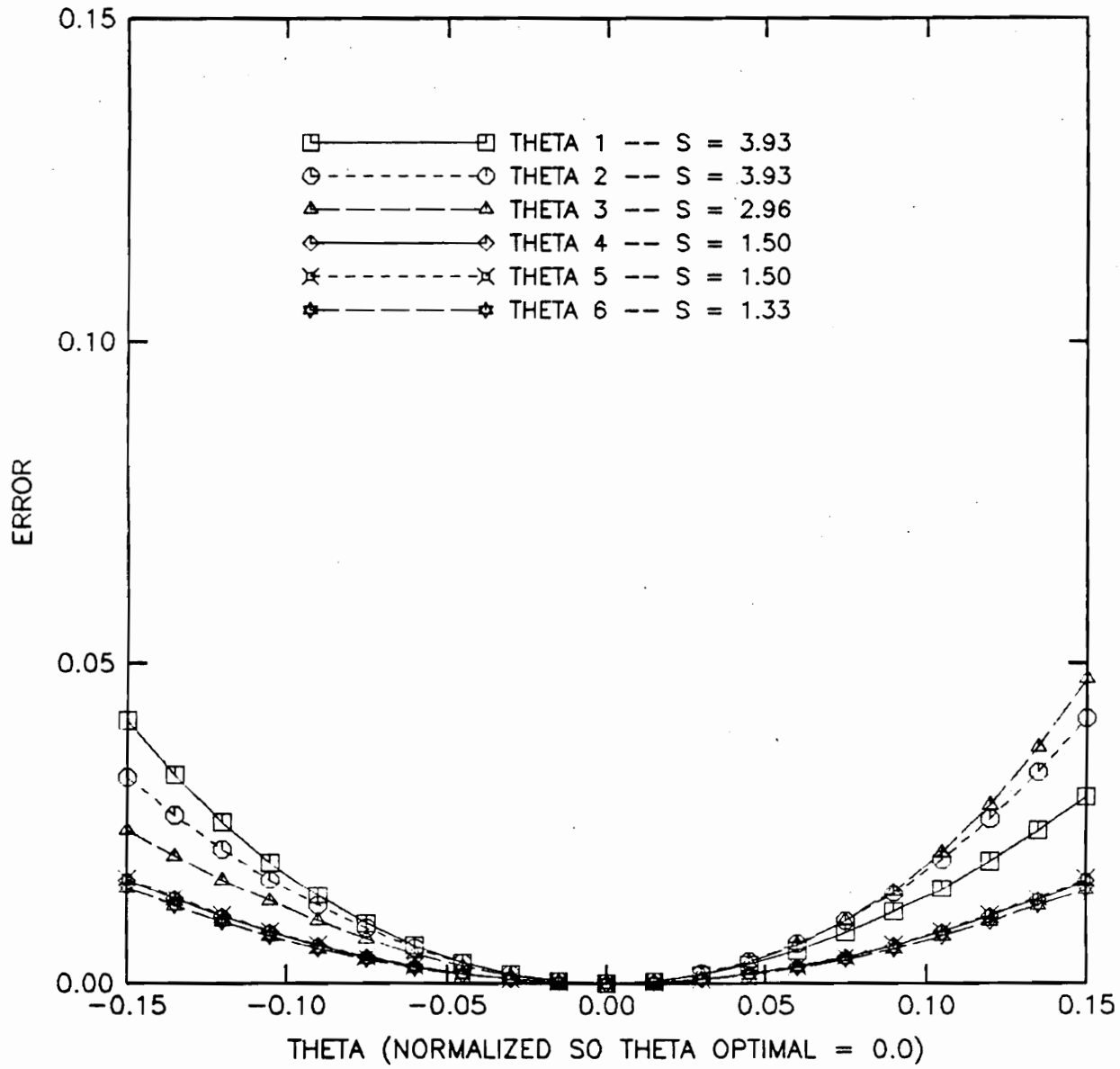

Figure 50. LP1, Error criterion for PRLL parameters (N = 6)

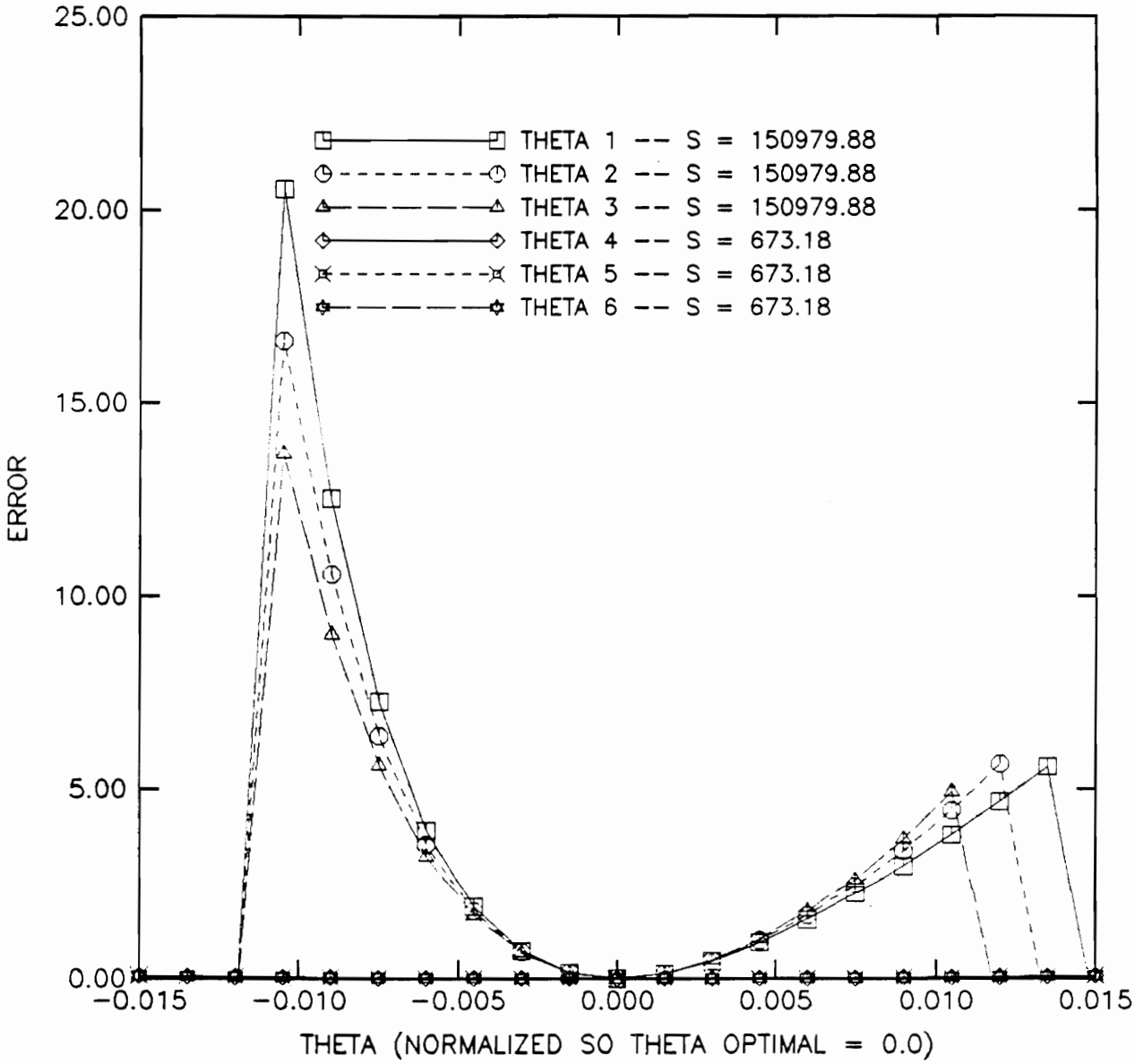

Figure 51. LP2, Error criterion for DII parameters (N = 25)

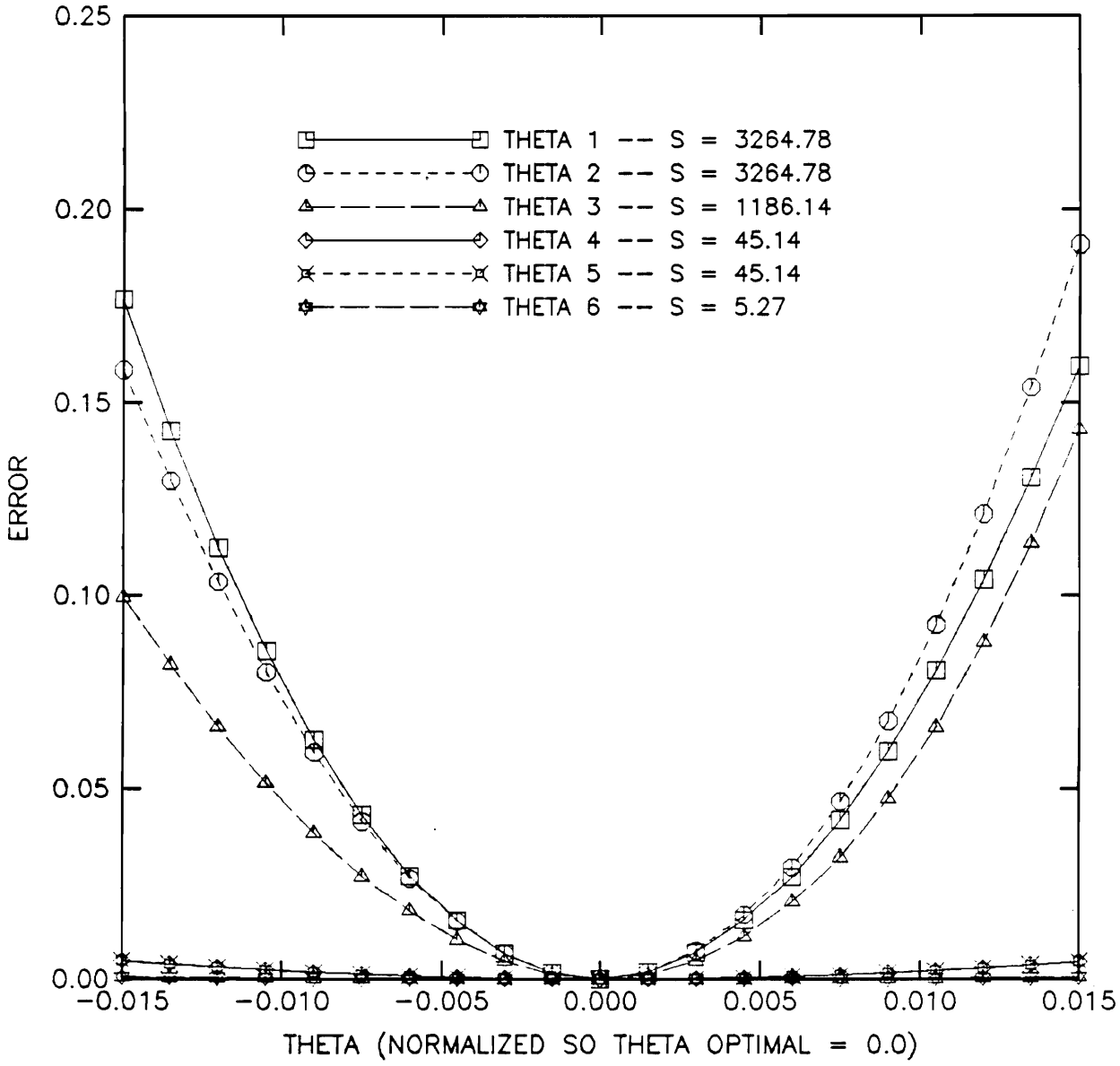

Figure 52. LP2, Error criterion for PRLL parameters (N = 25)

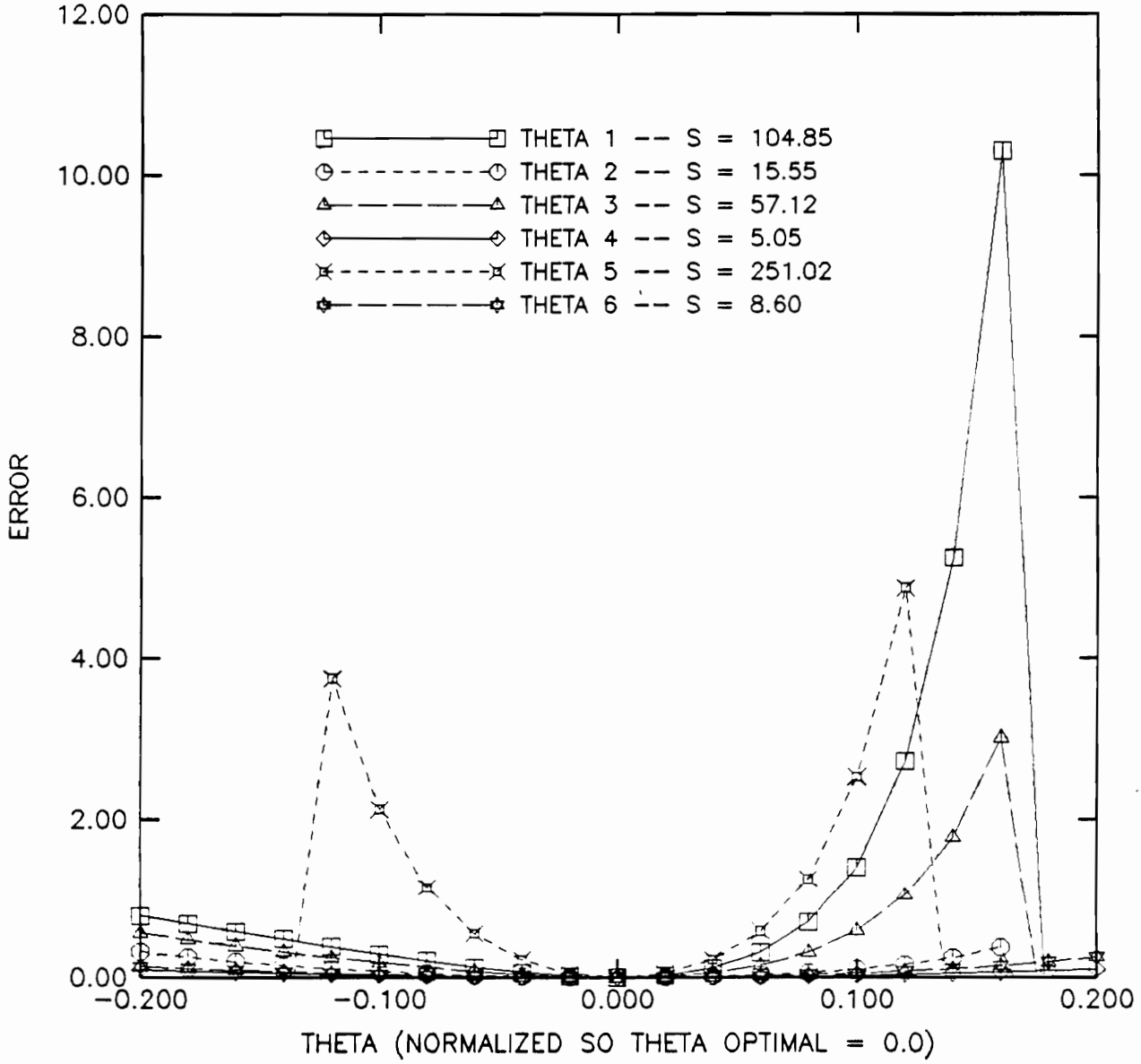

Figure 53. LP3, Error criterion for DGHR parameters (N = 20)

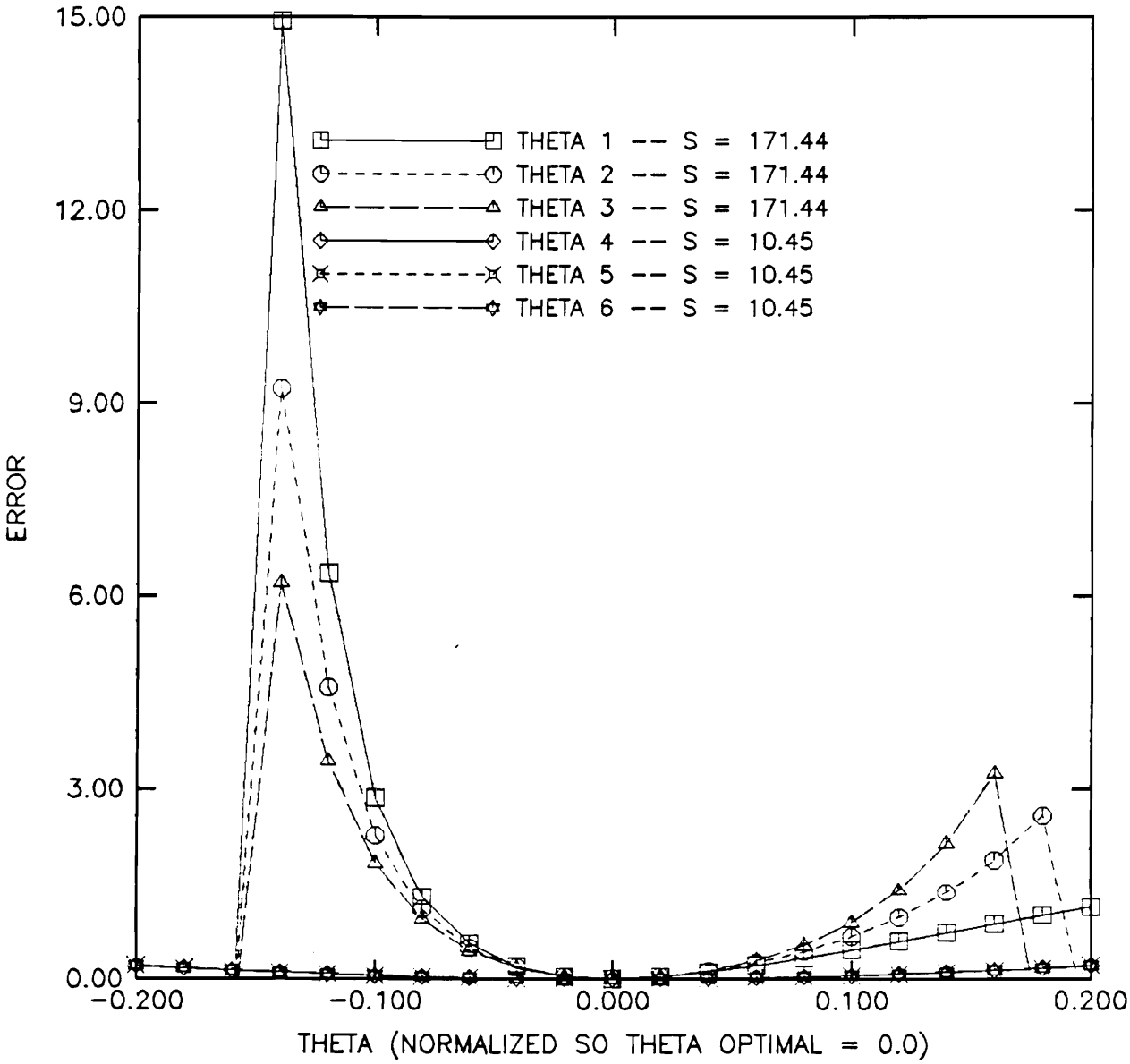

Figure 54. LP3, Error criterion for DII parameters (N = 20)

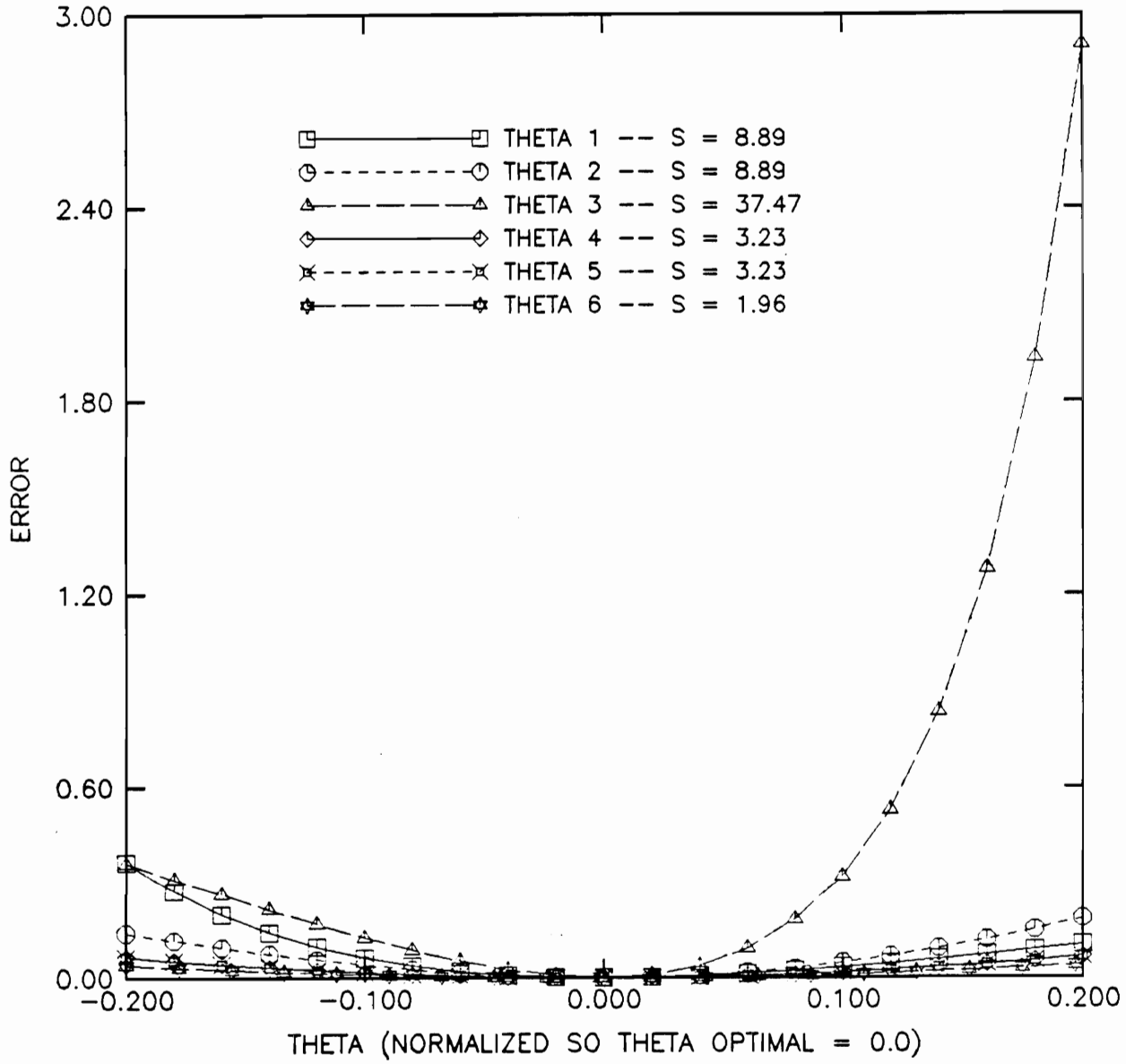

Figure 55. LP3, Error criterion for PRLL parameters (N = 20)

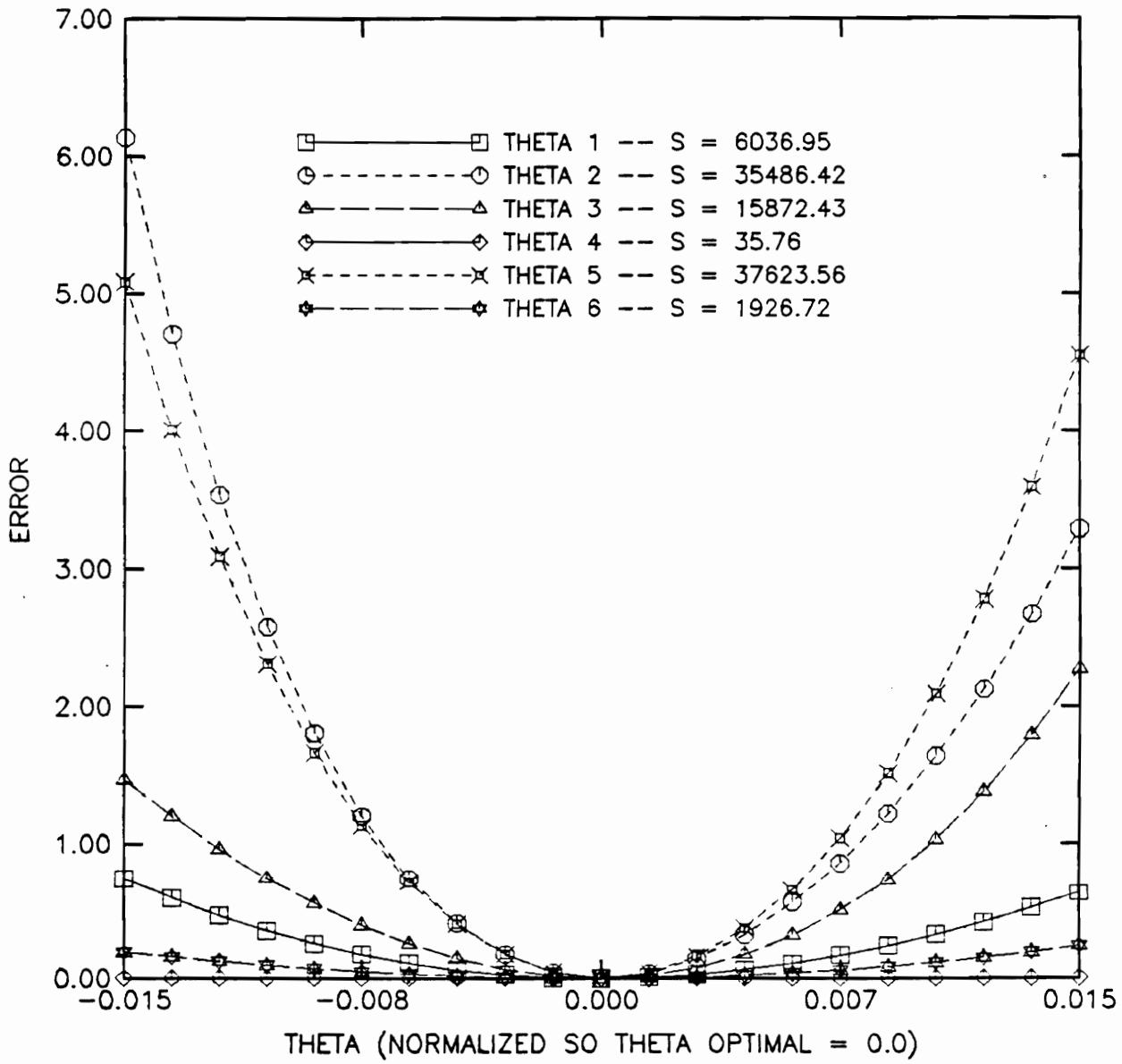

Figure 56. HP1, Error criterion for DGHR parameters (N = 20)

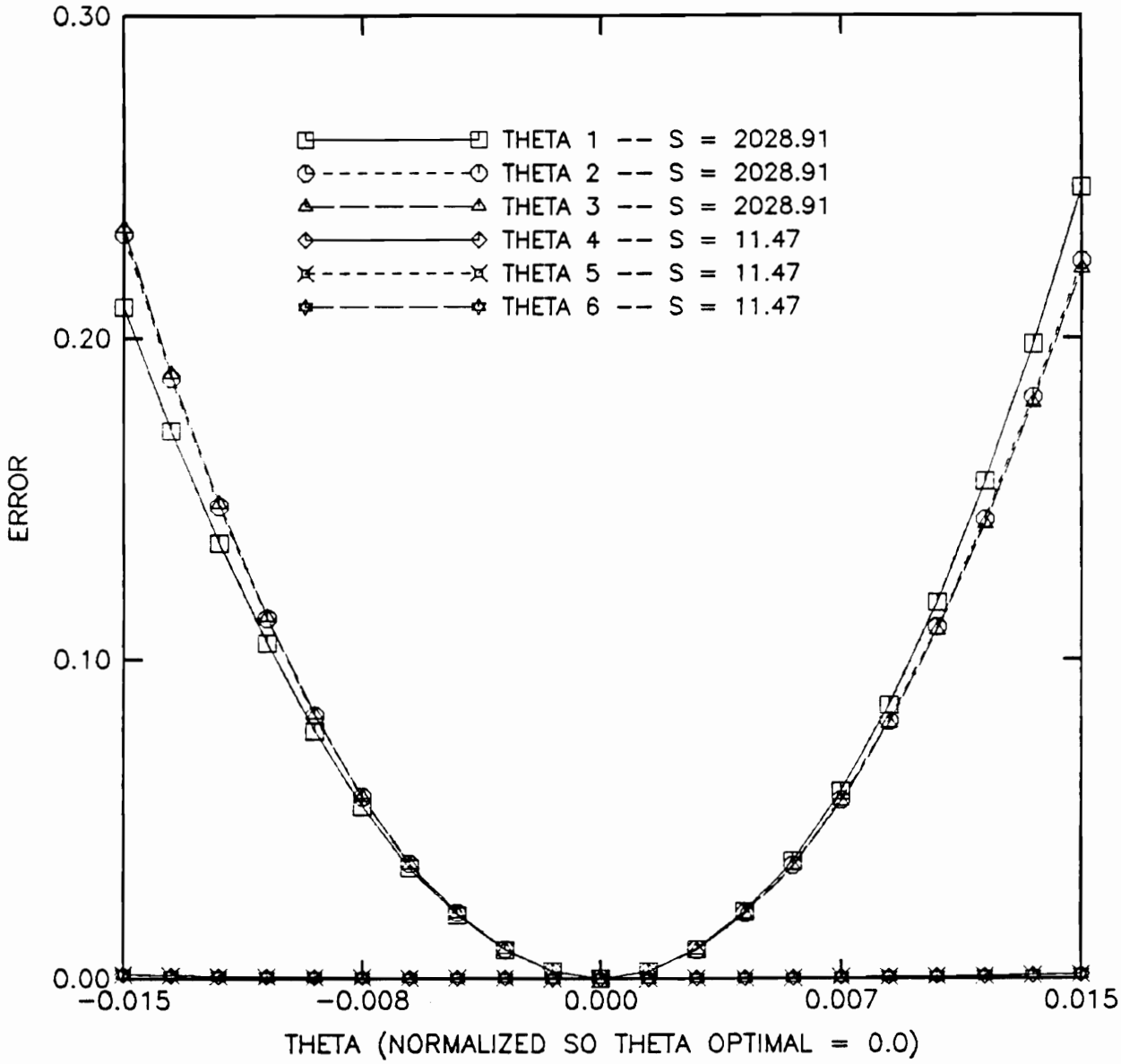

Figure 57. HP1, Error criterion for DII parameters (N = 20)

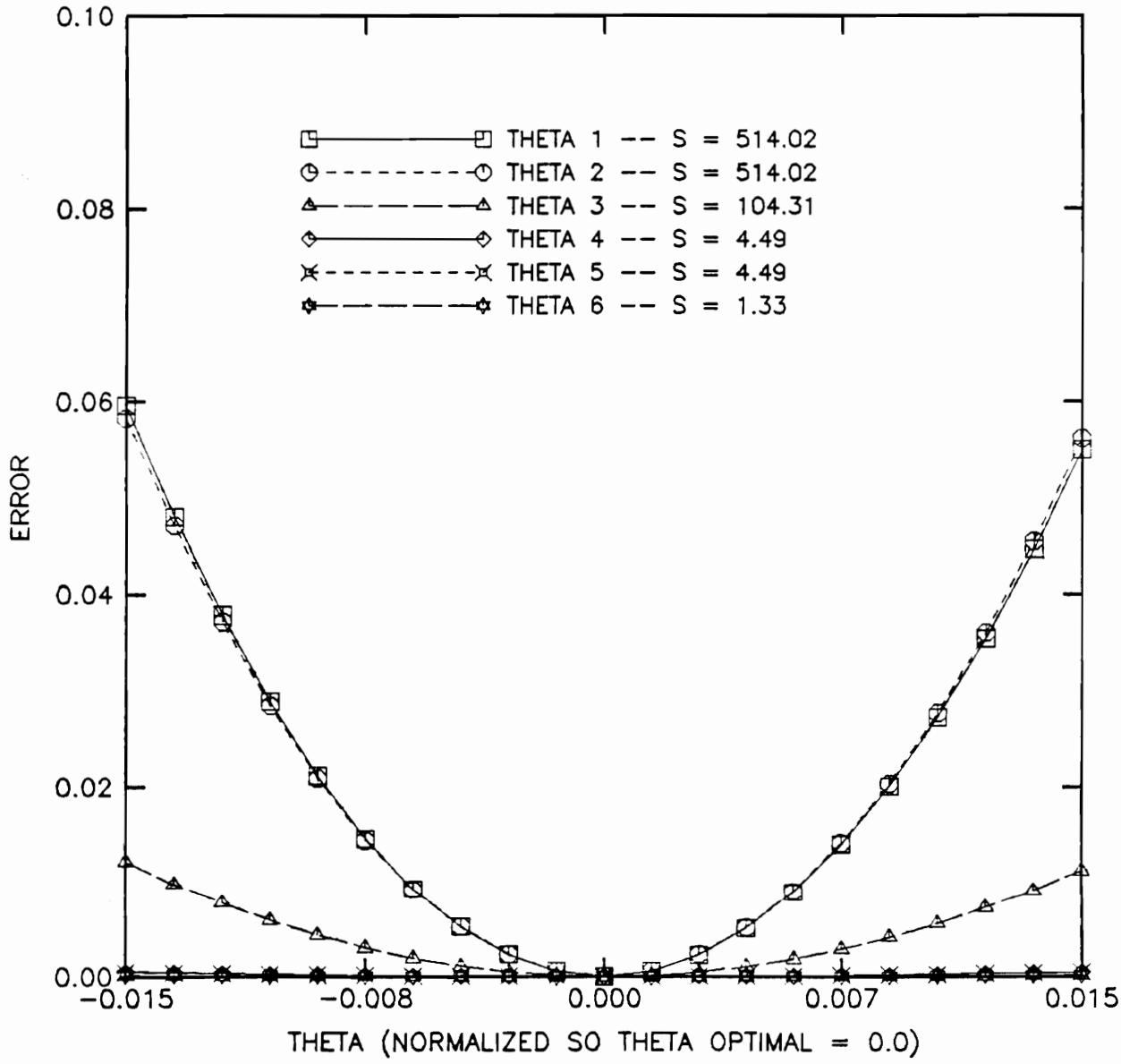

Figure 58. HP1, Error criterion for PRLL parameters (N = 20)

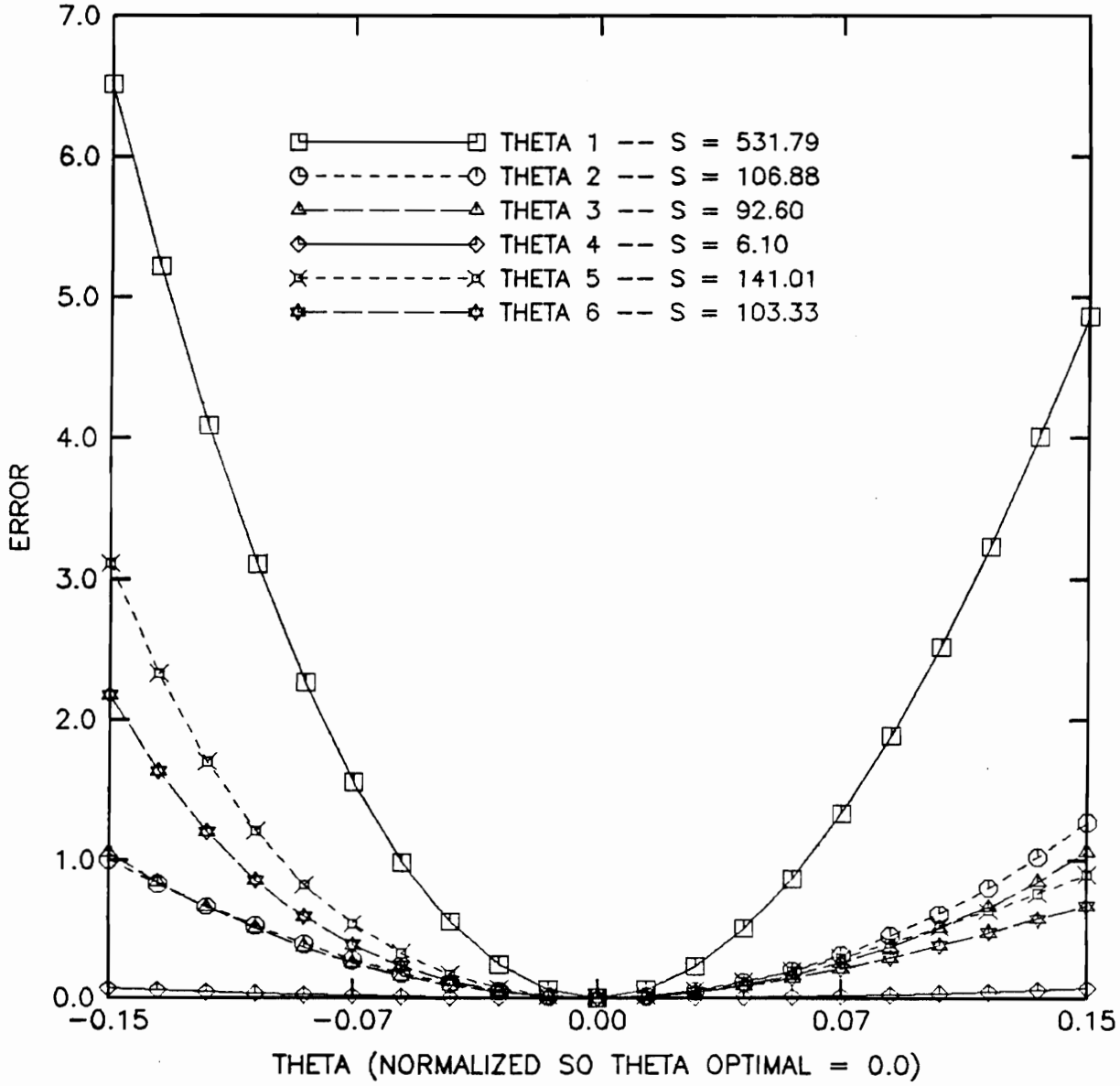

Figure 59. BP1, Error criterion for DGHR parameters (N = 20)

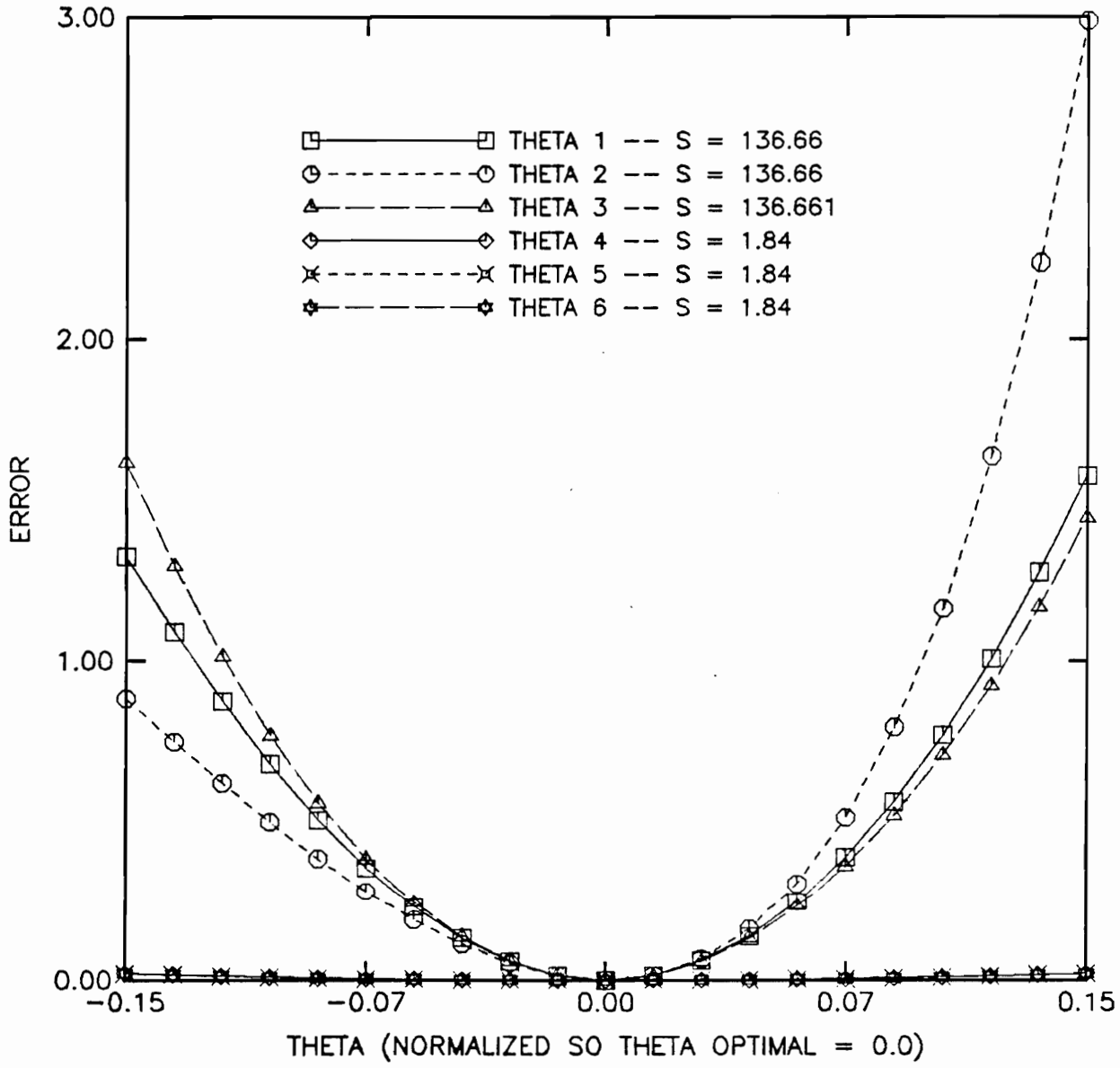

Figure 60. BP1, Error criterion for DII parameters (N = 20)

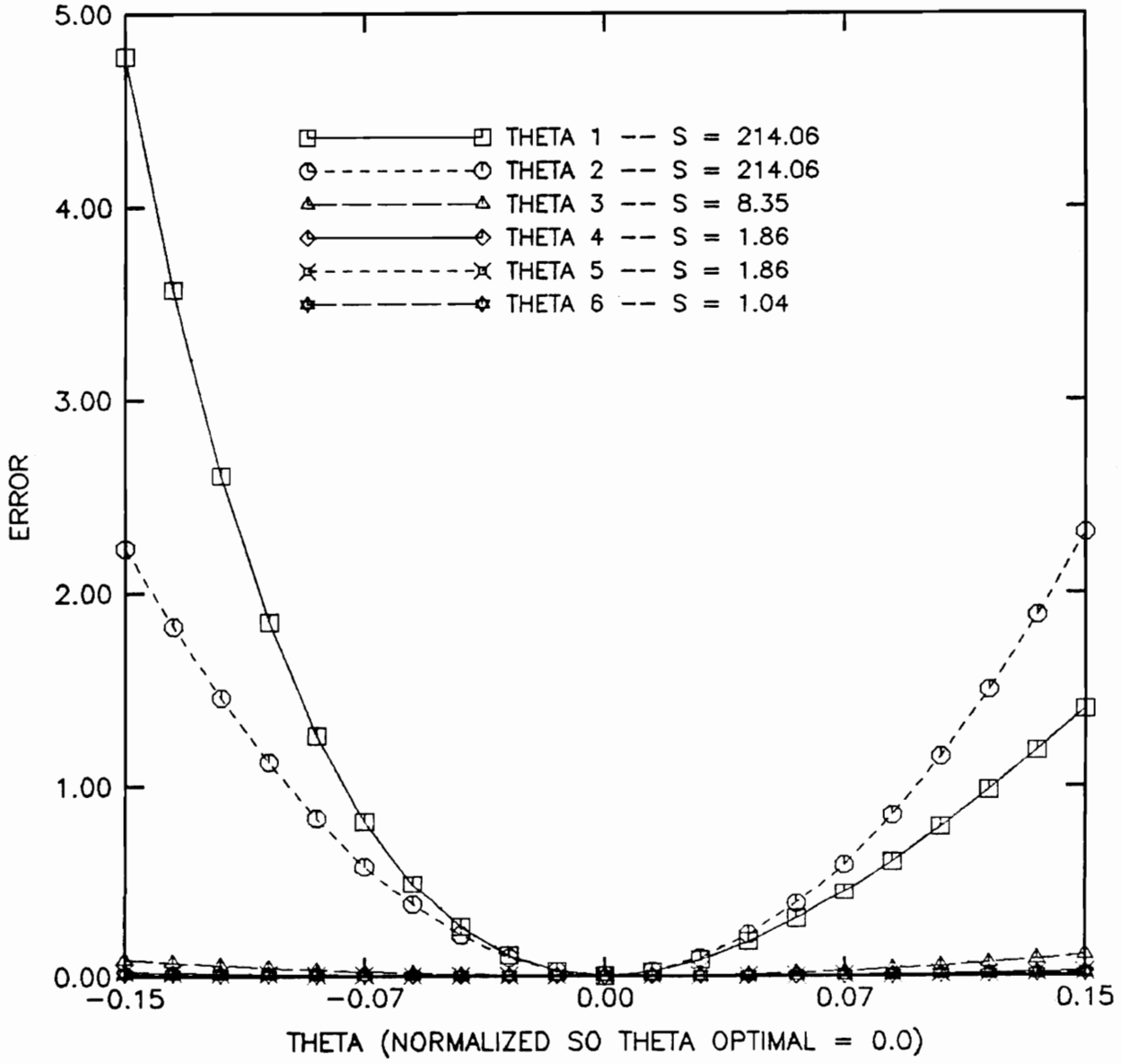

Figure 61. BP1, Error criterion for PRLL parameters (N = 20)

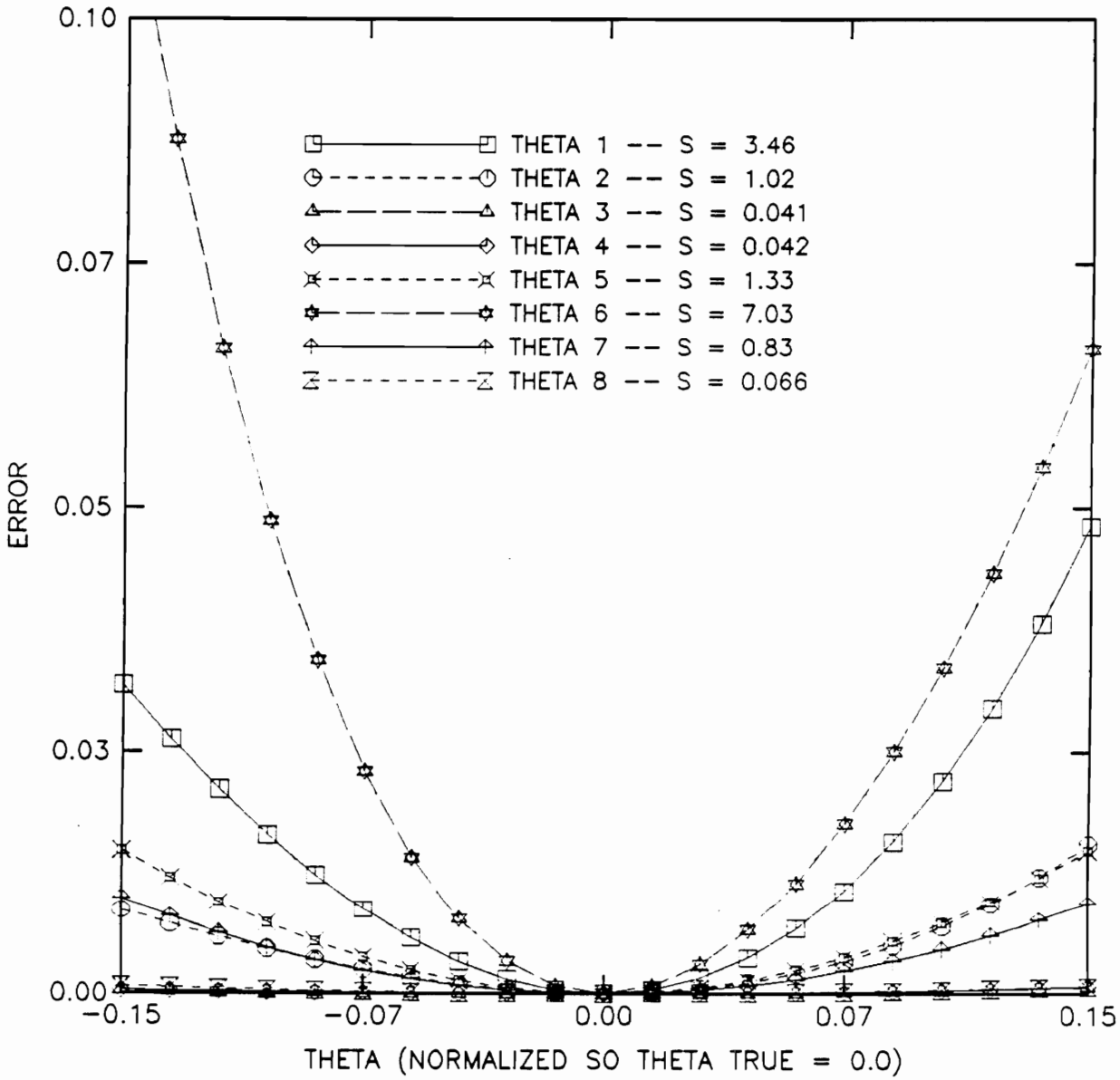

Figure 62. BP2, Error criterion for DGHR parameters (N = 20)

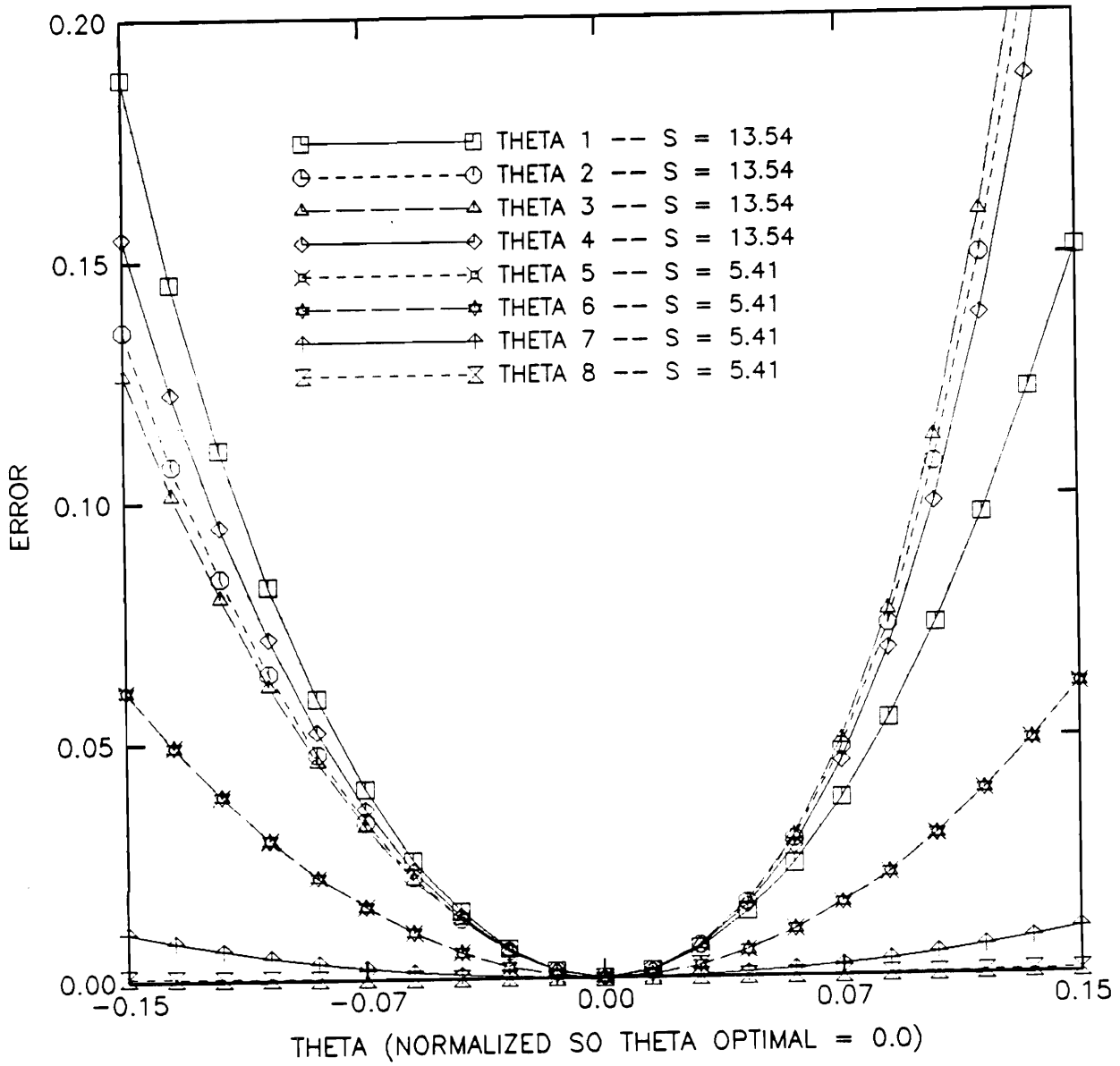

Figure 63. BP2, Error criterion for DII parameters (N = 20)

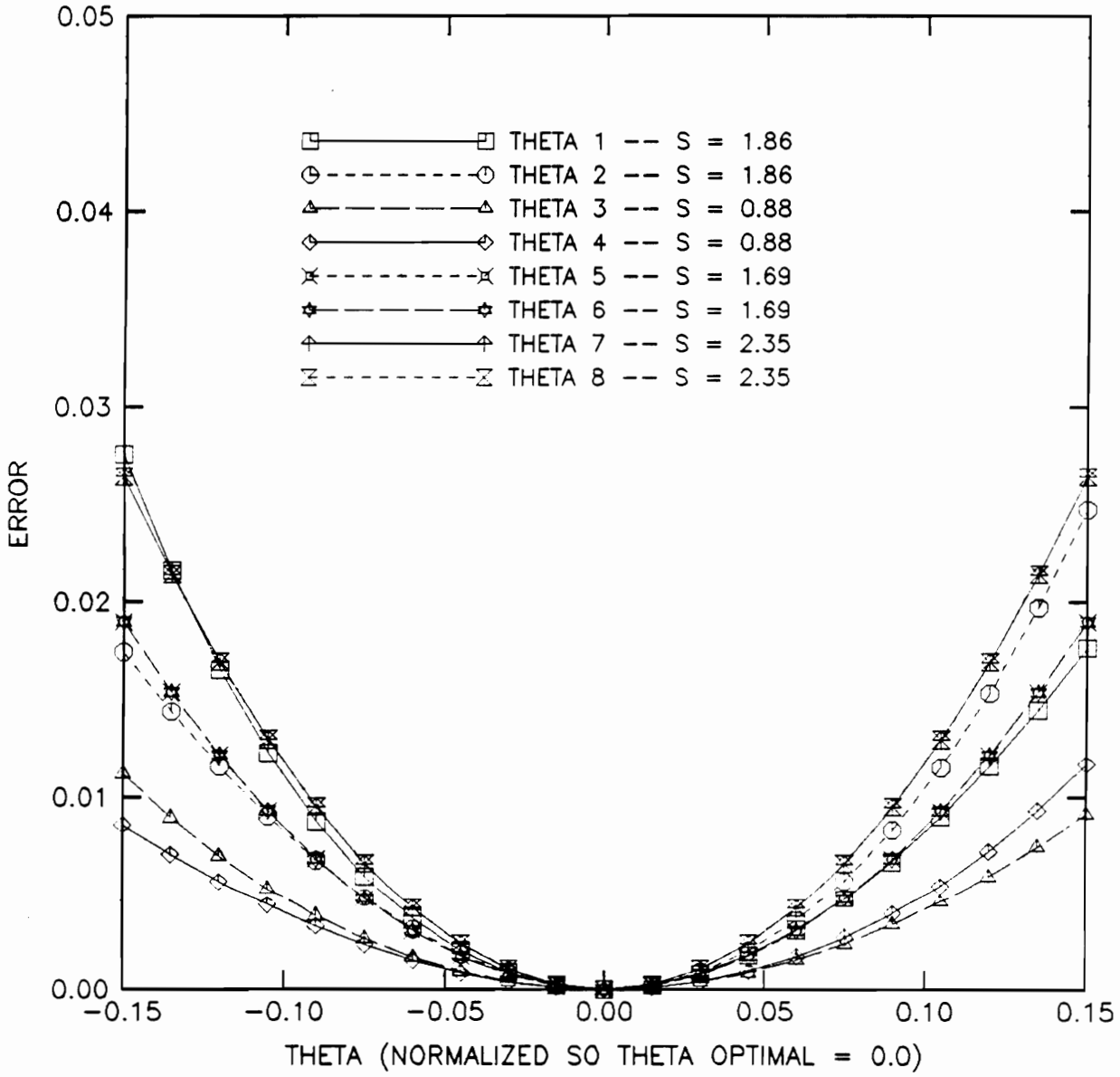

Figure 64. BP2, Error criterion for PRLL parameters (N = 20)

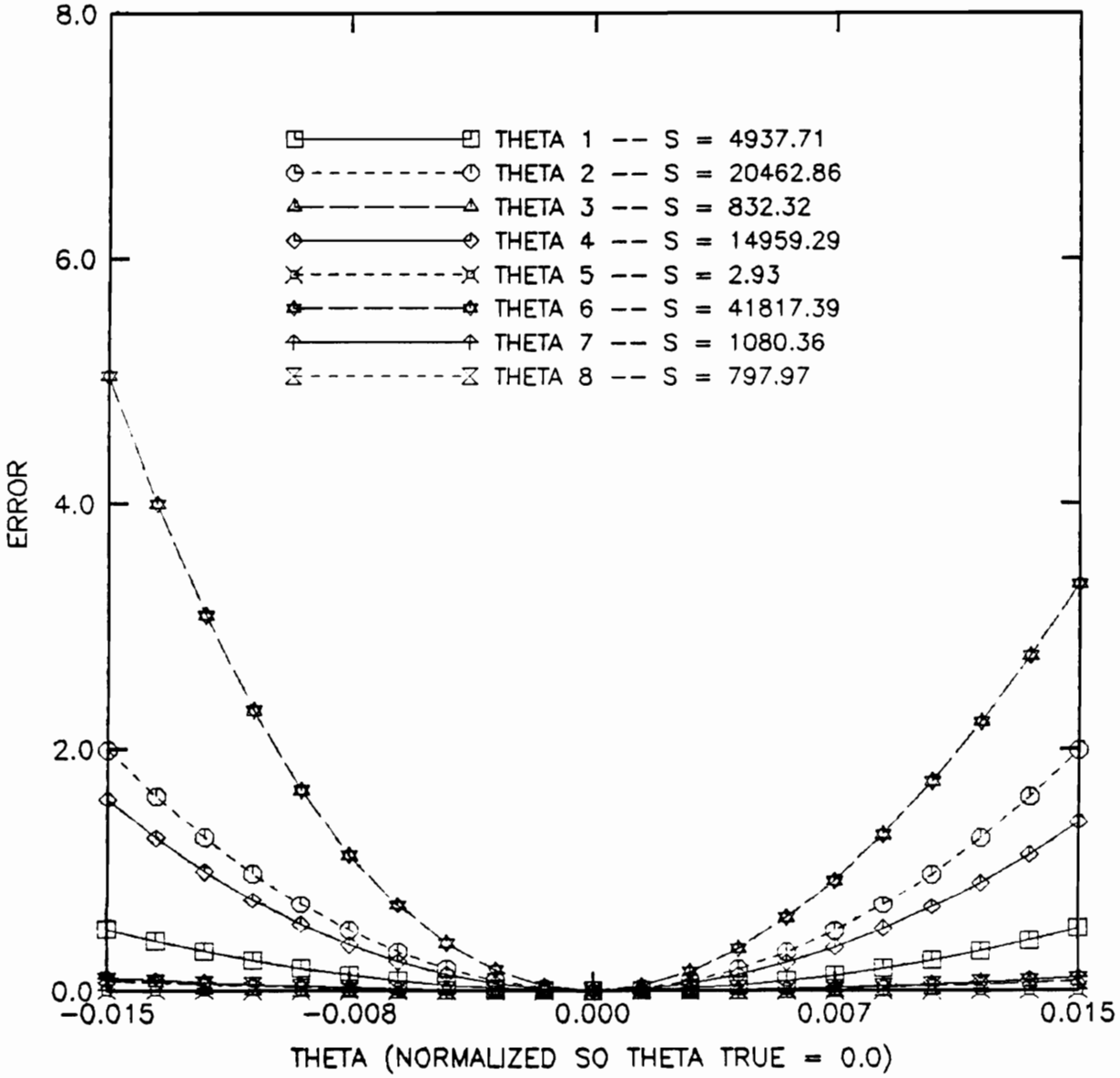

Figure 65. SHY, Error criterion for DGHR parameters (N = 25)

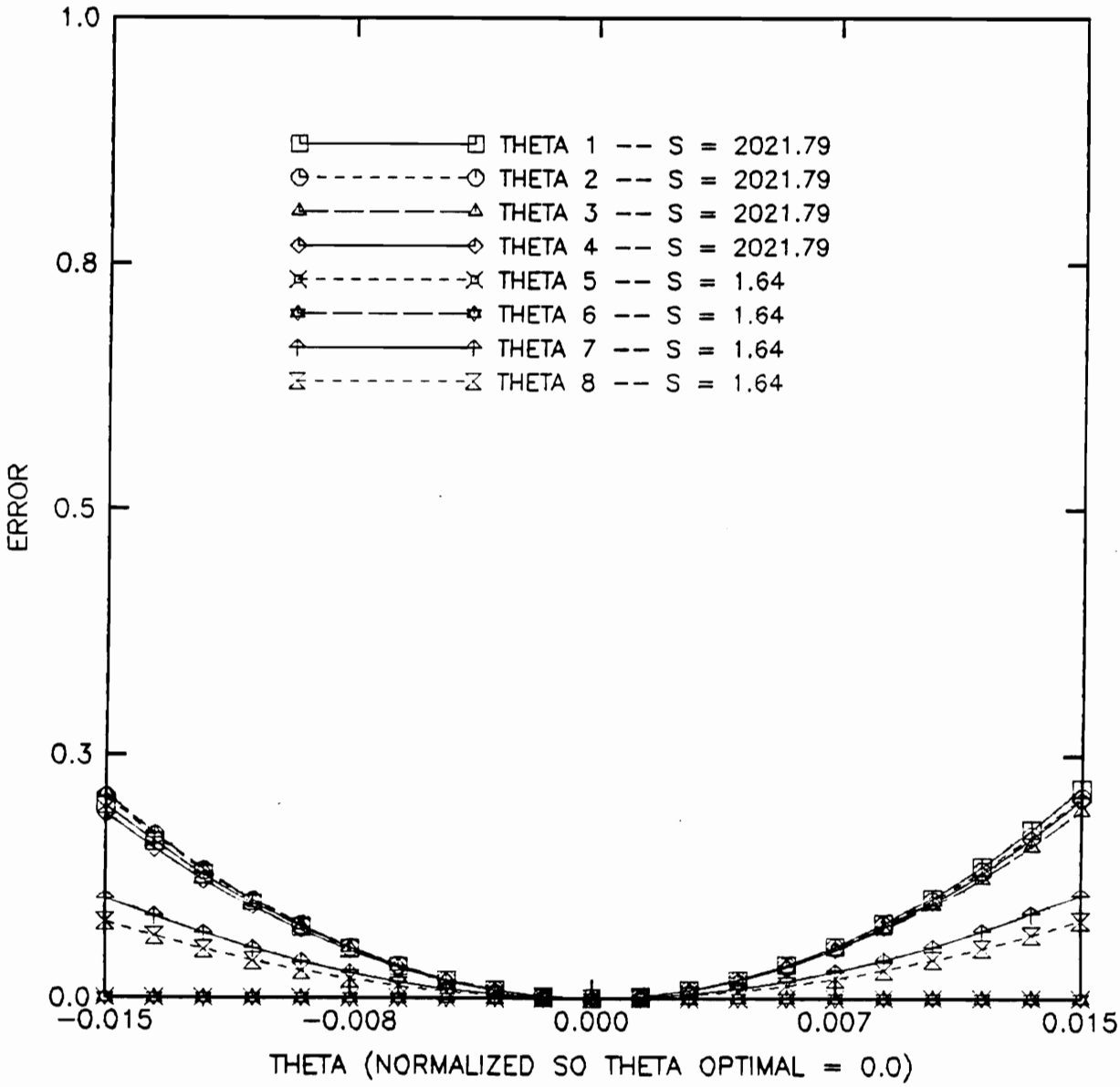

Figure 66. SHY, Error criterion for DII parameters (N = 25)

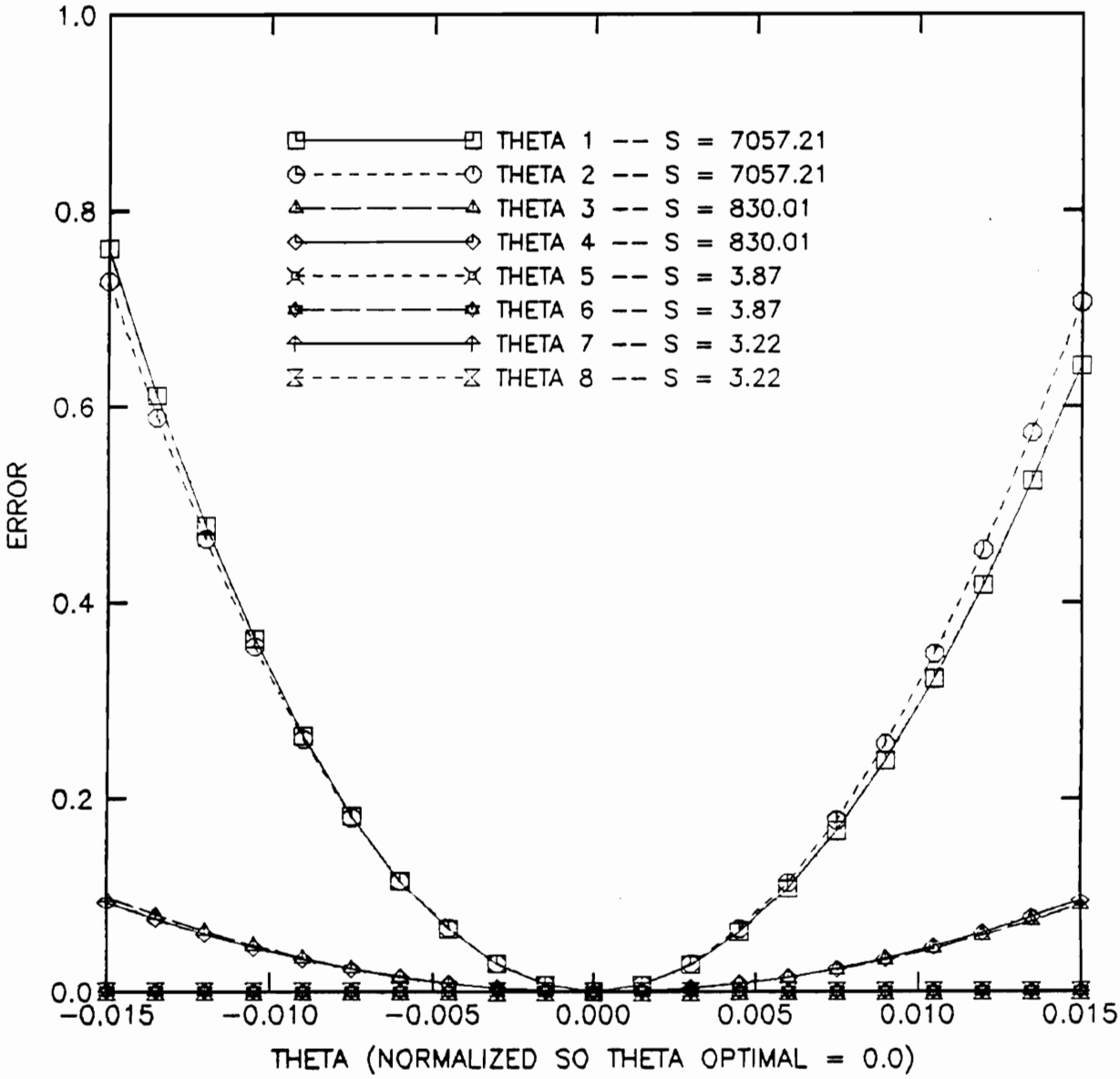

Figure 67. SHY, Error criterion for PRLL parameters (N = 25)

Appendix C. Computing τ

This appendix contains the information necessary to compute the time constant τ for an arbitrary system. The routine is written in double precision arithmetic, using VSPASCAL on the IBM mainframe VM2 at Virginia Polytechnic Institute and State University. The correlations necessary to build the Fisher Information Matrix are calculated using the algorithm first given in [10].

The eigen-decomposition is performed using the double precision IMSL routine DEVCSF. This subroutine computes all the eigenvalues and eigenvectors of a real symmetric matrix. In addition, a call to the IMSL routine DEPISF provides a check on the accuracy of the determined eigenvalues and eigenvectors. The routine DEVCSF first uses many orthogonal similarity transformations to reduce the input matrix to tridiagonal form. This tridiagonal matrix is then fed into an implicit QL algorithm to determine the eigenvalues and eigenvectors. This is a very stable and accurate procedure [41].

The performance index computed in DEPISF is a rough measurement of accuracy based on the norms of the residuals of a computed eigenvalue/eigenvector pair (theoretically, these norms are 0, but no closed form method exists for finding the eigen-pairs), on the norms of the decomposed matrix and eigenvector, and on the machine precision used. This index was first developed as part of the EISPAK project at the Argonne National Laboratory. As a further check, the norm of the

residuals themselves is also computed, i.e. the norm of $Ax - \lambda x$ where λ is the eigenvalue and x is its associated eigenvector. Finally, the orthogonality of the computed eigenvectors is computed since they are theoretically orthogonal for a symmetric matrix. This information gives strong indications of the accuracy of the computation for τ.

This brief information is given because the first routine used to decompose the Fisher matrix was based on the Jacobi iteration. This procedure was determined to be incapable of producing accurate eigenvalue/eigenvector pairs when the Fisher matrix was reasonably ill-conditioned. The numerical problems associated with this procedure were uncovered only when such systems were studied, and the convergence behavior did not follow the (erroneously computed) τ predicted path. A change to the more accurate IMSL decomposition routine fixed this problem, but this is an indication that care should be exercised when computing τ!

Appendix D. The Simulation Software

This appendix contains some information necessary to reproduce the simulations performed in the body of the dissertation. The code itself is not considered to be particularly beneficial, and so is not included here[7] . The purpose of this appendix is merely to briefly acquaint the reader with the scope and magnitude of the simulation software.

All software is written in VSPASCAL for the IBM mainframe VM2 at Virginia Polytechnic Institute and State University[8] . As a consequence, the routines are double precision. Pascal was chosen as the language for readability considerations (since over 5000 lines of code were written) rather than speed of computation. Also, FORTRAN routines can be accessed quite easily as necessary. This combination works quite well.

A simulation routine for each structure was written, with the one used for the PRLL structure being the most readily adaptable to any arbitrary state-space structure. Several different versions of each routine exist -- one which uses the fast covariance generator of [10] to compute the gradients and impulse responses necessary in Algorithm (A.1), another which uses the identified coefficients themselves in associated state-space filters for those computations, and two more corresponding likewise for Algorithm (A.2). Since Algorithm (A.2) is a square-root algorithm, the resulting

---

[7] The software is available upon request to the author

[8] An IBM 3090 vector processor

parameter estimates are essentially twice as accurate as the estimates in Algorithm (A.1). Algorithm (A.2) also has the added advantage that the parameter correlation matrix must always be positive definite, while Algorithm (A.1) suffers in comparison. This lack of numerical accuracy lead to the use of simulation software for Algorithm (A.2), especially if the system to be identified has poles with radii close to 1.

The software is commented, and all input and output files are carefully described in the source code. Because of computational requirements, all simulations were run in batch mode, preferably after midnight or on weekends. The average simulation run is about 5 minutes, with code which has been partially optimized (compiler vectorized) for VM2.

Appendix E. The Stability Projections

This appendix contains a detailed description of the stability projections used in Algorithm (A.1) and Algorithm (A.2). Two projections are used: pole/zero radii scaling and μ projections.

E.1 Pole/Zero Radii Scaling

Within each identification procedure, a stability check on the identified parameters is performed. A root-finding algorithm could be used to determine accurately the exact pole locations. However, as this procedure would be time-consuming, a different approach using the fast Levinson algorithm is used to determine the reflection coefficients corresponding to the identified system. It is well-known that if one of these reflection coefficients has magnitude greater than or equal to 1 the system is not stable. If this is the case, an easily performed pole radii scaling can be affected. However, since the exact location of the offending pole(s) is unknown, the amount of scaling necessary for the required stability is unknown, and the scaling-stability-check must be performed an indefinite number of times. This problem is not dealt with here, but should be considered for real time applications. The radii of the zeroes are scaled also because the DGHR structure contains

both the pole and zero locations in the state transition matrix, and so the two radii are strongly coupled. For the DII structure, the pole/zero radii scaling r is achieved by the procedure in Figure 68. For the PRLL structure, the pole/zero radii scaling r is achieved by the procedure in Figure 69. For the DGHR structure, the pole/zero radii scaling r is achieved by the procedure in Figure 70. To see how the scaling works for the DII and PRLL structures, a sketch of the proofs is provided. A complete proof will be provided for the more complicated DGHR structure.

Examine equation (3.4.1). From the procedure in Figure 68, note that a new transfer function has been created

$$H(r^{-1}z) = \frac{b_1 rz^{-1} + b_2 r^2 z^{-2} + \cdots + b_m r^m z^{-m}}{1 + a_1 rz^{-1} + a_2 r^2 z^{-2} + \cdots + a_n r^n z^{-n}} = \frac{B(r^{-1}z)}{A(r^{-1}z)}$$

It is a well known property of polynomials that if ρ is a root of $A(z)$, i.e. if $A(\rho) = 0$, then $r\rho$ is a root of $A(r^{-1}z)$. Clearly then, all poles and zeros of the DII structure have had their radii scaled by the factor r. The PRLL structure is a combination of 2^{nd}-order DII subfilters as seen in equation (3.4.2), and so the same analysis holds here as well.

That the scaling is correct for the DGHR structure is shown by induction. From [3], the characteristic polynomial of the system (3.4.4) is

$$\begin{aligned} \Pi_k(\rho) &= (\rho - a_k)\Pi_{k-1}(\rho) - \gamma_k \Pi_{k-2}(\rho) \qquad \text{for } 2 < k \le n \\ \Pi_1(\rho) &= \rho - a_1 \\ \Pi_0(\rho) &= 1 \end{aligned}$$

The scale factor r is entered in such a way that the a_k's are now ra_k and $\gamma_2, \gamma_3, \ldots, \gamma_n$ are now $r^2\gamma_i$'s. This new system then has characteristic polynomial

$$\begin{aligned} \tilde{\Pi}_k(\rho') &= (\rho' - ra_k)\tilde{\Pi}_{k-1}(\rho') - r^2\gamma_k \tilde{\Pi}_{k-2}(\rho') \qquad \text{for } 2 < k \le n \\ \tilde{\Pi}_1(\rho') &= \rho' - ra_1 \\ \tilde{\Pi}_0(\rho') &= 1 \end{aligned}$$

Now let $\rho' = r\rho$. Then

$$\tilde{\Pi}_1(\rho') = r\rho - ra_1 = r\Pi_1(\rho)$$

Thus, the roots are scaled by r! Now, for k = 2

$$\tilde{\Pi}_2(\rho') = (r\rho - ra_2)\tilde{\Pi}_1(\rho') - r^2\gamma_2\tilde{\Pi}_0(\rho') = r^2(\rho - a_2)\Pi_1(\rho) - r^2\gamma_2\Pi_0(\rho) = r^2\Pi_2(\rho)$$

Now assume that $\tilde{\Pi}_k(\rho') = r^k\Pi_k(\rho)$. Then

$$\tilde{\Pi}_{k+1}(\rho') = r^k(r\rho - ra_{k+1})\Pi_k(\rho) - r^{k-1}r^2\gamma_{k+1}\Pi_{k-1}(\rho) = r^{k+1}\Pi_{k+1}(\rho)$$

Thus, the zeros of $\tilde{\Pi}_n(\rho')$ are the roots of $\Pi_n(\rho)$ scaled by r, which is precisely the desired outcome. The zeros of the DGHR structure are determined by deleting the first column and first row of the state transition matrix in equation (3.4.4), and so a similar argument shows that their radii have also been scaled. Finally, γ_1 must be multiplied by the factor r (which merely scales all impulse response values) so that the scaled system impulse response is exactly that found by the scaling given for the DII and PRLL structures. Note that this additional scaling is not really necessary in any of the structures since the z^0 term is assumed to be zero in the MA part of all the identified systems.

```
For k: = 1 ... n do
    θ_k: = r^k θ_k
    θ_{n+k}: = r^k θ_{n+k}
```

Figure 68. The procedure for DII pole/zero radii scaling

```
num_subf: = trunc( (n − 1)/2 ) + 1

For k: = 1 ... num_subf do
    if 2k ≤ n then
        θ_{2k−1}: = r^2 θ_{2k−1}
        θ_{2k}: = r θ_{2k}
        θ_{2k−1+n}: = r^2 θ_{2k−1+n}
        θ_{2k+n}: = r θ_{2k+n}
    else
        θ_{2k−1}: = r θ_{2k−1}
        θ_{2k−1+n}: = r θ_{2k−1+n}
```

Figure 69. The procedure for PRLL pole/zero radii scaling

For $k := 1 \ldots n+1$ do
    $\theta_k := r\theta_k$
For $k := 2 \ldots n$ do
    $\theta_{n+k} := r^2\theta_{n+k}$

Figure 70. The procedure for DGHR pole/zero radii scaling

E.2 Successive Reduction of the Estimate Correction Term

The μ projection is presented as described in [76]. In step 1 of Algorithm (A.1) and Algorithm (A.2), a correction term is added to the old parameter vector estimate Θ_{k-1} to determine the new estimate Θ_k. To implement the μ scaling, one should merely check the stability of Θ_k . If it is stable, then no projection is required, and the algorithm is repeated for time k + 1. However, if the updated parameter vector is unstable, then the correction term is scaled by the factor μ, where $0 \leq \mu < 1$. The scaled correction term is then added to Θ_{k-1}, resulting in a new Θ_k. This process of scaling the correction term is repeated until Θ_k achieves the desired stability.

One very desirable feature of the μ scaling is that if $\mu = 0$, the algorithms are recursive in a strict manner, as the projection will always take a fixed amount of time. Note that in this case, measurements which move the parameter estimates out of the stability region are ignored (in the parameter vector update only, but not in computing the Hessian approximation!).

Appendix F. Calculating SNR

Since we are concerned with the (A)PR problem, a note about what SNR means is needed. We know the energy in the (infinite) impulse response of the true system. Denote this energy as E_{signal}. To compute the noise energy, denoted E_{noise}, we merely take the variance of the noise (which is 1.0 from the IMSL routine RNNOA -- this subroutine produces zero-mean, white Gaussian noise of unit variance) and multiply it by the number of noise samples used. For example, if N = 20, then $E_{noise} = 20$. If the noise is scaled by α, the SNR is

$$SNR = 10 \log_{10} \left(\frac{E_{\text{signal}}}{\alpha^2 E_{\text{noise}}} \right)$$

Note that E_{signal} may be computed using the fast covariance generator described in [10,23,26]. When N is large relative to the "effective" impulse response length, E_{signal} is very close (1 or 2% higher) to the energy in the actually used portion of the impulse response. If desired, the exact noise values can be used for a particular noise realization to compute an exact SNR. One other important note is that for noisy measurements, increasing N decreases the SNR, since the added impulse response measurements are almost all noise.

Appendix G. An Efficient Gradient-Based Iteration for Direct Form II Sensitivity Reduction

This appendix[9] is included for general information pertaining to the extension of the Master of Science work [24] on digital filter sensitivity and quantization noise power.

G.1 Introduction

Previously, we have determined that direct form II digital filter sensitivity (and thus the output quantization noise power) can be reduced by adding pole/zero cancellation pairs [4,24]. We now consider the problem of determining the optimal location for the placement of the sensitivity reducing pole/zero cancellations. We use the nonlinear Newton method for this optimization since the required gradients are just ARMA auto- and cross-covariances which can be computed efficiently [10,23,26]. Many of the ARMA sequences have the same AR structure, differing only

[9] This appendix essentially appears in Proceedings of ICASSP'88 [22]

in the MA part. Our approach takes advantage of these redundancies, resulting in major time and computational savings. As for the usefulness of our method, we consider its use in designing the subfilters of a parallel form. Also, preliminary work shows that the method will work with the addition of more pole/zero cancellation pairs, as noted by Rao [98].

G.2 Sensitivity Reduction

The sensitivity minimization will be based on the following state space description for a digital filter with impulse response h_n and rational transfer function H(z):

$$x_{k+1} = Ax_k + Bu_k \tag{1}$$

$$y_k = Cx_k + du_k \tag{2}$$

where x is the state vector, u is the input and y is the output. Note that A is an (nxn) matrix, B is an (nx1) vector, C is a (1xn) vector and d is a scalar. The system transfer function is

$$H(z) = C(zI - A)^{-1}B + d \tag{3}$$

The L_2 sensitivity measure S as given in [98] is

$$S \equiv \sum_l \frac{1}{2\pi j} \oint \frac{\partial H(z)}{\partial \gamma_l} \frac{\partial H(z^{-1})}{\partial \gamma_l} \frac{dz}{z} = \sum_l \frac{1}{2\pi j} \oint \left| \frac{\partial H(z)}{\partial \gamma_l} \right|^2 \frac{dz}{z} \tag{4}$$

where the γ_l are the non-structural coefficients (i.e. the coefficients which are $\neq 0$ or $\neq \pm 1$) of the {A, B, C} state space description. The integration is evaluated in a counterclockwise direction on the unit circle. Consider the sensitivity measure of direct form II filters; a form whose difference

equation has coefficients identical to those of its state space form. Assume we are given the ideal system transfer function

$$H(z) = \frac{N(z)}{D(z)} = \frac{\sum_{j=0}^{m} b_j z^{-j}}{1 - \sum_{j=1}^{n} a_j z^{-j}} = \frac{\prod_{j=1}^{m} (1 - z_j z^{-1})}{\prod_{j=1}^{n} (1 - p_j z^{-1})} \tag{5}$$

where the p_j are the simple poles of H(z). The sensitivity measure S, of a direct form II filter is [24]

$$S = \frac{1}{2\pi j} \oint \sum_{j=1}^{n} \left| \frac{\partial H(z)}{\partial a_j} \right|^2 + \sum_{i=1}^{m} \left| \frac{\partial H(z)}{\partial b_i} \right|^2 \frac{dz}{z} \tag{6}$$

Since the direct form II state space form is trivial to compute, the idea of reducing its sensitivity -- without altering its form -- was pursued [4]. There, the idea of placing pole/zero cancellation pairs was introduced, and we noted that an n^{th}-order optimal form has n(n + 2) non-trivial coefficients and the block-optimal form has 4n while the $(n+2)^{th}$ -order (with added degrees of freedom) direct form II has only 2(n + 2) non-trivial coefficients. Note that this begins to be **beneficial for systems with order as low as 2.** As the order of the original system grows, computational savings become more pronounced.

G.3 The Fast Gradient Algorithm

We now look at finding the optimal location for placement of a pole/zero cancellation pair for direct form II filters. Any optimization procedure could be used, but we use the gradient-based methods since the gradients are ARMA auto- and cross-covariances which can be solved efficiently by the techniques mentioned previously [10,23,26]. The derivations are straightforward but tedious, so that we will primarily outline the steps and give the results. Two different cases are examined. The first, that of adding one real pole/zero cancellation pair, yields a simpler solution than the second, that of adding a complex conjugate set of pole/zero cancellation pairs. In both cases, the Newton method was used.

First we look at adding a single real pole/zero cancellation pair. Taking the partial derivatives of equation (6) and denoting

$$\tilde{H}(z,\alpha) = \frac{(1-\alpha z^{-1})N(z)}{(1-\alpha z^{-1})D(z)} = \frac{A(z)}{A(z)}H(z) = H(z) \tag{7}$$

yields the sensitivity function

$$\begin{aligned} S(\alpha) = {} & \frac{m+1}{2\pi j}\oint \frac{1}{A(z)D(z)}\;\frac{1}{A(z^{-1})D(z^{-1})}\;\frac{dz}{z} \\ & + \frac{n+1}{2\pi j}\oint H(z)\,\frac{1}{A(z)D(z)}\,H(z^{-1})\,\frac{1}{A(z^{-1})D(z^{-1})}\;\frac{dz}{z} \end{aligned} \tag{8}$$

where α is the real pole/zero cancellation pair location added to reduce system sensitivity and output quantization noise power. For implementing the Newton method to find the minimum of equation (8) with respect to α, we determine the derivative $S_{\alpha}(\alpha)$ to be

$$S_\alpha(\alpha) = 2\frac{(m+1)}{2\pi j}\oint \frac{z^{-1}}{A^2(z)D(z)}\ \frac{1}{A(z^{-1})D(z^{-1})}\ \frac{dz}{z}$$
$$+ 2\frac{(n+1)}{2\pi j}\oint H(z)\frac{z^{-1}}{A^2(z)D(z)}\ H(z^{-1})\frac{1}{A(z^{-1})D(z^{-1})}\ \frac{dz}{z} \tag{9}$$

This we recognize as the weighted sum of two ARMA cross-covariances:

$$S_\alpha(\alpha) = 2(m+1)\sigma_{xy}\left[\frac{z^{-1}}{A^2(z)D(z)}, \frac{1}{A(z)D(z)}\right]$$
$$+ 2(n+1)\sigma_{xy}\left[\frac{N(z)z^{-1}}{A^2(z)D^2(z)}, \frac{N(z^{-1})}{A(z)D^2(z)}\right]$$

where $\sigma_{xy}[H(z), G(z)]$ denotes the cross-covariance at lag zero of the outputs x and y respectively of the ARMA systems H(z) and G(z) respectively, when both are driven by the same unit-variance white noise input [10]. Taking the derivative of equation (9) yields the sum of 2 ARMA auto-covariance evaluations and 2 ARMA cross-covariance evaluations:

$$S_{\alpha\alpha}(\alpha) = 2(m+1)\sigma_{xy}\left[\frac{2z^{-2}}{A^3(z)D(z)}, \frac{1}{A(z)D(z)}\right]$$
$$+ 2(m+1)\sigma_{xx}\left[\frac{z^{-1}}{A^2(z)D(z)}\right]$$
$$+ 2(n+1)\sigma_{xy}\left[\frac{2N(z)z^{-2}}{A^3(z)D^2(z)}, \frac{N(z)}{A(z)D^2(z)}\right]$$
$$+ 2(n+1)\sigma_{xx}\left[\frac{N(z)z^{-1}}{A^2(z)D^2(z)}\right]$$

We can then find the pole/zero cancellation pair location for minimum sensitivity with the Newton iteration

$$\alpha_{i+1} = \alpha_i - \frac{S_\alpha(\alpha_i)}{S_{\alpha\alpha}(\alpha_i)} \tag{10}$$

Test cases (in Section 4) show the iteration to converge quickly because the sensitivity function is well-behaved. Note that no savings can be realized in the AR decomposition in this case. However, we can realize savings in the required polynomial multiplications, and as we shall see next in the more important (and complex) case of complex pole/zero additions, we can achieve savings in both polynomial multiplication and AR decomposition.

We now consider the more complex case of adding a complex-conjugate set of pole/zero cancellation pairs. We write the added pole/zero cancellation in terms of the corresponding independent variables: radius and angle. The sensitivity can then be written (as in equation (8))

$$S(r,\theta) = \frac{m+2}{2\pi j}\oint \left|\frac{1}{B(z)D(z)}\right|^2 \frac{dz}{z} + \frac{n+2}{2\pi j}\oint \left|H(z)\,\frac{1}{B(z)D(z)}\right|^2 \frac{dz}{z} \tag{11}$$

where

$$B(z) = 1 - 2r\cos\theta z^{-1} + r^2 z^{-2}$$

Here, we need to find the first-order partials with respect to r and θ as well as the second-order partials with respect to r and θ and the cross-term partial with respect to both r and θ. Since, as in the previous case, these partial derivative computations turn out to require ARMA cross- and auto-covariance evaluations only, the results are given directly.

$$S_r(r,\theta) = 2(m+2)\sigma_{xy}\left[\frac{2\cos\theta z^{-1} - 2rz^{-2}}{B^2(z)D(z)}, \frac{1}{B(z)D(z)}\right]$$
$$+2(n+2)\sigma_{xy}\left[\frac{N(z)(2\cos\theta z^{-1} - 2rz^{-2})}{B^2(z)D^2(z)}, \frac{N(z)}{B(z)D^2(z)}\right]$$

$$S_\theta(r,\theta) = 2(m+2)\sigma_{xy}\left[\frac{-2r\sin\theta z^{-1}}{B^2(z)D(z)}, \frac{1}{B(z)D(z)}\right]$$
$$+2(n+2)\sigma_{xy}\left[\frac{N(z)(-2r\sin\theta z^{-1})}{B^2(z)D^2(z)}, \frac{N(z)}{B(z)D^2(z)}\right]$$

$$S_{rr}(r,\theta) = 2(m+2)\sigma_{xy}\left[\frac{(8\cos^2\theta - 2)z^{-2} - 12r\cos\theta z^{-3} + 6r^2z^{-4}}{B^3(z)D(z)}, \frac{1}{B(z)D(z)}\right]$$
$$+2(m+2)\sigma_{xx}\left[\frac{2\cos\theta z^{-1} - 2rz^{-2}}{B^2(z)D(z)}\right]$$
$$+2(n+2)\sigma_{xy}\left[\frac{N(z)((8\cos^2\theta - 2)z^{-2} - 12r\cos\theta z^{-3} + 6r^2z^{-4})}{B^3(z)D^2(z)}, \frac{N(z)}{B(z)D^2(z)}\right]$$
$$+2(n+2)\sigma_{xx}\left[\frac{N(z)(2\cos\theta z^{-1} - 2rz^{-2})}{B^2(z)D^2(z)}\right]$$

$$S_{\theta\theta}(r,\theta) = 2(m+2)\sigma_{xy}\left[\frac{-2r\cos\theta x^{-1} + 4r^2(1+\sin^2\theta)z^{-2} - 2r^3\cos\theta z^{-3}}{B^3(z)D(z)}, \frac{1}{B(z)D(z)}\right]$$
$$+2(m+2)\sigma_{xx}\left[\frac{-2r\sin\theta z^{-1}}{B^2(z)D(z)}\right]$$
$$+2(n+2)\sigma_{xy}\left[\frac{N(z)(-2r\cos\theta x^{-1} + 4r^2(1+\sin^2\theta)z^{-2} - 2r^3\cos\theta z^{-3})}{B^3(z)D^2(z)}, \frac{N(z)}{B(z)D^2(z)}\right]$$
$$+2(n+2)\sigma_{xx}\left[\frac{N(z)(-2r\sin\theta z^{-1})}{B^2(z)D^2(z)}\right]$$

$$S_{r\theta}(r,\theta) = 2(m+2)\sigma_{xy}\left[\frac{-2\sin\theta z^{-1} - 4r\cos\theta\sin\theta z^{-2} + 6r^2\sin\theta z^{-3}}{B^3(z)D(z)}, \frac{1}{B(z)D(z)}\right]$$
$$+2(m+2)\sigma_{xy}\left[\frac{-2r\sin\theta z^{-1}}{B^2(z)D(z)}, \frac{2\cos\theta z^{-1} - 2rz^{-2}}{B^2D(z)}\right]$$
$$+2(n+2)\sigma_{xy}\left[\frac{N(z)(-2\sin\theta z^{-1} - 4r\cos\theta\sin\theta z^{-2} + 6r^2\sin\theta z^{-3})}{B^3(z)D^2(z)}, \frac{N(z)}{B(z)D^2(z)}\right]$$
$$+2(n+2)\sigma_{xy}\left[\frac{N(z)(-2r\sin\theta z^{-1})}{B^2(z)D^2(z)}, \frac{N(z)(2\cos\theta z^{-1} - 2rz^{-2})}{B^2D^2(z)}\right]$$

The iteration is then given by

$$r_{l+1} = r_l - \frac{S_{\theta\theta}(r_l, \theta_l)S_r(r_l, \theta_l) - S_{r\theta}(r_l, \theta_l)S_\theta(r_l, \theta_l)}{\Lambda_l}$$
$$\theta_{l+1} = \theta_l - \frac{S_{rr}(r_l, \theta_l)S_\theta(r_l, \theta_l) - S_{r\theta}(r_l, \theta_l)S_r(r_l, \theta_l)}{\Lambda_l} \tag{12}$$

where

$$\Lambda_l = S_{rr}(r_l, \theta_l)S_{\theta\theta}(r_l, \theta_l) - S^2_{r\theta}(r_l, \theta_l)$$

Again, test cases from Section 4 show the iteration to converge quickly. Note from the above expressions that the only AR decompositions necessary are those of $B^4(z)D^2(z)$ and $B^4(z)D^4(z)$.

These iterations are simple minimizations, and because the required calculations consist only of ARMA cross- and auto-covariances, they can be solved in closed form and in a fast and efficient manner.

G.4 Examples

Let us illustrate by example that our approach indeed reduces the sensitivity and that our optimization procedure indeed works. The system with transfer function [50]

$$H(z) = \frac{0.07930672z^{-1} + 0.02301695z^{-2} + 0.023175236z^{-3}}{1 - 1.97486115z^{-1} + 1.55616124z^{-2} - 0.453768131z^{-3}} \tag{13}$$

has a direct form II sensitivity S = 93.71.

A single real pole/zero pair is added and the resulting sensitivity as a function of the location of the real pole/zero cancellation pair is given in Figure 71. At the minimum point the sensitivity is comparable to that of the cascade realization (S = 43.51). With an initial guess for the single real pole/zero cancellation pair $\alpha_0 = 0.2$, the Newton method yields (to a tolerance of 0.001) the

sensitivity S = 36.60 with the single real pole/zero cancellation pair at $\alpha = -0.952450$ added. The added pole/zero pair has increased the system order by one, thus adding two non-trivial coefficients above the number required for the original order direct form II model. The sensitivity of the filter has been reduced, but has the transfer function been changed in the process? Ideally, a pole/zero cancellation will leave the system transfer function unchanged, but without infinite precision wordlengths, the impulse response will change, however imperceptibly. Results show that the system function has hardly been changed at all. Further improvement in sensitivity is realized when a complex conjugate pair of pole/zero cancellations is added. From the sensitivity surface of Figure 72, a location in the z-plane is found which has a sensitivity lower than the minimum sensitivity achieved by adding only a single, real pole/zero cancellation pair. The Newton method in two variables yields a sensitivity (0.001 tolerance) S = 18.56 with a pair of pole/zero cancellations added at radius $r = 0.9082$ and angle $\theta = \pm 93.13°$. The iteration starting conditions are $r_0 = 0.95$ and $\theta_0 = 110°$. This sensitivity is comparable to the sensitivity of the parallel description (S = 15.70) and about twice as sensitive as the optimal form (S = 8.82). In this case four non-trivial coefficients are added.

We now make an important observation; why do we do this? Even with these four non-trivial coefficients added, the sensitivity measure S for the original order parallel form is lower than the reduced sensitivity 5^{th} -order direct form II, and at less computational effort. Three reasons exist:

1. The direct form II is trivial to compute (i.e. no root-finding is necessary).
2. The parallel form is in reality the sum of isolated direct form II subfilters. Thus, we can treat the subfilters as above and actually reduce the total sensitivity using the present method. For example, adding a real pole/zero cancellation at -0.843739 to the 2^{nd}-order block formed from the two complex conjugate poles in the parallel implementation of the filter described by equation (13) yields a sensitivity of 10.13. Note that the overall filter is now a 4^{th} -order filter and thus has 8 non-trivial coefficients, only 2 more than before. If instead a complex conjugate pair of pole/zero cancellations is added to the 2^{nd}-order block, this results in a sensitivity of S = 9.61. The extension of these ideas to higher order systems is clear.

3. Sensitivity is really a lower bound estimate of quantization noise power, the real quantity of interest.

Figure 73 compares the output quantization noise power of the optimal and the various parallel implementations of the 3rd-order filter. Note that the higher order reduced sensitivity parallel forms have lower output quantization noise power at almost every bit wordlength than the 3rd-order parallel form filter. In fact, **one or the other of these parallel forms actually has lower output quantization noise power than the optimal form at most wordlengths.**

Finally, we note that adding more pole/zero cancellation pairs can further reduce the system sensitivity. For example, placing an additional pole/zero pair at radius $r = 0.9327$ and $\theta = \pm 64.43°$ in the 5th-order direct form II filter given above further reduces the sensitivity, from $S = 18.56$ down to $S = 14.76$.

What is important to gain from these examples is that the sensitivity measure S is only a linear system approximation to a nonlinear system property, and so S really only indicates suitable candidate filters for low output quantization noise power. After determining the candidates, we must simulate them at the desired wordlengths to distinguish between them. In the end, it is the particular application that dictates how to trade off the computational effort for output signal to noise ratio.

G.5 Conclusions

We have given the sensitivity measure S for general state-space digital filters. Next, the direct relationship between the pole and zero sensitivities and the sensitivity measure was exploited to reduce the system output quantization noise power of direct form II digital filters by the introduction of judiciously placed pole/zero cancellation pair(s). Relatively low-order filters designed this way are competitive with optimal designs, and higher-order filters may be designed

using our technique on the isolated direct form II sub-filters of a parallel or cascade implementation. An efficient and fast gradient algorithm is given which determines the optimal locations for these pole/zero cancellation pairs. Finally, the sensitivity may be further reduced by adding more pole/zero cancellation pairs.

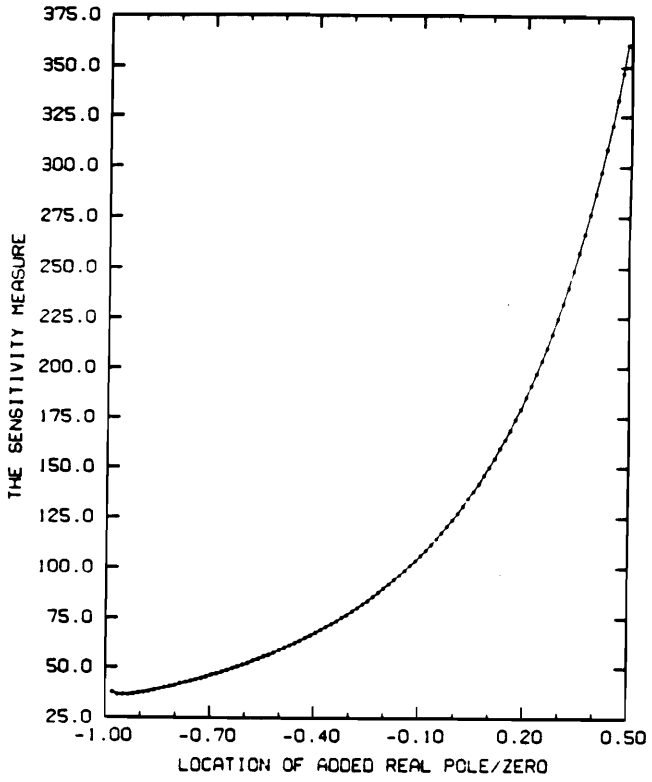

Figure 71. Sensitivity of fourth-order direct form II implementations

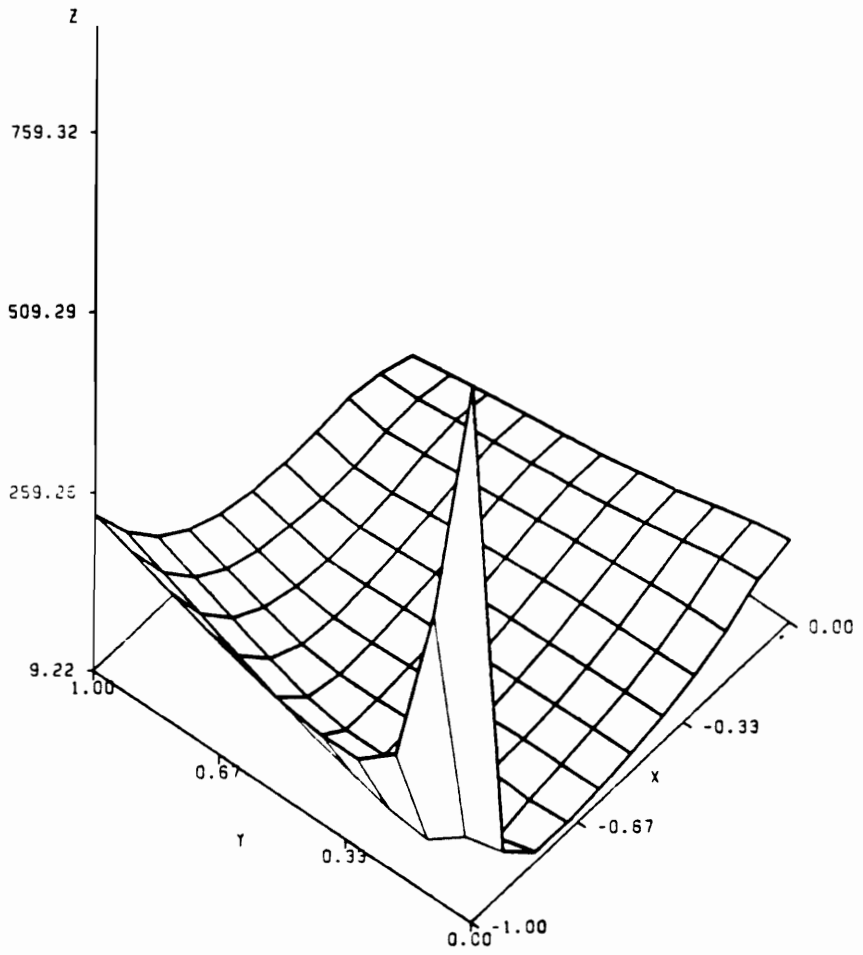

Figure 72. Sensitivity of fifth-order direct form II implementations

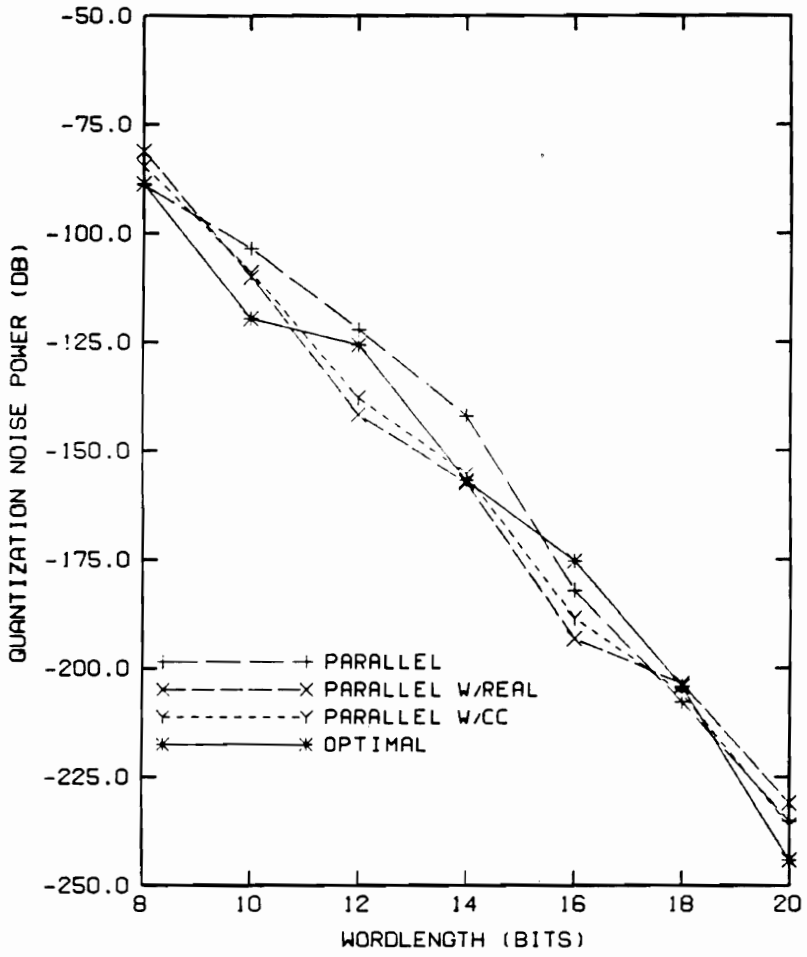

Figure 73. Comparison of the optimal and reduced sensitivity parallel forms

Appendix H. Arbitrary Input DII and PRLL Gradient Computations

In this appendix, the gradient components are derived for the case of arbitrary input (see [102,104]). They are provided for completeness, while offering no direct insight into the measure τ. Note that gradient expressions for the CSCD and lattice forms may be found [104].

H.1 The DII Parameterization

From the parameterization given in equation (3.4.1), we have the associated time-varying difference equation

$$y(t) = \sum_{k=1}^{m} b_k(t)x(t-k) + \sum_{k=1}^{n} a_k(t)y(t-k) \qquad (H.1.1)$$

For purposes of comparison with the PRLL structure, it is assumed that m = n to that the PRLL structure does not have any direct feedthrough-only component sub-section. Then the gradient vector corresponding to the parameter vector given in Chapter 3 will be

$$\Phi_t = [\alpha_1(t)\ \alpha_2(t)\ \ldots\ \alpha_n(t)\ \beta_1(t)\ \beta_2(t)\ \ldots\ \beta_n(t)]$$

where, for $1 \leq k \leq n$, the elements are

$$\begin{aligned} \alpha_k(t) &= \frac{\partial y(t)}{\partial a_k(t)} \\ \beta_k(t) &= \frac{\partial y(t)}{\partial b_k(t)} \end{aligned} \qquad (H.1.2)$$

The gradient may be simplified by noticing that [104] the k^{th} gradient component is the output of the time-varying MA filter

$$\begin{aligned} \alpha_k(t) &= y(t-k) + \sum_{i=1}^{n} a_i(t)\alpha_k(t-i) \\ \beta_k(t) &= x(t-k) + \sum_{i=1}^{n} a_i(t)\beta_k(t-i) \end{aligned} \qquad (H.1.3)$$

By noting that near convergence, $a_i(t) \simeq a_i(t+1)$, one can approximate the gradient elements as

$$\begin{aligned} &\alpha_k(t) \simeq \alpha_1(t-k+1) \text{ for } k = 2, \ldots, n \\ &\beta_k(t) \simeq \beta_1(t-k+1) \text{ for } k = 2, \ldots, n \end{aligned} \qquad (H.1.4)$$

H.2 The PRLL Parameterization

From the parameterization given in equation (3.4.2), we note that the filter output $y(t)$ is the sum of the p sub-filter outputs, i.e.

$$y(t) = \sum_{i=1}^{p} y_i(t) \tag{H.2.1}$$

where

$$y_i(t) = \sum_{j=1}^{2} \xi_{ij}(t)x(t-j) + \sum_{j=1}^{2} v_{ij}y_i(t-j)$$

The gradient components for $i = 1, \ldots, p$ and $j = 1,2$ are then

$$\begin{aligned} \alpha_{ij}(t) &= \frac{\partial y(t)}{\partial v_{ij}(t)} = \frac{\partial y_i(t)}{\partial v_{ij}(t)} \\ \beta_{ij}(t) &= \frac{\partial y(t)}{\partial \xi_{ij}(t)} = \frac{\partial y_i(t)}{\partial \xi_{ij}(t)} \end{aligned} \tag{H.2.2}$$

These components should be placed appropriately in the vector Φ_t as given in Chapter 3. Following from the DII structure equation (H.1.3), the gradient elements can be computed as

$$\begin{aligned} \alpha_{ij}(t) &= y_i(t-j) + \sum_{k=1}^{2} v_{ik}(t)\alpha_{ij}(t-j) \\ \beta_{ij}(t) &= x(t-j) + \sum_{k=1}^{2} v_{ik}(t)\beta_{ij}(t-j) \end{aligned} \tag{H.2.3}$$

Notice that the exact gradient computation is much simpler computationally than the DII computation given in equation (H.1.3). However, since only 2^{nd}-order DII sub-filters are used, the

approximation results in a savings of only one-half, instead of the n times available in the DII structure gradient computation.

List of References

1. S. T. Alexander, "A Simple Noniterative Speech Excitation Algorithm Using the LPC Residual," *IEEE Trans. Acoust. Speech, Sig. Proc.*, vol. ASSP-33, no. 3, pp. 432-434, May 1985.
2. B. D. O. Anderson and C. R. Johnson, "Exponential Convergence of Adaptive Identification and Control Algorithms," *Automatica*, vol. 18, no. 1, pp. 1-13, January 1982.
3. S. Barnett and C. Storey, *Matrix Methods in Stability Theory*, Barnes and Noble, Inc., New York, 1970.
4. A. A. Beex and V. E. DeBrunner , "Reducing Sensitivities of Direct Form Digital (Sub) Filter Structures by Increasing System Order," *IEEE Trans. Cir. and Sys.*, vol. CAS-36, no. 3, pp. 438-442, March 1989.
5. A. A. Beex, "Robust Approximate Stochastic Modeling and Partial Realization," *Invited submission to the 1988 IFAC Symposium on System Identification and Parameter Estimation*, Beijing, People's Republic of China, pp. 1399-1403, 1421, August 1988.
6. A. A. Beex, "ARMA Modeling of Covariance Sequences," *Workshop on Spectral Estimation*, Boston, MA, pp. 41-44, October 1986.
7. A. A. Beex, "Stable Approximate Stochastic Partial Realizations from Noisy Covariances," *7th Int. Symp. on the Mathematical Theory of Networks and Systems (MTNS-85)*, Stockholm Sweden, June 10-14, 1985. In *Modelling, Identification and Robust Control*, eds. C. I. Byrne and A. Lindquist, North-Holland, Amsterdam, pp. 489-498, 1986.
8. A. A. Beex, "ARMA Covariance Realization from Noisy Data," *ICASSP'86*, Tokyo, Japan, pp. 2747-2750, April 8-11, 1986.
9. A. A. Beex, *personal communication,* Blacksburg, VA, November 1985.
10. A. A. Beex, "Efficient Generation of ARMA Cross Covariance Sequences," *ICASSP'85*, Tampa, FL, pp. 327-330, March 1985.
11. A. A. Beex and L. L. Scharf, "Covariance Sequence Approximation for Parametric Spectrum Modeling," *IEEE Trans. Acoust., Speech, Sig. Proc.*, vol. ASSP-29, no. 5, pp. 1042-1052, October 1981.
12. S. Bingulac, J. H. Chow and J. R. Winkelman, "Simultaneous Generation of Sensitivity Functions -- Transfer Function Matrix Approach," *Automatica*, vol. 24, no. 2, pp. 239-242, 1988.
13. R. L. Carroll, "New Adaptive Algorithms in Lyapunov Synthesis," *IEEE Trans. Autom. Control*, vol. AC-21, no. 2, pp. 246-249, April 1976.

14. M. Catelani, G. Iuculano, A. Liberatore, S. Manetti and M. Marini, "Improvements to Numerical Testability Evaluation," *IEEE Trans. on Instr. and Meas.*, vol. IM-36, no. 4, pp. 902-907, Dec. 1987.
15. H.-F. Chen, *Recursive Estimation and Control for Stochastic Systems*, Wiley Series in Probability and Mathematical Statistics, John Wiley & Sons, New York, NY, 1985.
16. H.-F. Chen and L. Guo, "Convergence rate of least-squares identification and adaptive control for stochastic systems," *Int. J. Control*, vol. 44, no. 5, pp. 1459-1476, May 1986.
17. H.-F. Chen and L. Guo, "Optimal Adaptive Control and Consistent Parameter Estimates for ARMAX Model with Quadratic Cost," *SIAM J. Control and Optimization*, vol. 25, no. 4, pp. 845-867, July 1987.
18. H.-F. Chen and L. Guo, "Adaptive control via consistent estimation for deterministic systems," *Int. J. Control*, vol. 45, no. 6, pp. 2183-2202, June 1987.
19. M. Cookey, H. J. Trussell and I. J. Won, "Seismic Deconvolution by Multipulse Methods," *IEEE Trans. Acoust., Speech, Sig. Proc.*, vol. ASSP-38, no. 1, pp. 156-160, January 1990.
20. A. A. H. Damen and A. K. Hajdasinski, "Practical Tests with Different Approximate Realizations Based on the Hankel Matrix," *Eindhoven University of Technology Internal Report*, Eindhoven, Netherlands, May 1982. Conference version: "Practical tests with different approximate realizations based on the singular value decomposition of the Hankel matrix," in *Identification and System Parameter Estimation. 6th IFAC Symposium*, Arlington, Virginia, pp. 809-814, June 1982, editor G. A. Bekey (cover misprint: R. Isermann), Pergamon Press, Oxford, UK, 1982.
21. A. A. H. Damen, P. M. J. Van den Hof and A. K. Hajdasinski, "The Page Matrix: An excellent tool for noise filtering of Markov parameters, order testing and realization," *Eindhoven University of Technology Report 82-E-127*, Eindhoven, Netherlands, August 1982.
22. V. E. DeBrunner and A. A. Beex, "An Efficient Gradient-Based Iteration for Direct Form II Sensitivity Reduction," *ICASSP'88*, New York, NY, pp. 1806-1809, April 1988.
23. V. E. DeBrunner and A. A. Beex, "Sensitivity Analysis of Digital Filter Structures," *SIAM J. Matrix Anal. Appl.*, vol. 9, no. 1, pp. 106-125, January 1988.
24. V. E. DeBrunner, "Sensitivity Analysis of Digital Filters," *M. S. Thesis*, Virginia Polytechnic Institute and State University, Blacksburg, VA, 24061, April 1986.
25. V. E. DeBrunner and A. A. Beex, "Sensitivity of Structures for the Identification of Linear Systems from Impulse Response Data," *ICASSP'89*, Glasgow, Scotland UK, pp. 2214-2217, May 1989.
26. C. J. Demeure and C. T. Mullis, "The Euclid Algorithm and the Fast Computation of Cross-Covariance and Autocovariance Sequences," *IEEE Trans. Acoust., Speech, Sig. Proc.*, vol. 37, no. 4, pp. 545-552, April 1989.
27. S. Deng, "Optimal adaptive control and consistent parameter estimate for deterministic systems with quadratic cost," *Int. J. Control*, vol. 47, no. 6, pp. 1603-1612, June 1988.
28. E. Denman, T. Hasselman, C. T. Sun, J. N. Juang, J. Junkins, F. Udwadia, V. Venkayya and M. Kamat, "Identification of Large Space Structures on Orbit," *Final Report for the period September 1985 to August 1986*, prepared for the Air Force Rocket Propulsion Laboratory, Air Force Space Technology Center, Space Division, Air Force Systems Command, Edwards Air Force Base, California 93523-5000, report #F04611-85-C-0092, September 1986.
29. J. E. Dennis Jr. and R. B. Schnabel, *Numerical methods for unconstrained optimization and nonlinear equations*, Prentice-Hall series in computational mathematics, Prentice-Hall, Englewood Cliffs, NJ, 1983.
30. U. B. Desai, *Modelling and Application of Stochastic Processes*, Kluwer Academic Press, Kluwer Academic Publishers, Boston, MA, 1986.
31. U. B. Desai, "Approximation of Stochastic Systems: Reduced-Order Estimator and Controller," 22nd *IEEE Conf. on Decision and Control*, San Antonio, TX, pp. 1254-1259, December 1983.

32. U. B. Desai and D. Pal, "A Realization Approach to Stochastic Model Reduction and Balanced Stochastic Realizations," 21st *IEEE Conf. on Decision and Control*, Orlando, FL, pp. 1105-1112, December 1982.
33. P. Eykhoff, *System Identification: Parameter and State Estimation*, Wiley-Interscience Publication, John Wiley & Sons, New York, NY, 1974.
34. H. Fan and M. Nayeri, "Counter Examples to Stearns' Conjecture on Error Surfaces of Adaptive IIR Filters," *ICASSP'88*, New York, NY, vol. 3, pp. 1568-1571, April 1988.
35. A. Fettweis, "On Sensitivity and Roundoff Noise in Wave Digital Filters," *IEEE Trans. Acoust., Speech, Sig. Proc.*, vol. ASSP-22, no. 5, pp. 383-384, October 1974.
36. P. Flandrin, F. Magand and M. Zakharia, "Generalized Target Description and Wavelet Decomposition," *IEEE Trans. Acoust., Speech, Sig. Proc.*, vol. ASSP-38, no. 2, pp. 350-352, February 1990.
37. J. B. Foley and F. M. Boland, "A Note on the Convergence Analysis of LMS Adaptive Filters with Gaussian Data," *IEEE Trans. Acoust., Speech, Sig. Proc.*, vol. ASSP-36, no. 7, pp. 1087-1089, July 1988.
38. P. M. Frank, *Introduction to System Sensitivity Theory*, Academic Press (a subsidiary of Harcourt Brace Hovanovich, Publishers), New York, 1978.
39. W. A. Gardner, "Introduction to Einstein's Contribution to Time-series Analysis," *IEEE ASSP Magazine.*, vol. 4, no. 2, pp. 4-5, October 1987.
40. K. F. Gauss, "Theoria motus corporum coelestium. English translation: Theory of the Motion of the Heavenly Bodies," Dover Publishing (1963), New York, NY, 1809.
41. G. H. Golub and C. F. Van Loan, *Matrix Computations*, The John Hopkins University Press, Baltimore, Maryland, 1983.
42. W. B. Gragg and A. Lindquist, "On the Partial Realization Problem," *SIAM J. Linear Algebra, App.*, vol. 50, pp. 277-319, 1983.
43. A. K. Hajdasinski and A. A. H. Damen, "Realization of the Markov Parameter Sequences Using the Singular Value Decomposition of the Hankel Matrix," *Eindhoven University of Technology Report 79-E-95*, Eindhoven, Netherlands, May 1979.
44. A. K. Hajdasinski, P. M. J. Van den Hof and A. A. H. Damen, "Naive Approximate Realizations of Noisy Data," 9th *Biennial World Congress, IFAC*, Budapest, Hungary, vol. 2, pp. 699-704, July, 1984.
45. M. T. Hanna and M. Simaan, "Minimally Sensitive Digital Filters for Array Data Processing," *ICASSP'87*, Dallas, TX, vol. 4, pp. 2348-2351, April 1987.
46. P. Harshavardhana, E. A. Jonckheere and L. M. Silverman, "Stochastic Balancing and Approximation-Stability and Minimality," *IEEE Trans. Autom. Control*, vol. AC-29, no. 8, pp. 744-746, August 1984.
47. P. Harshavardhana and E. A. Jonckheere, "Stochastic Balancing and Approximation: Stability and Minimality," 22nd *IEEE Conf. Dec. and Control*, San Antonio, TX, pp. 1260-1265, December 1983.
48. M. Hestenes, *Conjugate Direction Methods in Optimization*, Springer-Verlag, New York, 1980.
49. S. Horvath, Jr., "A new adaptive recursive LMS filter," in *Digital Signal Processing*, V Cappellini and A. G. Constantinides, Editors, New York, Academic Press, pp. 21-26, 1980.
50. S. Y. Hwang, "Minimum Uncorrelated Unit Noise in State-Space Digital Filtering," *IEEE Trans. Acoust. Speech, Sig. Proc.*, vol. ASSP-25, no. 4, pp. 273-281, August 1977.
51. M. Iwatsuki, M. Kawamata and T. Higuchi, "Synthesis of Minimum Sensitivity Structures in Linear Systems," *ICASSP'86*, Tokyo, Japan, pp. 501-504, April 1986.
52. L. B. Jackson, "Roundoff Noise Bounds Derived from Coefficient Sensitivities for Digital Filters," *IEEE Trans. Cir. and Sys.*, vol. CAS-23, no. 8, pp. 481-485, August 1976.
53. D. A. Johns, W. M. Snelgrove and A. S. Sedra, "State-Space Adaptive Recursive Filters," *ISCAS'88*, Espoo, Finland, pp. 2153-2156, June 1988.
54. R. M. Johnstone, C. R. Johnson, R. R. Bitmead and B. D. O. Anderson, "Exponential convergence of recursive least squares with exponential forgetting factor," *Systems & Control Letters*, vol. 2, no. 2, pp. 77-82, August 1982.

55. R. Kalaba and K. Spingarn, *Control, Identification, and Input Optimization*, Plenum Press, Plenum Publishing Corp., New York, NY, 1982.
56. R. Kalaba, "Sensitivity of Parameter Estimates to Observations, System Identification, and Optimal Inputs," *Applied Mathematics and Computation*, no. 7, pp. 225-235, 1980.
57. R. E. Kalman, "On partial realizations, transfer functions and canonical forms," *Acta. Polytech. Scand.*, vol. MA31, pp. 9-32, 1979.
58. L. G. Kraft, "Controllable Form State Variables Obtained from an Arbitrarily Fast Adaptive Observer," *Proc. IEEE Conf. Dec. Control and 15th Symp. on Adaptive Processes*, pp. 1088-1094, 1976.
59. J. M. Krause and P. P. Khargonekar, "Parameter Information Content of Measurable Signals in Direct Adaptive Control," *IEEE Trans. Autom. Control*, vol. AC-32, no. 9, pp. 802-810, September 1987.
60. G. Kreisselmeier, "The Generation of Adaptive Law Structures for Globally Convergent Adaptive Observers," *IEEE Trans. Autom. Control*, vol. AC-24, no. 3, pp. 510-513, June 1979.
61. G. Kreisselmeier, "Adaptive Observers with Exponential Rate of Convergence," *IEEE Trans. Autom. Control*, vol. AC-22, no. 1, pp. 2-8, February 1977.
62. S. Y. Kung and K. S. Arun, "Approximate Realization Methods for ARMA Estimation," *ISCAS'83*, Newport Beach, CA, pp. 105-109, May 1983.
63. S. Y. Kung, "Partial Realizations: Existence, Uniqueness and Minimality," *ISCAS'82*, Rome, Italy, pp. 911-915, May 1982.
64. S. Y. Kung and D. W. Lin, "A State-Space Formulation for Optimal Hankel-Norm Approximations," *IEEE Trans. Autom. Control*, vol. AC-26, no. 4, pp. 942-946, August 1981.
65. S. Y. Kung and D. Lin, "Optimal Hankel-Norm Model Reductions: Multivariable Systems," *IEEE Trans. Autom. Control*, vol. AC-26, no. 4, pp. 832-852, August 1981.
66. S. Y. Kung, "Optimal Hankel-Norm Model Reductions -- Scalar Systems," *Joint Automatic Control Conf.*, vol. 2, paper FA8-D, San Francisco, CA, August 1980.
67. S. Y. Kung, "A New Identification and Model Reduction Algorithm via Singular Value Decompositions," *12th Asilomar Conf. on Cir., Sys. and Computers*, pp. 705-714, Pacific Grove, CA, November 1978.
68. D. K. Lindner, "The Dual GHR," *Proc. of the 22nd Annual Allerton Conf. on Comm., Control, Comput.*, Monticello, IL, pp. 745-752, September 1984.
69. D. K. Lindner, "Near aggregation, the dual GHR and pole-zero cancellation," *Int. J. Control*, vol. 48, no. 2, pp. 705-727, August 1988.
70. D. K. Lindner and J. Babendreier, "A Trajectory Analysis of Near Aggregation," *IEEE Trans. Autom. Control*, vol. AC-35, no. 5, pp. 474-477, May 1988.
71. D. K. Lindner and W. R. Perkins, "The Generalized Hessenberg Representation and Near Aggregation," *Automatica*, vol. 24, no. 2, pp. 267-270, March 1988.
72. D. K. Lindner, J. Babendreier and A. M. A. Hamdan, "The Dual GHR, zeros, and residues," *Systems & Control Letters*, vol. 10, pp. 245-250, 1988.
73. D. K. Lindner, J. Babendreier and A. M. A. Hamdan, "Measures of Controllability and Observability and Residues" *Internal Report, Bradley Department of Electrical Engineering, VPI&SU, Blacksburg, VA, 24061 USA*, June 1987.
74. L. Ljung, "Analysis of Recursive Stochastic Algorithms," *IEEE Trans. Autom. Control*, vol. AC-22, no. 4, pp. 551-575, August 1977.
75. L. Ljung, "Analysis of a General Recursive Prediction Error Identification Algorithm," *Automatica*, vol. 17, no. 1, pp. 89-99, January 1981.
76. L. Ljung and T. Söderström, *Theory and Practice of Recursive Identification*, MIT Press, Cambridge, MA, 1983.
77. W.-S. Lu and E. B. Lee, "Optimal Structural Sensitivity of Linear Systems with Time Delays," *ACC'87*, Minneapolis, MN, pp. 1925-1930, June 1987.
78. D. G. Luenberger, *Optimization by Vector Space Methods*, John Wiley and Sons, Inc., New York, 1969.
79. J. Makhoul, "On Matching Correlation Sequences by Parametric Spectral Models," *ICASSP'87*, Dallas, TX, vol. 2, pp. 995-998, April 1987.

80. G. Menga and N. Sundararajan, "Stochastic Modeling of Mean-Wind Profiles for In-Flight Wind Estimation -- A New Approach to Lower Order Stochastic Realization Schemes," *IEEE Trans. Autom. Control*, vol. AC-27, no. 3, pp. 547-558, June 1982.
81. S. Mittnik, "Time Series Estimation via Approximate Realization Theory," *Washington University, Department of Economics, Working Paper #89*, St. Louis, MO, 1986.
82. S. Mittnik, "Linear Realization Theory and Time Series Estimation: The Initial State Problem," *Washington University, Department of Economics, Working Paper #90*, St. Louis, MO, 1986.
83. B. C. Moore, "Principal Component Analysis in Linear Systems: Controllability, Observability, and Model Reduction," *IEEE Trans. Autom. Control*, vol. AC-26, no. 1, pp. 17-32, February 1981.
84. J. B. Moore, "Strong Consistency of Least-Squares Identification Algorithms," *Automatica*, vol. 14, pp. 505-509, September 1978.
85. A. P. Morgan and K. S. Narendra, "On the Uniform Asymptotic Stability of Certain Linear Nonautonomous Differential Equations," *SIAM J. Control Optimiz.*, vol. 15, no. 1, pp. 5-24, January 1977.
86. R. Moses, P. Stoica, B. Friedlander and T. Söderström, "An Efficient Linear Method of ARMA Spectral Estimation," *ICASSP'87*, Dallas, TX, vol. 4, pp. 2077-2080, April 1987.
87. C. T. Mullis and R. A. Roberts, "Synthesis of Minimum Roundoff Noise Fixed Point Digital Filters," *IEEE Trans. Cir. and Sys.*, vol. CAS-23, no. 9, pp. 551-562, September 1976.
88. B. R. Musicus, "An Iterative Algorithm for Finding Stable Solutions to the Covariance or Modified Covariance Autoregressive Modeling Methods," *ICASSP'82*, Paris, France, pp. 244-247, April 1982.
89. A. Nehorai and P. Stoica, "Adaptive Algorithms for Constrained ARMA Signals in the Presence of Noise," *ICASSP'87*, Dallas, TX, vol. 2, pp. 1003-1006, April 1987.
90. M. Nayeri and W. K. Jenkins, "Analysis of Alternative Realizations of Adaptive IIR Filters," *ISCAS'88*, Espoo, Finland, pp. 2157-2160, June 1988.
91. A. V. Oppenheim and R. W. Schafer, *Digital Signal Processing*, Prentice-Hall, Inc., Englewood Cliffs, NJ, 1975.
92. A. Parker, S. T. Alexander and H. J. Trussell, "Low bit rate speech enhancement using a new method of multiple impulse excitation," *ICASSP'84*, San Diego, CA, pp. 1.5.1-1.5.4, April 1984.
93. A. I. Perov, "Sensitivity Analysis of Adaptive Filtration Algorithms," *Izvestia VUZ. Radioelektronika*, vol. 29, no. 3, pp. 71-75, 1986.
94. R. Pouliquen, J. Estapa and J. Richalet, "Identification by Frequency Methods and Sensitivity Functions," 2nd *IFAC Symp. on Sys. Sensitivity and Adaptivity*, Dubrovnik, Yugoslavia, pp. 108-123, August 1968.
95. S. C. Puthenpura and N. K. Sinha, "Robust Identification from Impulse and Step Responses," *IEEE Trans. Indus. Elect.*, vol. IE-34, no. 3, pp. 366-370, August 1987.
96. S. C. Puthenpura, N. K. Sinha and O. P. Vidal, "Application of M-Estimation in Robust Recursive System Identification," *Proc. IFAC Symp. Stochastic Control*, Vilnius, USSR, pp. 23-29, June 1986.
97. B. D. Rao, "Sensitivity Analysis of State Space Methods in Spectrum Estimation," *ICASSP'87*, Dallas, TX, vol. 3, pp. 1517-1520, April 1987.
98. D. V. B. Rao, "Analysis of Coefficient Quantization Errors in State-Space Digital Filters," *IEEE Trans. Acoust., Speech, Sig. Proc.*, vol. ASSP-34, no. 1, pp. 131-139, February 1986.
99. A. Rault, J. Richalet and R. Pouliquen, "Identification and Sensitivity," 2nd *IFAC Symp. on Sys. Sensitivity and Adaptivity*, Dubrovnik, Yugoslavia, pp. 93-107, August 1968.
100. J. Rissanen, "Recursive Identification of Linear Systems," *SIAM J. Control*, vol. 9, no. 3, pp. 420-430, August 1971.
101. S. Shokoohi, "Block-Balanced Realizations," *ISCAS'84*, Montreal, Canada, pp. 825-829, May 1984.
102. J. J. Shynk, "Adaptive IIR Filtering Using Parallel-Form Realizations," *IEEE Trans. Acoust., Speech, and Sig. Proc.*, vol. ASSP-37, no. 4, pp. 519-533, April, 1989.

103. J. J. Shynk, "Adaptive IIR Filtering," *IEEE ASSP Magazine*, vol. 6, no. 2, pp. 4-21, April, 1989.
104. J. J. Shynk, "Performance of Alternative Adaptive IIR Filter Realizations," 21st *Asilomar Conference on Signals, Systems & Computers*, pp. 144-150, November 2-4, 1987, Pacific Grove, California.
105. S. Singhal and B. S. Atal, "Improving performance of multipulse LPC coders at low bit rates," *ICASSP'84*, San Diego, CA, pp. 1.3.1-1.3.4, April 1984.
106. N. K. Sinha and B. Kuszta, *Modeling and Identification of Dynamic Systems*, Van Nostrand Reinhold Electrical/Computer Science and Engineering Series, Van Nostrand Reinhold Company, New York, NY, 1983.
107. T. Söderström, "On model structure testing in system identification," *Int. J. Control*, vol. 26, no. 1, pp. 1-18, January 1977.
108. T. Söderström and P. Stoica, "On Some Identification Techniques for Adaptive Filtering," *IEEE Trans. Cir. and Sys.*, vol. CAS-35, no. 4, pp. 457-461, April 1988.
109. V. Solo, "The Convergence of AML," *IEEE Trans. Autom. Control*, vol. AC-24, no. 6, pp. 958-962, December 1979.
110. J. Staar, "A Study of MBH-type Realization Algorithms," *Automatica*, vol. 17, no. 3, pp. 523-533, May 1981.
111. S. D. Stearns, "Error surfaces of recursive adaptive filters," *IEEE Trans. Cir. and Sys.*, vol. CAS-28, no. 6, pp. 603-606, June 1981.
112. P. Stoica, R. L. Moses, B. Friedlander and T. Söderström, "Maximum Likelihood Estimation of the Parameters of Multiple Sinusoids from Noisy Measurements," *IEEE Trans. Acoust., Speech, Sig. Proc.*, vol. ASSP-37, no. 3, pp. 378-392, March 1989.
113. Virginia L. Stonick and S. Thomas Alexander, "Global Optimal IIR FIlter Design and ARMA Estimation Using Homotopy Continuation Methods," *ICASSP'90*, Albuquerque, NM, 1990.
114. Virginia L. Stonick and S. Thomas Alexander, "On Reduced Computational Methods for Global IIR Filtering," *ISCAS'90*, New Orleans, LA, 1990.
115. V. Tavsonoglu, "The Necessary and Sufficient Conditions for Minimum Roundoff Noise in Second-Order State-Space Digital Filters and Their Optimal Synthesis," *IEEE Trans. Cir. and Sys.*, vol. CAS-34, no. 6, pp. 669-677, June 1987.
116. V. Tavsonoglu and L. Thiele, "Optimal Design of State-Space Digital Filters by Simultaneous Minimization of Sensitivity and Roundoff Noise," *IEEE Trans. Cir. and Sys.*, vol. CAS-31, no. 10, pp. 884-888, October 1984.
117. L. Thiele, "On the Sensitivity of Linear State-Space Systems," *IEEE Trans. Cir. and Sys.*, vol. CAS-33, no. 5, pp. 502-510, May 1986.
118. A. Thowsen, "Identifiability of dynamic systems," *Int. J. Systems Sci.*, vol. 9, no. 7, pp. 813-825, July 1978.
119. R. J. Vaccaro and F. Li, "A State-Space Approach to Positive Sequences," *ICASSP'87*, Dallas, TX, vol. 3, pp. 1304-1307, April 1987.
120. J. Vandewalle and J. Staar, "Modelling of Linear Systems: Critical Examples, Problems and Numerically Reliable Approaches," *ISCAS'82*, Rome, Italy, pp. 915-918, May 1982.
121. E. Walter, *Identifiability of State Space Models*, Lecture Notes in Biomathematics, Springer-Verlag, New York, NY, 1982.

Vita

Victor DeBrunner graduated from Auburn University in Auburn, Alabama with a Bachelor degree in Electrical Engineering in March of 1984. He attended Virginia Polytechnic Institute and State University in Blacksburg, Virginia, where he completed a Master of Science degree in Electrical Engineering with an emphasis in digital signal processing. He anticipates receiving his Ph.D. in Electrical Engineering there in May of 1990. His goals are to teach and do research at the university level.

His research interests are in the areas of system identification, spectral estimation, digital filter design and adaptive beamforming; his hobbies include swimming, weight-lifting, reading about history and travel.

He is a member of Eta Kappa Nu, Tau Beta Pi, Phi Kappa Phi, and the IEEE (Societies: Acoustics, Speech, and Signal Processing; Circuits and Systems; and Communications).